



FACULTY OF SCIENCES AND TECHNOLOGY

DEPARTMENT OF CIVIL ENGINEERING

LABORATORY OF HYDRAULICS, WATER RESOURCES AND ENVIRONMENT

**MODELLING THE INFLUENCE OF STORM MOVEMENT AND
WIND-DRIVEN RAINFALL ON OVERLAND FLOW IN URBAN AREAS**

by

Jorge Manuel Guieiro Pereira Isidoro

Master of Science in Civil Engineering

Supervisor

Prof. Dr. João Luís Mendes Pedroso de Lima

Full Professor of the University of Coimbra

Thesis submitted to the Civil Engineering Department, Faculty of Sciences and Technology of the University of Coimbra, in the fulfilment of the requirements for the degree of Doctor of Philosophy in Civil Engineering, with specialization in Hydraulics, Water Resources and Environment

Coimbra, 2012

ABSTRACT

In the second half of the 20th century and in the beginning of this new century the world has witnessed a historic increase in urban population. This demographic reality implies a greater exposure and vulnerability of these populations to risks of natural and anthropogenic origin. Urban flooding associated with heavy rainfall fits under both these risks. One consequence of changes to the natural hydrological cycle, *e.g.*, lower infiltration capacity by ground-sealing, combined with population growth and the concentration of economic activities, is a heightened awareness of the increased occurrence and magnitude of urban floods, not to mention the associated loss of tangible and intangible assets. A thorough understanding of the reasons underlying this reality is thus fundamental to the development of tools (*e.g.*, plans, models and techniques) to mitigate the consequences of intense rainfall over urban areas.

The main objective of this thesis is to contribute to a better understanding of the processes associated with urban flooding caused by heavy rainfall. Particular attention has been paid to the analysis of the effects triggered by the simultaneous occurrence of wind and rain on overland flow in urban areas, a subject on which there are not very many studies.

The research work that establishes the foundation of this thesis was mainly based on physical simulations in the laboratory. Computer simulation techniques were also used, in particular to develop a digital terrain model and obtain runoff hydrographs associated with moving rainstorms, by means of numerical approximation and analytical derivation. Simulated rainfall tests were performed on physical models of urban areas. The rainfall simulator consisted of a movable structure with nozzles which could generate wind speed fields. These laboratory tests were applied to several scenarios with different precipitation intensity conditions (*e.g.*, stationary and moving rainfall, with and without wind). These scenarios made it possible to study how the density, height and rooftop connectivity of buildings influence overland flow. Laboratory tests were also carried out to investigate how the configuration of hillslopes influences overland flow and sediment loss, under static and moving intense rainstorms. Computer simulation was used to establish comparisons with some of the laboratory tests' observations and to perform an applied GIS-based study of the temporal evolution of urban occupation.

From the results obtained it can be concluded that the combined action of wind, rainfall and storm movement causes significant and systematic changes on overland flow. Peak and time of base flow are particularly affected by these actions.

The research carried out with physical models also showed that different characteristics of the urban structure (*e.g.*, density of high-rise buildings), under the same rainfall conditions, led to different overland flow hydrographs and that, in natural surfaces, hillslope configuration is a key factor in overland flow and water erosion processes.

RESUMO

Na segunda metade do século XX e no início deste novo século tem-se assistido a um aumento histórico da população urbana. Esta realidade demográfica acarreta uma maior exposição e vulnerabilidade destas populações aos riscos de origem natural e antrópica. As cheias urbanas associadas a precipitações intensas enquadram-se em ambos estes riscos. Efeito das alterações ao ciclo hidrológico natural, *e.g.*, diminuição da capacidade de infiltração por impermeabilização do terreno, e da maior concentração de habitantes e de atividades económicas, é perceptível o aumento da ocorrência e da magnitude de cheias em áreas urbanas, bem como das perdas tangíveis e intangíveis associadas. Um profundo conhecimento das razões que levam a esta realidade é pois fundamental para a criação das ferramentas (*e.g.*, planos, modelos e técnicas) que permitam mitigar os efeitos decorrentes das precipitações intensas em meio urbano.

O principal objetivo desta tese é o de contribuir para um melhor conhecimento dos processos associados às cheias urbanas causadas por precipitações intensas. Para o cumprir foram investigados diversos aspetos sobre o processo de precipitação-escoamento. Foi dada particular importância à análise dos efeitos causados pela ocorrência simultânea de vento e chuva no escoamento superficial em zonas urbanas, tema sobre o qual existem poucos estudos.

A atividade de investigação que consubstancia esta tese baseou-se principalmente na simulação física em laboratório. Foram também utilizadas técnicas de simulação computacional, nomeadamente para desenvolver um modelo digital de terreno e obter – por aproximação numérica e derivação analítica – hidrogramas de escoamento superficial associados a chuvas móveis. Recorrendo a um simulador de chuva foram realizados ensaios de precipitação simulada sobre modelos físicos de zonas urbanas. O simulador de chuva consiste numa estrutura móvel onde podem ser adaptados nebulizadores e a partir da qual é possível gerar campos de velocidade do vento. Estes ensaios foram realizados sob vários cenários com diferentes condições de precipitação intensa (*e.g.*, chuvadas estáticas e móveis, com e sem vento). Estes cenários permitiram estudar a influência que a densidade, altura e conectividade de coberturas de edifícios têm no escoamento superficial. Foram também realizados ensaios laboratoriais para investigar de que forma a geometria das encostas influencia o escoamento superficial e o transporte de sedimentos, para chuvas estáticas e móveis de elevada intensidade. A simulação computacional foi utilizada para estabelecer comparações com algumas das observações realizadas em

laboratório e para realizar um estudo aplicado, com base em modelos SIG, sobre a evolução temporal da ocupação urbana.

Com os resultados obtidos pode concluir-se que a ação combinada do vento e da chuva e o movimento das células de precipitação provocam alterações significativas e sistemáticas no escoamento superficial. Os caudais de ponta e os tempos de base do escoamento são particularmente afetados pelas ações referidas.

O trabalho realizado com base em modelos físicos permitiu também constatar que diferentes características do edificado (*e.g.*, densidade de edifícios altos) conduziram, para as mesmas condições de precipitação, à obtenção de diferentes hidrogramas de escoamento superficial e que, em superfícies naturais, a forma das encostas é um fator preponderante para os processos de escoamento superficial e erosão hídrica.

ACKNOWLEDGEMENTS

A PhD thesis can be seen from two orthogonal perspectives: a horizontal plane, where a large tangle of paths is visible (almost to the horizon) and a vertical plane full of high's and low's that, from this instant and point of view, looks somewhat like a rollercoaster. Completion of this thesis would not have been possible without the people that helped me choosing the most fruitful paths and showing me that after a big dive, a fast rise is always near. It is to those people that the next words are addressed.

First of all to my scientific supervisor, Professor João de Lima from the University of Coimbra, whose creativity, objectivity, high quality standards and support allowed me to take this task to completion. It was him who taught me what research really is. Thank you very much João for your time, patience and friendship.

To my research colleagues Ina Vertommen, Sílvia Carvalho, Romeu Gerardo and Diana Coimbra and to the members of the University of Coimbra faculty João Vieira and Jorge Leandro – all of them now good friends – for their advices, time spent on fruitful discussion, helping in the laboratory experiments and friendship. To the latter, especial thanks for the direct contribution to some chapters of this work are owed. To Mr. Joaquim Cordeiro, technical assistant on the Laboratory of Hydraulics, Water Resources and Environment, I wish to express my gratitude for his help on the preparation of the rainfall simulator and the physical models.

To Professor Maria Isabel de Lima, from the Polytechnic Institute of Coimbra, to which I am grateful for the fruitful discussions on some of the topics presented in this thesis and for reviewing some of the papers submitted to journals and conferences.

To my friends and colleagues at University of Algarve for their support, opinions and many, many hours of discussion about several issues related to this work. Among others, I would like to express thanks to Carlos Silva, José Rodrigues and Rui Lança. A special recognition to David Pereira for his help on some computer-related issues is particularly owed. To Vera Rocheta, my cabinet colleague, I must show gratitude for her understanding of my lack of time and for having to listen for too many hours of classical music...

Finally, I must address a special acknowledgement to my parents for their general support and to Ana for... everything else!

FINANCIAL SUPPORT

This thesis was partially funded by research project “*Experimental and Numerical set-up for validation of the Dual-Drainage (sewer/surface) concept in an Urban Flooding framework*” (PTDC/ECM/105446/2008) and PhD grant SFRH/PROTEC/49736/2009, both supported by the **Portuguese Foundation for Science and Technology (FCT)**.

During the course of this thesis (4 years), research was also partially funded by the following projects supported from FCT:

POCI/AMB/58429/2004
PTDC/GEO/73114/2006
PTDC/CLI/67180/2006
PTDC/ECM/70456/2006
PTDC/AAC-AMB/101197/2008

An acknowledgement is owed to the following institutions and programmes that provided financial support to this thesis:

European Regional Development Fund (ERDF), Operational Programme 'Thematic Factors of Competitiveness' (COMPETE);

Institute of Marine Research – Marine and Environmental Research Centre (IMAR–CMA), Coimbra, Portugal;

University of Algarve (UAlg), Faro, Portugal;

Faculty of Sciences and Technology of the University of Coimbra (FCTUC), Coimbra, Portugal.



CONTENTS

1. Scope and introduction	3
1.1 Motivation and Research Context.....	3
1.2 Organization of the Thesis.....	5
1.3 Objectives	6
1.4 Publications and Conferences	7
2. Literature review.....	15
2.1 Overland Flow.....	15
2.1.1 Components of surface flow.....	15
2.1.2 Overland flow on urban areas – Conditioning factors	16
2.1.2.1 Rainfall water	17
2.1.2.2 Storm movement	21
2.1.2.3 Wind-driven rainfall	23
2.1.2.4 Land use and topography	25
2.2 Urban Floods.....	27
2.2.1 Flash floods in urban areas	28
2.2.2 Consequences of urbanization	31
2.2.3 GIS-based flood models	33
2.3 Influence of Storm Movement and Wind-Driven Rainfall.....	35
2.3.1 Overland flow in urban environments.....	35
2.3.1.1 Field studies	38
2.3.1.2 Laboratory experiments	39
2.3.1.3 Numerical methods	42
2.3.1.4 Analytical solutions.....	44
2.3.2 Overland flow on natural surfaces	46
2.3.3 Applications in other fields of civil engineering	49
2.4 Notation.....	51
2.5 References	51

3. Evolution of urbanization in a small urban basin: DTM construction for hydrologic computation	65
3.1 Introduction	65
3.2 Study Area Description	66
3.3 Geographical Information System Model	67
3.3.1 Geographical database	67
3.3.2 DTM construction	68
3.3.3 Drainage network representation	69
3.4 Evolution of the Urban Area	70
3.5 Flood Event Example	71
3.6 Conclusions	72
3.7 Acknowledgements	73
3.8 References	73
4. Influence of wind-driven rain on the rainfall-runoff process for urban areas: Scale model of high-rise buildings	77
4.1 Introduction	77
4.2 Rainfall Simulator and Scale Model	79
4.2.1 The rainfall simulator system	80
4.2.2 The scale model	81
4.2.3 The flow meter and data collection system	82
4.3 Methodology and Simulations	82
4.3.1 Calibration and validation	83
4.3.2 Rainfall spatial distribution	84
4.3.3 Wind characterization	85
4.3.4 Simulated storm scenarios	86
4.4 Results and Discussion	88
4.5 Summary and Conclusion	94
4.6 Acknowledgments	95
4.7 Notation	96
4.8 References	96

5. The study of rooftop connectivity on the rainfall-runoff process by means of a rainfall simulator and a physical model	103
5.1 Introduction	103
5.2 Methodology	105
5.2.1 Rainfall simulator	105
5.2.2 Physical model	107
5.2.3 Rainfall and wind distribution.....	108
5.2.3 Laboratory experiments procedure.....	109
5.3 Simulation Runs	110
5.4 Results.....	112
5.5 Discussion	115
5.6 Conclusions	118
5.7 Acknowledgments	119
5.8 Notation.....	120
5.9 References	120
6. Laboratory simulation of the influence of building height and storm movement on the rainfall-runoff process in impervious areas.....	127
6.1 Introduction	127
6.2 Laboratory Set-Up and Procedure.....	128
6.2.1 Rainfall simulator	129
6.2.2 Impervious flume and building elements.....	129
6.2.3 Rainfall and wind distributions	130
6.3 Results and Discussion.....	132
6.4 Conclusions	135
6.5 Acknowledgments	135
6.6 References	135
7. An analytical closed form solution for 1D linear kinematic overland flow under moving rainstorms	139
7.1 Introduction	139
7.2 Theory	141

7.2.1 Solution of the 1D linear kinematic wave equation for downstream (uniform) movement of a storm cell	143
7.2.2 Solution of the 1D linear kinematic wave equation for upstream (uniform) movement of a storm cell.....	145
7.3 Verification of the Analytical Solution.....	147
7.3.1 Comparison with another analytical solution	147
7.3.2 Comparison with a numerical approximation	149
7.3.3 Comparison with laboratory simulations	151
7.4 Applications	154
7.4 Conclusions	157
7.5 Acknowledgments	158
7.6 Notation	158
7.7 References	159
8. Incorporating moving storm effects into hillslope hydrology: results from multiple-slope soil flume.....	165
8.1 Introduction	166
8.2 Methods and Materials	167
8.2.1 Rainfall simulator	167
8.2.2 Soil flume	169
8.2.3 Storm characterization	169
8.2.4 Granulometric characterization.....	170
8.3 Results and Discussion.....	170
8.3.1 Hydrographs and sediment flux.....	170
8.3.2 Soil granulometric evolution	173
8.3.3 Relation between the sediment transported and discharge	174
8.4 Conclusions	176
8.5 Acknowledgements	176
8.6 References	176
9. Conclusions and future research.....	181
9.1 Conclusions	181
9.2 Future Research.....	185

LIST OF FIGURES

Figure 2.1 Rain cells with intensity above 20 mm/h over the Portuguese Algarve region, from 05:00am until 03:00pm of the 28 th November 2006 (left). Rain cell 9 speed during this period; dashed line is the rain cell mean speed (centre). Flooding in downtown Faro as a consequence of rain cell 9 passage (right)	18
Figure 2.2 Rainfall-runoff processes in the urban water cycle. Losses due to interception, surface storage, infiltration and evapotranspiration are identified. Dashed lines stand for indirect flow of water, which includes the fraction retrieved by plants and then transpired and the fraction that reaches the drainage basin surface and evaporates	21
Figure 2.3 Example of disdrometer (Thies Clima) available in the Laboratory of Hydraulics, Water Resources and Environment of the Civil Engineering Department of the Faculty of Sciences and Technology, University of Coimbra.....	24
Figure 2.4 Simplified scheme of the influence of wind on the terminal velocity of a raindrop. V_R is the raindrop terminal velocity for windless conditions (vertical rainfall), V_W is the horizontal wind velocity near the ground surface, V_{WDR} is the wind-driven affected raindrop terminal velocity and θ is the angle of incidence of the rainfall.....	25
Figure 2.5 Uniform depth of water in a 1.0 m wide rectangular open channel with a surface roughness K_S (Strickler coefficient) of $90 \text{ m}^{1/3} \cdot \text{s}^{-1}$, for a flow of 100 l/s and different surface slopes	27
Figure 2.6 Sewer sink clogged due to accumulation of leafs and pine tree needles carried by storm runoff (Quinta do Lago, Loulé, Portugal). The sewer sink trash rack was found completely covered after a flooding event which occurred on the 29 th September 2008 (left). A worker removes the accumulated leafs and pine tree needles, uncovering the sewer sink trash rack (right)	29
Figure 2.7 Urban flash floods due to short duration extreme intensity rainfall. On the 17 th February 1972, 78.5 mm of rain fell in one hour (MWC, 2007) over the Melbourne (Australia) business centre (left; Neville Bowler/Fairfax Syndication). On the 20 th February 2010, from 9:00am to 11:00am, 223 mm of rainfall was measured at the <i>Pico do Arieiro</i> (01/02M) meteorological station (de Lima <i>et al.</i> , 2010), causing 42 deaths, 100 injured and millions of Euros in damages (Luna <i>et al.</i> , 2011) that are currently still being repaired (right; Octávio Passos/AP)	30
Figure 2.8 Schematic hydrographs helps to illustrate the influence of urbanization in overland flow discharge.....	32

Figure 2.9 1960 RADAR image of Hurricane Abby approaching the coast of British Honduras, nowadays Belize. The complete eyewall cloud is perfectly defined (United States National Oceanic and Atmospheric Administration).....	37
Figure 2.10 A physical model of an urban area densely occupied by high-rise buildings is tested on the laboratory to obtain experimental data of the relation between building density, storm movement, wind-driven rainfall and overland flow. In these experiences, elements representing buildings could be removed and repositioned in order to obtain different building occupation densities	41
Figure 3.1 Location of Algarve and Cabanas de Tavira in the south of Portugal	67
Figure 3.2 Water courses in the Cabanas de Tavira urban area	67
Figure 3.3 Drainage network: (a) GRID; (b) flow directions; and (c) flow lines	69
Figure 3.4 Cabanas de Tavira GIS image.....	70
Figure 3.5 Development of the urban area in Cabanas de Tavira from 1991 to 2005 (see also Table 1)	71
Figure 3.6 Flood in Ribeira do Pocinho on 2 nd October 2007, next to tourist housing..	72
Figure 4.1 Rainfall simulator and electric fan system on a structure (a), scale model of a hypothetical high density urbanized area with high-rise buildings (b) and static pressure meter placed at the bottom of a cylindrical reservoir and data collecting system (c)	80
Figure 4.2 Constant pressure nozzle: hydraulic system scheme (a) and photograph of the operating system (b).....	81
Figure 4.3 Scale model: conceptual representation of building elements	82
Figure 4.4 Distribution of simulated rainfall intensity (isohyets every 25 mm/h) under the nozzle: without wind (a); with wind (b). Sketch of rainfall cell movement along the scale model (c)	85
Figure 4.5 Wind speed fields at 0.15 m (a), 1.00 m (b) and 2.00 m (c), from the fans. Sketch of wind speed fields' positions relative to the fans (d).....	86
Figure 4.6 Density of the high-rise building blocks used on the scale model	87
Figure 4.7 Notation used to define the hydrologic variables obtained through the experimental hydrographs.....	88
Figure 4.8 Dimensionless overland discharge hydrographs for: a) static rainfall without wind; b) static rainfall with wind; c) uphill moving rainfall without wind; d) uphill moving rainfall with wind; e) downhill moving rainfall without wind; f) downhill moving rainfall with wind	91

Figure 4.9 Uphill vs. Downhill dimensionless peak discharges for moving storms, without and with wind (in the legend ‘w’ refers to simulations with wind).....	94
Figure 4.10 Dimensionless hydrograph’s rising limb angle (α^*) for different high-rise building densities for (a) no-wind rainfall and (b) wind-driven rainfall scenarios	94
Figure 5.1 Left: Sketch of rainfall simulator comprising the pressurized system, moving structure and set of fans. Top right: Detail of constant pressure system and nozzle. Bottom right: Discharge measuring system consisting of a recipient equipped with a pressure sensor and data logger	106
Figure 5.2 Physical model. Left: Stand with steel sheet surface. Right: Building element made of expanded polystyrene.....	107
Figure 5.3 Spatial distributions of the storm cell rainfall intensity. Top: without wind. Bottom: with wind (and wind-speed spatial distribution at 1.35 m from the nozzle). Wind speed measured above physical model with no buildings	108
Figure 5.4 Sketch of the drainage basin geometry, storm movement directions, hydraulic circuit of the rainfall simulator, outlet and data collection.....	109
Figure 5.5 Rooftop connectivities used in the simulations	111
Figure 5.6 Discharge hydrographs. Top: Static storms; Centre: Downstream storms; Bottom: Upstream storms. Left: No-wind; Right: Wind-driven. The obtained peak flows are shown in the hydrographs	113
Figure 5.7 Notation used for the variables retrieved from the hydrographs. Discharge obtained from the output of the pressure sensor	114
Figure 5.8 Variables retrieved from the hydrographs as a function of rooftop connectivity. Top: Maximum peak discharges; Centre top: Base time of runoff; Centre bottom: Time of runoff initiation; Bottom: Slope of the rising limb of the hydrograph, for all rooftop connectivities and storm types; Left: no-wind rainfall; and Right: wind-driven rainfall	116
Figure 6.1 Experimental set-up comprising a wind-driven rainfall simulator (1, 2 and 5), an impervious flume (4) and polystyrene elements representing buildings (3) (elements with 0.20 m height, in the photograph)	129
Figure 6.2 Spatial distribution of simulated rain cells rainfall intensities (mm/h) at the flume surface: Top: no-wind scenario; Bottom: wind-driven scenario.....	130
Figure 6.3 Wind speed field (m/s) at vertical plane 1.00 m away from of the set of fans. Height is measured upwards from the flume geometrical centre	131
Figure 6.4 Sketch of different scenarios used in the laboratory experiments: a) static storm; b) upstream moving storm; and c) downstream moving storm. No-wind (left) and wind-driven (right) rainfalls are presented for each storm scenario	132

Figure 6.5 Experimental hydrographs. Left: no-wind rainfall; Right: wind-driven rainfall. Up: static storms; Centre: upstream moving storms; Bottom: downstream moving storms. Different building heights are represented by different colours	133
Figure 6.6 Runoff peak discharges (left, in l/s) and base times (right, in s) obtained for all the storm types and building heights. Different building heights are represented by different colours). In the figure NW stands for No-Wind rainfall and W for Wind-driven rainfall	134
Figure 6.7 Comparison of runoff peak discharges for the scenarios with and without buildings, no-wind and wind-driven rainfall. Different building heights are represented by different colours. Storm types (static, upstream and downstream) are specified	134
Figure 7.1 Sketch of a storm cell moving over a plane surface with unit width. “Downstream” refers to the storm cell’s movement in the flow direction	144
Figure 7.2 Sketch of a storm cell moving over a plane surface with unit width. “Upstream” refers to the storm cell’s movement opposite to the flow direction	146
Figure 7.3 Flood hydrographs obtained with the analytical solutions presented in this study and in Singh (1998) for (left) downstream and (right) upstream storm movements	149
Figure 7.4 Analytical solution and numerical approximation (presented in de Lima and Singh (2002)) of flood hydrographs for (left) downstream and (right) upstream storm movements	151
Figure 7.5 Sketch of the laboratory experiments. The simulated storm cell, generated by a moving sprinkler, moves over the laboratory flume	151
Figure 7.6 3D representation of the rainfall spatial distribution under the nozzle ...	153
Figure 7.7 Analytical solution and experimental simulation of flood hydrographs for (left) downstream and (right) upstream storm movement	153
Figure 7.8 Entire time-space domain hydrographs provided by the analytical solution for a catchment 100 m long and with a hydraulic coefficient (α) of 2.0, caused by a storm cell moving with a velocity of $0.5 \text{ m}\cdot\text{s}^{-1}$ and having $2.78\cdot 10^{-5} \text{ m}\cdot\text{s}^{-1}$ ($100 \text{ mm}\cdot\text{h}^{-1}$) rainfall intensity and a length of 250 m, for (left) downstream and (right) upstream storm movements.....	155
Figure 7.9 Hydrographs for a catchment with a length of 500 m, a slope of 1.0% and Strickler roughness coefficient of $100 \text{ m}^{1/3}\cdot\text{s}^{-1}$ ($\alpha=10$), caused by storm cells of (top) 100 m, (middle) 500 m and (bottom) 1000 m length and with a rainfall intensity of $2.78\cdot 10^{-5} \text{ m}\cdot\text{s}^{-1}$ ($100 \text{ mm}\cdot\text{h}^{-1}$) moving (left) downstream and (right) upstream, at a velocity of 0.5, 1.0 and $5.0 \text{ m}\cdot\text{s}^{-1}$	156

Figure 7.10 Discharge vs. drainage surface length in $t=20, 40$ and 60 s for (left) downstream and (right) upstream storm movements.....	157
Figure 8.1 Rainfall simulator system and soil flume.....	168
Figure 8.2 Position of nozzles, rainfall simulator movement and discharge point regarding the soil flume.....	168
Figure 8.3 Hillslope types used in the laboratory experiences	169
Figure 8.4 Runoff hydrographs and respective sediments fluxes for different storms and hillslopes types, for moving rains	171
Figure 8.5 Runoff hydrographs and respective sediments fluxes for different storms and hillslopes types, for static rains.	172
Figure 8.6 Percentages of the sand, silt and clay by the different storm types and hillslope	173
Figure 8.7 Relation between the sediment flux and discharge by the different combinations of the storm and hillslope types: Downhill moving storm (a); Uphill moving storm (b); Static – P1 (c); Static – P2 (d) and Static – P3 (e).....	174

LIST OF TABLES

Table 1.1 Articles in international journals (SCI-indexed) or journals type A or B (FCTUC).....	8
Table 1.2 Articles in proceedings of international conferences.....	9
Table 1.3 Abstracts and extended abstracts of international conferences.	10
Table 1.4 Articles in proceedings of national (Portuguese) conferences.	12
Table 1.5 Abstracts and extended abstracts of international (Portuguese) conferences	12
Table 3.1 Development of the urban area of Cabanas de Tavira over about 15 years.	71
Table 4.1 Duration of rainfall and simulator speed for different storm scenarios	84
Table 4.2 Scenarios used in the simulations	87
Table 4.3 Observed peak discharge, time to peak discharge, slope of the rising limb of the hydrograph, base time of runoff and average discharge, for all the experimental runs	89
Table 4.4 Relative differences of peak discharges (ΔQ_p^{rel}) for the with- and without- wind storms, for all the simulated scenarios' combinations (values in %)	93
Table 5.1 Storm types used in the laboratory simulations	111
Table 5.2 Rooftop connectivities used in the laboratory simulations (see Figure 5.5)	112
Table 5.3 Parameters obtained directly from the discharge hydrographs (see Figure 5.6)	114
Table 8.1 Runoff hydrographs and respective sediments fluxes for different storms and hillslopes types, for moving rains	173

CHAPTER 1

El habitante urbano que la observa a diario, dócil a sus necesidades, bajar mansa de la llave, no tiene idea de su idiosincrasia. No imagina con cuánta paciencia y astucia hay que manejar a esta nuestra gran amiga-enemiga; cuán a fondo hay que entender su índole altiva para poder someterla y doblegarla; cómo hay que "dorarle la píldora" para reducirla a nuestra voluntad, respetando -sin embargo- la suya. Por eso, el hidráulico ha de ser, ante todo, algo así como un psicólogo del agua, conocedor profundo de su naturaleza.

Enzo Levi

1. SCOPE AND INTRODUCTION

This thesis fits in the field of urban hydrology. The work addresses the influence of storm movement and wind-driven rain on the rainfall-runoff process in urban areas. The role of urbanization in the water cycle is also considered. The relation between some characteristics of urban areas (high-rise building density, building height and rooftop connectivity) and the resulting overland flow hydrographs for wind-driven moving storms over impervious surfaces are discussed. A study on the influence of hillslope configuration on overland flow and sediment loss is also included. Some supplementary themes are also presented and discussed (*e.g.*, GIS-based flood models), although in less detail.

The first part of this chapter explains the motivation to investigate this field of engineering and the context in which research was carried out. The organization of this work is then outlined by a brief overview of each chapter. Finally, the most specific issues that this thesis attempts to answer are listed in the form of open questions.

1.1 MOTIVATION AND RESEARCH CONTEXT

Why choose this field of study? A question without a single (and simple) answer but attempting to provide one may help to explain the motivation behind this work...

Urban floods pose high risks to people and assets. Economic activities, cultural heritage and the environment are also endangered by these phenomena. High intensity rainfall events tend to happen in nature but when they strike particularly exposed and vulnerable densely-populated areas the results may be catastrophic. The expansion of urban areas, highly noticeable in the second half of the 20th century and in the beginning of this new one, raises several issues such as an increase in the potentially affected population, reduced infiltration or inability of rainwater drainage systems to cope with the runoff generated by ever-expanding impervious areas. In Europe alone in the past few years floods have caused the death of hundreds of people, the displacement of hundreds of thousands more and thousands of millions of Euros in economic losses.

Flooding events depend on the multiple state variables that define their origins and so a better knowledge of these origins is a key factor for the more effective prevention, management and mitigation of urban floods. Even though absolute flood security is a utopian dream, proper flood management must be seen as essential to reducing flood vulnerability and exposure. This was the fundamental impetus to pursuing a research programme in this field. A better understanding of the physics of the rainfall-runoff process on urban area can significantly enhance the tools used by modellers and planners, *e.g.*, by attaining simulation models which are more accurate and faithful to the natural environment.

Even though some computer simulation was performed that involved creating a digital terrain model, programming a numerical approach and finding an original analytical solution, the research described in this thesis is mainly based on laboratory physical modelling. This laboratory work was carried out at the Civil Engineering Department of the Faculty of Sciences and Technology of the University of Coimbra (www.uc.pt/fctuc/dec), more precisely in the Laboratory of Hydraulics, Water Resources and Environment. Among its facilities this laboratory has a rainfall simulator that can simulate the movement of rain cells simultaneously with the occurrence of wind. The simulator had been used previously to this work, mainly for water erosion studies that have already been published in international journals and conference proceedings.

In order to carry out the research described in this thesis the rainfall simulator required the following improvements: (i) installation of an electronic frequency inverter to give a highly accurate control of the rainfall simulator speed, (ii) fitting of an additional hydraulic circuit to the nozzle intake to ensure instant rainfall start/stop and constant pressure, *i.e.*, constant rainfall intensity, during the simulations, and (iii) the fitting of a static pressure sensor and a data logger to allow the acquisition and collection of the overland flow discharged from the tested physical models with 1.0 s resolution. Besides these improvements to the rainfall simulator, physical models of buildings were also designed and constructed to simulate buildings of different geometries and layouts over an impervious area.

The research described in this thesis lay within the scope of the Hydraulics, Water Resources and Environment Research Line (HyWaRE) of the Institute of Marine Research – Marine and Environmental Research Centre (IMAR–CMA). The IMAR-CMA webpage provides more information about this research centre and can be found at: <http://www1.ci.uc.pt/imar/unit/>

1.2 ORGANIZATION OF THE THESIS

This thesis is divided in 9 chapters. The contents of each chapter are briefly summarized in the next paragraphs¹:

Chapter 1 gives an overview on the motivation to research in this field of engineering and on how the work was carried out, describes the organization of this document and, finally, identifies the objectives of this thesis.

Chapter 2 presents a literature review on several issues related to overland flow, urban floods, storm movement and wind-driven rainfall. A short comprehensive literature review on the influence of storm movement and wind-driven rainfall on impervious surfaces in urban areas is included.

Chapter 3 presents a study regarding the evolution of urbanization in Cabanas de Tavira (Portugal) and the construction of a Digital Terrain Model (DTM) of that area for flood modelling purposes. Cabanas de Tavira is a parish and a former fishing village in the municipality of Tavira (Algarve, Portugal) which, during the last decades, experienced intense urbanization due to touristic activities.

Chapter 4 presents the derivation of an analytical explicit solution for 1D overland flow in impervious areas under upstream and downstream moving rainstorms. Laplace transformation is used to solve the linear kinematic wave equation resulting of applying Zarmi's theory. Results obtained with the presented analytical solution were compared with another exact solution (derived with the characteristics method), a numerical approach and laboratory experiments.

Chapter 5 presents a laboratory study on the influence of storm movement and wind-driven rainfall on the rainfall-runoff processes for impervious surfaces in urban areas with different densities of high-rise buildings.

Chapter 6 presents a laboratory study on the influence of storm movement and wind-driven rainfall on the rainfall-runoff processes for impervious surfaces in urban areas with distinct building rooftop connectivities.

¹ A comprehensive abstract is provided at the beginning of the chapters which were published in journals and conference proceedings (Chapters 3 to 8).

Chapter 7 presents a laboratory study on the influence of building height, storm movement and wind-driven rainfall on the rainfall-runoff processes in impervious surfaces.

Chapter 8 presents a laboratory study on the effects of storm movement on hillslope hydrology, where a three-segment soil flume was used to obtain different hillslope configurations. Hydrographs and sedimentographs for different storm conditions and hillslope configurations are presented.

Chapter 9 summarizes the most important conclusions of this thesis and points out some topics for future research.

1.3 OBJECTIVES

The overall goal of this thesis is to contribute for a better knowledge of the influence of storm movement and wind-driven rain on the rainfall-runoff process in urban areas. Most specific objectives, in the form of open questions, are listed below.

For urban (impervious) areas:

- How does storm movement affect overland flow?
- How does wind-driven rainfall affect overland flow?
- Which effects does building density have on overland flow? How are these effects altered by the occurrence of wind-driven moving rainstorms?
- What effects do rooftop connectivities have on overland flow? How are these effects altered by the occurrence of wind-driven moving rainstorms?
- What effects do building heights have on overland flow? How are these effects altered by the occurrence of wind-driven moving rainstorms?
- Based on the linear kinematic wave theory is it possible to establish an exact solution of 1D overland flow under moving rainstorms? If so, what are the constraints and possible applications of that solution?
- Can building density, rooftop connectivity and building height contribute to flood prevention?

For natural (pervious) surfaces:

- How does hillslope configuration affect overland flow and erosion? How are these effects altered by storm movement?
- What are the most hazardous hillslope configurations for soil loss?

1.4 PUBLICATIONS AND CONFERENCES

Most chapters of the thesis were submitted to international peer-reviewed journals (Chapters 3 to 7). One chapter was published in the proceedings of an ASCE International Conference (Chapter 8). In this last article, the author of this thesis was not involved in the execution of the laboratory experiments and in the preparation of the figures.

With the exception of some layout-specific aspects, the chapters which reverted from published articles (Chapters 3 to 8) were not altered (see Table 1.1 and first article of Table 1.2).

The research described in this thesis was also presented in several international and national (Portuguese) conferences (Tables 1.2 to 1.5).

Table 1.1 Articles in international journals (SCI-indexed) or journals type A or B (FCTUC).

Chapter	Title of the article/thesis chapter	Journal	Authors	Status
3*	Evolution of urbanization in a small urban basin: DTM construction for hydrologic computation [B]	IAHS Red Book Series	Isidoro, J.M.G.P. , Rodrigues, J.I.J., Martins, J.M.R. & de Lima, J.L.M.P.	Published (2010, Vol. 336, 109–114)
4*	Influence of wind-driven rain on the rainfall-runoff process for urban areas: Scale model of high-rise buildings [SCI/A]	Urban Water Journal (<i>ISI IF: 0.691</i>)	Isidoro, J.M.G.P. , de Lima, J.L.M.P. & Leandro, J.	In press
5*	The study of rooftop connectivity on the rainfall-runoff process by means of a rainfall simulator and a physical model [SCI/B]	Zeitschrift für Geomorphologie (<i>ISI IF: 0.477</i>)	Isidoro, J.M.G.P. , de Lima, J.L.M.P. & Leandro, J.	In press
6*	Laboratory simulation of the influence of building height and storm movement on the rainfall-runoff process in impervious areas [SCI/B]	Journal of Flood Risk Management (<i>ISI IF: 1.176</i>)	Isidoro, J.M.G.P. & de Lima, J.L.M.P.	Submitted (under 1 st review)
7*	An analytical explicit solution for 1D kinematic overland flow under moving rainstorms [SCI/B]	Journal of Hydrologic Engineering (<i>ISI IF: 0.787</i>)	Isidoro, J.M.G.P. & de Lima, J.L.M.P.	Submitted (under 2 nd review)

[SCI] – SCI-indexed; [A/B] – Journal type A or B (FCTUC); *ISI IF* – ISI-Web of Knowledge Impact Factor (2010).

* – This chapter of the thesis reverted from the published article only with minor layout adjustments.

Table 1.2 Articles in proceedings of international conferences.

Chapter	Title of the article	Conference proceedings	Authors	Status
8*	Incorporating the Effect of Moving Storms into Hillslope Hydrology: Results from a Multiple-Slope Soil Flume [O]	World Environmental and Water Resources Congress, 22–26 May 2011, Palm Springs, CA, USA	<i>de Lima, J.L.M.P., Singh, V.P., Isidoro, J.M.G.P. & de Lima, M.I.P.</i>	Published (2011, ASCE Conference Proceedings 414 (146), 1398–1407)
7	Single-Equation Analytical Solution for 1D Overland Flow due to Moving Storms [O]	5 th International Perspective on Water Resources & the Environment Conference, 4–7 January 2012, Marrakech, Morocco	Isidoro, J.M.G.P. & de Lima, J.L.M.P.	Published (2012, Proceedings of the IPWE 2012, paper No. 104, CD-ROM)
4	<i>Respostas Hidrológicas de Zonas Urbanas com Diferentes Densidades de Edifícios Altos a Chuvadas Intensas - Experiências Laboratoriais</i> [O]	<i>SILUBESA - Simpósio Luso-Brasileiro de Engenharia Sanitária e Ambiental</i> , 12–15 October 2010, Porto, Portugal	Isidoro, J.M.G.P. & de Lima, J.L.M.P.	Published (2010, Proceedings of the 14 th SILUBESA, CD-ROM)

[O] – Oral presentation (presenting author in italic).

* – This chapter of the thesis reverted from the published article only with minor layout adjustments.

Table 1.3 Abstracts and extended abstracts of international conferences.

Chapter	Title of the abstract	Conference proceedings	Authors	Status
5	Evaluating the influence of rooftop connectivity on the rainfall-runoff processes by means of (wind-driven) rainfall simulation [O]	EGU General Assembly, 22–27 April 2012, Vienna, Austria	<i>Isidoro, J.M.G.P.</i> , de Lima, J.L.M.P. & Leandro, J.	Published (2012, Geophysical Research Abstracts, Vol. 14, EGU2012–2183)
8	A study of the effect of moving storms on hillslope hydrology using laboratory experiments [O]	EGU General Assembly, 22–27 April 2012, Vienna, Austria	<i>de Lima, J.L.M.P.</i> , Isidoro, J.M.G.P. , Singh, V.P. & de Lima, M.I.P.	Published (2012, Geophysical Research Abstracts, Vol. 14, EGU2012–3656)
7	Exact solution of the linear KWE for 1D overland flow under moving rainstorms [P]	EGU General Assembly, 22–27 April 2012, Vienna, Austria	Isidoro, J.M.G.P. & de Lima, J.L.M.P.	Published (2012, Geophysical Research Abstracts, Vol. 14, EGU2012–2139)
4	The influence of wind and moving rainshowers on runoff in urban areas with high-rise buildings [P]	10 th International Precipitation Conference, 23–25 June, 2011, Coimbra, Portugal	Isidoro, J.M.G.P. & de Lima, J.L.M.P.	Published (2011, Proceedings of the IPC–10, 183, 75)
2/3	Urban floods caused by intense rainfall events in the Algarve region [P]	10 th International Precipitation Conference, 23–25 June, 2011, Coimbra, Portugal	Isidoro, J.M.G.P. , de Lima, J.M.L.P. & de Lima, M.I.P.	Published (2011, Proceedings of the IPC–10, 182, 75–76)
4/8	Evaluation in the laboratory of the influence of storm movement on the hydrologic response of small areas [P]	EGU General Assembly, 3–8 April 2011, Vienna, Austria	Isidoro, J.M.G.P. & de Lima, J.L.M.P.	Published (2011, Geophysical Research Abstracts, Vol. 13, EGU2011-680)
4/8	Wind-driven rain effects on the hydrologic response of small basins [O]	13 th Biennial Conference ERB, 5–8 September 2010, Seggau Castle, Austria	<i>de Lima, J.M.L.P.</i> , Isidoro, J.M.G.P. & de Lima, M.I.P.	Published (2010, Book of Abstracts of the ERB 2010, 71–72)

[O] – Oral presentation (presenting author in italic); [P] – Poster presentation.

Table 1.3 (cont.) Abstracts and extended abstracts of international conferences.

Chapter	Title of the abstract	Conference proceedings	Authors	Status
4	The use of a scale model to study the hydrologic response of urban areas for different building densities [P]	EGU General Assembly, 2–7 May 2010, Vienna, Austria	Isidoro, J.M.G.P. & de Lima, J.L.M.P.	Published (2010, Geophysical Research Abstracts, Vol. 12, EGU2010-800)
4	The influence of high-rise buildings on urban stormwater response – a laboratory physical model [P]	EGU General Assembly, 19–14 April 2009, Vienna, Austria	Isidoro, J.M.G.P. , Rocheta, V.L.S. & de Lima, J.L.M.P.	Published (2009, Geophysical Research Abstracts, Vol. 11, EGU2009-1639)
3	<i>Evolução da Ocupação do Solo em Área Urbana – Implicações na Drenagem de Precipitações Intensas</i> [P]	<i>VI Congresso Ibérico de Gestão e Planeamento da Água</i> , 4–7 December 2008, Vitoria-Gasteiz, Spain	Isidoro, J.M.G.P. , Rodrigues, J.I.J., Martins, J.M.R. & de Lima, J.L.M.P.	Published (2008, Poster abstracts, CD-ROM)
4	The influence of high construction density on urban stormwater drainage - a physical model [P]	8 th International Conference on Urban Drainage Modelling, 7–12 September 2009, Tokyo, Japan	Isidoro, J.M.G.P. , Rocheta, V.L.S. & de Lima, J.L.M.P.	Published (2009, Book of abstracts, UDM-P46, CD-ROM)
2	Faro's Urban Basin Flood on the 28 th November 2006 [P]	EGU General Assembly, 13–18 April 2008, Vienna, Austria	Isidoro, J.M.G.P. , Campina, V.H.J.S. & de Lima, J.L.M.P.	Published (2008, Geophysical Research Abstracts, Vol. 10, EGU2008-A-05252)
4	Physical Modelling of Urban Drainage on an Area with High Construction Density on a 1:100 Scale [P]	EGU General Assembly, 13–18 April 2008, Vienna, Austria	Isidoro, J.M.G.P. & de Lima, J.L.M.P.	Published (2008, Geophysical Research Abstracts, Vol. 10, EGU2008-A-05238)
2/3	Runoff and associated transport processes in urban areas [P]	EGU General Assembly, 15–20 April 2007, Vienna, Austria	de Lima, J.L.M.P., Duarte, C.A.F., Isidoro, J.M.G.P. & de Lima, M.I.P.	Published (2007, Geophysical Research Abstracts, Vol. 9, EGU2007-A-07034)

[O] – Oral presentation (presenting author in italic); [P] – Poster presentation.

Table 1.4 Articles in proceedings of national (Portuguese) conferences.

Chapter	Title of the article	Conference proc.	Authors	Status
2	<i>Delimitação de Áreas Inundáveis por Acção Fluvial – Aplicação ao Rio Séqua/Gilão na área urbana de Tavira</i> [O]	10 th Congresso da Água, 21–24 March 2010, Alvor, Portugal	Isidoro, J.M.G.P. , Rocheta, V.L.S. & Lança, R.M.M.	Published (2010, Proceedings of the CA 2010, Paper 19, 14pp, CD-ROM)

[O] – Oral presentation (presenting author in italic).

Table 1.5 Abstracts and extended abstracts of national (Portuguese) conferences.

Chapter	Title of the abstract	Conference proc.	Authors	Status
2	<i>Cheias urbanas na região algarvia - Influência da maré na resposta dos sistemas de drenagem</i> [P]	10 th Congresso da Água, 21–24 March 2010, Alvor, Portugal	Isidoro, J.M.G.P. , de Lima, J.L.M.P. & de Lima, M.I.P.	Published (2010, Proceedings of the CA 2010, Poster 56, CD-ROM)
2	<i>A Inundação da Bacia Urbana de Faro do dia 28 de Novembro de 2006</i> [P]	9 th Congresso da Água, 2–4 April 2008, Cascais, Portugal	Isidoro, J.M.G.P. & de Lima, J.L.M.P.	Published (2008, Proceedings of the CA 2009, Poster 48, CD-ROM)
4	<i>Modelação Física à Escala 1:100 da Drenagem de Águas Pluviais em Meio Urbano com Elevada Densidade de Construção</i> [P]	9 th Congresso da Água, 2–4 April 2008, Cascais, Portugal	Isidoro, J.M.G.P. , Campina, V.H.J.S. & de Lima, J.L.M.P.	Published (2008, Proceedings of the CA 2009, Poster 49, CD-ROM)

[P] – Poster presentation.

CHAPTER 2

...Zeus claimed his wrath at the sight of the scorched earth; he pitied her, and wished to wash with water the ashes of ruin and the fiery wounds of the land. Then Rainy Zeus covered the whole sky with clouds and flooded all the earth.

Nonnus

Rainfall is never uniform nor static. Rainfall is always changing and moving. Rainfall movement is an important part of the rainfall process.

Jin Liang

2. LITERATURE REVIEW

This chapter presents the background for the research that led to this thesis. The focus is on the links between the conditioning factors of overland flow and urban floods. Special attention is given to storm movement and wind-driven rainfall, as well as to the tools used to evaluate their influence on overland flow in urban areas.

Three main subjects are addressed in this chapter: i) Overland flow, its importance in the hydrological cycle and conditioning factors; ii) Urban floods, their relation to urbanization and GIS-based flood models used in urban flood assessment, and iii) Influence of storm movement and wind-driven rainfall on surface hydrology and other fields of civil engineering.

2.1 OVERLAND FLOW

The term “overland flow” is often misused or contradictory in the literature. Because of this, some explanation about its physical meaning, its origins and its place in surface hydrology is presented first. The origins of the water that will turn into overland flow and the factors that condition the overland flow course are also discussed, especially for urban areas under rainfall. Particular attention is given to impermeable surfaces because of their predominance in urban areas.

2.1.1 COMPONENTS OF SURFACE FLOW

Overland flow (often called *runoff*, *surface runoff*, *sheet flow*, *sheet flood*, *sheet wash*, etc.) is one of the main components of the hydrologic cycle, studied within what is usually known as “Surface Hydrology”. However, after the earliest attempts to define this component, which were based on local observation (e.g., McGee, 1897), contradictory and/or incomplete definitions of overland flow and confusing classifications of the constituents of surface hydrology became widespread in the literature. For a more detailed analysis of this topic see Hogg (1982).

Despite most of the classifications for Surface Hydrology found in the literature showing varying levels of discrepancy it is still possible to establish a classification that fits in with many of the works in this field, e.g., Guy (1964), de Lima (1989a), Singh (1997b), Knödel *et al.* (2007) and Huggett (2011). In this classification all the water that runs over the ground surface is divided into *Overland Flow*, *Rill Flow* and

Stream Flow. Rill flow is flow in narrow and shallow irregular incisions into topsoil layers (rills). These structures may evolve into streams or rivers, larger fluvial structures where stream flow takes place. Water that runs immediately below the surface is the *Subsurface Flow*. Together, overland flow and subsurface flow result in *Runoff*. According to this classification, overland flow is divided into *Sheet Flow* and *Sheet Flood*, both representing the flow of a thin, continuous film of water until it converges in a rill or another fluvial structure. Differences in sheet flow and sheet flood are only related to issues of frequency of occurrence and magnitude. Sheet flows are more common and have less magnitude.

Attention should be given to the difference between surface runoff and overland flow. The following definition of *Surface Runoff* is often-cited within the scope of quantitative geomorphology and was given by Horton (1933): *Neglecting interception by vegetation, surface runoff is that part of the rainfall that is not absorbed by the soil by infiltration, i.e., surface runoff includes channel flow (rill and stream flows).*

A possible definition of overland flow was given by van Loon (2001): *Overland flow is that part of the surface water that moves over the soil surface, while not being concentrated in channels of a given size.* This definition embraces a discussion about where overland flow ends and channel flow starts since, according to the same author, this can only be defined subjectively and approximately. However, we can give more precision to van Loon's definition of overland flow if the spatially distributed characteristics of this phenomenon are taken into account, while channel flow solely relates to points in space. Thus, in order to clarify this issue the following definition of overland flow is proposed: *Overland flow comprises all non-point surface water flows.*

Since this thesis is focused on urban environments, where land is largely covered with impervious elements (*e.g.*, roads and buildings), rainfall-generated subsurface flow is almost negligible. In order to maintain some fidelity with the literature consulted, the terms "overland flow" and "runoff" are used synonymously to express the former in accordance with the surface hydrology classification presented above.

2.1.2 OVERLAND FLOW ON URBAN AREAS – CONDITIONING FACTORS

Physically, overland flow is the transfer of a mass of water from one area to another that satisfies the definition expressed in Chapter 2.1.1. Possible origins of the water

are rainfall, ice and snowmelt, irrigation, exfiltration and dew (this last originates what hydrologists refer as *occult rainfall*). Since the water travels over the ground surface, overland flow is influenced both by the factors that determine the origins of water and the factors that constrain its course, namely, the topography, geology, soil type, land use and flow control measures (*e.g.*, flood control and mitigation of water erosion).

Because this thesis deals with intense rainfall events over urban areas, only rainfall water was studied and most of the work regards impervious areas, and so, storm properties (*e.g.*, storm movement), land use (*e.g.*, urbanized areas) and topography (*e.g.*, slope) becomes, in this scope, the most important conditioning factors of overland flow. Despite this, some of the work presented may be extrapolated for other origins of water (*e.g.*, snowmelt) or drainage basin features (*e.g.*, natural surfaces with low permeability).

2.1.2.1 Rainfall water

The primary condition for rainfall initiation is the saturation of air with water vapour originated by evaporation from wetted surfaces (*e.g.*, sea) or large scale transpiration (*e.g.*, forests). Large masses of saturated air can be carried by wind from other locations, and so, rainfall does not occur necessarily in the same locations where the air has been saturated with water vapour. The second condition is the cooling of the saturated air, generally caused by the lifting of the saturated air masses. The following lifting mechanisms, which are able to form clouds, can be differentiated (*e.g.*, Ackerman and Knox, 2011): *Orographic*, when the air is lifted as it moves over a mountain range; *Convictional*, when the air near the earth surface is heated by solar energy becoming less dense than the air around it and rises; *Convergent*, when the air near the earth surface flowing together from different directions collides and originates an upward movement, and finally; *Frontal*, when the warm air (less dense) is forced to rise over the cooler air (more dense). These designations of the lifting mechanisms are usually applied to differentiate and name the rainstorm types (*e.g.*, convictional rainstorm). The third condition is the condensation of the water vapour in the troposphere. Since a non-gaseous surface must be involved so water vapour can transit to the liquid state (Wallace and Hobbs, 2006), the condensation of water is triggered by the existence of small solid or liquid particles (around 0.2 μm) entitled cloud condensation nuclei (CCNs), usually, salt crystals from the oceans, combustions products, dust and ash. The fourth and last condition for rainfall to initiate is the

raindrops growth. This growth occurs due to water droplets coalescence, *i.e.*, as the cloud droplets (around 10 μm) collide against each other their size increases until they start to fall through the cloud. In their way downwards, by colliding with the smaller droplets, larger droplets capture more water. This process continues until the resulting droplet is heavy enough to fall out of the cloud and reach the ground as rain (or snow) before it can evaporate. A complete description on rainstorms formation and rainfall initiation can be found in, *e.g.*, Wallace and Hobbs (2006), Shuttleworth (2012).

A rainstorm can be characterized by a number of factors, which are dependent of the rainstorm type, such as its location, magnitude, extent, direction, timing, velocity, geographic and spatial distribution, structure of the rain cells, peak intensities, *etc.* In this study more attention was given to features related to the rainstorm velocity and spatial distribution. Slow-moving rainstorms with regular intensities can be equally – or even more – destructive than high-intensity fast-moving rainstorms; Figure 2.1 shows an example: using RADAR (RADio Detection And Ranging) imagery to track the rain cells with intensity above 20 mm/h that passed over the Algarve region (South of Portugal) from 05:00am until 03:00pm of the 28th November 2006 (left), it was possible to calculate these rain cells mean speeds, which ranged from 38.2 to 57.8 km/h, excluding rain cell 9 which had a mean velocity of 15.4 km/h (centre) and stayed for approximately 120 min over the urban area of Faro (approximately 40000 hab.) causing some havoc (right).

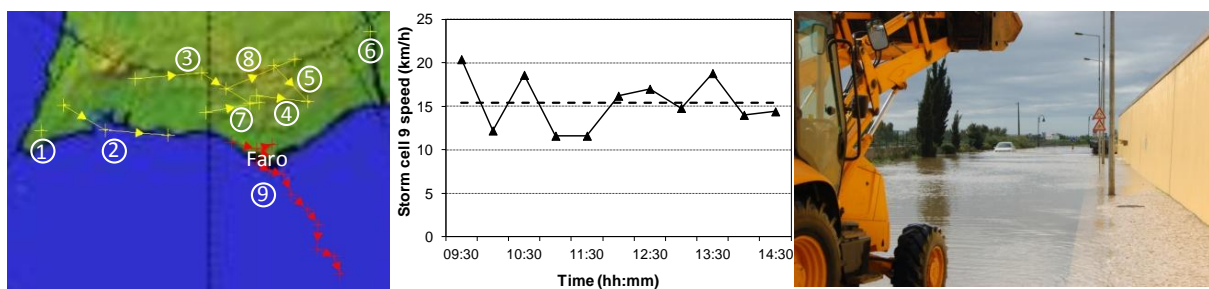


Figure 2.1 Rain cells with intensity above 20 mm/h over the Portuguese Algarve region, from 05:00am until 03:00pm of the 28th November 2006 (left). Rain cell 9 speed during this period; dashed line is the rain cell mean speed (centre). Flooding in downtown Faro as a consequence of rain cell 9 passage (right).

In urban areas, other components of the hydrologic cycle related to losses of water as interception, infiltration, evaporation and surface storage also influence the rainfall-runoff process. However, in the case of intense rainfall events, this influence may be relatively small or even negligible. Those losses, also called as *Hydrological*

Abstractions, are usually incorporated in empirical methods to estimate runoff (*e.g.*, Soil Conservation Service runoff curve number method).

Intercepted water regards to the fraction of water that wets and adheres to surfaces above ground and that, subsequently, will evaporate and thus return to the atmosphere without becoming runoff or groundwater. Losses due to interception are more important in forested drainage basins than in urban drainage basins, and the highly impervious urban developments, with low vegetation or tree cover, have little interception (*e.g.*, Marsalek *et al.*, 2008).

Infiltration is the vertical movement of water into the soil, governed by gravity and capillarity forces. This component of the hydrologic cycle becomes proportionally less important as the urbanized areas become more impermeable; however, a proper quantification of infiltration is essential in urban hydrology design (*e.g.*, pervious pavements, detention basins and low-impact developments (LIDs) for flood mitigation purposes). Infiltration is highly dependent of soil properties, which are difficult and expensive to characterize due to their spatial and/or temporal variability (*e.g.*, granulometric distribution and moisture content). To overcome this issue, in urban hydrologic studies it is usual to model the behaviour of infiltration by using sets of discrete entities forming a topological space that, under certain assumptions and limitations, approximates the natural distributed system behaviour (lumped models). Horton and Green-Ampt are examples of lumped models to assess infiltration, having widespread use in hydrology.

Evaporation is the process where water transforms into water vapour and is lost to the atmosphere. Since air temperature plays a major role in evaporation and urban areas are usually characterized by having higher values of air temperature (compared to non-urbanized areas), these areas may have a 5 to 20% higher rate of evaporation (Geiger *et al.*, 1987). An example of the influence of urban areas in local climate is the urban “heat island effect” (*e.g.*, Oke, 1973; Parker, 2010), responsible for a local increase of the air temperature by 4 to 6 °C when compared to the surrounding areas. For a more in-depth review on this phenomenon – that can produce significant localized climate changes – and on the methodologies used to quantify its effects see *e.g.*, Stewart (2011). Notwithstanding its limited interest for hydrologic studies regarding high intensity rainfall events in urbanized areas, it shall be referred that the processes of evaporation and transpiration (the loss of water vapour from the plants) are usually combined into “Evapotranspiration”. If evapotranspiration is not limited by the water input, the total amount of water that would be lost that way is called by

Potential Evapotranspiration. Most common methods to estimate these values are the Penman equation (for evaporation) and the Thornthwaite equation (for evapotranspiration). An in-depth review on the existing methods to estimate evaporation and evapotranspiration can be found in *e.g.*, Chang (2009).

Surface storage regards the water which accumulates in depressions on the surface of a drainage basin and is then lost by evaporation or infiltration, thus not becoming runoff. The surface coverage (*e.g.*, asphalt) and slope, soil type and antecedent moisture conditions (*e.g.*, due to previous rainfall) are within the most important factors affecting surface storage (van Lanen *et al.*, 2004). Despite the existence of some formulae to estimate surface storage losses (*e.g.*, Linsley *et al.*, 1982) it is usual in urban hydrologic modelling to employ empirical values, ranging from of 1.6 to 6.4 mm (ASCE, 1996). By modifying surface roughness, *e.g.*, due to urbanization, depression storage may play a significant role in the surface hydrologic response (Peng *et al.*, 2002).

Figure 2.2 schematizes the urban water cycle processes referred above. Rainfall water evaporates both due to interception and surface storage, before infiltrating or becoming runoff. The infiltrated fraction of water percolates both ways in the unsaturated and the saturated zone. Water in these zones may be lost by evaporation, if it reaches the drainage basin surface by capillarity, or by transpiration of the plants, which retrieve the water from the soil.

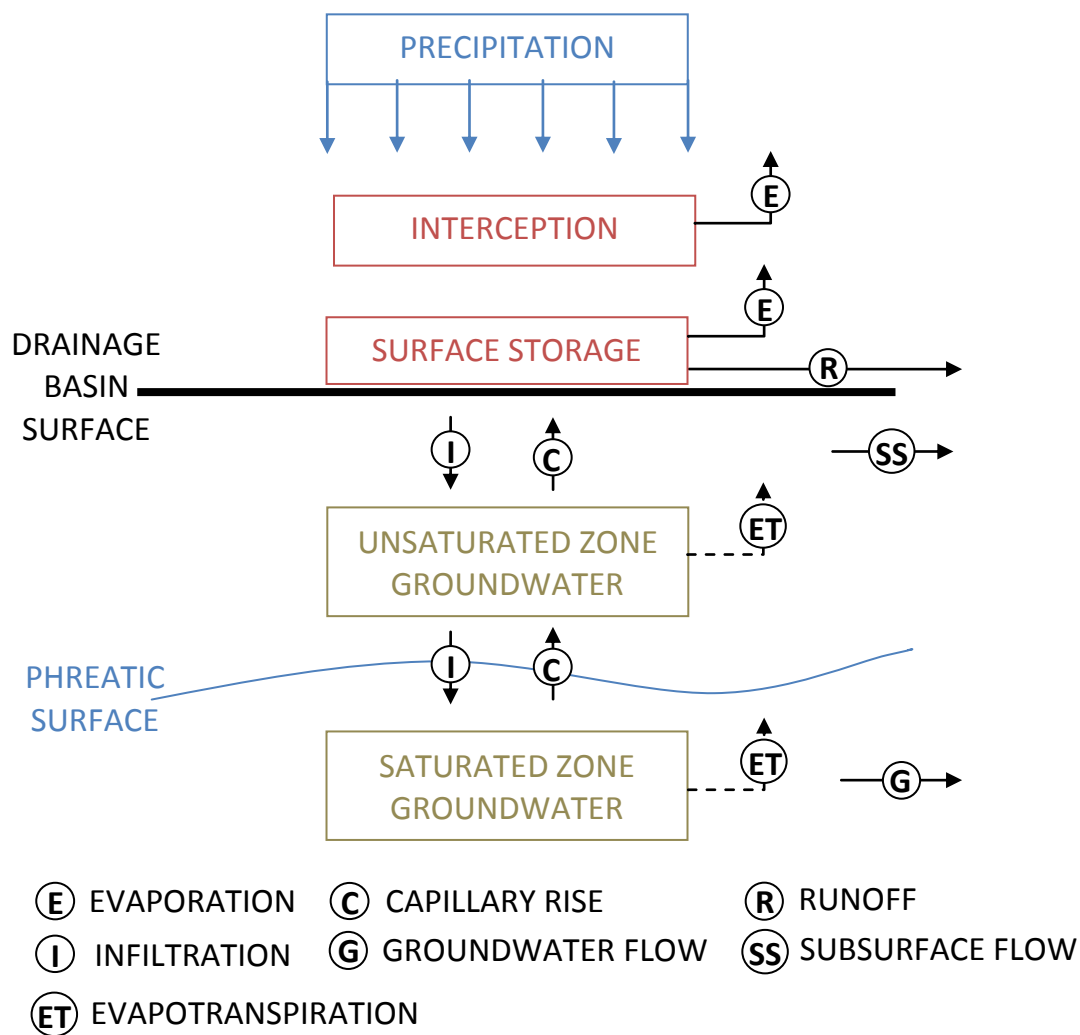


Figure 2.2 Rainfall-runoff processes in the urban water cycle. Losses due to interception, surface storage, infiltration and evapotranspiration are identified. Dashed lines stand for indirect flow of water, which includes the fraction retrieved by plants and then transpired and the fraction that reaches the drainage basin surface and evaporates.

2.1.2.2 Storm movement

In the case of moving storms, four characteristics of the rainstorms influence the overland flow hydrographs (Singh, 2002b; Liang, 2010). These features are: (i) the storm direction, which can be upstream, downstream, transverse or forming any angle with the main slope of a drainage basin; (ii) the storm areal coverage, that may be partial or full; (iii) the storm speed, which normally can range from 2 to 60 km/h (Singh, 1997a), and (iv) the duration of the storm activity, which is highly variable as it depends on the storm velocity and size.

Storm direction, measured by the angle to the stream or to the main slope in the drainage basin, has a strong influence on peak discharge and on the overland flow

hydrograph shape (de Lima and Singh, 2002). Most studies found in the literature focused only in the downstream and the upstream direction, where it is shown that comparing to downstream moving storms, upstream moving storms hydrographs are usually characterised by an earlier rise, lower peak discharge, milder steepness of the rising limb and longer base time. A laboratory study on angular storm movement, for a pervious drainage basin (soil flume), showed that the storm movement along directions different from the steepest slope led to hydrologic responses ranging between the responses of downstream and upstream moving storms (de Lima *et al.*, 2009).

Areal coverage regards to the fraction of a drainage basin on which rainfall occurs during a rainstorm event. Partial areal coverage of a drainage basin by a rainstorm means that the storm is not large enough to cover the entire basin or, in the case of a moving storm, that the storm duration is limited in time and so, it never covers the basin completely. Singh (2002b) found that in a planar drainage basin with the same areal coverage and for the same storm duration, the peak discharge is greater for downstream moving storms than for upstream moving storms and the time to peak takes place much later for upstream moving storms than for downstream moving storms.

Storm speed is a very important feature of a rainstorm. It influences, among other factors, the rainfall duration over a drainage basin and the total amount of rainfall volume (see, *e.g.*, Figure 2.1). Accordingly to Singh (1997a) rainstorms most frequently move at a speed ranging from 7 to 35 km/h, or about 2 to 10 times the average stream flow speed. Singh (1998) and de Lima and Singh (2003) found that, both for upstream and downstream moving storms, the highest relative peak discharge is attained when the storm velocity equals the mean overland flow velocity.

The duration of a rainstorm may be analysed from two different points of view: the duration of the rainstorm by itself, *i.e.*, the time it takes for a rainstorm to form, raise, travel, decay and disintegrate, and the duration in which a rainstorm stays over a drainage basin, *i.e.*, the lapse of time it takes from the instant a rainstorm enters a drainage basin until it leaves it. In the context of this thesis this last point of view is the most important, because urban areas are relatively small when compared with the spatial extension travelled by a rainstorm throughout its lifetime. The duration of a rainstorm over a drainage basin is a consequence of the rainstorm size and speed. This factor is important for attaining the overland flow hydrograph. An overland flow hydrograph develops into an equilibrium hydrograph if its peak equals the peak

rainfall excess intensity times the drainage basin area. If this last value is not attained, then the hydrograph remains in partial equilibrium (Singh, 2002b). Consequently, moving storms may originate hydrographs with a steady plateau, despite the equilibrium is, or is not, attained.

2.1.2.3 Wind-driven rainfall

The combined action of wind and rainfall produce changes in the spatial and temporal distribution of rainfall. Despite this fact is known for a long time (*e.g.*, Fourcade, 1942), nowadays it is still usual to consider windless conditions on rainfall-runoff process studies and engineering design. Wind-driven raindrops fall through a wind field under gravitational and drag forces, thus gaining horizontal speed. This causes raindrops to be redistributed in specific patterns (Blocken *et al.*, 2006) and to strike the ground surface at an angle deviated from the vertical (*e.g.*, de Lima, 1990; Erpul *et al.*, 2003).

First measurements of wind-driven rainfall took place almost 200 years ago (Middleton, 1969) [cited in Blocken (2004)] and have evolved since then. In the last decades this subject has been studied by many authors, namely in the fields of earth science and meteorology, *e.g.*, Sharon (1980) measured angles resultant of wind-driven rainfall to be within a range of 40° to 60° (from the vertical) for wind speeds of 10 m/s. Rainfall measurements reported in the literature point out that wind-driven rainfall is highly variable in time and space, and that should be addressed in hydrologic studies, namely in hillslope hydrology, runoff and erosion studies, and in the design of rainfall monitoring networks (*e.g.*, Blocken *et al.*, 2006). Besides these, wind-driven rainfall is also important for research in fields such as agriculture and meteorology. de Lima (*e.g.*, 1989b; 1989c; 1989d) found that the wind intensity and direction have influence in the effective rainfall patterns and in the mechanics of the overland flow process on hillslopes. The shape, size, angle and terminal velocity of raindrops, splash shape and shear stress in the water-air boundary were found to be particularly affected by the existence of wind. Wind-driven rainfall may also be responsible for errors in rainfall measurements when using individual above-ground gauges (*e.g.*, de Lima, 1990; Blocken and Carmeliet, 2004).

The angle between wind-driven raindrops and a vertical axis can be measured by means of photography or video. This angle can also be estimated by a trigonometric approach if the average horizontal wind speed near the ground surface and the

average terminal vertical speed of raindrops are known. The latter can be attained using formulae (e.g., Beard, 1976; Wang and Pruppacher, 1977) or by means of using specific equipments like disdrometers (see Figure 2.3) or optical rain spectrometers.



Figure 2.3 Example of disdrometer (Thies Clima) available in the Laboratory of Hydraulics, Water Resources and Environment of the Civil Engineering Department of the Faculty of Sciences and Technology, University of Coimbra.

Because the wind-affected raindrops gain an additional component of horizontal kinetic energy, their impact velocity is often greater than the terminal vertical velocity for raindrops in windless conditions (vertical rainfall). Figure 2.4 schematizes the referred components of the terminal velocity of a raindrop.

Inclined rainfall has a considerable importance in hillslope hydrology since the horizontal component of the terminal velocity of a raindrop may add, or reduce, the overland flow momentum, respectively if the wind is blowing in the downstream (downslope) direction or in the upstream (upslope) direction. de Lima (1989b) showed that in impervious surfaces upslope blowing winds caused a delay in the initiation of overland flow and an increase in the depth of water along the surface.

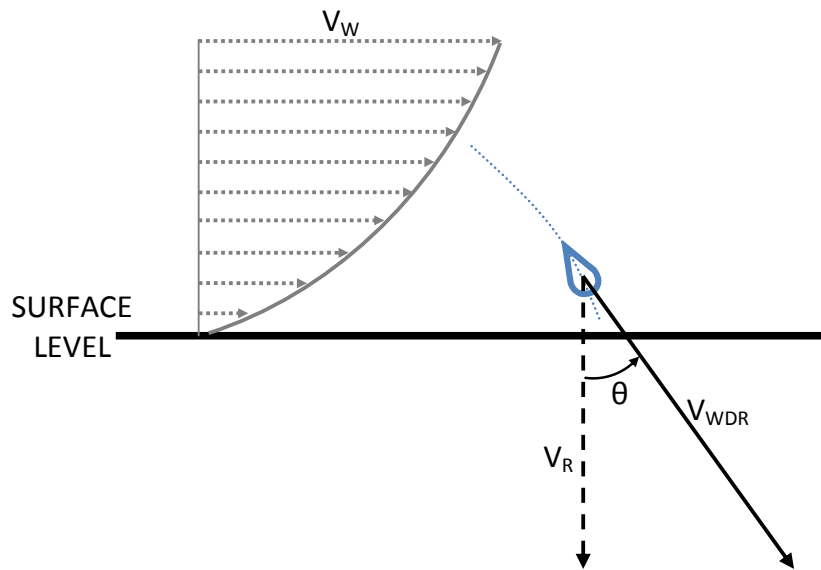


Figure 2.4 Simplified scheme of the influence of wind on the terminal velocity of a raindrop. V_R is the raindrop terminal velocity for windless conditions (vertical rainfall), V_W is the horizontal wind velocity near the ground surface, V_{WDR} is the wind-driven affected raindrop terminal velocity and θ is the angle of incidence of the rainfall.

While in windless conditions rainfall only wets horizontal and sloped surfaces, wind-driven rainfall also wets vertical surfaces (*e.g.*, building facades), thus having particular importance on urban areas. In a set of studies on the influence of wind-driven rainfall on the rainfall-runoff process in highly urbanised areas (Isidoro *et al.*, 2012a; Isidoro *et al.*, 2012b; Isidoro and de Lima, 2012b), wind-driven rainfall showed to reduce the differences on the overland flow hydrographs (*e.g.*, peak discharge and base time) caused by the increase in building density and building height, and by the different rooftop connectivities. These differences were partly due to the increase in the collision of raindrops with the buildings, caused by the horizontal speed component of wind-driven rainfall.

Wind-driven rainfall also has an important effect over natural surfaces. Wind causes significant changes in the raindrops trajectory and frequency, which may lead to considerable effects on the soil detachment process (Erpul *et al.*, 2003).

2.1.2.4 Land use and topography

Regarding the factors related to the drainage basins, two features having more influence on overland flow in urban areas stand out: the natural terrain sealing due to the construction of roads, buildings, driveways, *etc.* and the drainage basins topography, namely the surface slope, which condition the flow speed and depth.

Veldkamp and Fresco (1996) defines land use as the human activities that are directly related to land, uses its resources or interferes with the ecological processes. A good example of the influence of land use in overland flow is given by USEPA (2003): while in the natural terrain 25% of rainfall water infiltrates into the aquifers and only 10% becomes runoff, in highly urbanized areas more than 50% of all rainfall water becomes runoff and deep infiltration is only a fraction of what it was back in the natural terrain conditions.

Modifications of the natural, economical or/and political conditions promote biophysical or/and human demands, ultimately leading to land use changes (O’Callaghan, 1996). Even for non-hydrologists it is easy to understand that *e.g.*, the deforestation and posterior urbanization of a hypothetical area would promote major changes in the water cycle, namely by the increase in runoff. These kind of severe changes in land use have been thoroughly analysed by several authors for the last decades; however, in urbanized areas, more subtle changes in runoff may be noticed due to small scale alterations, *e.g.*, different building densities – easily detectable in downtown and suburban areas – have a marked influence on overland flow (Isidoro *et al.*, 2012a; 2012c).

The morphology of urban areas, *i.e.*, the construction land plots (real estate structures), the street network and their evolution over time, is a very important factor to the rainfall-runoff process in urban areas (Rodriguez *et al.*, 2008), affecting flow depths and velocities. Therefore, urban planning has a major relevance on urban rainwater drainage systems and flood mitigation. Particular care should be taken when defining the spatial distribution of urban physical structures (*e.g.*, building patterns) that may strongly interfere with urban runoff and flood events (*e.g.*, James and Korom, 2001).

From a hydrological point of view, the slope of a drainage basin is one of its most important physiographic factors. Using a simple empirical turbulent flow equation (Gauckler-Manning-Strickler equation) the uniform depth of water, in a fictional 1.0 m wide rectangular open channel with a surface roughness K_s (Strickler coefficient) of $90 \text{ m}^{1/3} \cdot \text{s}^{-1}$, was established for a flow of 100 l/s and different surface slopes (Figure 2.5). As the slope decreases to near-zero values, flow depth increases exponentially, and so, this really simple demonstration helps to illustrate the importance of the drainage basin slope in overland flow.

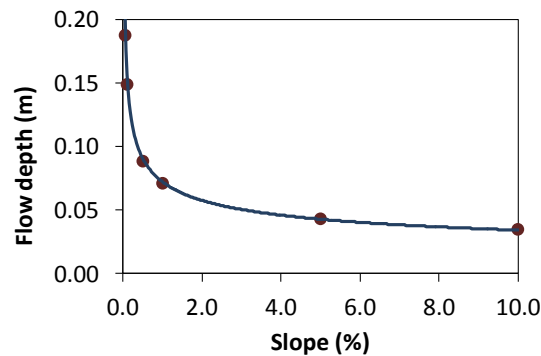


Figure 2.5 Uniform depth of water in a 1.0 m wide rectangular open channel with a surface roughness K_s (Strickler coefficient) of $90 \text{ m}^{1/3} \cdot \text{s}^{-1}$, for a flow of 100 l/s and different surface slopes.

Drainage basins with an almost flat topography are thus prone to accumulate water, which is a synonym of low discharge. This yields a severe problem for flat or gently sloped urban areas under intense rainfall scenarios. Moreover, in these urban areas drainage systems also have low-sloped longitudinal profiles, and so, neither the overland flow nor the drainage systems promote extensive discharge of stormwater, and so, urban areas with these topographical characteristics may suffer from more frequent and intense flooding events.

2.2 URBAN FLOODS

Urban floods may have multiple origins and magnitudes. Fluvial flooding due to intense precipitation on large basins may cause destruction over hundreds of square kilometres. Coastal urban areas may be severely affected by sea storms. Coastal areas may also be prone to tsunamis – extreme waves caused by seismic activity or major undersea landslides – which are capable of moving inward land for kilometres with massive destruction, or by the storm surge effect – an offshore rise of the sea level due to a low pressure weather system – typical of tropical areas. Snowmelt is another important origin for urban floods. Areas located at the base of mountain ranges where snow and ice accumulate during wintertime may suffer from flash floods during springtime snowmelt; in this period of time the flow rate in rivers may increase rapidly, causing fluvial flooding. Low-lying areas underlined by aquifers may suffer from a rise of the phreatic surface after long periods of sustained high intensity rainfall. Urban floods may also have anthropogenic origins, like the rupture of water supply systems (*e.g.*, pipes) or dam/dyke failure, the latter with the potential of catastrophic consequences.

This chapter initially presents a review of the literature on a particular type of urban flood: flash floods caused by intense rainfall events. Afterwards a discussion is made on the role of urbanization – the conversion of other types of land use to uses associated with the growth of population and economy (Weng, 2001) – on these kind of events, *i.e.*, how does the physical growth of urban areas interferes in the urban water cycle. Finally, some issues related to GIS-based models used in this field of work are presented.

2.2.1 FLASH FLOODS IN URBAN AREAS

What is a “flash flood”? And how does it differentiate from a “regular flood”? Accordingly to the literature the answer to these questions may be given by the following definition (ACTIF, 2004): *A flash flood can be defined as a flood that threatens damage at a critical location in the catchment, where the time for the development of the flood from the upstream catchment is less than the time needed to activate warning, flood defence or mitigation measures downstream of the critical location.*

This last definition, among several others available in the literature, was chosen not for what it says, but because of what it does not say. It does not say how much is damaged, it does not establish the time for the development of the flood and it is a bit obscure about what is “a critical location in the catchment”. However, this definition, by covering the totality of circumstances, gives a very good frame for the discussion of these issues. In this Chapter, and despite flash floods may be triggered without rainfall (*e.g.*, after dam failure) and may occur almost anywhere (*e.g.*, in a forested area), attention is focused on flash floods that are triggered by intense rainfall events and occur in urban areas.

Flash floods exhibit a quick overland flow peak within a very short time (*e.g.*, Bailly-Comte *et al.*, 2008; Toukourou *et al.*, 2011). The United States National Weather Service (USNWS) specifies that flash floods occur from few minutes to six hours of the contributory event and that are usually characterized by raging torrents with the capability of sweeping everything in front of them (USNWS, 2002). Due to the very short lapse of time, it is almost impossible to take actions between the rainfall events and the consequent flooding, therefore, the best way to anticipate these occurrences is via an effective rainfall forecast. Technology allowed the development of high resolution temporal and spatial rainfall measurement, either at a point (rain gauges),

spatially distributed (ground-based RADARs and satellites orbiting the Earth) or along a straight line (microwave links). However, rainstorms are highly dynamic systems, and so, it is necessary to extrapolate in time, *i.e.*, to forecast, how will the rainstorm cells evolve. Despite this thesis does not focus on flood forecasting, some references are given for a more in-depth analysis on this subject (*e.g.*, Maskey, 2004; Sivapalan, 2006; Sene, 2008; Ackerman and Knox, 2011).

In the developed countries, urban areas are usually served by rainwater drainage systems. In these systems, large numbers of spatially distributed sewer sinks, gutters and downspouts drain runoff water from the streets, pathways and rooftops into a network of pipes placed underground. The collected rainwater flows in the pipes generally only due to gravity and is finally discharged to a natural water body (*e.g.*, river). Since these systems are usually designed for a rainfall intensity/duration associated with a given return period, theoretically, rainfall events that exceed the design intensity/duration will produce runoff on streets and pathways because the systems will not be able to cope with such discharges; however, this issue is not so straightforward, since runoff will also depend on the wet antecedent conditions of the drainage basin. Overland flow from surrounding natural catchments may also flow into urban areas and easily surpass the sewer system hydraulic capacity. This hydraulic capacity is often reduced by natural or anthropogenic factors (*e.g.*, obstruction of sewer sinks by leafs or trash) that may severely compromise the systems efficiency (Figure 2.6).



Figure 2.6 Sewer sink clogged due to accumulation of leaves and pine tree needles carried by storm runoff (Quinta do Lago, Loulé, Portugal). The sewer sink trash rack was found completely covered after a flooding event which occurred on the 29th September 2008 (left). A worker removes the accumulated leaves and pine tree needles, uncovering the sewer sink trash rack (right).

Lack of maintenance of urban stormwater drainage systems is not the only reason for serious flash flood episodes. Ancient towns or fast-growing cities often suffer from poor land-use planning (e.g., Figure 2.7; left). Downslope-located urban areas may be severely unprotected from extreme rainfall events (e.g., Figure 2.7; right). Rainstorm types (see Chapter 2.1.2.1) may also have regional predominance, e.g., at the tropics and mid-latitudes intense rainfall events are primarily associated with the existence of convective rain cells, rainstorm structures that are capable of originating flash floods in small drainage basins like the ones typical of the Mediterranean environment (Rebora and Ferraris, 2006).



Figure 2.7 Urban flash floods due to short duration extreme intensity rainfall. On the 17th February 1972, 78.5 mm of rain fell in one hour (MWC, 2007) over the Melbourne (Australia) business centre (left; Neville Bowler/Fairfax Syndication). On the 20th February 2010, from 9:00am to 11:00am, 223 mm of rainfall was measured at the *Pico do Arieiro* (01/02M) meteorological station (de Lima *et al.*, 2010), causing 42 deaths, 100 injured and millions of Euros in damages (Luna *et al.*, 2011) that are currently still being repaired (right; Octávio Passos/AP).

Accordingly to the Directive 2007/60/EC of the European Parliament and of the Council on the assessment and management of flood risks: *Floods have the potential to cause fatalities, displacement of people and damage to the environment, to severely compromise economic development and to undermine the economic activities of the Community.* However, major flood disasters may also provide opportunities to accelerate the rate at which flood management policies are implemented, and so, key factors in this processes appear to be a combination of environmental, behavioural and contextual drivers (Johnson *et al.*, 2005). In an increasingly interconnected world it also seems reasonable to surmise that, in the next decades, participatory governance may help to shape the flood risk management policies.

2.2.2 CONSEQUENCES OF URBANIZATION

Seventy years take us apart from the following definition of Urbanization by Tisdale (1942): *Urbanization is a process of population concentration. It proceeds in two ways: the multiplication of points of concentration and the increase in size of individual concentrations. It may occasionally or in some areas stop or actually recede, but the tendency is inherent in society for it to proceed until it is inhibited by adverse conditions.*

Recent data available in reports from official entities and in research articles (e.g., Satterthwaite *et al.*, 2010; Wu, 2010; Madlener and Sunak, 2011; Kabisch and Haase, 2011) validate Tisdale's definition on urbanization and proves its actuality. The following two sentences (UN, 2011) give a clear outlook on this issue:

For the first time in history, more people live now in urban than in rural areas. In 2010, urban areas are home to 3.5 billion people, or 50.5 per cent of the world's population. In the next four decades, all of the world's population growth is expected to take place in urban areas, which will also draw in some of the rural population through rural to urban migration.

The current levels of urbanization are unprecedented and so is the number and size of the world's largest cities. In 1950, there were only two megacities, that is, cities with at least 10 million inhabitants, and five cities with populations ranging from 5 million to 10 million inhabitants. Today, there are 21 megacities, including 17 in the developing world.

Urbanization thus implies anthropogenic changes within natural systems. Because nowadays many cities show fast and sometimes uncontrolled growth, these changes are probably more important than ever. According to Buhl *et al.* (2006) this happens at many scales and is clearly visible e.g., in the developing countries, where simultaneously to the highly increasing expansion of main urban centres, slums, shantytowns and squatter settlements are also expanding and currently account as one half of all the global urbanization processes. It is thus predictable that, at least for some countries, urbanized areas will continue expanding (Nuisl *et al.*, 2009) for a long period which, accordingly to some authors, it is still not foreseeable (e.g., Haase, 2009).

One of the most important changes that urbanization causes in a natural system is the profound alteration of the “natural hydrological cycle” into what is sometimes called as the “urban water cycle”. Urbanization generally imply compaction of soils and increased impervious coverage of land, *e.g.*, by construction of roads and buildings (*e.g.*, Arnold Jr. and Gibbons, 2006). This causes infiltration and surface roughness to decrease when compared to natural terrain. For these reasons, and because many of the urban drainage systems currently in use were not designed for such land occupation (*e.g.*, Isidoro *et al.*, 2010) or to extreme storm conditions (*e.g.*, Schmitt *et al.*, 2004) urban growth enhances the magnitude and recurrence of floods (*e.g.*, Yuan and Bauer, 2007; Grimm *et al.*, 2008), leading to stormwater overland flow hydrographs with higher discharged volumes and peaks, earlier start and sharper rise (Figure 2.8). In small drainage basins, where the impervious covered area tends to be relevant, the impact of urbanization on the hydrological processes may be particularly significant in increasing flash floods occurrence (Nunes *et al.*, 2009). Regarding these issues, Schilling (1991) anticipated that for all the industrialized countries the next decades will be characterized by exceptionally high expenditures on stormwater drainage systems renovation.

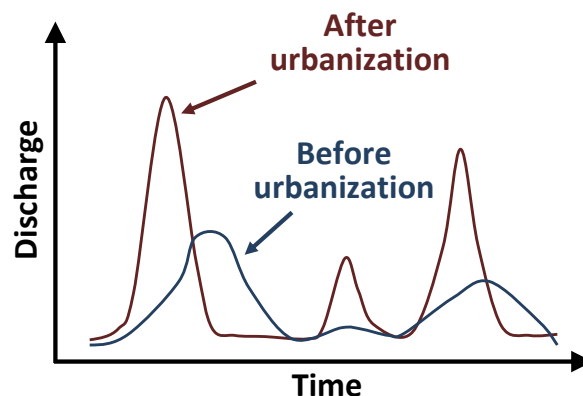


Figure 2.8 Schematic hydrographs helps to illustrate the influence of urbanization in overland flow discharge.

Consequences of urbanization on the water cycle are not restricted to overland flow. Paving may change the process of groundwater recharge, restricting it only to the unpaved areas (*e.g.*, parks). If infiltration is severely decreased phreatic surface levels may decline (*e.g.*, Jat *et al.*, 2009; Thurston *et al.*, 2010), giving origin to other problems as *e.g.*, well failures or salt water intrusion. The decline of groundwater recharge due to reduced infiltration in urban areas is however controversial, since leakage from water supply pipes, wastewater disposal or excess irrigation of amenity areas may compensate, or even surpass, that effect (*e.g.*, Foster, 2001; Howard, 2002).

Whereas urbanization has a marked effect on the water cycle, its impacts can be minimized if proper choices are made from an early stage in the development process. The minimization of connected impervious cover (*e.g.*, downspout disconnection) or an approach to the natural hydrological cycle by infiltrating and abstracting runoff at the source (*e.g.*, pervious pavements and green roofs) are examples of more suitable management choices which can reduce flooding risk (*e.g.*, Walsh *et al.*, 2005). Furthermore, it should be kept in mind that, ignoring the effects of urbanization on the water cycle and the consequential increase of flash flood events of higher frequency and magnitude, it is also an externalization of the costs of proper urban management, because flash floods involves the imposition of foreign costs upon others and thus disregards the legal maxim of *sic utere tuo ut alienum non laedas*¹ (Kochan, 2006).

2.2.3 GIS-BASED FLOOD MODELS

Geographical Information Systems (GIS) are application-oriented database management systems that, by merging cartography, statistical analysis and database tools, possess a powerful capability to analyze spatial information and process large quantities of data. These systems are capable of digitally representing real world objects by using vector and raster data. By integrating GIS with hydrologic models it is possible *e.g.*, to identify areas of potential flood risk, assess groundwater contamination susceptibility or define possible scenarios for water resources management purposes. This Chapter pretends to give a brief illustration on how GIS became nowadays a natural support for flood models and to list the most important advantages of GIS-based models in flood management and flood risk assessment.

Early uses of GIS in flood studies have some decades (*e.g.*, Davis, 1978) but its generalization took some time to take place. Berry and Sailor (1987) referred that, notwithstanding the value of spatial relationships to hydrology, there was a lack of a more extensive integration of GIS in applied hydrologic models such as storm water modelling, where the spatial characteristics of entire drainage basins continued to be many times aggregated into one or more too simplistic parameters. Correia *et al.* (1998) claimed on how much there was to gain in incorporating hydraulic flood modelling capabilities in GIS; and how much there was to gain with it in terms of engineering practice. Al-Sabhan *et al.* (2003) evidenced that the available hydrologic models, despite innovative and robust, were poorly suited to real time applications

¹ Use what is yours in a way that you don't harm what is another's.

and often not well integrated with GIS spatial datasets. In the last years, however, GIS-based flood models have evolved significantly and integration of hydrologic models with GIS is nowadays seen as perfectly normal, as referred by Alaghmand *et al.* (2010).

GIS have a powerful capacity to deal with large quantities of spatially distributed data. Singh and Fiorentino (1996) link this potentiality of GIS models with the needs of hydraulic modelling: *The GIS technology has the ability to capture, store, manipulate, analyze, and visualize the diverse sets of geo-referenced data. On the other hand, hydraulic is inherently spatial and hydraulic models have large spatially distributed data requirements.* Prasad (1997) focus on the noteworthy flexibility GIS-based flood models enjoy, pointing out the following reasons: (i) After a GIS database is created the required time for hydrologic simulation is no longer a constraining factor and the modeller gets additional time to investigate more scenarios that may lead to an optimum solution; (ii) Updating or modifying the GIS database to study the impact of changes in a drainage basin (*e.g.*, urbanization) is easy, and (iii) Production of outputs can be done in diverse formats as *e.g.*, texts, tables, graphics or thematic maps. Prasad (1997) also refers that the improved accuracy of results obtained by GIS-based hydrologic simulation comes from the capability that these models have to integrate hydrologic regional parameters, and to allow for a more judicial extrapolation of empirical synthetic frequency curves and computation of frequency curves for modified drainage basin conditions. The potential of GIS visualization tools to estimate probable flood damage is referred by Clark (1998) as one of the main advantages of using GIS-based models for flood management.

Correia *et al.* (1998) refer the advantages that GIS has on the integration and manipulation of information not intended only for technical purposes and how that information is easily reached by the public. This easier communication with the public is also focused by Correia *et al.* (1999) who alert for some fragilities of GIS-based flood models, *e.g.*, that those models may be misleading if the hydrologic and hydraulic models are not adequate, that very powerful GIS have better capabilities but are less flexible and less portable, and that simple GIS have increased flexibility but are not so powerful. Nevertheless, the advantages of the powerful and the simpler systems can be used if the systems conversion and interfacing capabilities are properly exploited.

The last years have shown a great evolution on GIS-based flood models. Prediction and presentation of near-real-time flood extension for decision makers and the public

(Mioc *et al.*, 2007) and simulation of contrasting scenarios – including both economic costs and benefits – to be considered for implementation in the context of long term sustainability by key actors (Jolma *et al.*, 2008) are examples of the potential that GIS-based flood models have to integrate diverse types of information, display the interlinked simulation results and assist on decision-making. From these examples it is possible to surmise that GIS-based flood models will continue to show major developments on the years ahead.

2.3 INFLUENCE OF STORM MOVEMENT AND WIND-DRIVEN RAINFALL

This chapter initially presents some aspects related to the influence of storm movement and wind-driven rainfall on overland flow in urban environments. The different tools used in hydrology to study this influence on impervious areas are thoroughly reviewed, namely, in field studies, laboratory experiments, numerical methods and analytical solutions. Two brief reviews on the importance of storm movement and wind-driven rainfall in overland flow over natural surfaces, and in other fields of civil engineering (*e.g.*, construction) are also presented.

2.3.1 OVERLAND FLOW IN URBAN ENVIRONMENTS

Some misunderstanding about the expressions “*Storm movement*” and “*Wind-driven rainfall*” (also referred as “*Driving rainfall*”) subsist in the literature given that, sometimes, these expressions are abusively used. Storm movement regards the displacement of a rain cell (or a group of rain cells) over a given area. It may range from seconds or minutes, at a small urban drainage basin, to hours or days, at the river basin scale (Liang, 2010). Without the existence of wind near the ground level rainfall will only have vertical speed (vertical rainfall), despite it comes from a static or a moving storm. However, if wind exists near the ground level, the rain will gain horizontal speed and will be carried by the wind thus having a non-vertical trajectory (inclined rainfall). This latter description corresponds to wind-driven rain, which, as explained, only depends on the existence of wind near the ground level, regardless if the rainfall is originated by a static or by a moving storm. These phenomena are thus independent, *i.e.*, wind-driven rainfall can occur without storm movement and vice-versa.

Both the rain cell movement and the occurrence of wind affect the temporal and spatial distribution of natural rainfall, thus modifying the input of the rainfall-runoff process. This has been proved for several times during the last decades (*e.g.*, Yen and Chow, 1968; de Lima *et al.*, 2011). According to Beven (2004) we need to model the rainfall-runoff process in hydrology to extrapolate the available hydrological measurements, both in space and time. In space, so we may attain knowledge on the hydrological processes where measured data is not obtainable. In time, so we may forecast impacts of hydrological change where measurements are impossible to be carried out. Incorporation of the storm movement and wind-driven-rain effects on the rainfall-runoff process is thus a way to achieve a better simulation of the real systems.

Urban environments have singular characteristics regarding the rainfall-runoff process. The increased imperviousness of the terrain (see Chapters 2.2.2 and 3) and the existence of buildings (see Chapters 4, 5 and 6) promote considerably changes in the natural water cycle. The intensity of human activities, measurable by socio-economical indexes (*e.g.*, electricity consumption, GDP per capita, total industrial output value and population density), can produce localized changes in climate and thus induce an additional pressure to the modified water cycle. An example of it is the “urban heat island” phenomenon (see Chapter 2.1.2.1).

Knowing and quantifying the influence of storm movement and wind on the spatial distribution of rainfall intensity in urban areas is far from being a stress-free task. It obliges to have the relevant data acquired within short spatial and temporal intervals over sometimes large areas. Obtaining this kind of information is possible through the use of technological resources. RADAR is a tool used since World War II for rainfall detection (see Figure 2.9) that is still in use nowadays with a global widespread employ in meteorology, naturally, with great technological advancements. Basically, using microwaves RADARs measure the power of targets existing in the atmosphere, as raindrops or hailstones and convert it into reflectivity. Because reflectivity is proportional to the concentration of the detected targets, and mostly to their sizes, reflectivity is then finally converted into rainfall intensity.

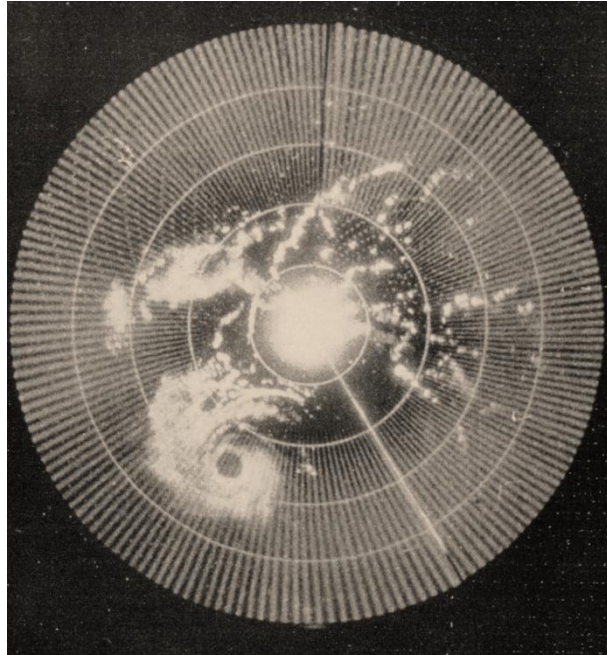


Figure 2.9 1960 RADAR image of Hurricane Abby approaching the coast of British Honduras, nowadays Belize. The complete eyewall cloud is perfectly defined (United States National Oceanic and Atmospheric Administration).

Like in RADAR, microwaves are nowadays being used for flood forecast purposes in urban areas but within a different technology. Actual communication demands led to setting up networks of microwave antennas in most of the urban areas. This allowed using commercial microwave communication links to predict the spatial distribution of rainfall intensity has been studied by some authors in the last years (*e.g.*, David *et al.*, 2009; Zinevich *et al.*, 2009). Recent advances on this purpose include the use of cellular networks (*e.g.*, Overeem *et al.*, 2011).

RADAR and commercial microwave communication links are technologies based in the disturbances (scattering and absorption) of microwave radio propagation caused by rainfall, and thus, have advantages over traditional rain gauge networks as the absence of additional installation and maintenance costs (Rayitsfeld *et al.*, 2012), and the higher robustness (Minda and Nakamura, 2005). Moreover, because these resources are many times available near – or within – the population centres, they are capable of giving real-time distribution of rainfall intensity with enough resolution for flash flood forecast purposes.

2.3.1.1 FIELD STUDIES

Field studies enable the acquisition of hydrological relevant data in real systems, with natural or artificially imposed rainfall conditions, providing a helpful visualization on the rainfall-runoff process under moving storms and/or wind-driven rainfall. The results obtained can be used to verify and calibrate computational models; however, field campaigns are expensive and highly time-consuming, and thus, careful design of equipments and appropriate preparation of experimental protocols must be taken into account when preparing this kind of studies.

Rainfall simulators, which are used to impose artificial rainfall, allow the elimination of the unpredictable variability of natural rainfall by permitting a controllable, reliable and predictable simulation of rainfall events. A rainfall simulator is required to produce an accurate reproduction of the physical features of natural rainfall; however, some tolerance may be given in the interests of simplicity and cost (Hudson, 1993). Often-cited Meyer (1988) refers that: *The goal of rainfall simulator research should be the collection of accurate, useful data, not a perfect rainfall simulator*. Despite rainfall simulators cannot meticulously replicate natural rainfall, they still are the best technique to study overland flow generation (Reaney, 2003).

From RADAR and rain gauge data acquired during summer storms, which occurred from 1969 to 1972 and led to the flooding of house basements in the city of Ottawa (Canada), Austin and Austin (1974) found that these flooding events were likely the result of slow moving storms, which could have more influence on the overland flow hydrograph than faster moving storms. The authors also referred that these features of storm dynamics seemed to be more important than either the maximum instantaneous rainfall rate or the total accumulated rainfall.

Despite the restrictions, when compared to nowadays technologies based on remote sensing, rain gauge networks for storm tracking were widely used in the early studies of storm movement influence on overland flow. Shearman (1977) tracked the paths of 230 storms using 15 rain gauges of the Surrey and Greater London Council areas (England) to characterize local storm events and compute storm dynamics as the speed, direction and frequency of storms. Based on two field studies in Cardington and Winchcombe (England,) in which a total of 219 storms were analysed, Marshall (1980) described a method to estimate the speed and direction of moving rainstorms based on cross-correlations between all pairs of rain gauges of a given network for

different time lags. The method was also capable of providing information about the rainstorm's spatial and temporal structures.

The most recent field studies reported in the literature are based in Niemczynowicz's long-term rainfall and discharge measurements taken in the city of Lund (Sweden), where more than 90% of the city area was served by a stormwater drainage system. Niemczynowicz (1984b) measured the runoff caused by intense rainfall events over the city for more than 17 months. The storm movement was characterized using a network of 12 automatic rain gauges with 1-minute resolution. Maximum discharges were found to take place for storms moving downstream which the same speed than the average flow velocity in the stormwater drainage system. By applying three distinct storm track methods it was shown that when the rainfall data acquired from rain gauges is consistent the storm movement pattern can be easily – however subjectively – recognized, and that the information about the spatial distribution and kinematics of short-duration rainfall events helps to diminish errors in overland flow simulation on urban areas (Niemczynowicz, 1987). Using rainfall data from 10 events to simulate single-event overland flows, Niemczynowicz (1988) showed that the use of information acquired with a 12 rain gauge network or with only 3 rain gauges, but complement with rainfall movement parameters, gave similarly good results, and so, that a sound knowledge of the storm dynamics could overcome the shortcomings caused by lack of higher-density rain gauge networks.

Interdisciplinary experimental studies in a variety of climate and physiographic conditions allow the investigation on the scale and dynamics of spatial rainfall variability (Berndtsson and Niemczynowicz, 1988). These authors referred that by bridging the gaps between researchers and engineers some errors and uncertainties, usual in the modelling of hydrological processes in which the rainfall is a driving force, may be overcome. The influence of storm movement over a drainage basin on the shape of the discharge hydrographs is an example of those errors and uncertainties, which are seldom addressed in engineering applications.

2.3.1.2 LABORATORY EXPERIMENTS

Laboratory simulation allows the analysis of a given hydrological process taking place in a well-characterized setting. The characteristics of rainfall (*e.g.*, spatial distribution of rainfall intensity) and the environmental conditions (*e.g.*, air temperature) can thus be controlled and repeated, permitting an individually analysis of their influence on

the studied hydrologic process. As with field studies (see Chapter 2.3.1.1) the results obtained in the laboratory can be used to verify and calibrate computational models and, because laboratory physical simulation is also expensive and highly time-consuming, the same requirements regarding equipment design and protocol delineation must be fulfilled. Rainfall simulators have also a widespread use in laboratory experimentation of the rainfall-runoff process, since in indoor conditions the spatial and temporal distribution of the rainfall events can be accurately reproduced for n -times.

First laboratory studies on the influence of storm movement on overland flow consisted on two experiments with rainstorms moving upstream and downstream Amorocho and Orlob (1961) [cited in Liang (2010)]. From these experiments it was suggested that storm movement could influence the runoff hydrographs.

Consistent experimentation on the influence of moving storms on overland flow over impervious surfaces started at the University of Illinois, where a 12 m square V-shaped drainage basin experimental system with 400 raindrop producers was established. With this equipment Marcus (1968) [cited in Singh (1997a)] studied how moving storms influenced the distribution of overland flow over time. The same equipment was used by Yen and Chow (1968; 1969) to investigate the influence of moving storms on surface runoff by means of dimensional analysis of the resulting hydrographs. These authors found that storms moving upstream produced a smaller peak discharge than downstream moving storms. This was confirmed by Roberts and Klingman (1970) and Townson and Ong (1974) that run controlled experiments on the conditions affecting the runoff hydrographs. Among other runoff affecting-factors, storm movement showed to produce systematic changes in the flood hydrographs. Peak discharges and the hydrograph's recession limbs showed to be largely affected by the storm movement.

Hall *et al.* (1989) described the development of an installation capable of simulating spatial and temporal controlled rainfall intensities with natural rainfall drop-size distribution and terminal velocity. The rainfall simulator had, accordingly to the authors, enough flexibility to simulate *stationary, spatially uniform, constant or variable intensity rainfalls; stationary, spatially non-uniform, constant or variable intensity rainfalls; and moving storms, of either constant shape (uniform in space) or growing or decaying with time during their movement*. Despite this installed capacity, studies on its use in storm movement research were not found in the literature.

In order to assess the effects of storm velocity and direction in the runoff response de Lima and Singh (2000; 2003) used a sprinkling-type rainfall simulator with the ability to move over rails to simulate moving storms. The simulations showed that, when compared with downstream moving storms, storms moving upstream produced hydrographs with earlier rise, lower peak discharge and longer base time. Both for storms moving in the downstream and upstream directions, the highest ratio of peak discharge to total discharged volume was obtained for a storm velocity equal to the average overland flow velocity. After installing a set of 11-fans to simulate wind-driven rainfall and other upgrades (*e.g.*, automatic measurement and logging of runoff data), Isidoro *et al.* (2012a; 2012b) and Isidoro and de Lima (2012b) used the same laboratory rainfall simulator to study the influence of high-rise building density, rooftop connectivity and building height on the rainfall-runoff process in impervious areas under wind-driven rainfall (Figure 2.10). From these studies it was concluded that disregarding the density of high-rise buildings, the rooftop connectivity and the building height could lead to under- or over-estimation of important hydrologic parameters (*e.g.*, peak discharge, runoff base time) which are indispensable to the design of urban drainage systems.

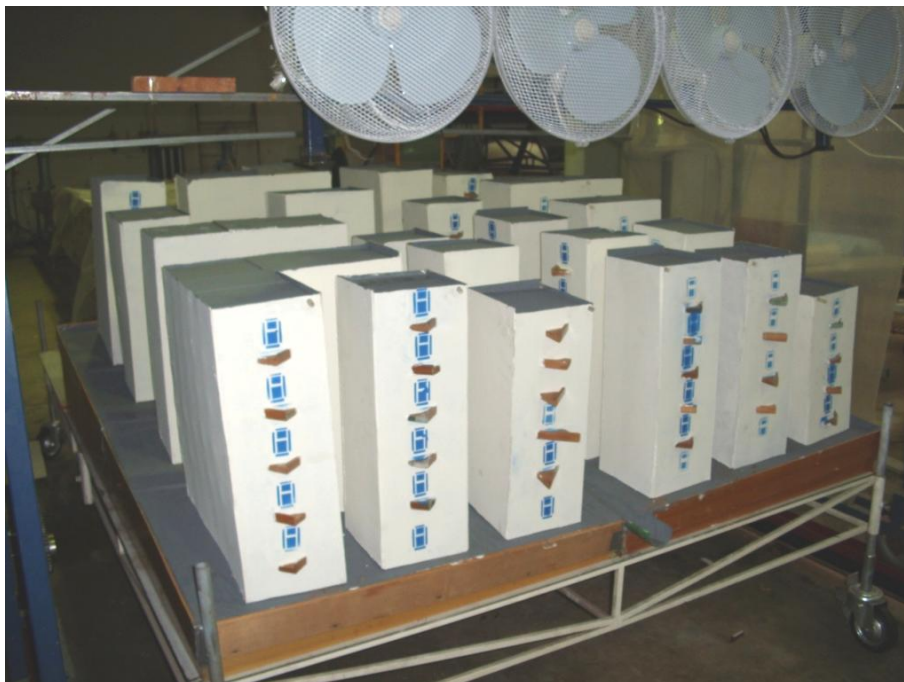


Figure 2.10 A physical model of an urban area densely occupied by high-rise buildings is tested on the laboratory to obtain experimental data of the relation between building density, storm movement, wind-driven rainfall and overland flow. In these experiences, elements representing buildings could be removed and repositioned in order to obtain different building occupation densities.

2.3.1.3 NUMERICAL METHODS

Advantages of numerical simulation in hydrology and hydraulics are widely reported. The suitability to create and explore diverse scenarios, easiness on modifying input conditions, capability to obtain (approximate) solutions where no exact solution exists and low cost for equipment and development are, among other advantages, often-reported. Nonetheless these advantages, the use of numerical methods also have some difficulties as model parameterization and quantification of uncertainty in the results. Despite the evolution of computational capabilities, some more sophisticated high-resolution numerical models may be significantly time consuming. Calibration of numerical models (*e.g.*, using field measurements) is also frequently expensive.

A numerical model was the tool used in the first published article (Yen and Chow, 1968) about the influence of storm movement on runoff (Maksimov, 1964). The model showed that the storm movement was clearly associated with changes in the magnitude of the peak discharge.

After the work of Maksimov several authors started using numerical schemes to indentify changes in the overland flow hydrographs caused by storm movement. Marcus (1968) [cited in Liang (2010)] applied the continuity and momentum equations to study the overland flow and channel unsteady flow caused by moving storms, finding less than 10% of discrepancy between the experimental results and the ones obtained by the approximate dynamic-wave approach model. A distributed model to simulate how moving storms in different directions influenced runoff (Surkan, 1974) showed that peak discharge and average flow rate were most sensitive to the change of the storm direction and speed. Stephenson (1984) simulated runoff hydrographs from a storm travelling down a drainage basin using an implicit scheme proposed by Brakensiek (1967) due to its accuracy and swift calculation. It was concluded that the storm movement reduced the peak flow, unless in the downstream storm movement where the model did not showed any change in the peak runoff rate.

Overland flow sensibility to storm direction and speed became an important research field. A circular conceptual drainage basin was modelled to show that smaller catchments are more sensitive to storm movement than larger ones (Ngirane-Katashaya and Wheater, 1985). In this circular drainage basin, downstream moving storms originated, for almost all storm speeds, higher peak discharges than upstream

moving storms. Peak discharge of downstream moving storms initially augmented with increasing storm speed, reached a maximum and then declined. The upstream moving storms showed an increase of the peak discharge, although at a decreasing rate, for all the simulated storm speeds. The relation between storm and channel-flow speeds was studied for a hypothetical 50-year return period moving storm (Foroud *et al.*, 1984). When moving downstream, the time to peak flow showed to be nondependent of the storm speed, if the latter exceeded channel-flow velocity. The difference in the time to peak flow of a downstream moving storm and an equivalent stationary rainstorm were negligible; however, when compared to the equivalent stationary rainstorm, upstream storm movement storms led to higher times to peak flow, also dependant on the storm's velocities.

The Storm Water Management Model (SWMM – United States Environmental Protection Agency), a dynamic rainfall-runoff simulation model developed in 1971 primarily for urban areas and used for single event or long-term simulation of runoff, was the tool that Niemczynowicz (1984a) used to simulate a conceptual drainage basin and study the relations between storm movement parameters (*e.g.*, duration, intensity, velocity and direction of rainstorms) and their influence on peak discharge. The SWMM was also used by Niemczynowicz (1984b and 1988) to simulate the rainfall-runoff process in Lund (Sweden) due to moving rainstorms (see Chapter 2.3.1.1).

A finite element runoff model called CASC was developed by Julien *et al.* (1988) for spatially varied overland simulation of cascades of planes, and converging and expanding drainage basin geometries. The CASC model was applied by Richardson and Julien (1989) with the objective of simulating one-dimensional overland flow under moving storm blocks over a simple open book geometry drainage basin and to compare the results with the obtained by means of laboratory experimentation (Yen and Chow, 1968). Ogden *et al.* (1995) also used the CASC model for 1D and 2D runoff simulation on simple planar and complex topography under moving storms, concluding that the upstream storm movement reduces the magnitude of the hydrograph peak and that the 2D runoff geometries are much more sensitive to storm speed than to storm direction.

Based on the non-linear kinematic wave model de Lima and Singh (2002) emphasized the importance of the rainfall intensity spatial patterns on overland flow under moving storms. The hydrographs of hypothetical storms with different patterns, lengths and speeds, moving up and down an impervious plane surface, were

compared. Significant differences in the hydrograph shapes were noticed. It was also observed that the influence of storm patterns in the runoff decreased as the storm speed increased. Another non-linear kinematic wave model was developed by Lee and Huang (2007) to simulate runoff originated by moving storms over an overland plane and a V-shaped drainage basin. The numerical model was validated using laboratory data. The results showed that runoff can attain equilibrium discharge for downstream moving storms, even if the storm length is shorter than the drainage basin length, and that the rainfall duration is smaller than the time to equilibrium of the drainage basin for static uniform storms. These findings are opposed to conventional hydrology, which presuppose that for the maximum discharge be attained, the storm duration must be at least equal to the time to equilibrium (*e.g.*, Saghafian and Julien, 1995; Singh, 2002b).

Kinematic- and dynamic-wave models were used to evaluate the runoff response to moving storms in impervious areas (Liang, 2010). Comparison of both models showed that the kinematic-wave model overestimated the peak discharge for downstream moving storms, probably due to the backwater effect which cannot be described by such models; however, the kinematic-wave model produced a good simulation of runoff caused by upstream moving storms. The dynamic-wave allowed very good results in the simulation of runoff produced by both downstream and upstream moving storms. This study also showed that the interaction between backwater in the channel reaches and incoming lateral flows have a marked influence in the flood propagation process.

2.3.1.4 ANALYTICAL SOLUTIONS

Analytical solutions for runoff under moving storms have been derived only in the last two decades. Exact solutions of wind-driven rainfall (inclined rainfall) induced runoff are not yet known to exist. Analytical-based models are far less demanding on computational capacity than numerical-based models and can help to give an important insight on specific hydrological processes. However, exact solutions are only applicable to a limited number of problems with very particular conditions.

Empirically-based synthetic storms were initially used to obtain exact solutions for overland flow caused by moving storms. Using an algebraic linear time-area curve model, Jensen (1984) observed that moving rainfall blocks changed the shape, peak and time to peak of the runoff hydrographs. To evaluate the influence of storm

movement on urban drainage systems, Sargent (1981) simulated the passage of a spatially and temporally distributed synthetic storm, at a range of speeds and directions, across a number of very simplistic hypothetical drainage basins. The results showed that the consequences of storm movement in runoff could, under some circumstances, affect pipe network design. Disregarding the storm movement showed to result in a significant over-estimation of the runoff peak and volume (thus to an overdesign of drainage systems) which seemed to be more significant for larger urban drainage basins (Sargent, 1982).

Analytical studies of the rainfall-runoff process over complex basins gave a step forward with the research on how the storm movement influence overland flow. Bengtsson (1991) derived analytical solutions for runoff caused by moving storms with time-varying rain intensity over a complex drainage basin, assuming constant concentration times for the distinct systems within the basin. The storm movement showed to influence the peak runoff, especially in elongated basins. In another work, Wang and Chen (1996) used a linear spatially distributed model based on ordinary differential equations to represent the rainfall-runoff process for sub-basins – in series or parallel – which are assembled to obtain, via Laplace transforms, a general equation for the whole drainage basin. A unit-step function was used to represent the rainfall excess of each sub-basin. When compared with upstream moving storms, discharge hydrographs from downstream moving rainstorms showed to be characterized by higher peak flows and shorter base times.

Analytical solutions for flow resulting from storms moving up and down a plane were derived by Singh (1998, 2002a, 2002b) who used the characteristics method to solve the nonlinear kinematic wave equations. The flows, caused both by moving and static storms, were compared and significant influence on peak flow, time to peak and hydrograph shape caused by storm movement was observed. Peak flow and time to peak flow for downstream and upstream moving storms showed dependence of storm velocity. Storms moving in the flow direction caused higher peak and steeper hydrograph's limbs. Highest peak discharge, both for downstream and upstream moving storms, happened when the storm velocity was equal to the flow velocity. In the downstream moving storms, the hydrographs crest was longer for storms with higher velocity than for lower velocity storms, while in the upstream moving storms this influence showed to be of less importance. The characteristics method was also used to solve the nonlinear kinematic wave model of overland flow with time-varying rainfall on a sloping plane (Mizumura and Ito, 2011a). This solution was compared – and fitted satisfactorily – with experimental data obtained from a semi-V-shaped

drainage basin at the Kanazawa Institute of Technology (Japan). Further research showed that for low-speed storms moving upstream and downstream, the difference of the water depths at the drainage basin outlet is proportional to the speed of the moving rainstorm (Mizumura and Ito, 2011a). In this work, it was also observed that the water depth peak occurs for equal speeds of the moving storm and the overland flow, and that the moving storm speed effect is larger for drainage basins with milder bottom slope or lower Strickler roughness coefficient.

Based on Zarmi's hypothesis (Zarmi *et al.*, 1983), *i.e.*, linear kinematic wave equation and using Laplace transforms, Isidoro and de Lima (2012a) derived an exact closed form solution for the entire space-time domain of the overland flow hydrograph. The continuous solution – which enables evaluation of the discharge over time for the total drainage plane surface – was validated through comparison with another exact solution (Singh, 1998), a numerical simulation (de Lima and Singh, 2002) and experimental laboratory runs using an impermeable flume and a rainfall simulator (see Chapter 7). The continuous solution fitted perfectly with the exact solution and the numerical simulation, and was capable to capture satisfactorily the shape of the experimentally-obtained hydrographs.

2.3.2 OVERLAND FLOW ON NATURAL SURFACES

Despite this thesis is mainly focused on impervious areas it is appropriate to outline some aspects of storm movement and wind-driven rainfall on overland flow in natural surfaces, since this kind of coverage also exists on urban areas (*e.g.*, parks and outdoor recreation complexes).

The influence of storm movement and wind-driven rainfall on the hydrologic cycle in natural surfaces has undergone greater attention from researchers, when compared to impervious areas related research. Hydrological studies on natural basins do not need data with such short spatial and temporal intervals as on urban areas; however, natural drainage basins occupy much larger areas and are usually less densely instrumented (*e.g.*, with rain gauges) than urban areas. It is relevant to mention the importance that remote sensing has on this subject. Remote sensing using satellite technology allowed expanding our knowledge about rainfall distribution globally. The first operational meteorological satellite was the TIROS I (Television InfraRed Observation Satellites – TIROS) which was launched in 1960 (Smith *et al.*, 1986), but the first satellite dedicated to measure rainfall (Tropical Rainfall Measuring Mission –

TRMM) was only launched in 1997 (Kidd and Levizzani, 2011). By acquiring real-time meteorological data over large areas, satellite technology is an essential tool for environmental processes modelling, namely, for the forecast of rainstorm events and flood simulation. For an in-depth review of recent developments on weather satellites see *e.g.*, Kidd *et al.* (2009).

In natural surfaces, storm movement and wind-driven rainfall have a particular influence on soil detachment, rill and gully formation and sediment transport, thus being intrinsically related with water erosion processes. The next paragraphs show some examples of studies in this field. These references do not pretend to exhaustively list the work published in the field but only to illustrate the range of themes addressed in the literature, which is vast.

Laboratory rainfall simulation is a useful way of determining the effect of the drainage basin properties (shape, slope, size, drainage pattern and soil pattern) and the rainfall characteristics (intensity and direction of storm movement) on the outflow hydrographs. Black (1972) conducted a series of laboratory tests on this subject, concluding that the laboratory models exhibited hydrologic responses similar to those that would be found in a wide range of real drainage basins. Moreover it was observed that, the drainage basin shape, individually, does not have a major influence on peak magnitude but its eccentricity is an important – and easily measured – expression which affects not only peak flows, but also other parameters of the hydrographs (*e.g.*, time to peak).

A physically-based model was proposed by Watts and Calver (1991) to study the rainfall-runoff process for moving storms over a hypothetical drainage basin with 100 km² dominated by subsurface flow. Different scenarios were analysed (*e.g.*, storm speed, direction and intensity) and, for all the scenarios, downstream moving storms caused higher runoff peaks than upstream moving storms, with the highest differences happening for storms with speed and direction near the average peak channel velocity. Despite the results of these experiments evidenced a similar behaviour with drainage basins that are dominated by overland flow, the differences in peak runoff between downstream and upstream moving storms are much smaller than the observed in the latter.

To study the influence of storm movement on the water erosion process for different surface slopes, de Lima *et al.* (2003) used a rainfall simulator with the ability to move over rails and developed a slope-adjustable soil flume. Results showed a marked

influence of the storm velocity and direction on the water erosion process. Soil loss caused by downstream moving storms proved to be higher than the caused by upstream moving storms. The increase in surface slope showed to augment the relative differences between soil losses, both for downstream and upstream moving storms. Storm velocity also showed to affect runoff volume and the associated soil loss. The increase of storm velocity showed to promote a reduction of soil loss, both for upstream and downstream moving storms. The absolute and relative differences between soil loss yields for upstream and downstream moving storms were also reduced as the storm speed increased.

In recent years particular attention has been given to the combined action of wind and rainfall, namely through laboratory and field experimentation using rainfall simulators. A laboratory wind tunnel facility equipped with a rainfall simulator was used by Erpul *et al.* (2005) to assess the effect of wind velocities on sand detachment. Wind-driven and windless rainfall was simulated over splash cups filled with sand. A kinetic energy sensor was used to measure rainfall energy and the results confirmed that the observed sand detachment was related to the calculated energy flux. Uncertainty in rainfall measurements caused by the occurrence of wind were reported in a field study on the hydrologic impacts of tropical mountain deforestation to increase pasture area in Costa Rica, carried by a team of the VU University Amsterdam (Bruijnzeel, 2006). In this study it was showed that high runoff to rainfall ratios may reflect unmeasured wind-driven rainfall inputs, instead of high fog-water inputs as is commonly assumed. This study also showed that wind-driven rainfall inputs can be expected to vary enormously in space due to the variations in exposure to prevailing winds, presence or absence of intercepting obstacles (*e.g.*, tall trees vs. short grass) and hillslope steepness.

The temporal evolution of the granulometric distribution of sediments transported in overland flow, generated by static and moving storms, was studied by de Lima *et al.* (2008) by means of laboratory experimentation. In these experiments a rainfall simulator and a slope-adjustable soil flume were used. Storm movement was generated by moving the rainfall simulator, with constant speed, in the downstream and upstream directions over the flume, which was set at different slopes. Storm movement showed to have an important influence on the grain-size characteristics of overland flow transported sediments. Downstream moving storms produced higher stream power than static and upstream moving storms. Using the same rainfall simulator over a multiple-slope soil flume, de Lima *et al.* (2011) studied the influence of storm movement at the hillslope scale confirming the previous findings. Hillslopes

with the lowest slope near the discharge section showed to suffer less erosion, with sediments depositing mostly in that area; on the other hand, when the highest slope was near the discharge section, strong surface erosion and the formation of deeper ridges were observed. In another laboratory study, Ran *et al.* (2012) carried out a set of experiments to study the influence of rainfall characteristics on runoff generation and soil erosion. From the hydrographs generated by rainfall events with different intensities, durations, moving directions, positions and no-rainfall intervals (dry-cycles), it was observed that most of the downstream moving storms events were characterized by a later rise of the hydrograph and a higher runoff peak, and that the runoff and erosion rate peaks appeared at the same time when the storms moved in the downstream direction.

To overcome the limitations of laboratory research and, at the same time, make possible to investigate, in the field, the interactions between wind and rainfall under comparable conditions, Fister *et al.* (2012) developed a Portable Wind and Rainfall Simulator (PWRS) to study the soil loss processes which are associated with wind and water erosion, namely with wind-driven rainfall erosion. The PWRS showed to be capable of reproducing the natural wind and rain conditions, therefore being adequate for comparative soil erosion studies in the field. A different kind of approach was taken by Valette *et al.* (2012) who developed a numerical rainfall generator for small-scale simulation of rainfall-induced processes as soil loss or soil surface crusting. The numerical generator produce the input of the rainfall-runoff process by originating series of individual raindrops, according to a given hyetograph and a spatial distribution, and at the same time, satisfying an imposed size distribution. The outputs of the numerical generator showed a good reproducibility of observed data, thus allowing an adequate simulation of experimental or natural rainfall events.

2.3.3 APPLICATIONS IN OTHER FIELDS OF CIVIL ENGINEERING

Wind-driven rainfall is also an important subject for other areas in the field of Civil Engineering beyond hydrology, *e.g.*, in building science where quantifying wind-driven rainfall action on buildings facades and studying their responses has been a subject of research over the last years (*e.g.*, Blocken and Carmeliet, 2004). However, because *e.g.*, wind-driven rainfall is an essential boundary condition for studies related to the hygrothermal performance and durability of historical and contemporary building facades, much research work still needs to be done (Blocken

and Carmeliet, 2010). Experimental, semi-empirical and numerical methods have been employed on research in this field: experimental methods consist basically in the measurement of wind-driven rainfall using specific rain gauges with vertical apertures; semi-empirical methods are usually based on the analysis of relationships between wind-driven rainfall and the influencing climatic parameters (*e.g.*, wind speed and rainfall intensity), and numerical methods allow calculating the movements of raindrops (*e.g.*, around a building), thus being an important help on the reveal of the inherent complexity of wind-driven rainfall. For an in-depth review on wind-driven rain on building science see Blocken (2004) and Blocken and Carmeliet (2004).

The influence of wind-driven rainfall on surface discoloration patterns of a stone building, studied by Tang *et al.* (2004) and Tang and Davidson (2004), is an example of how knowing more about the wind-driven-rainfall behaviour may be applied in buildings science, *e.g.*, for heritage building conservation. The observed stained patterns were found to be associated with the non-uniform distribution of wind-driven rainfall, and as the result of wind, rainfall and building geometry interactions. Another study on the effect of wind-driven rainfall in masonry walls (Rydock and Gustavsen, 2007) showed that the observed maximum rain spell intensities striking at walls placed at different angles is related to the average angular distributions of annual wind-driven rainfall data. This may be of particular interest for masonry walls in building facades with relative risk of repeated penetration by rainfall water, where quantitative wind-driven rainfall data is not available.

The effects of wall-absorbed rainfall water for wind-driven rainfall conditions were assessed from an estimative of the average catch-ratio distribution over building facades (Hens, 2010). This estimative was obtained through a combination of computational (computer fluid dynamics) and empirical (raindrop-trajectory tracing) methods. The results showed that effects of absorbed rain water in wall assemblies can be acceptably well estimated using the actual computer tools, but the runoff water over the walls presents complexity that cannot yet be addressed by existing models. Computer fluid dynamics was the tool used by van Hooff *et al.* (2010) to simulate 3D wind flow and wind-driven rainfall for twelve distinctive stadium configurations representative of a wide range of real stadiums. Stadium geometry and roof slope showed to influence the areas of the stand wetted by wind-driven rainfall. Stadium open roofs and corners showed to promote particular wind-driven rainfall distributions.

2.4 NOTATION

The following symbols are used in this chapter:

C	capillary rise;
E	evaporation;
ET	evapotranspiration;
G	groundwater flow;
I	infiltration;
K_S	Strickler coefficient;
R	runoff;
SS	subsurface flow;
V_R	raindrop terminal velocity for windless conditions;
V_W	horizontal wind velocity near the ground level;
V_{WDR}	wind-driven affected raindrop terminal velocity;
θ	angle of incidence of the rainfall.

2.5 REFERENCES

Ackerman, S.A. and Knox, J.A., 2011. *Meteorology: Understanding the Atmosphere*. 3rd ed. London: Jones & Bartlett Publishers.

ACTIF – Achieving Technological Innovation in Flood Forecasting, 2004. *Future EC research needs under the EC sixth framework for flood and drought forecasting* [online]. EC Research Project: Project Reference No. EVK1-CT-2002-80014. Available from: <http://www.actif-ec.net/documents/ACTIFResearchNeedsfor%20FP6V1.4.pdf> [Accessed 4 Jan 2012].

Alaghmand, S., bin Abdullah, R., Abustan, I. and Vosoogh, B., 2010. GIS-based river flood hazard mapping in urban area (a case study in Kayu Ara river basin, Malaysia). *International Journal of Engineering and Technology*, 2 (6), 488–500.

Al-Sabhan, W., Mulligan, M. and Blackburn, G.A., 2003. A real-time hydrological model for flood prediction using GIS and the WWW. *Computers, Environment and Urban Systems*, 27 (1), 9–32.

Amorocho, J. and Orlob G.T., 1961. Nonlinear analysis of hydrologic systems. *In: Water Resources Center Contribution Vol. 40*. Berkeley, CA: University of California, 74–77.

Arnold Jr., C.L. and Gibbons, C.J., 1996. Impervious Surface Coverage: The Emergence of a Key Environmental Indicator. *Journal of the American Planning Association*, 62 (2), 243–258.

ASCE – American Society of Civil Engineers/Task Committee on Hydrology Handbook of Management Group D, 1996. *Hydrology handbook*. 2nd ed. ASCE Manuals and reports on engineering practice No. 28. New York, NY: ASCE Publications.

Austin G.L. and Austin L.B., 1974. The use of radar in urban hydrology. *Journal of Hydrology*, 22 (1–2), 131–142.

Bailly-Comte, V., Jourde, H., Roesch, A. and Pistre, S. (2008) Mediterranean flash flood transfer through karstic area. *Environmental Geology*, 54 (3), 605–614.

Beard, K.V., 1976. Terminal velocity and shape of cloud and precipitation drops aloft. *Journal of Atmospheric Sciences*, 33 (5), 851–864.

Bengtsson, L., 1991. Effective concentration time for design storms in complex urban basins. *Atmospheric Research*, 27 (1–3), 137–150.

Berndtsson R. and Niemczynowicz, J., 1988. Spatial and temporal scales in rainfall analysis – Some aspects and future perspectives. *Journal of Hydrology*, 100 (1–3), 293–313.

Berry, J.K. and Sailor, J.K., 1987. Use of a geographic information system for storm runoff prediction from small urban watersheds. *Environmental Management*, 11 (1), 21–27.

Beven, K.J., 2004. *Rainfall-runoff modelling: the primer*. Chichester: John Wiley and Sons.

Black, P.E., 1972. Hydrograph responses to geomorphic model watershed characteristics and precipitation variables. *Journal of Hydrology*, 17 (4), 309–329.

Blocken, B. and Carmeliet, J., 2004. A review of wind-driven rain research in building science. *Journal of Wind Engineering and Industrial Aerodynamics*, 92 (13), 1079–1130.

Blocken, B. and Carmeliet, J., 2010. Overview of three state-of-the-art wind-driven rain assessment models and comparison based on model theory. *Building and Environment*, 45 (3), 691–703.

Blocken, B., 2004. *Wind-driven rain on buildings: measurements, numerical modelling and applications*. Thesis (PhD). Catholic University of Leuven.

Blocken, B., Poesen, J. and Carmeliet, J., 2006. Impact of wind on the spatial distribution of rain over micro-scale topography: numerical modelling and experimental verification. *Hydrological Processes*, 20 (2), 345–368.

Brakensiek, D.L., 1967. Kinematic flood routing. *Transactions of the American Society of Agricultural and Biological Engineers*, 10 (3), 340–343.

Bruijnzeel, L.A., 2006. *Hydrological impacts of converting tropical montane cloud forest to pasture, with initial reference to Northern Costa Rica* [online]. Final Technical Report for Project R7991, DFID Forestry Research Programme. Amsterdam, VU University Amsterdam. Available from: http://www.falw.vu/~fiesta/reports/R7991_Final%20Technical%20Report_Jan00.pdf [Accessed 18 Jan 2012].

Buhl, J., Gautrais, J., Reeves, N., Solé, R.V., Valverde, S., Kuntz, P. and Theraulaz, G., 2006. Topological patterns in street networks of self-organized urban settlements. *The European Physical Journal B*, 49 (4), 513–522.

- Chang, J-h, 2009. *Climate and agriculture: an ecological survey*. New Brunswick, NJ: Transaction Publishers.
- Clark, M.J., 1998. Putting water in its place: A perspective on GIS in hydrology and water management. *Hydrological Processes*, 12 (6), 823–834.
- Correia, F.N., Rego, F.C., Saraiva, M.G. and Ramos, I., 1998. Coupling GIS with hydrologic and hydraulic flood modelling. *Water Resources Management*, 12 (3), 229–249.
- Correia, F.N., Saraiva, M.G. and Silva, F.N., 1999. Innovative approaches to integrated floodplain management. In: R. Casale and C. Margottini, eds. *Floods and Landslides: Integrated Risk Assessment*. Berlin: Springer-Verlag, 199–244.
- David, N., Alpert, P. and Messer, H., 2009. Technical note: Novel method for water vapour monitoring using wireless communication networks measurements. *Atmospheric Chemistry and Physics*, 9 (7), 2413–2418.
- Davis, D.W., 1978. Comprehensive flood plain studies using spatial data management techniques. *Journal of the American Water Resources Association*, 14 (3), 587–604.
- de Lima, J.L.M.P. and Singh V.P., 2002. The influence of the pattern of moving rainstorms on overland flow. *Advances in Water Resources*, 25 (7), 817–828.
- de Lima, J.L.M.P. and Singh, V.P., 2000. The influence of storm movement on overland flow – Laboratory experiments under simulated rainfall. In: V.P. Singh, I.W. Seo and J.H. Sonu, eds. *Hydrologic Modeling – Proceedings of the International Conference on Water, Environmental, Ecology, Socio-economics and Health Engineering (WEESHE)*, 18–21 October 1999 Seoul. Highlands Ranch, CO: Water Resources Publications, 101–111.
- de Lima, J.L.M.P. and Singh, V.P., 2003. Laboratory experiments on the influence of storm movement on overland flow. *Physics and Chemistry of the Earth*, 28 (6–7), 277–282.
- de Lima, J.L.M.P., 1989a. *Overland flow under rainfall: Some aspects related to modelling and conditioning factors*. Thesis (PhD). Wageningen University.
- de Lima, J.L.M.P., 1989b. Overland flow under simulated wind-driven rain. In: V.A. Dodd and P.M. Grace, eds. *Agricultural Engineering Vol. 1 – Land and Water Use, Proceedings of the 11th International Congress on Agricultural Engineering*, 4–8 September 1989 Dublin. Rotterdam: A.A. Balkema, 493–500.
- de Lima, J.L.M.P., 1989c. Raindrop splash anisotropy: slope, wind and overland flow velocity effects. *Soil Technology*, 2 (1), 71–78.
- de Lima, J.L.M.P., 1989d. The influence of the angle of incidence of the rainfall on the overland flow process. In: M.L. Kavvas, ed. *New Directions for Surface Water Modeling*. IAHS Publication Vol. 181. Wallingford: IAHS Press, 73–82.
- de Lima, J.L.M.P., 1990. The effect of oblique rain on inclined surfaces: a nomograph for the rain-gauge correction factor. *Journal of Hydrology*, 115 (1–4), 407–412.

de Lima, J.L.M.P., Singh, V.P. and de Lima, M.I.P., 2003. The influence of storm movement on water erosion: Storm direction and velocity effects. *Catena*, 52 (1), 39–56.

de Lima, J.L.M.P., Singh, V.P., Isidoro, J.M.G.P. and de Lima, M.I.P., 2011. Incorporating the effect of moving storms into hillslope hydrology: Results from a multiple-slope soil flume. In: R.E. Beighley II and M.W. Killgore, eds. *Proceedings of the 2011 World Environmental and Water Resources Congress: Bearing Knowledge for Sustainability*, 22–26 May 2011 Palm Springs, CA. Reston, VA: ASCE Publications, 1398–1407.

de Lima, J.L.M.P., Souza, C.S. and Singh, V.P., 2008. Granulometric characterization of sediments transported by surface runoff generated by moving storms. *Nonlinear Processes in Geophysics*, 15 (6), 999–1011.

de Lima, J.L.M.P., Tavares, P., Singh, V.P. and de Lima, M.I.P., 2009. Investigating the nonlinear response of soil loss to storm direction using a circular soil flume. *Geoderma*, 152 (1–2), 9–15.

de Lima, M.I.P., de Lima, J.L.M.P. and Coelho, M.F.E.S., 2010. Extreme precipitation in the Madeira Island: the event of February 20, 2010. *10th International Precipitation Conference*, 23–25 June 2010 Coimbra. Coimbra: University of Coimbra/IMAR.

Erpul, G., Gabriels, D. and Norton, L.D., 2003. The combined effect of wind and rain on the interrill erosion processes. In: D. Gabriels, G. Ghirardi, D.R. Nielsen, I.P. Sentis and E.L. Skidmore, eds. *Invited presentations College on Soil Physics 2003*, ICTP Lecture Notes 18, 3–21 March 2003 Trieste. Trieste: Abdus Salam International Centre for Theoretical Physics, 173–182.

Erpul, G., Gabriels, D. and Norton, L.D., 2005. Sand detachment by wind-driven raindrops. *Earth Surface Processes and Landforms*, 30 (2), 241–250.

European Parliament and Council Directive 2007/60/EC of 23 October 2007 on the assessment and management of flood risks.

Fister, W., Iserloh, T., Ries, J.B. and Schmidt, R.-G., 2012. A portable wind and rainfall simulator for in situ soil erosion measurements. *Catena*, 91 (1), 72–84.

Foroud, N., Broughton, R.S. and Austin, G.L., 1984. The effects of a moving rainstorm on direct runoff properties. *Journal of the American Water Resources Association*, 20 (1), 87–91.

Foster, S.S.D., 2001. The interdependence of groundwater and urbanisation in rapidly developing cities. *Urban Water*, 3 (3), 185–192.

Fourcade, H.G., 1942. Some notes on the effect of the incidence of rain on the distribution of rainfall over the surface of unlevel ground. *Transactions of the Royal Society of South Africa*, 29 (3), 235–254.

Geiger, W.F., Marsalek, J., Rawls, W.J. and Zuidema, F.C., eds., 1987. *Manual on Drainage in Urban Areas: Volume I – Planning and Design of Drainage Systems*. Studies and reports in hydrology No. 43. Paris: UNESCO/IHP.

Grimm, N.B., Faeth, S.H., Golubiewski, N.E., Redman, C.L., Wu, J., Bai, X. And Briggs, J.M., 2008. Global change and the ecology of cities. *Science*, 319, 756–760.

Guy, H.P., 1964. An analysis of some storm-period variables affecting stream sediment transport. In: *Sediment Transport in Alluvial Channels*. Washington, DC: US Geological Survey, E1–E46.

- Haase, D., 2009. Effects of urbanisation on the water balance – A long-term trajectory. *Environmental Impact Assessment Review*, 29 (4), 211–219.
- Hall, M.J., Johnston, P.M. and Wheater, H.S., 1989. Evaluation of overland flow models using laboratory catchment data. I. An apparatus for laboratory catchment studies. *Hydrological Sciences Journal – Journal des Sciences Hydrologiques*, 34 (3), 277–288.
- Hens, H., 2010. Wind-driven rain: from theory to reality. In: *Proceedings of Thermal performance of the exterior envelopes of whole buildings XI*, 5-9 December 2010 Clearwater Beach, FL. ASHRAE, 10pp.
- Hogg, S.E., 1982. Sheetfloods, sheetwash, sheetflow, or ...? *Earth-Science Reviews*, 18 (1), 59–76.
- Horton, R.E., 1933. The role of infiltration in the hydrologic cycle. *Transactions of the American Geophysical Union*, (14), 446–460.
- Howard, K.W.F., 2002. Urban groundwater issues – An introduction. In: K.W.F. Howard and R.G. Israfilov, eds. *Current Problems of Hydrogeology in Urban Areas, Urban Agglomerates and Industrial Centres – Proceedings of the NATO Advanced Research Workshop*, 29 May – 1 June 2001 Baku. Dordrecht: Kluwer Academic Publishers, 1–15.
- Hudson, N., 1993. *Field measurement of soil erosion and runoff*. Vol. 68 of FAO Soils Bulletin. Rome: UN/FAO.
- Huggett, R.J., 2011. *Fundamentals of Geomorphology*. 3rd ed. Abingdon: Routledge.
- Isidoro, J.M.G.P., Rodrigues, J.I.J., Martins, J.M.R. and de Lima, J.L.M.P., 2010. Evolution of urbanization in a small urban basin: DTM construction for hydrologic computation. In: A. Hermann, S.A. Schumann, L. Holko, I. Littlewood, L. Pfister, P. Warmerdam and U. Schroder, eds. *Proceedings of the International Workshop on Status and Perspectives of Hydrology in Small Basins*, IAHS Red Book Series No. 336, 30 March 2 April 2009 Goslar-Hahnenklee. Wallingford: IAHS, 109–114.
- Isidoro, J.M.G.P. and de Lima, J.L.M.P., 2012a. An analytical closed form solution for 1D linear kinematic overland flow under moving rainstorms. *Journal of Hydrologic Engineering* (revised manuscript).
- Isidoro, J.M.G.P. and de Lima, J.L.M.P., 2012b. Laboratory simulation of the influence of building height and storm movement on the rainfall-runoff process in impervious areas. *Journal of Flood Risk Management* (submitted).
- Isidoro, J.M.G.P., de Lima, J.L.M.P. and Leandro, J., 2012a. Influence of wind-driven rain on the rainfall-runoff process for urban areas: Scale model of high-rise buildings. *Urban Water Journal* (in press).
- Isidoro, J.M.G.P., de Lima, J.L.M.P. and Leandro, J., 2012b. The study of rooftop connectivity on the rainfall-runoff process by means of a rainfall simulator and a physical model. *Zeitschrift für Geomorphologie* (in press).
- James, L.D. and Korom, S.F., 2001. Lessons from Grand Forks: Planning structural flood control measures. *Natural Hazards Review*, 2 (1), 22–32.

- Jat, M.K., Khare, D. and Garg, P.K., 2009. Urbanization and its impact on groundwater: a remote sensing and GIS-based assessment approach. *The Environmentalist*, 29 (1), 17–32.
- Jensen, M., 1984. Runoff pattern and peak flows from moving block rains based on linear time-area curve. *Nordic Hydrology*, 15 (3), 155–168.
- Johnson, C.L., Tunstall, S.M. and Penning-Rowsell, E.C., 2005. Floods as Catalysts for Policy Change: Historical Lessons from England and Wales. *International Journal of Water Resources Development*, 21 (4), 561–575.
- Jolma, A., Ames, D.P., Horning, N., Mitasova, H., Neteler, M., Racicot, A. and Sutton, T., 2008. Environmental modeling using open source tools. In: S. Shekhar and H. Xiong, eds. *Encyclopedia of GIS*. New York, NY: Springer-Science+Business Media, 275–279.
- Julien, P.Y., Moglen, G.E. and Sunada, G.U., 1988. *CASC Users Manual – A Finite Element Method for Spatially Varied Overland Flow Simulation*, Report No CER 87–88 GEO7. Fort Collins, CO: Colorado State University Center for Geosciences.
- Kabisch, H. and Haase, D., 2011. Diversifying European agglomerations: evidence of urban population trends for the 21st century. *Population, Space and Place*, 17 (3), 236–253.
- Kidd, C. and Levizzani, V., 2011. Status of satellite precipitation retrievals. *Hydrology and Earth System Sciences*, 15 (4), 1109–1116.
- Kidd, C., Levizzani, V. and Bauer, P., 2009. A review of satellite meteorology and climatology at the start of the twenty-first century. *Progress in Physical Geography*, 33 (4), 474–489.
- Knödel, K., Lange, G. and Voigt, H.-J., eds., 2007. *Environmental Geology: Handbook of Field Methods and Case Studies*. Berlin: Springer-Verlag.
- Kochan, D.J., 2006. Runoff and reality: Externalities, economics, and traceability issues in urban runoff regulation. *Chapman Law Review*, 9 (2), 409–433.
- Lee, K.T. and Huang, J.K., 2007. Effect of moving storms on attainment of equilibrium discharge. *Hydrological Processes*, 21 (24), 3357–3366.
- Liang, J., 2010. *Evaluation of Runoff Response to Moving Rainstorms*. Thesis (PhD). Marquette University.
- Linsley, R.K., Kohler, M.A. and Paulhus, J.L.H., 1982. *Hydrology for Engineers*. 3rd ed. New York, NY: McGraw-Hill Book Company.
- Luna, T., Rocha, A., Carvalho, A.C., Ferreira, J.A. and Sousa, J., 2011. Modelling the extreme precipitation event over Madeira Island on 20 February 2010. *Natural Hazards and Earth System Sciences*, 11 (9), 2437–2452.
- Madlener, R. and Sunak, Y., 2011. Impacts of urbanization on urban structures and energy demand: What can we learn for urban energy planning and urbanization management? *Sustainable Cities and Society*, 1 (1), 45–53.
- Maksimov, V.A., 1964. Computing runoff produced by a heavy rainstorm with a moving center. *Soviet Hydrology*, 5, 510–513.

- Marcus, N., 1968. *A Laboratory and Analytical Study of Surface Runoff Under Moving Rainstorms*. Thesis (PhD). University of Illinois at Urbana-Champaign.
- Marsalek, J., Jiménez-Cisneros, B.E., Malmquist, P.-A., Karamouz, M., Goldenfum, J. and Chocat, B., 2008. *Urban Water Cycle Processes and Interactions*. Urban Water Series Vol. 2. Paris: UNESCO/IHP.
- Marshall, R.J., 1980. The estimation and distribution of storm movement and storm structure, using a correlation analysis technique and rain-gauge data. *Journal of Hydrology*, 48 (1–2), 19–39.
- Maskey, S., 2004. *Modelling Uncertainty in Flood Forecasting Systems*. Thesis (PhD). TU Delft.
- McGee, W.J., 1897. Sheetflood erosion. *Geological Society of America Bulletin*, 8, 87–112.
- Meyer, L.D., 1988. Rainfall simulators for soil conservation research. In: R. Lal, ed. *Soil Erosion Research Methods*. Ankeny, IA: Soil and Water Conservation Society, 75–95.
- Middleton, W.E.K., 1969. *Invention of the Meteorological Instruments*. Baltimore, MD: The John Hopkins Press.
- Minda, H. and Nakamura, K., 2005. High temporal resolution path-average rain gauge with 50-GHz band microwave. *Journal of Atmospheric and Oceanic Technology*, 22 (2), 165–179.
- Mioc, D., Gengsheng L., Anton, F. and Nickerson, B.G., 2007. Decision support for flood event prediction and monitoring. *Geoscience and Remote Sensing Symposium*, 23–28 July 2007 Barcelona. IEEE International, 2439–2442.
- Mizumura, K. and Ito, Y., 2011a. Analytical solution of nonlinear kinematic wave model with time-varying rainfall. *Journal of Hydrologic Engineering*, 16 (9), 736–746.
- Mizumura, K. and Ito, Y., 2011b. Influence of moving rainstorms on overland flow of an open book type using kinematic wave. *Journal of Hydrologic Engineering*, 16 (11), 926–935.
- MWC – Melbourne Water Corporation, 2007. *Port Phillip and Westernport Region Flood Management and Drainage Strategy*. Melbourne: Melbourne Water.
- Ngirane-Katashaya, G.G. and Wheeler, H.S., 1985. Hydrograph sensitivity to storm kinematics. *Water Resources Research*, 21 (3), 337–345.
- Niemczynowicz, J., 1984a. Investigation of the Influence of rainfall movement on runoff hydrograph: Part I – Simulation on conceptual catchment. *Nordic Hydrology*, 15 (2), 57–70.
- Niemczynowicz, J., 1984b. Investigation of the influence of rainfall movement on runoff hydrograph: Part II—Simulation on real drainage basins in the City of Lund. *Nordic Hydrology*, 15 (2), 71–84.
- Niemczynowicz, J., 1987. Storm tracking using rain gauge data. *Journal of Hydrology*, 93 (1–2), 135–152.
- Niemczynowicz, J., 1988. The rainfall movement – a valuable complement to short-term rainfall data. *Journal of Hydrology*, 104 (1–4), 311–326.

- Nuissl, H., Haase, D., Lanzendorf, M. and Wittmer, H., 2009. Environmental impact assessment of urban land use transitions – a context-sensitive approach. *Land Use Policy*, 26 (2), 414–424.
- Nunes, J.P., de Lima, J.L.M.P. and Ferreira, A.J.D., 2009. Modelling the impact of urbanization on hydrological extremes. In: W. Chelmicki and J. Siwek, eds. *12th Biennial International Conference of the Euromediterranean Network of Experimental and Representative Basins (ERB)*, 18–20 September 2008 Krakow. Paris: UNESCO/IHP, 41–47.
- O’Callaghan, J.R., 1996. *Land use: the interaction of economics, ecology and hydrology*. London: Chapman & Hall.
- Ogden, F.L., Richardson, J.R. and Julien, P.Y., 1995. Similarity in catchment response 2: Moving rainstorms. *Water Resources Research*, 31 (6), 1543–1547.
- Oke, T.R., 1973. City size and the urban heat island. *Atmospheric Environment*, 7 (8), 769–779.
- Overeem, A., Leijnse, H. and Uijlenhoet, R., 2011. Measuring urban rainfall using microwave links from commercial cellular communication networks. *Water Resources Research*, 47, W12505, doi:10.1029/2010WR010350.
- Parker, D.E., 2010. Urban heat island effects on estimates of observed climate change. *WIREs Climate Change*, 1 (1), 123–133.
- Peng, G., Leslie, L.M. and Shao, Y., 2002. *Environmental modelling and prediction*. Berlin: Springer-Verlag.
- Prasad, T., 1997. GIS Applications for Flood Simulation and Management. In: B. Misra, ed. *Geographic information system and economic development: conceptual applications*. New Delhi: Mittal Publications, 49–56.
- Ran, Q., Su, D., Li, P. and He, Z., 2012. Experimental study of the impact of rainfall characteristics on runoff generation and soil erosion. *Journal of Hydrology*, 424–425, 99–111.
- Rayitsfeld, A., Samuels, R., Zinevich, A., Hadar, U. and Alpert, P., 2012. Comparison of two methodologies for long term rainfall monitoring using a commercial microwave communication system. *Atmospheric Research*, 104–105, 119–127.
- Reaney, S.M., 2003. *Modelling runoff generation and connectivity for semi-arid hillslopes and small drainage basins*. Thesis (PhD). University of Leeds.
- Rebora, N. and Ferraris, L., 2006. The structure of convective rain cells at mid-latitudes. *Advances in Geosciences*, 7, 31–35.
- Richardson, J.R. and Julien, P.Y., 1989. One-dimensional modelling of moving rainstorms. In: B.C. Yen, ed. *Catchment Runoff and Rational Formula*. Littleton, CO: Water Resources Publications, 155–167.
- Roberts, M.C. and Klingeman, P.C., 1970. The influence of landform and precipitation parameters on flood hydrographs. *Journal of Hydrology*, 11 (4), 393–411.
- Rodriguez, F., Andrieu, H. and Morena, F., 2008. A distributed hydrological model for urbanized areas – Model development and application to case studies. *Journal of Hydrology*, 351 (3–4), 268–287.

- Rydock, J.P. and Gustavsen, A., 2007. A look at driving rain spells at three cities in Great Britain. *Building and Environment*, 42 (3), 1386-1390.
- Saghafian, B. and Julien P.Y., 1995. Time to equilibrium for spatially variable watersheds. *Journal of Hydrology*, 172 (1-4), 231-245.
- Sargent, D.M., 1981. An investigation into the effects of storm movement on the design of urban drainage systems: Part 1. *The Public Health Engineer*, 9 (2), 201-207.
- Sargent, D.M., 1982. An investigation into the effects of storm movement on the design of urban drainage systems: Part 2. Probability analysis. *The Public Health Engineer*, 10 (2), 111-117.
- Satterthwaite, D., McGranahan, G. and Tacoli, C., 2010. Urbanization and its implications for food and farming. *Philosophical Transactions of the Royal Society B*, 365 (1554), 2809-2820.
- Schilling, W., 1991. Rainfall data for urban hydrology: what do we need? *Atmospheric Research*, 27 (1-3), 5-21.
- Schmitt, T.G., Thomas, M. and Ettrich, N., 2004. Analysis and modeling of flooding in urban drainage systems. *Journal of Hydrology*, 299 (3-4), 300-311.
- Sene, K., 2008. *Flood Warning, Forecasting and Emergency Response*. Berlin: Springer.
- Sharon, D., 1980. The distribution of hydrologically effective rainfall incident on sloping ground. *Journal of Hydrology*, 46 (1-2), 165-188.
- Sharon, D., Adar, E. and Lieverman, G., 1983. Observations on the differential hydrological and/or erosional response of opposite-lying slopes, as related to incident rainfall. *Israel Journal of Earth Sciences*, 32, 71-74.
- Shearman, R.J., 1977. The speed and direction of movement of storm rainfall patterns with reference to urban storm sewer design. *Hydrological Sciences Bulletin*, 22 (3), 421-431.
- Shuttleworth, W.J., 2012. *Terrestrial Hydrometeorology*. Chichester: Wiley-Blackwell.
- Singh, V. P., 1998. Effect of the direction of storm movement on planar flow. *Hydrological Processes*, 12 (1), 147-170.
- Singh, V.P. and Fiorentino, M., eds., 1996. *Geographical Information Systems in Hydrology*. Dordrecht: Kluwer Academic Publishers.
- Singh, V.P., 1997a. Effect of spatial and temporal variability in rainfall and watershed characteristics on stream flow hydrograph. *Hydrological Processes*, 11 (12), 1649-1669.
- Singh, V.P., 1997b. *Kinematic Wave Modeling in Water Resources: Environmental Hydrology*. New York, NY: John Wiley and Sons.
- Singh, V.P., 2002a. Effect of the duration and direction of storm movement on infiltrating planar flow with full areal coverage. *Hydrological Processes*, 16 (7), 1479-1511.
- Singh, V.P., 2002b. Effect of the duration and direction of storm movement on planar flow with full and partial areal coverage. *Hydrological Processes*, 16 (17), 3437-3466.

- Sivapalan, M., ed., 2006. *Predictions in ungauged basins: promise and progress*. IAHS Publication Vol. 303. Wallingford: IAHS Press.
- Smith, W.L., Bishop, W.P., Dvorak, V.F., Hayden, C.M., McElroy, J.H., Mosher, F.R., Oliver, V.J., Purdom, J.F. and Wark, D.Q., 1986. *Science*, 231 (4737), 455–462.
- Stephenson, D., 1984. Kinematic study of effects of storm dynamics on runoff hydrographs. *Water SA*, 10 (4), 189–196.
- Stewart, I.D., 2011. A systematic review and scientific critique of methodology in modern urban heat island literature. *International Journal of Climatology*, 31 (2), 200–217.
- Surkan, A.J., 1974. Simulation of storm velocity effects on flow from distributed channel networks. *Water Resources Research*, 10 (6), 1149–1160.
- Tang, W. and Davidson, C.I., 2004. Erosion of limestone building surfaces caused by wind-driven rain: 2. Numerical modeling. *Atmospheric Environment*, 38 (33), 5601–5609.
- Tang, W., Davidson, C.I., Finger, S. and Vance, K., 2004. Erosion of limestone building surfaces caused by wind-driven rain: 1. Field measurements. *Atmospheric Environment*, 38 (33), 5589–5599.
- Thurston, H.W., Taylor, M.A., Shuster, W.D., Roy, A.H. and Morrison, M.A., 2010. Using a reverse auction to promote household level stormwater control. *Environmental Science & Policy*, 13 (5), 405–414.
- Tisdale, H., 1942. The process of urbanization. *Social Forces*, 20 (3), 311–316.
- Toukourou, M., Johannet, A., Dreyfus, G. and Ayrat, P-A., 2011. Rainfall-runoff modeling of flash floods in the absence of rainfall forecasts: the case of “Cévenol flash floods”. *Applied Intelligence*, 35 (2), 178–189.
- Townson, J.M. and Ong, H.S., 1974. A laboratory study of runoff caused by line storm moving over a conceptual catchment. *Water Services*, Aug, 266–269.
- Umback, C.R. and Lembke, W.D., 1966. Effect of wind on falling water drops. *Transactions of the ASABE*, 9 (6), 805-808.
- USEPA – United States Environmental Protection Agency, 2003. *Guidance Specifying Management Measures for Sources of Nonpoint Pollution in Coastal Waters*. EPA 840-B-92-002. Washington, DC: USEPA Office of Water.
- UN – United Nations, 2011. *Population Distribution, Urbanization, Internal Migration and Development: An International Perspective*. ESA/P/WP/223. New York, NY: UN Publication.
- USNWS – United States National Weather Service, 2002. *Definitions and general terminology*. NWS Manual 10–950. Silver Spring, MD: NWS.
- Valette, G., Prévost, S., Léonard, J. and Lucas, L., 2012. A virtual discrete rainfall simulator. *Environmental Modelling & Software*, 29 (1), 51–60.

- van Hooff, T., Blocken, B. and van Harten, M., 2011. 3D CFD simulations of wind flow and wind-driven rain shelter in sports stadia: Influence of stadium geometry. *Building and Environment*, 46 (1), 22–37.
- van Lanen, H.A.J., Fendeková, M., Kupczyk, E., Kasprzyk, A. and Pokojski, W., 2004. Flow Generating Processes. In: L.M. Tallaksen and H.A.J. van Lanen, eds. *Hydrological Drought – Processes and Estimation Methods for Streamflow and Groundwater*. Developments in Water Science No. 48. Amsterdam: Elsevier Science B.V., 53–96.
- van Loon, E.E., 2001. *Overland flow: interacting models with measurements*. Thesis (PhD). Wageningen University.
- Veldkamp, A. and Fresco, L.O., 1996. CLUE: a conceptual model to study the Conversion of Land Use and its Effects. *Ecological Modelling*, 85 (2–3), 253–270.
- Vivoni, E.R., Entekhabi, D., Bras, R.L. and Ivanov, V.Y., 2007. Controls on runoff generation and scale-dependence in a distributed hydrologic model. *Hydrology and Earth System Sciences*, 11(5), 1683–1701.
- Wallace, J.M. and Hobbs, P.V., 2006. *Atmospheric science: an introductory survey*. 2nd ed. London: Academic Press.
- Walsh, C.J., Fletcher, T.D. and Ladson, A.R., 2005. Stream restoration in urban drainage basins through redesigning stormwater systems: Looking to the drainage basin to save the stream. *Journal of the North American Benthological Society*, 24 (3), 690–705.
- Wang, G.-T. and Chen, S., 1996. A linear spatially distributed model for a surface rainfall-runoff system. *Journal of Hydrology*, 185 (1–4), 183–198.
- Wang, P.K. and Pruppacher, H.R., 1977. Acceleration to terminal velocity of cloud and raindrops. *Journal of Applied Meteorology*, 16 (3), 275–280.
- Watts, L.G. and Calver, A., 1991. Effects of spatially-distributed rainfall on runoff for a conceptual catchment. *Nordic Hydrology*, 22 (1), 1–14.
- Weng, Q., 2001. Modeling urban growth effects on surface runoff with the integration of remote sensing and GIS. *Environmental Management*, 28 (6), 737–748.
- Wu, J., 2010. Urban sustainability: an inevitable goal of landscape research. *Landscape Ecology*, 25 (1), 1–4.
- Yen, B.C. and Chow, V.T., 1968. *A Study of Surface Runoff Due to Moving Rain Storms*. Civil Engineering Studies, Hydraulic Engineering Series No. 17. Champaign, IL: University of Illinois at Urbana-Champaign.
- Yen, B.C. and Chow, V.T., 1969. A laboratory study of surface runoff due to moving rainstorms. *Water Resources Research*, 5 (5), 989–1006.
- Yuan, F. and Bauer, M., 2007. Comparison of impervious surface area and normalized difference vegetation index as indicators of surface urban heat island effects in Landsat imagery. *Remote Sensing of Environment*, 106 (3), 375–386.

Zarmi, Y., Asher, J.B. and Greengard, T., 1983. Constant velocity kinematic analysis of an infiltrating microcatchment hydrograph. *Water Resources Research*, 19 (1), 277–283.

Zinevich, A., Messer, H. and Alpert, P., 2009. Frontal Rainfall Observation by a Commercial Microwave Communication Network. *Journal of Applied Meteorology and Climatology*, 48 (7), 1317–1334.

CHAPTER 3

Floods are natural phenomena which cannot be prevented. However, some human activities (such as increasing human settlements and economic assets in floodplains and the reduction of the natural water retention by land use) and climate change contribute to an increase in the likelihood and adverse impacts of flood events.

The European Parliament and the Council

3. EVOLUTION OF URBANIZATION IN A SMALL URBAN BASIN: DTM CONSTRUCTION FOR HYDROLOGIC COMPUTATION

Abstract: The expansion of the urban area (urbanization), which increases impervious areas like roads, car parks and buildings (roofs), has a major influence on urban flooding caused by high intensity rainfall events. Population and urban expansion go hand in hand and hence the risks to people and property rise. A Digital Terrain Model (DTM) of an area located in the south of Portugal (Cabanas de Tavira, Tavira) was conceived and developed with the objective of implementing a computational hydrological simulation tool. This area has seen a noteworthy increase in urban occupancy. As the natural drainage system, which largely consists of two flow lines, cannot drain the flow caused by intense precipitation flooding frequently occurs. The flow lines obtained with this DTM show small differences compared with those inferred from the available cartography, indicating that the DTM can be a suitable approximation to the real topography.

Keywords: GIS; DTM; Urbanization; Hydraulic computation

3.1 INTRODUCTION

The expansion of urban area promotes the increase of impervious areas. This fact, in association with several urban drainage systems that are currently in use, will enhance the magnitude and recurrence of floods, because those systems were not conceived for such soil occupation conditions. Adding to this, local effects of urbanization on the climate are important, causing surface and atmospheric changes due to the existence of new surface materials, the construction of buildings, roads and other infrastructures promoting energy and water exchanges and airflow (Grimmond, 2007). This paper presents the first phase of a study on the influence of urbanization on urban flooding as a consequence of high intensity rainfall events. It focuses on the construction of a Digital Terrain Model (DTM) of the actual situation in a small drainage basin in the south of Portugal with a Mediterranean climate, where impervious areas have been increasing. This growth has been especially marked in the last few years with the construction of urban tourism infrastructure in Cabanas de Tavira, Algarve, in the form of tourist apartments and resorts. This DTM was

conceived and developed with the goal of creating a computational hydrological simulation tool for the basin.

The natural drainage system is mainly composed of two small watercourses (Ribeira da Canada and Ribeira do Pocinho), which demonstrably have insufficient capacity to transport storm water, frequently leading to flooding.

The use of GIS techniques provides better hydrological models since they give a more reliable representation of physical features and processes (*e.g.*, Brandt *et al.*, 2004; Efstratiadis *et al.*, 2008) and DTMs are among the most important data sources for deriving variables used by hydrologic and hydraulic models (Bales and Wagner, 2009). Even taking into consideration all their associated uncertainties (Wechsler, 2006), GIS-based models have recently been adapted for use in flood forecast and flood management (*e.g.*, Dietrich *et al.*, 2008).

The next stage will see the inclusion of algorithms for rainfall–runoff and associated transport process modelling, and then simulations of the urban tissue in different years will be performed.

3.2 STUDY AREA DESCRIPTION

Cabanas de Tavira is a parish and a former fishing village in the municipality of Tavira, Algarve, Portugal. With around 1000 permanent residents, it has become a popular tourist destination, mainly in summer, because of its white sand beach, Praia de Cabanas, located on an island which is part of the Ria Formosa Natural Park. Fishing and tourism are the principal economic activities.

Cabanas de Tavira is located near the coastline of the east side of Algarve, the southernmost district of Portugal (Figure 3.1).

Portuguese military maps (2005) and field observation show that two watercourses can be defined: Ribeira da Canada and Ribeira do Pocinho, respectively W and E of Cabanas de Tavira (Figure 3.2). Ribeira da Canada has a basin area of around 3.8 km², a main stream length of 10.9 km with an average slope of 1.0%. Ribeira do Pocinho has a basin area of around 1.1 km² and a main stream length of 1.5 km with an average slope of 1.5%.

Land use is essentially pastures and orchards on the upper areas of the basins and urban development's on the lower, covering approximately one third of the total basin area.



Figure 3.1 Location of Algarve and Cabanas de Tavira in the south of Portugal.

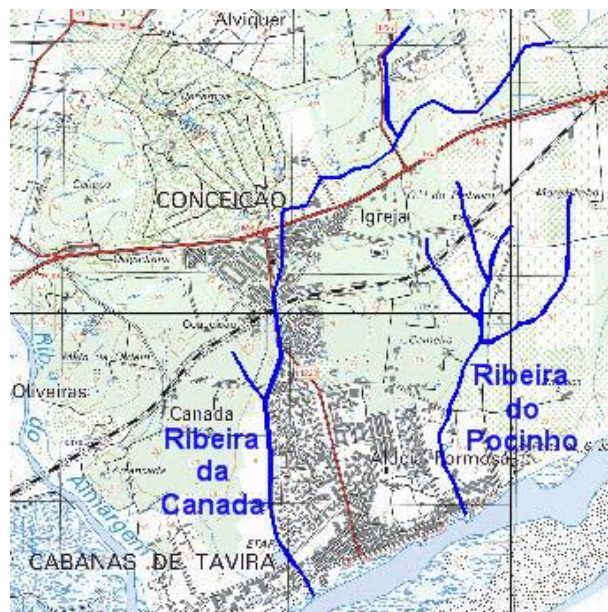


Figure 3.2 Water courses in the Cabanas de Tavira urban area.

3.3 GEOGRAPHICAL INFORMATION SYSTEM MODEL

3.3.1 GEOGRAPHICAL DATABASE

A database was created from data available in miscellaneous formats from different sources. This database integrates a topographic numerical model established by a Triangulated Irregular Network (TIN) and six sets of vectorial geo-objects. Each set

was created according to the type of geometrical element used in the representation – point, line, polygon – and in the nature of the represented entities.

For simplification, we shall generally refer to each set of data as a “theme”, both for geo-objects and for the DTM itself. Each theme forms one layer or parcel of representation (necessarily incomplete) of the occurrences considered in this work.

The six vector themes are: (a) two themes of points (one with a sample of elevation points and another with the position of existing trees); (b) three themes of linear elements (data related to the roads, railways and a sample of equidistant level curves, 1.0 m apart); (c) one theme of polygons (representing the area occupied by buildings).

3.3.2 DTM CONSTRUCTION

The TIN integrating the geographical database was constructed from a topographic numerical model defined by a set of elevation points and by a sample of equidistant level curves 1.0 m apart, provided by a topographic survey carried out in 2002, by photogrammetric restitution. “Hard breaklines” (rupture lines associated with discontinuities on the surface slope) were not considered for the construction of this TIN.

Breaklines are an important resource for TIN definition. Because triangle edges cannot intersect those lines, it is possible to generate a more accurate topographic surface. This simplification was adopted in this first phase of work, but in future developments the TIN will have to be reconstructed and applied in detailed hydrological models in order to incorporate the discontinuities associated with roads and railways.

The DTM obtained, represented by the TIN, matches a topologically validated three-dimensional surface where there are no gaps or overlaps between adjacent triangles, thus allowing the identification of the main elements of a topographic surface: slopes, valleys and ridges.

3.3.3 DRAINAGE NETWORK REPRESENTATION

Bearing in mind the goals of this work and the set of spatial analysis tools available, the software is operating with the data sets expressed in matrix format. A GRID numerical surface model, with 0.5 m resolution, was built by converting the TIN (Figure 3.3a). GRID is a geo-referenced matrix form implemented in ArcGis software.

The resulting image, which contains some depressions as a consequence either of the natural terrain configuration or of errors made during the classification of cartographic elements, was then analysed. The depressions were corrected to achieve a more consistent surface flow model. Using this model, flow directions (Figure 3.3b) and flow accumulation areas were estimated in order to define valleys and consequently flow lines (Figure 3.3c). Flow lines become apparent in those valleys and they are represented and classified according to Strahler's classification, which defines the hierarchy for the drainage network. Using these elements it was then possible to identify and delimit all the sub-basins that contributed to the respective flow lines.

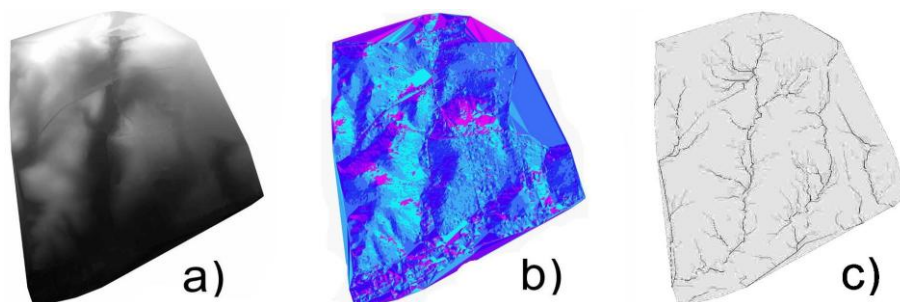


Figure 3.3 Drainage network: (a) GRID; (b) flow directions; and (c) flow lines.

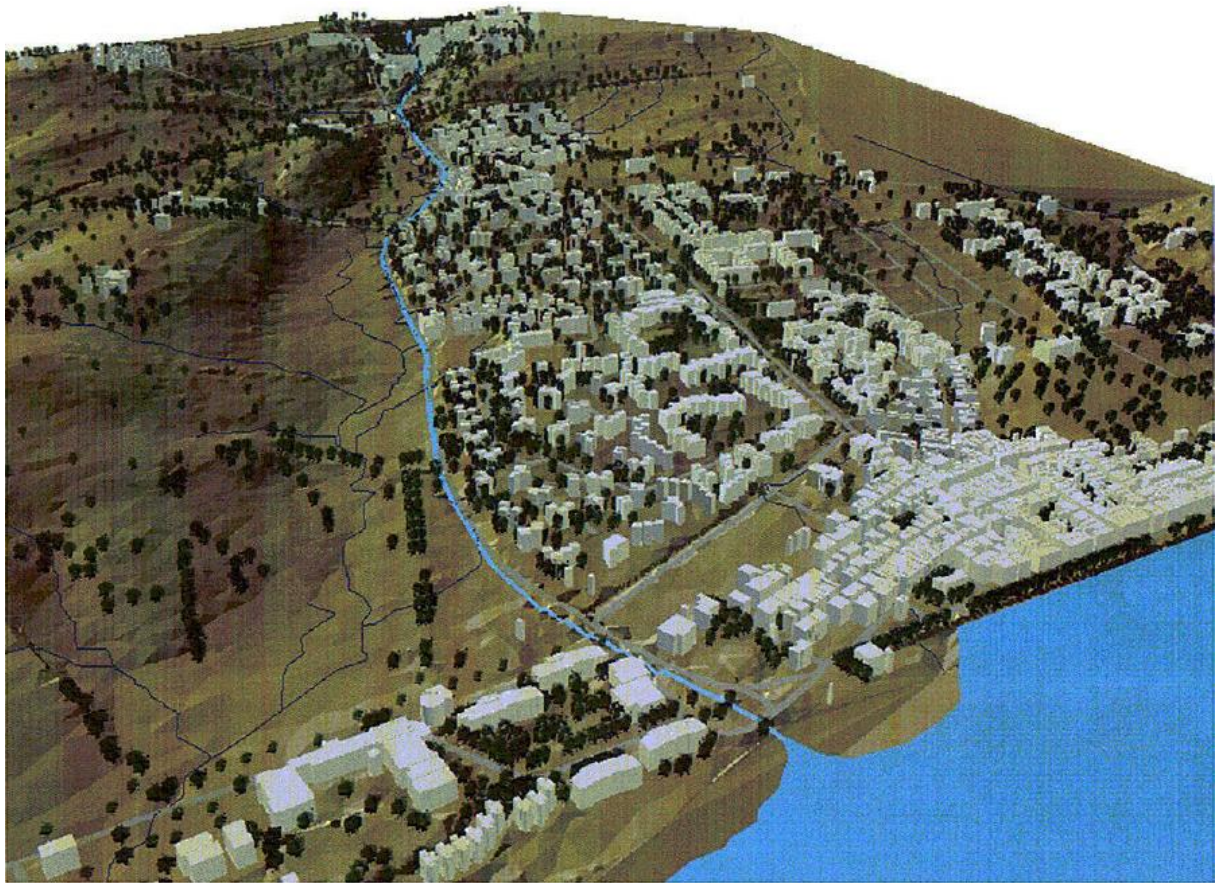


Figure 3.4 Cabanas de Tavira GIS image.

A combination of the geographical model with the drainage network is presented in Figure 3.4.

3.4 EVOLUTION OF THE URBAN AREA

The development of the urban area in Cabanas de Tavira can be seen from aerial photographs (Figure 3.5). Urban areas were defined by using a CAD tool and were classified as “High Density Area” if the area is mainly occupied by buildings and roads and “Medium Density Area” if the area is occupied by a lower density of constructions with significant areas of gardens and parks.

The urban occupation has expanded considerably in Cabanas de Tavira in the last few years, leading to higher peak discharges and recurrent flood events, as shown from the analysis of historical records. A comprehensive hydro-meteorological network is presently being installed in the drainage basin in order to calibrate hydrological

models which will provide a better insight into the impact of urbanization on small urban basins in the south of Portugal.



Figure 3.5 Development of the urban area in Cabanas de Tavira from 1991 to 2005 (see also Table 3.1).

Table 3.1 Development of the urban area of Cabanas de Tavira over about 15 years.

Year	High density area (km ²)	Medium density area (km ²)
1991	0.21	0.19
1997	0.26	0.19
2002	0.36	0.23
2005	0.39	0.24

Table 3.1 shows areas of high and medium density construction over a period of about 15 years. The increase in these values leads to higher runoff coefficients and therefore to the more frequent and intense urban flooding of the village Cabanas de Tavira.

It can be seen that the urban area has suffered an increment of more than 50% in the last 15 years. With this kind of information DTMs can be adapted according to the chronological evolution of urbanization, thus allowing the analysis and interpretation of hydrological consequences.

3.5 FLOOD EVENT EXAMPLE

On the 2nd October 2007 there was continuous rainfall in Cabanas de Tavira from 05:00am until 10:30am, with the highest intensity from 07:45am until 08:45am. The Doppler radar images of the storm obtained from the *Instituto Nacional de*

Meteorologia (Portuguese Meteorological Office) showed rainfall intensities exceeding the 20 mm/h level.

Cabanas de Tavira suffered from flooding during the period of higher rainfall intensity, when the tide was low (drainage of the lower urban areas depends on the tide level) (Figure 3.6).



Figure 3.6 Flood in Ribeira do Pocinho on 2nd October 2007, next to tourist housing.

The use of a simple hydrological model (rational method) computed a peak flow of about 1.3 m³/s. Based on the Intensity-Duration-Frequency (IDF) curves for the Algarve region indicated by Portuguese legislation, the return period estimated for the event was five years. This and other events will be analysed using the hydrologic computation tool that is being developed.

3.6 CONCLUSIONS

The DTM developed seems to provide a good discretisation for application with numerical overland flow models, particularly concerning the definition of flow lines and corresponding drainage basins. The obtained flow lines exhibit small differences compared with those inferred from the available maps, showing that the generated model can be a good approximation to the real topography. Some known

discontinuity lines will be incorporated in future work and this will improve the quality of the model. The future work also aims at combining information on the evolution of urbanization with algorithms to model rainfall–runoff and associated transport processes. This will allow quantifying the influence of an increase in imperviousness on the response of an urban drainage system to intense precipitation events of various return periods.

3.7 ACKNOWLEDGEMENTS

This study was undertaken with the support of projects PTDC/GEO/73114/2006, PTDC/CLI/67180/2006 and PTDC/ECM/70456/2006 from the Portuguese Foundation for Science and Technology (FCT – Fundação para a Ciência e a Tecnologia – www.fct.mctes.pt/).

3.8 REFERENCES

- Bales, J.D. and Wagner, C.R., 2009. Sources of uncertainty in flood inundation maps. *Journal of Flood Risk Management*, 2, 139–147.
- Brandt, C., Robinson, M. and Finch, J.W., 2004. Anatomy of a catchment: the relation o physical attributes of the Plynlimon catchments to variations in hydrology and water status. *Hydrology and Earth System Sciences*, 8 (3), 345–354.
- Dietrich, J., Trepte, S., Wang, Y., Schumann, A.H., Voß, F., Hesser, F.B. and Denhard, M., 2008. Combination of different types of ensembles for the adaptive simulation of probabilistic flood forecasts: hindcasts for the Mulde 2002 extreme event. *Nonlinear Processes in Geophysics*, 15, 275–286.
- Efstratiadis, A., Nalbantis, I., Koukouvinos, A., Rozos, E. and Koutsoyiannis, D., 2008. HYDROGEIOS: a semi-distributed GIS-based hydrological model for modified river basins. *Hydrology and Earth System Sciences*, 12, 989–1006.
- Grimmond, S., 2007. Urbanization and global environmental change: local effects of urban warming. *The Geographical Journal*, 173, 83–88.
- Wechsler, S., 2006. Uncertainties associated with digital elevation models for hydrologic applications: a review. *Hydrology and Earth System Sciences*, Discuss. 3, 2343–2384.

CHAPTER 4

4. INFLUENCE OF WIND-DRIVEN RAIN ON THE RAINFALL-RUNOFF PROCESS FOR URBAN AREAS: SCALE MODEL OF HIGH-RISE BUILDINGS

Abstract: The hydrological response of impervious urban areas with varying building densities to the combined action of wind and rain is not well understood. Exploratory laboratory simulations were conducted using a scale model of a hypothetical high density urbanized area with high-rise buildings. 72 runs were conducted for static and moving storms in upstream and downstream directions, with and without wind, for different building densities and for an average rainfall intensity of 120 mm/h. The laboratory experiments show that building density and the spatial and temporal distribution of rainfall that results from wind and storm movement have a clear influence on the hydrological response to rainstorms. Increased urbanization promotes a higher peak discharge, a longer base time and reduces the slope of the hydrographs rising limbs, while wind-driven rain attenuates these effects. Downhill storm movement promotes a faster hydrological response and a higher discharge peak than uphill movement.

Keywords: Experimental methods; Rainfall-runoff analysis; Urban flooding; Urban hydrology

4.1 INTRODUCTION

Moving storms are a natural phenomenon with a major influence on the rainfall-runoff process. Ignoring the storm movement can result in a considerable over- and underestimation of runoff volumes and peaks (*e.g.*, Maksimov, 1964; Yen and Chow, 1969; Wilson *et al.*, 1979; Jensen, 1984; Singh, 1998; de Lima and Singh, 2000; Singh, 2002; de Lima and Singh, 2002; de Lima *et al.*, 2003; Nunes *et al.*, 2006). Urban development modifies the flood hydrographs of the natural basin (Campana *et al.*, 2001; Chen *et al.*, 2009; Leandro *et al.* 2009), and it is important to understand rainfall-runoff in densely urbanized areas in order to assess pollutant and soil transport, design urban drainage and wastewater treatment systems, evaluate diffuse pollution, and also for flood control and flood management systems.

Major problems of urbanization related to urban floods are the increase of impervious areas (Hollis, 1975; Dawson, 2008) and the difficulty of forecasting urban

growth and future climate change (Mentens *et al.*, 2006; Nie *et al.*, 2009), which may cause drainage systems to become inadequate. To a smaller scale, urbanization also affects local climate (Bornstein and LeRoy, 1990; Quattrochi *et al.*, 1998; Bornstein and Lin, 2000; Gluch *et al.*, 2006; Carraça and Collier, 2007), because, for instance, the addition of new surface materials through the construction of buildings, roads and other infrastructure promotes energy and water exchange which affects local atmospheric conditions (Grimmond, 2007). Moreover, urban impervious areas produce faster hydrological responses than natural pervious areas, even for low rainfall intensity (Dayaratne and Perera, 2008), resulting in overland flow even for precipitation events with short return period (*e.g.*, $T_R=2$ years).

The urbanization impact on runoff in urban areas is documented in the literature (*e.g.*, James, 1965; Hollis, 1975; Booth, 1991) and it is still an important area of research (Farahmand *et al.*, 2007; Nunes *et al.*, 2009; Isidoro *et al.*, 2010). Urbanization has proceeded rapidly since the end of the 19th century (Antrop, 2000) and the overall percentage of the urban-dwelling population rose from 13% in 1900 to 49% in 2005, a figure expected to reach 60% in 2030 (UN, 2005). All this indicates that the total amount of urbanized land will continue to increase for some countries (Nuisl *et al.*, 2009) and that there is no end in sight for this trend (Haase, 2009).

A laboratory rainfall simulator can reproduce a large range of hydrologic conditions on a plot scale where the spatial and temporal characteristics of precipitation can be controlled (*e.g.*, de Lima *et al.*, 2002). This is important when analyzing events with high spatial and temporal variability, like moving storms. The benefits of the rainfall simulation approach have been studied by some authors when researching overland flow (*e.g.*, Meyer, 1965; Bryan and Poesen, 1989; Cerdà *et al.*, 1997) and including the analysis of the effects of urbanization growth (*e.g.*, Pappas *et al.*, 2008).

Most methods used in hydrologic studies assume a constant rain storm that arrives and disappears instantaneously over the drainage area, as opposed to natural rainfall, which is highly variable both in time and space (*e.g.*, Huff, 1967; Eagleson, 1978; Sharon, 1980; de Lima, 1998; Willems, 2001; de Lima *et al.*, 2005). These methods therefore fail to take into account the effect on the runoff response caused by a storm's movement across the drainage area. The effect of wind-driven rain on rainfall distribution is also an important issue for runoff and erosion studies (*e.g.*, Sharon *et al.*, 1983; Erpul *et al.*, 2003; Blocken *et al.*, 2006) and a topic of interest in other areas of engineering such as urban construction (*e.g.*, Choi, 1994; Kumaraperumal *et al.*, 2007; Tariku *et al.*, 2008).

The objective of this scaled study was to quantify and describe the influence of the density of high-rise buildings in impervious urban areas on the rainfall-runoff process, under wind-driven rain. Regarding the scaled model, the term 'density of high-rise buildings' refers to the percentage of catchment area occupied by buildings of a similar height. Experiments were carried out using a 1:100 scale model of a hypothetical high density urbanized area with high-rise buildings and a rainfall simulator. The simulations included static and dynamic rainfall (moving upstream from and downstream to the catchment outlet), for different building densities.

4.2 RAINFALL SIMULATOR AND SCALE MODEL

The laboratory apparatus consisted of a rainfall simulator attached to a moving structure (Figure 4.1a), above a hypothetical 1:100 scale model of a high density urbanized area with high-rise buildings (Figure 4.1b). A discharge measuring system (water level pressure transducer placed at the bottom of a cylindrical reservoir) allowed data collection at 1.0 s intervals via a computer (Figure 4.1c). Each component is described below.

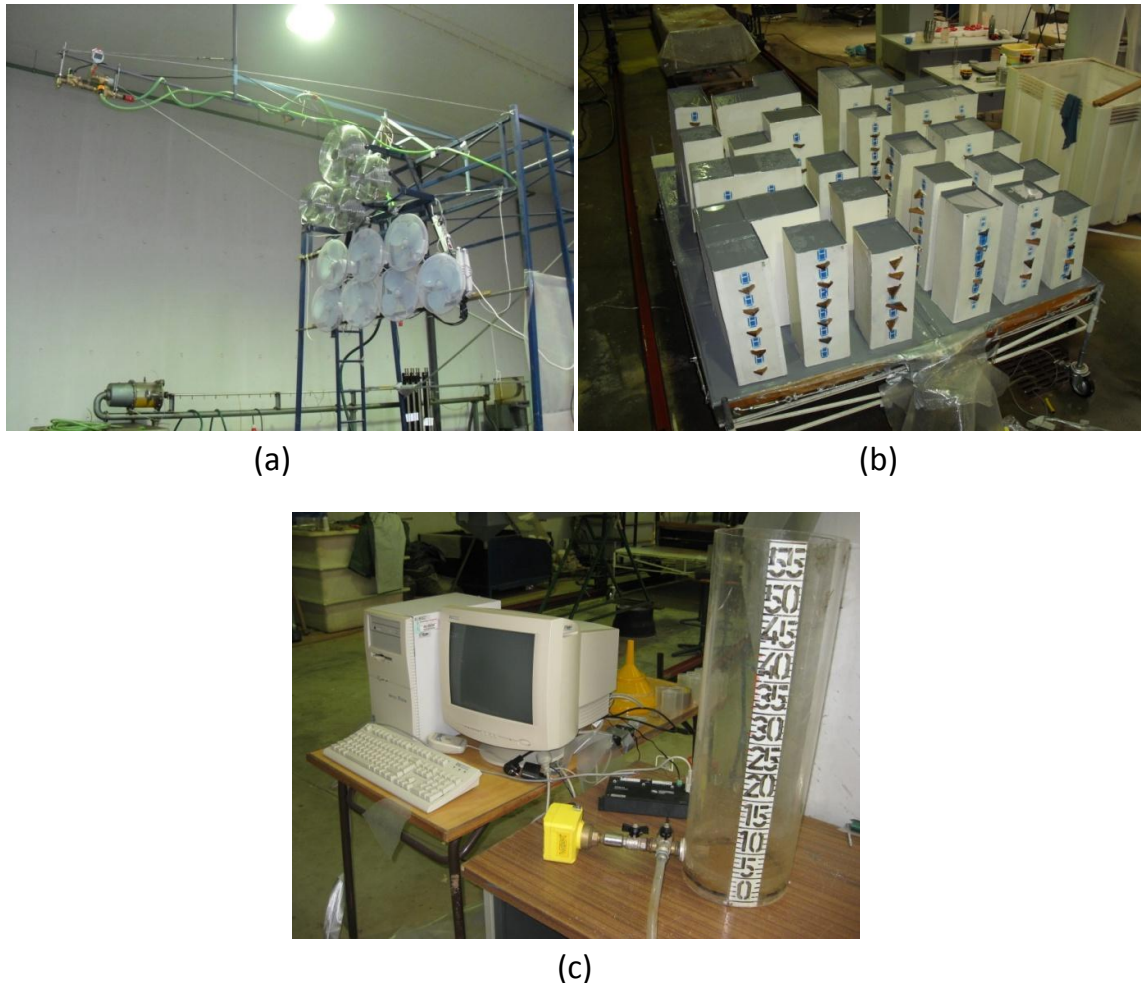


Figure 4.1 Rainfall simulator and electric fan system on a structure (a), scale model of a hypothetical high density urbanized area with high-rise buildings (b) and static pressure meter placed at the bottom of a cylindrical reservoir and data collecting system (c).

4.2.1 THE RAINFALL SIMULATOR SYSTEM

The rainfall simulator system comprises a constant water level reservoir, a pump and a set of flexible rubberized hoses (pressurized system). The structure bearing the rainfall simulator moves along 2 rails. It is powered by 2 electric motors and operated by a control panel. The pressurized system outlet is a sprinkler system with 1 downward-oriented full-cone nozzle (Spraying Systems Co.) equipped with a flow control valve and pressure gauge.

Moving storms are restricted to forward and backward movements on the rails and are automatically controlled by a switch panel. The effect of wind on rainfall is simulated by a set of 11 fans mounted on the upper part of the moving structure. The flow control valve and pressure gauge are attached to a rod connected to the moving structure. The relative position of the fans and the nozzle does not change when the

assembly moves. Further details on the rainfall simulator can be found in de Lima and Singh (2003).

To assure constant pressure on the nozzle from the start to the end of the rainfall event, the hydraulic system presented in Figure 4.2 was added to the downstream end of the pressurized system. It comprises a pressure reduction valve after the water intake (via a reinforced plastic hose), followed by a T junction with 2 outflow sections: one with a remote controlled retention valve followed by the full-cone nozzle, and another with a pressure gauge and a valve to cause a local head loss, followed by a return hose. The pressure reduction valve after the water intake prevents the loss of pressure in the system caused by hose elasticity, and so ensures a constant pressure level throughout each rainfall event. The return hose is controlled by the head loss valve eliminating excess pressure when the electric retention valve is closed. Since the regulated pressure in the head loss valve is slightly lower than that regulated in the pressure reduction valve, a constant flow drains continuously in the return hose. This flow is negligible compared with the rainfall sprayed on the scale model.

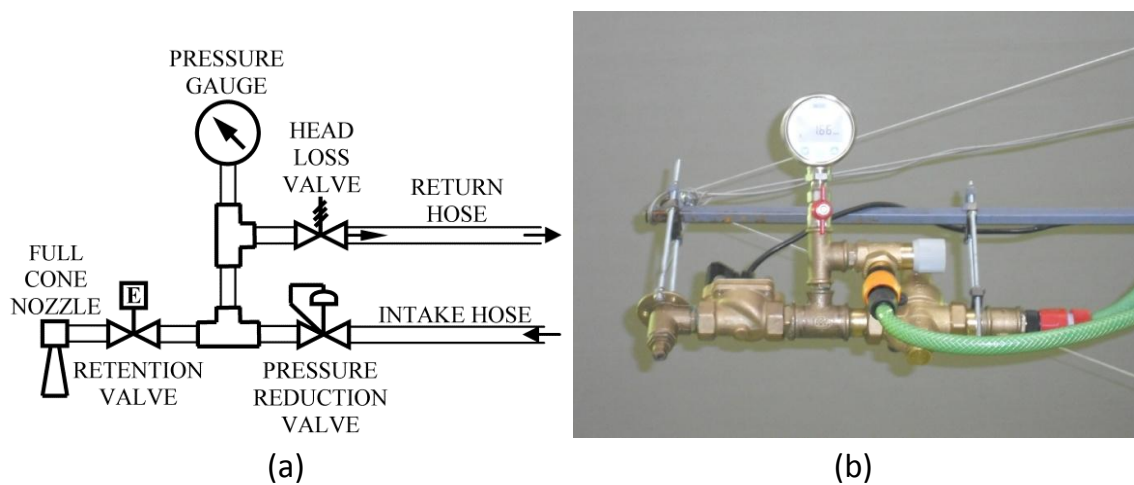


Figure 4.2 Constant pressure nozzle: hydraulic system scheme (a) and photograph of the operating system (b).

4.2.2 THE SCALE MODEL

A 1:100 scale physical model was built to represent a hypothetical urban area of $200 \times 200 \text{ m}^2$, with a high density of high-rise buildings (rectangular three dimensional elements representing medium to large buildings of approximately 20 storeys), with an average h/b ratio of building height to street width of approximately 4:1 (Figure 4.3). Scale model longitudinal and transversal slopes are, respectively, 10.0% and

2.5%, consisting of one longitudinal and three transversal semicircular (15 mm radius) surface drains (Figure 4.4c).

The model's bottom surface was made of medium density fibreboard (MDF) for the structural elements and particleboard for the coatings. Panels of painted extruded polystyrene were glued to the particleboard revetment in order to allow the scale buildings to be fitted and removed. Elements representing the buildings were made from plywood. Both buildings and pavements were painted to provide an impervious surface with similar surface roughness.

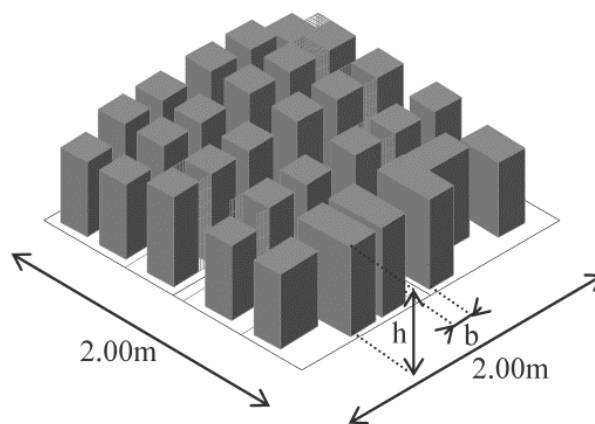


Figure 4.3 Scale model: conceptual representation of building elements.

4.2.3 THE FLOW METER AND DATA COLLECTION SYSTEM

To obtain the overland flow hydrographs for each rainfall event a cylindrical reservoir 0.14 m in diameter and 0.60 m deep was placed at the outlet of the scale model. The reservoir had a high-sensitivity pressure transducer (VEGA Bar 20) connected to a data logger (Campbell Scientific Ltd. CR510) with a collection interval of 1.0 s. This system was linked via a RS232 interface (Campbell Scientific Ltd. SC32A) to a computer (Intel Pentium III processor, 640 MB RAM) enabling the continuous monitoring of the sensitivity pressure measurements and data logging.

4.3 METHODOLOGY AND SIMULATIONS

A series of laboratory simulations were conducted to obtain the hydrographs in the hypothetical scale model basin. Flood hydrographs were obtained for the following conditions: with or without wind (use of the electric fans); upstream, downstream or

static rain (regulating the structure movement with the switch panel); density of buildings (different number of buildings); downhill or uphill storm movement (storm moving in the main slope direction, downwards or upwards). With this experimental setup it was possible to reconstitute the complete flood hydrographs at the outlet of the scale model.

In order to study the flood hydrographs and limit to a manageable size the number of parameters studied, the following assumptions were taken into account: the area in the scaled model was set impermeable, a single rainfall pattern with a constant moving velocity was defined, and both buildings and pavements were set with the same surface roughness. This allows to isolating the influence of storm movement, wind-driven rain and density of buildings on the shapes of the flood hydrographs, while other factors such as catchment characteristics, land use and soil moisture are kept constant.

4.3.1 CALIBRATION AND VALIDATION

Prior to the rainfall-runoff simulations and data collection, the sensitivity of the pressure transducer was calibrated and validated in order to guarantee the data's accuracy (minute, second, pressure). The range which provided the correct measurements was found to be 100-475 mm (Figure 4.1c). This was obtained by checking the quality fitting of a trend line to the data collected previously.

In order to achieve comparable flood hydrographs, a number of preliminary tests were run to guarantee that the same volume of water was discharged for each simulation. This depended on: (1) the duration of the rainfall event, (2) wind effect for the static simulations (the structure being motionless), (3) structure movement and (4) effect of wind for the dynamic simulations (with the structure in motion). For the static simulations the duration of the rainfall (T_r) was set to 55 s and 74 s, and for the dynamic simulations the structure was set to move at 4.2×10^{-2} m/s and 4.0×10^{-2} m/s, respectively for the scenarios without wind and with wind. These values were set to guarantee a total runoff volume of 7.2 litres (which assured that all pressure measurements were within the previously established range). Accordingly to the exposed, the simulator speed and the duration of rainfall over the scale model is expressed in Table 4.1. For the static simulations the duration of rainfall equals the period in which the nozzle valve is opened, while for the dynamic simulations, it

equals the time that each rainfall cell takes to completely cross the scale model (obtained by the cell length/structure velocity ratio).

Table 4.1 Duration of rainfall and simulator speed for different storm scenarios.

Storm movement	Existence of wind	Duration of rainfall (s)	Simulator speed ($\times 10^{-2}$ m/s)
Static	Without wind	55	0.0
Static	With wind	74	0.0
Dynamic	Without wind	52	4.2
Dynamic	With wind	113	4.0

4.3.2 RAINFALL SPATIAL DISTRIBUTION

Two rainfall spatial distributions (rainfall cells) were used: all simulations without wind distribution were approximately symmetrical (Figure 4.4a) and all simulations with wind distribution were distorted (Figure 4.4b). The simulator produced the same discharge for the entire set of experiments. Differences at the scale model level, for static and moving storms, are only in the spatial and temporal distribution of rainfall intensity as the total precipitated volume obtained was approximately the same in all the scenarios. The storm movement, upstream and downstream, was assumed constant and reproduced by displacing one of these rainfall cells across the scale model. Upstream storm refers to the movement of the rainfall simulator nozzle, along the middle axis of the scale model, from the lowest point (outlet) to the highest. Downstream refers to movement of the rainfall simulator nozzle in the opposite direction (Figure 4.4c). During the dynamic simulations, the rainfall simulator travelled the entire length of the rail system, allowing the rainfall cell to cross over the full extension of the scale model.

Rainfall intensity was determined by the nozzle size and type, the water pressure and the height of nozzle above the model's surface. The operating pressure, registered on the pressure gauge, was set at 145 kPa. The vertical distance from the nozzle to the middle point of the scale model surface was 2.0 m. The average rainfall intensity was 120 mm/h. The spatial variation of the rainfall intensity was obtained by weighing the water captured, for a 4 min duration rainfall, in a 0.3 m spaced grid of uniformly arranged receptacles that covered all the rainfall-affected area. This measurement was taken 3 times for both rainfall distributions, to obtain statistical representativeness. The diameter and fall velocity ranges of raindrops, measured at the scale model level by means of a laser precipitation monitor (Thies LPM), were 0.125-3.000 mm and 0.2-6.6 m/s. The most frequent measurements were 0.750 mm

and 3.4 m/s, respectively. The values are within the range found in literature (e.g., Coutinho and Tomás, 1995)

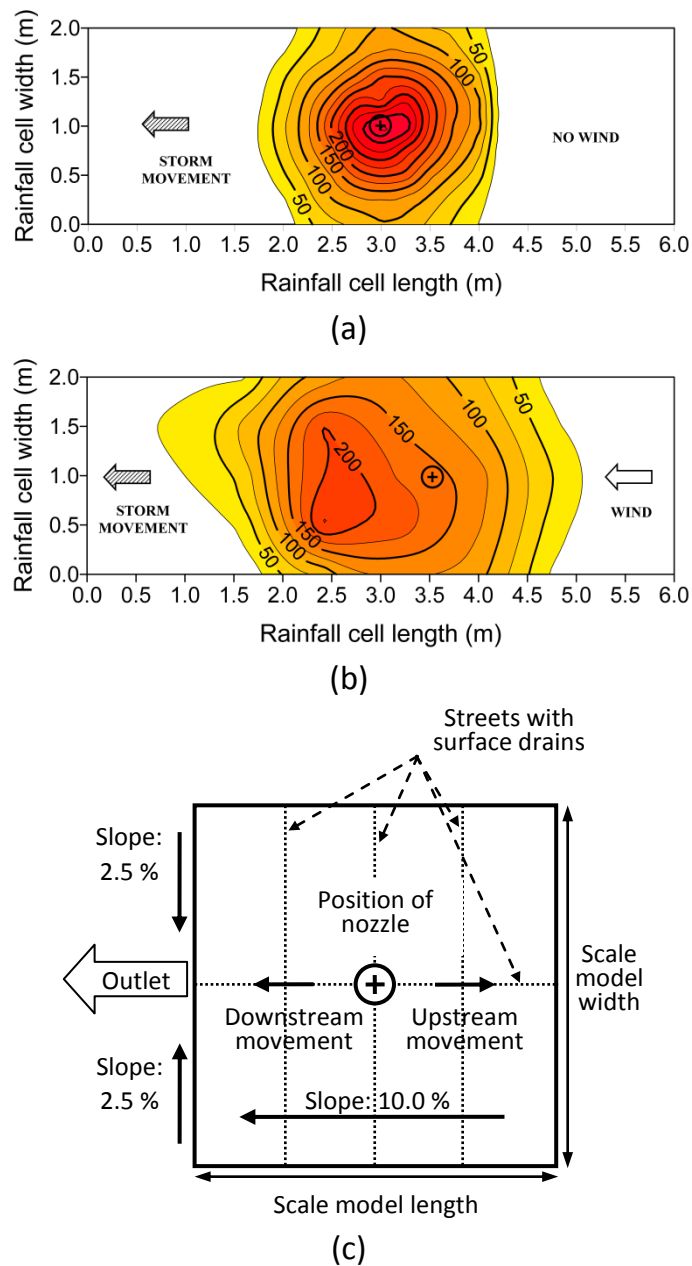


Figure 4.4 Distribution of simulated rainfall intensity (isohyets every 25 mm/h) under the nozzle: without wind (a); with wind (b). Sketch of rainfall cell movement along the scale model (c).

4.3.3 WIND CHARACTERIZATION

The wind velocity fields were obtained by an anemometer (Deuta-Werke ANEMO) placed at different grid points on an orthogonal mesh. The mesh of 0.15 m spaced grid points was spatially established (with thin nylon lines). The sides of the grids

were 2.0 m and the wind speed was measured at all the grid points (Figure 4.5). The measured values are within the range found in literature (e.g., Shearman, 1977).

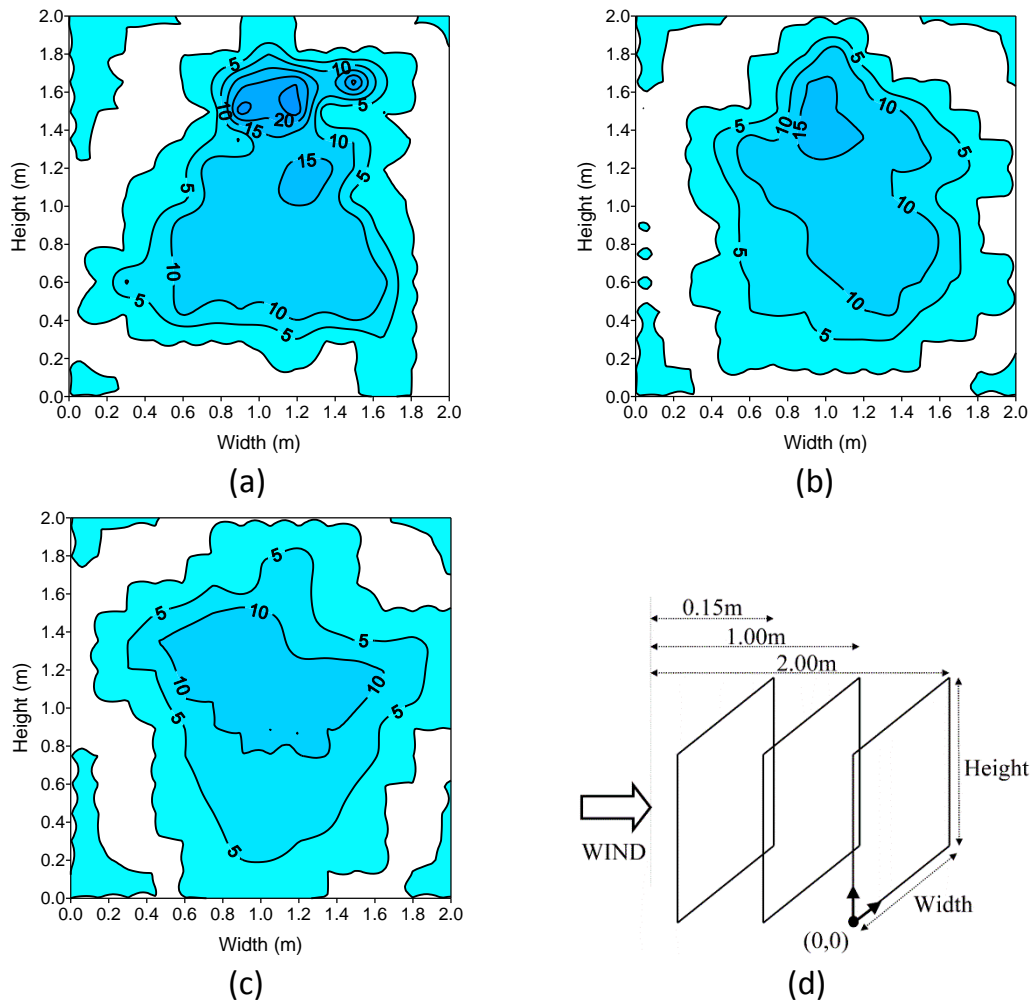


Figure 4.5 Wind speed fields at 0.15 m (a), 1.00 m (b) and 2.00 m (c), from the fans. Sketch of wind speed fields' positions relative to the fans (d).

4.3.4 SIMULATED STORM SCENARIOS

The influence of high-rise buildings on the rainfall-runoff process in (impervious) urban areas, in wind-driven rain conditions, was studied by performing simulations to obtain the flood hydrographs for each combination of different scenarios (Table 4.2). Each simulation was repeated 3 times for statistical representativeness, with a total of 72 events being simulated.

Table 4.2 Scenarios used in the simulations.

Storm movement	Existence of wind	Density of high-rise buildings (%)	Storm movement direction
Static	Without wind	0.0	Uphill
Dynamic	With wind	12.5	Downhill
		25.0	
		37.5	

The density of high-rise blocks was changed by placing these blocks in specific areas of the model (Figure 4.6). This occupancy was defined with the purpose of obtaining a similar density of buildings throughout the model for all the simulated scenarios.

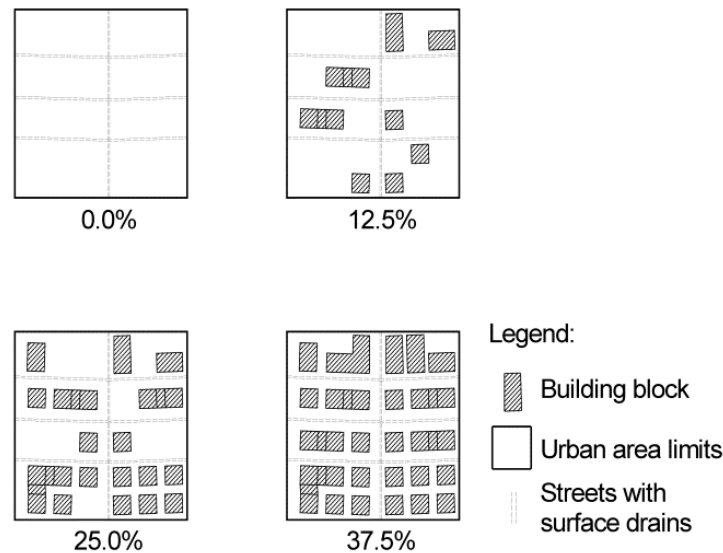


Figure 4.6 Density of the high-rise building blocks used on the scale model.

Each simulation started 15 minutes after the end of the previous event, so that the moisture content of the scale model was approximately the same for all scenarios. In fact, because of the scaled model slope and impervious surface, only a few water drops remained in the surface after each precipitation event due to the water surface tension and viscosity forces. Thus, the initial moisture content had negligible effect on the flood hydrographs. Before the first simulation in each session, the scale model was dampened by the rainfall simulator for 5 minutes, followed by a 15-minute drying period. For each simulation, the time interval from the instant the first raindrop touched the model until the establishment of runoff was measured and registered manually.

4.4 RESULTS AND DISCUSSION

The information acquired by the data collection system was plotted into a series of flood hydrographs, which were used to determine the following variables (Figure 4.7): Time to peak (T_p), is the time it takes since the initiation of flow at the scale model outlet until the highest discharge is attained; Base time of runoff (T_b), is the time it takes since the initiation of flow at the scale model outlet until a zero discharge is measured; Peak discharge (Q_p), is the highest measured discharge value; Average discharge (Q_m), is the total discharged volume per time unit during the base time of runoff; Angle between the rising limb of the hydrograph and the horizontal axis (α), is the angle between the time axis (horizontal axis) and the rising limb of the hydrograph, measured on the hydrograph itself. T_r is the duration of the rainfall event.

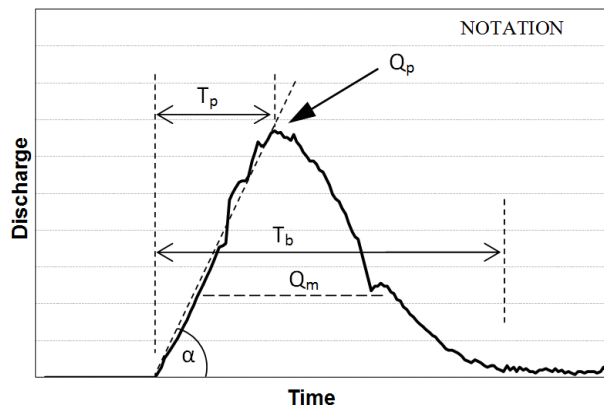


Figure 4.7 Notation used to define the hydrologic variables obtained through the experimental hydrographs.

The variables obtained are summarized on Table 4.3. For the same total volume of rainfall the presence of buildings causes a slower hydrologic response and reduces discharge peaks. Higher construction density promotes the collision of raindrops into buildings' walls and roofs, increasing the travel time of overland flow.

Table 4.3 Observed peak discharge, time to peak discharge, slope of the rising limb of the hydrograph, base time of runoff and average discharge, for all the experimental runs.

Simulated storm scenario	Without wind					With wind				
	$Q_p^{(a)}$	$T_p^{(b)}$	$\alpha^{(c)}$	$T_b^{(d)}$	$Q_m^{(e)}$	$Q_p^{(a)}$	$T_p^{(b)}$	$\alpha^{(c)}$	$T_b^{(d)}$	$Q_m^{(e)}$
Static storm Density: 0.0%	0.141	19	0.49	90	0.08	0.108	21	0.37	109	0.07
Static storm Density: 12.5%	0.122	26	0.26	103	0.06	0.099	25	0.26	124	0.06
Static storm Density: 25.0%	0.113	31	0.22	124	0.05	0.094	39	0.14	133	0.05
Static storm Density: 37.5%	0.118	43	0.16	134	0.05	0.089	45	0.12	165	0.04
Uphill moving storm Density: 0.0%	0.122	69	0.16	123	0.05	0.106	76	0.10	150	0.05
Uphill moving storm Density: 12.5%	0.108	73	0.14	139	0.05	0.094	77	0.08	157	0.04
Uphill moving storm Density: 25.0%	0.101	71	0.12	154	0.04	0.078	79	0.07	164	0.04
Uphill moving storm Density: 37.5%	0.092	79	0.11	157	0.04	0.078	79	0.07	178	0.04
Downhill moving storm Density: 0.0%	0.139	72	0.23	105	0.06	0.108	65	0.13	139	0.05
Downhill moving storm Density: 12.5%	0.129	73	0.19	108	0.06	0.097	74	0.10	145	0.04
Downhill moving storm Density: 25.0%	0.106	73	0.17	125	0.05	0.087	65	0.09	153	0.04
Downhill moving storm Density: 37.5%	0.104	82	0.13	134	0.05	0.080	78	0.08	166	0.04

(a) Q_p – Peak discharge ($\times 10^{-3} \text{ m}^3/\text{s}$).

(b) T_p – Time to peak (s).

(c) α – Angle between the rising limb of the hydrograph and the horizontal axis ($^\circ$).

(d) T_b – Base time of runoff (s).

(e) Q_m – Average discharge ($\times 10^{-3} \text{ m}^3/\text{s}$).

Increased building densities reduced the peak discharge. This effect is minimized by the effect of wind-driven rain (Table 4.3). As an example of this, comparing the 37.5% building density and the scenarios without buildings, the peak discharge falls (values in $\times 10^{-3} \text{ m}^3/\text{s}$) from 0.141 to 0.118 (16%), 0.122 to 0.092 (25%) and 0.139 to 0.104 (25%) respectively for the static, uphill and downhill storms (without wind), and from 0.108 to 0.089 (18%), 0.106 to 0.078 (26%) and 0.108 to 0.080 (26%) respectively for the static, uphill and downhill storms (with wind).

The steepness of the rising limb of the flood hydrographs is also affected by the density of high-rise buildings. Table 4.3 shows that an increase in building density promotes a weaker hydrologic response, and that wind-driven rain reduces the rising limb slopes of the hydrographs, compared to the scenarios without wind, for static and moving (uphill and downhill) rainfall. Comparing the 37.5% building density and the scenarios without-buildings, there is a reduction of the rising slope of the hydrograph (values in °) from 0.49 to 0.16 (67%), 0.16 to 0.11 (31%) and 0.23 to 0.13 (43%) respectively for the static, uphill and downhill storms (without wind), and from 0.37 to 0.12 (68%), 0.10 to 0.07 (30%) and 0.13 to 0.08 (38%) respectively for the static, uphill and downhill storms (with wind).

Figure 4.8 show the dimensionless hydrographs, whereby the measured discharge (vertical axis) is divided by the precipitation intensity (120 mm/h) and the scale model surface area (4.00 m²), while time (horizontal axis) is divided by the duration of rainfall (see Table 4.1). The dimensionless overland flow hydrographs presented in Figure 4.8 exhibit noticeable differences with respect to the shapes, rising limb times and peak discharges for the different scenarios.

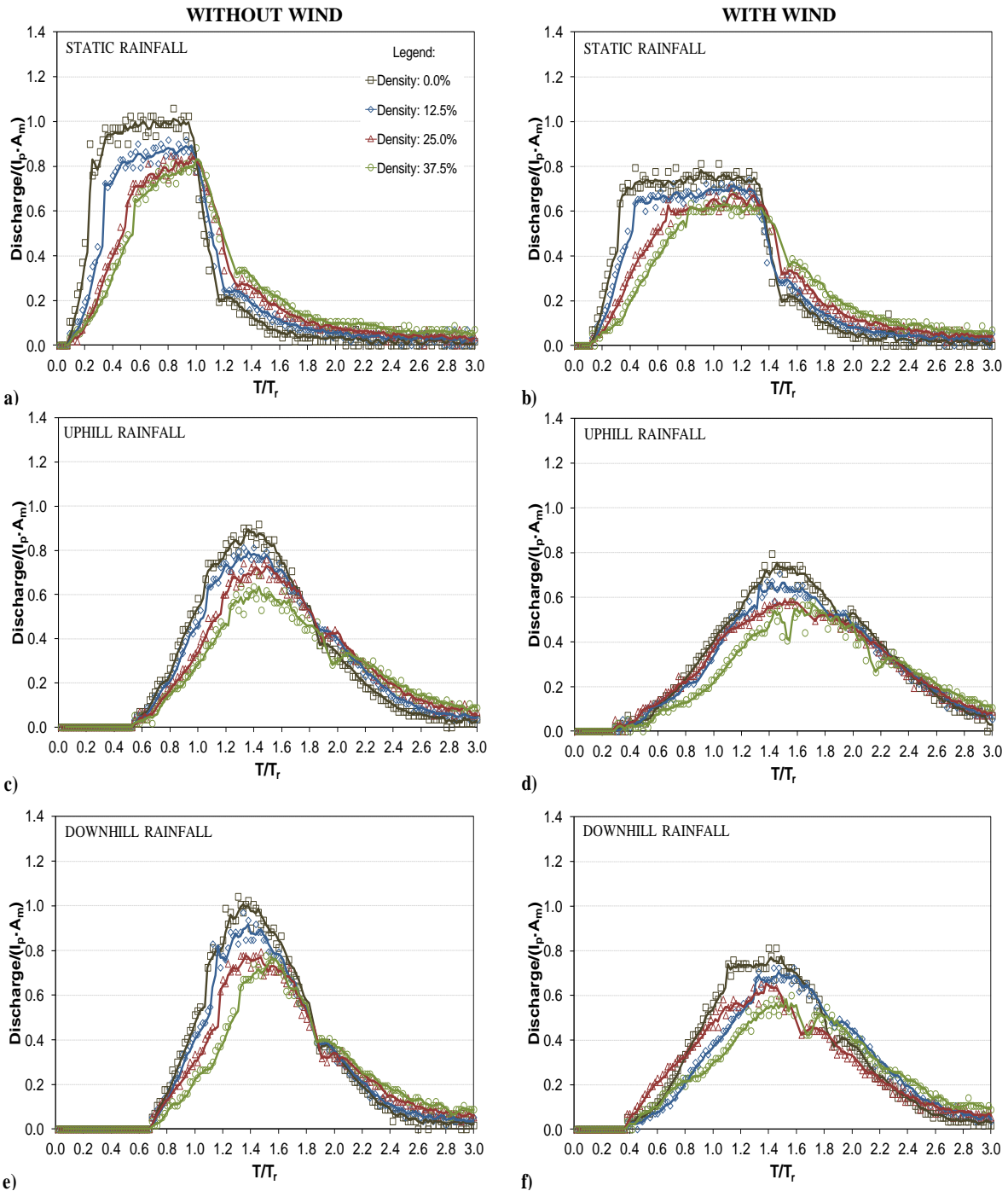


Figure 4.8 Dimensionless overland discharge hydrographs for: a) static rainfall without wind; b) static rainfall with wind; c) uphill moving rainfall without wind; d) uphill moving rainfall with wind; e) downhill moving rainfall without wind; f) downhill moving rainfall with wind.

Dimensionless flood hydrographs of the static storms (Figures 4.8a and 4.8b) show an earlier rise of the rising limb, because the rainfall begins to fall at once on the scale model, as opposed to the moving storms where the rainfall cell has to travel along the model. Therefore, it takes approximately 30 s for the surface runoff to reach the outlet. Uphill-moving storms produce flood hydrographs (Figures 4.8c and 4.8d) with

earlier runoff start time, lower peak discharge, less steep rising limb, and longer base time compared with downhill-moving storms (Figures 4.8e and 4.8f). This is in accordance with the results obtained by other authors (*e.g.*, de Lima and Singh, 2002; de Lima *et al.*, 2003; Nunes *et al.*, 2006).

For downhill moving storms, higher peak flow can be explained by the horizontal components of the raindrops velocities which are in the same direction of flow, while for an uphill moving storm those components are against the flow. This means that (the component of) the momentum transferred to overland flow by rainfall is in the same direction of the flow, thus “pushing” a larger volume of water downhill.

For uphill moving storms, the momentum is against the flow direction, thus retarding the last, and therefore increasing the base time, which will diminish the peak discharge. Also when the storm is moving in the uphill direction, raindrops will first start to fall near the outlet section, meaning that runoff will initiate nearer that section, thus a sooner rise will happen than on a downhill moving storm, in which the arrival of water contribution from the upper areas will be delayed.

Lower base time of downhill moving storm, when compared to uphill moving storms, is a consequence of the steeper rise of the hydrographs limb. For the same runoff volumes, due to the previously explained, discharge values for downhill storm movement are higher, and thus the base time is lower.

Comparing the scenarios without wind (Figures 4.8a, 4.8c and 4.8e) with wind-driven rain (Figures 4.8b, 4.8d and 4.8f) the former dimensionless hydrographs show lower peak discharges, less steep rising and recession limbs and longer base times, because of the spread of the rainfall cell (Figures 4.4a and 4.4b), and/or higher building interception.

The effect of wind-driven rain on peak discharge can also be observed in Table 4.4, which presents the relative differences of the measured peak discharges for the without- and with-wind scenarios ($\Delta Q_p^{rel} = (Q_{p_{without\ wind}} - Q_{p_{with\ wind}}) / Q_{p_{without\ wind}}$), for all the simulated scenarios' combination of storm movement and building densities. Highlighted figures correspond to ΔQ_p^{rel} for the same building density, showing that the occurrence of wind has a good effect on lowering the discharge peak for all the simulated storms (static, uphill and downhill) and building densities, mainly because of the lateral interception of raindrops by the buildings.

Table 4.4 Relative differences of peak discharges (ΔQp^{rel}) for the with- and without-wind storms, for all the simulated scenarios' combinations (values in %).

Wind		Without wind												
Density of buildings		0.0%			12.5%			25.0%			37.5%			
	Storm movement	Static	Uphill	Downhill	Static	Uphill	Downhill	Static	Uphill	Downhill	Static	Uphill	Downhill	
		With wind	0.0%	Static	23.33	11.54	22.03	11.54	0.00	16.36	4.17	-6.98	-2.22	8.00
Uphill	25.00			13.46	23.73	13.46	2.17	18.18	6.25	-4.65	0.00	10.00	-15.38	-2.27
Downhill	23.33			11.54	22.03	11.54	0.00	16.36	4.17	-6.98	-2.22	8.00	-17.95	-4.55
12.5%	Static		30.00	19.23	28.81	19.23	8.70	23.64	12.50	2.33	6.67	16.00	-7.69	4.55
	Uphill		33.33	23.08	32.20	23.08	13.04	27.27	16.67	6.98	11.11	20.00	-2.56	9.09
	Downhill		31.67	21.15	30.51	21.15	10.87	25.45	14.58	4.65	8.89	18.00	-5.13	6.82
25.0%	Static		33.33	23.08	32.20	23.08	13.04	27.27	16.67	6.98	11.11	20.00	-2.56	9.09
	Uphill		45.00	36.54	44.07	36.54	28.26	40.00	31.25	23.26	26.67	34.00	15.38	25.00
	Downhill		38.33	28.85	37.29	28.85	19.57	32.73	22.92	13.95	17.78	26.00	5.13	15.91
37.5%	Static		36.67	26.92	35.59	26.92	17.39	30.91	20.83	11.63	15.56	24.00	2.56	13.64
	Uphill		45.00	36.54	44.07	36.54	28.26	40.00	31.25	23.26	26.67	34.00	15.38	25.00
	Downhill		43.33	34.62	42.37	34.62	26.09	38.18	29.17	20.93	24.44	32.00	12.82	22.73

Notes: Negative relative ΔQp^{rel} value ($Qp^{without\ wind} < Qp^{with\ wind}$)
 ΔQp^{rel} for the same storm movement and buildings density
 ΔQp^{rel} values equal or above 30.00%

Generally, ΔQp^{rel} values fall from the bottom left to the top right corners of Table 4.4. This indicates that for static, uphill and downhill moving storms, wind-driven rain induces a consistent reduction of overland flow in urban impervious surfaces, which becomes more important as the density of high-rise buildings increases.

Table 4.4 shows that ΔQp^{rel} grows with increasing building density for a without-wind storm scenario as reference (ΔQp^{rel} values increase from top to bottom in all columns – e.g., first column from the left, starts with 23.33, 25.00 and 23.33, and ends with 36.67, 45.00 and 43.33, respectively for static, uphill and downhill storms). ΔQp diminishes with increasing building density for a with-wind storm scenario as reference (ΔQp values decrease from left to right on all lines – e.g., first line from the top, starts with 23.33, 11.54 and 22.03, and ends with 8.00, -17.95 and -4.55, respectively for static, uphill and downhill storms).

Figure 4.9 further illustrates the differences in the dimensionless peak discharge for uphill vs. downhill moving rainfall. This difference is plotted for the scenarios with and without the occurrence of wind, for different high-rise building density. Downhill moving storms clearly produce higher peak discharges (all points are located below the 1:1 line).

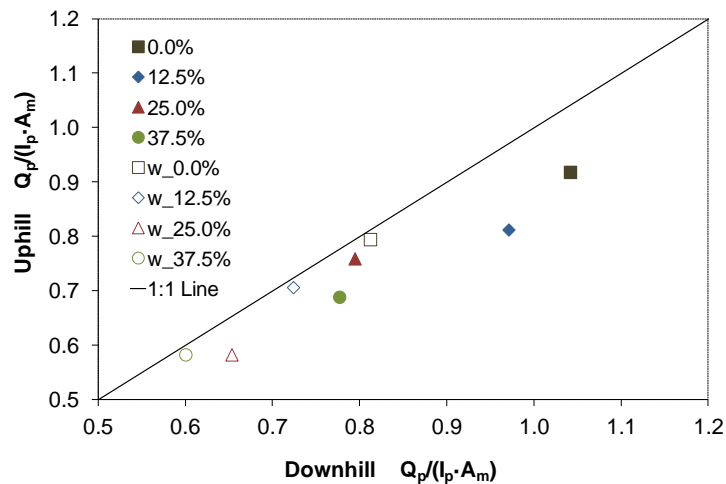


Figure 4.9 Uphill vs. Downhill dimensionless peak discharges for moving storms, without and with wind (in the legend ‘w’ refers to simulations with wind).

The dimensionless hydrographs rising limb angles (α^*) for the no-wind and wind-driven rainfall scenarios, for different densities of high-rise buildings are presented in Figure 4.10). The increase of the density of high-rise buildings is linearly correlated with the decrease of the hydrographs rising limb steepness, regardless of the type of storm. R^2 for downhill, static, and uphill rainfall is, respectively, 0.98, 0.97 and 0.96 for the no-wind rainfall, while for the wind-driven rainfall it is 0.96, 0.94 and 0.87.

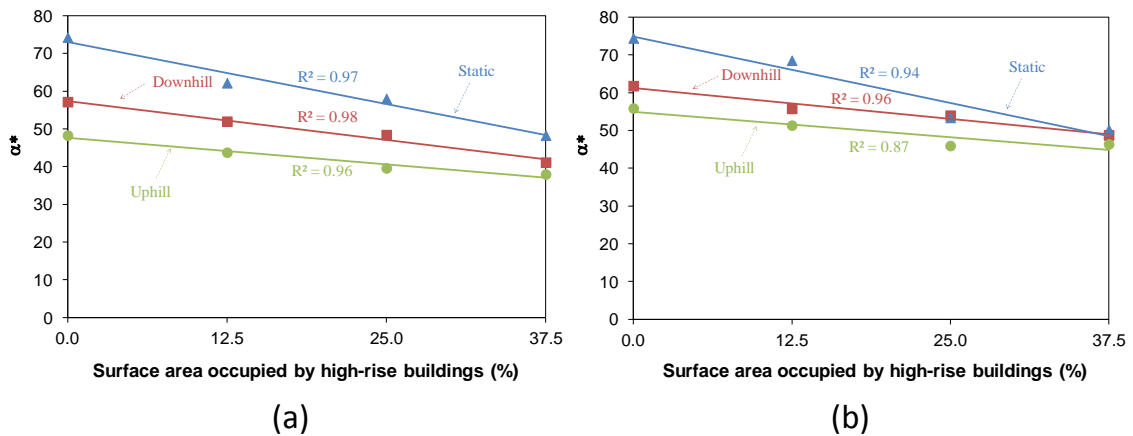


Figure 4.10 Dimensionless hydrograph's rising limb angle (α^*) for different high-rise building densities for (a) no-wind rainfall and (b) wind-driven rainfall scenarios.

4.5 SUMMARY AND CONCLUSION

One of the major issues in urban areas is the faster hydrological response of the urbanized catchment compared with natural areas, when exposed to extreme precipitations (see Introduction). The laboratory simulations described in this work

stress that the density of high-rise buildings, the spatial and temporal distribution of rainfall, the occurrence of wind, and the rain cell movement all have an influence on the overland flow in an urban environment, particularly on the changes caused on the shapes, peak discharges, base times and steepness of the flood hydrographs.

The following conclusions can be drawn from these experiments: (1) storm cell direction affects peak discharge and steepness of the rising limb of the hydrograph, and these are higher for downhill movement than for uphill; (2) increased density of high-rise buildings, for the same impervious urban area and without the occurrence of wind, has the favourable effect of lowering the discharge peak and increasing the overland discharge base time; (3) wind-driven rain reduces the differences mentioned above (because of higher lateral interception by the buildings); (4) steepness of rising limbs of hydrographs for the wind-driven and without-wind rainfall scenarios have linear variations with respect to the evolution of high-rise building density. Thus it is likely that the disregard of the density of high-rise buildings in real systems, as shown in the scaled model, can lead to under- or over-estimation of important hydrologic parameters (*e.g.*, peak discharge), which are indispensable to the design of urban drainage systems.

Future development of this work will include laboratory experiments to cover a wider range of conditions, including high-rise building clusters, acceleration and deceleration of rain cell movement, other rainfall intensity patterns, other wind speed fields, infiltrating surfaces, and different terrain slopes. Confirmation of these results in urban areas will also be attempted.

4.6 ACKNOWLEDGMENTS

The laboratory experiments described in this study were conducted at the Laboratory of Hydraulics, Water Resources and Environment in the Department of Civil Engineering of the Faculty of Science and Technology, University of Coimbra (Portugal). This research was supported by projects PTDC/ECM/105446/2008 and PTDC/AAC-AMB/101197/2008, funded by the Portuguese Foundation for Science and Technology (FCT) and by the Operational Programme “Thematic Factors of Competitiveness” (COMPETE), shared by the European Regional Development Fund (ERDF). The first author wishes to acknowledge FCT for PhD grant SFRH/PROTEC/49736/2009. The authors also wish to express their gratitude to Eng.

Vitor Campina and Mr. Joaquim Cordeiro for their help constructing the scale model, and to the anonymous reviewers for their pertinent comments and suggestions.

4.7 NOTATION

The following symbols are used in this chapter:

A_m	scale model surface area;
I_p	rainfall intensity;
Q_m	average discharge;
Q_p	peak discharge;
T	time;
T_b	base time of runoff;
T_p	time to peak discharge;
T_r	duration of the rainfall;
T_R	return period;
V_{WDR}	wind-driven affected raindrop terminal velocity;
b	street width;
h	building height;
ΔQ_p^{rel}	relative difference of peak discharges for the with- and without-wind storms;
α	angle of the rising limb of the hydrograph;
α^*	angle of the rising limb of the hydrograph (dimensionless);
θ	angle of incidence of the rainfall.

4.8 REFERENCES

Antrop, M., 2000. Background concepts for integrated landscape analysis. *Agriculture, Ecosystems & Environment*, 77 (1-2), 17–28.

Blocken, B., Poesen, J. and Carmeliet, J., 2006. Impact of wind on the spatial distribution of rain over micro-scale topography – numerical modelling and experimental verification. *Hydrological Processes*, 20 (2), 345–368.

- Booth, D. B., 1991. Urbanization and the Natural Drainage System – Impacts, Solutions and Prognosis. *The Northwest Environmental Journal*, 7 (1), 93–118.
- Bornstein, R. and LeRoy, M., 1990. Urban barrier effects on convective and frontal thunderstorms. *In: Preprint Volume, 4th AMS Conference on Mesoscale Processes, 25-29 June 1990 Boulder, CO. American Meteorological Society*, 508–516.
- Bornstein, R. and Lin., Q., 2000. Urban heat islands and summertime convective thunderstorms in Atlanta: Three case studies. *Atmospheric Environment*, 34 (3), 507–526.
- Bryan, R.B. and Poesen, J., 1989. Laboratory experiments on the influence of slope length on runoff, percolation and rill development. *Earth Surface Processes and Landforms*, 14 (3), 211–231.
- Campana, N.A. and Tucci, C.E.M., 2001. Predicting floods from urban development scenarios: case study of the Diluvio Basin, Porto Alegre, Brazil. *Urban Water*, 3 (1), 113–124.
- Carraça, M.G.D. and Collier, C.G., 2007. Modelling the impact of high rise buildings in urban areas on precipitation initiation. *Meteorological Applications*, 14 (2), 149–161.
- Cerdà, A., Ibáñez, S. and Calvo, A., 1997. Design and operation of a small and portable rainfall simulator for rugged terrain. *Soil Technology*, 11 (2), 163–170.
- Chen, Y., Xu, Y. and Yin, Y., 2009. Impacts of land use change scenarios on storm-runoff generation in Xitiao basin, China. *Quaternary International – Larger Asian Rivers: Climate Change, River Flow and Sediment Flux*, 208 (1-2), 121–128.
- Choi, E.C.C., 1994. Determination of wind-driven-rain intensity on building faces. *Journal of Wind Engineering and Industrial Aerodynamics*, 51 (1), 55–69.
- Coutinho, M.A. and Tomás, P.P., 1995. Characterization of raindrop size distributions at the Vale Formoso Experimental Erosion Center. *Catena*, 25, 187–197.
- Dawson, R. J., Speight, L., Hall, J.W., Djordjevic, S., Savic, D. and Leandro, J., 2008. Attribution of flood risk in urban areas. *Journal of Hydroinformatics*, 10 (4), 275–288.
- Dayaratne, S. T. and Perera, B. J. C., 2008. Regionalisation of impervious area parameters of urban drainage models. *Urban Water Journal*, 5 (3), 231–246.
- de Lima, J.L.M.P. and Singh V.P., 2002. The influence of the pattern of moving rainstorms on overland flow. *Advances on Water Resources*, 25 (7), 817–828.
- de Lima, J.L.M.P. and Singh V.P., 2003. Laboratory experiments on the influence of storm movement on overland flow. *Physics and Chemistry of the Earth, Parts A/B/C*, 28 (6–7), 277–282.
- de Lima, J.L.M.P., and Singh V.P., 2000. The influence of storm movement on overland flow – Laboratory experiments under simulated rainfall *In: V.P. Singh, I.W., Seo, J.H. Sonu, ed. Hydrologic Modeling – Proceedings of the International Conference on Water, Environmental, Ecology, Socio-economics and Health Engineering, 18–21 1999 October, Seoul. Fort Collins, CO: Water Resources*, 101–111.

de Lima, J.L.M.P., de Lima, M.I.P. and Singh, V. P., 2005. The importance of the direction, speed, intensity and length of moving storms on water erosion. In: A.F. Cano, R.O. Silla and A.R. Mermut, ed. *Advances in GeoEcology 36 – Sustainable Use and Management of soils – Arid and semiarid regions*. Reiskirchen, Germany: Catena Verlag, 163–176.

de Lima, J.L.M.P., Singh, V.P. and de Lima, M.I.P., 2003. The influence of storm movement on water erosion: storm direction and velocity effects. *Catena*, 52, 39–56.

de Lima, J.L.M.P., Torfs, P.J.J.F. and Singh, V.P., 2002. A mathematical model for evaluating the effect of wind on downward-spraying rainfall simulators. *Catena*, 46, 221–241.

de Lima, M.I.P., 1998. *Multifractals and the temporal structure of rainfall*. Thesis (PhD). Wageningen Agricultural University, The Netherlands.

Eagleson, P.S., 1978. Climate, soil and vegetation: the distribution of annual precipitation derived from observed storm sequences. *Water Resources Research*, 14 (5), 713–721.

Erpul, G., Norton, L.D. and Gabriels, D., 2003. Sediment transport from interrill areas under wind-driven rain. *Journal of Hydrology*, 276 (1–4), 184–197.

Farahmand, T., Fleming, S.W. and Quilty, E.J., 2007. Detection and visualization of storm hydrograph changes under urbanization: an impulse response approach. *Journal of Environmental Management*, 85 (1), 93–100.

Gluch, R., Quattrochi, D.A. and Luvall, J.C., 2006. A multi-scale approach to urban thermal analysis. *Remote Sensing of Environment*, 104 (2), 123–132.

Grimmond, S., 2007. Urbanization and global environmental change: local effects of urban warming. *The Geographical Journal*, 173 (1), 83–88.

Haase, D., 2009. Effects of urbanisation on the water balance – A long-term trajectory. *Environmental Impact Assessment Review*, 29 (4), 211–219.

Hollis, G.E., 1975. The Effect of Urbanization on Floods of Different Recurrence Interval. *Water Resources Research*, 11 (3), 431–435.

Huff, F.A., 1967. Time distribution of rainfall in heavy storms. *Water Resources Research*, 3 (4), 1007–1019.

Isidoro, J.M.G.P., Rodrigues, J.I.J., Martins, J.M.R. and de Lima, J.L.M.P., 2009. Evolution of urbanization in a small urban basin: DTM construction for hydrologic computation. In: A. Herrmann & S. Schumann, ed. *Status and Perspectives of Hydrology in Small Basins*, 30 March – 2 April 2009 Goslar-Hahnenklee, Germany: IAHS, 336, 109–114.

James, L.D., 1965. Using a Digital Computer to Estimate the Effects of Urban Development on Flood Peaks. *Water Resources Research*, 1 (2), 223–234.

Jensen, M., 1984. Runoff pattern and peak flows from moving block rains based on linear time-area curve. *Nordic Hydrology*, 15 (3), 155–168.

Kumaraperumal, A., Sanders, C.H., Baker, P.H., Galbraith G.H. and McGlinchey D., 2007. Analyzing wind-driven rain on a building façade using the laser precipitation monitor (LPM). In: Sixth

international Conference on Indoor Air Quality, Ventilation & Energy Conservation in Building, Sendai, Japan: Tohoku University, 365-375.

Leandro, J., Chen, A.S., Djordjevic, S. and Savic, D.A., 2009. Comparison of 1D/1D and 1D/2D coupled (sewer/surface) hydraulic models for urban flood simulation. *Journal of Hydraulic Engineering*, 135 (6), 495–504.

Maksimov, V.A., 1964. Computing runoff produced by a heavy rainstorm with a moving center. *Soviet Hydrology*, 5, 510–513.

Meyer, L.D., 1965. Simulation of rainfall for soil erosion research. *In: Transactions of the ASAE*, 8, 63–64.

Mentens, J., Raes, D. and Hermy, M., 2006. Green roofs as a tool for solving the rainwater runoff problem in the urbanized 21st century? *Landscape and Urban Planning*, 77 (3), 217–226.

Nuissl, H., Haase, D., Lanzendorf, M. and Wittmer, H., 2009. Environmental impact assessment of urban land use transitions – a context-sensitive approach. *Land Use Policy*, 26 (2), 414–424.

Nie, L., Lindholm, O., Lindholm, G., and Syversen, E., 2009. Impacts of climate change on urban drainage systems - a case study in Fredrikstad, Norway. *Urban Water Journal*, 6(4), 323–332.

Nunes, J.P., de Lima, J.L.M.P. and Ferreira, A.J.D., 2009. Modelling the impact of urbanization on hydrological extremes. *In: W. Chelmicki and J. Siwek, ed. Hydrological extremes in small basins – 12th Biennial International Conference of the ERB, Krakow, 18–20 September 2008. Paris: IHP–UNESCO*, 41–47.

Nunes, J.P., de Lima, J.L.M.P., Singh, V.P., de Lima, M.I.P. and Vieira, G.N., 2006. Numerical modeling of surface runoff and erosion due to moving rainstorms at the drainage basin scale. *Journal of Hydrology*, 330, (3–4), 709–720.

Pappas, E.A., Smith, D.R., Huang, C., Shuster, W.D. and Bonta, J.V., 2008. Impervious surface impacts to runoff and sediment discharge under laboratory rainfall simulation. *Catena*, 72 (1), 146–152.

Quattrochi, D., Luvall, J., Estes, M., Lo, C., Kidder, S., Hafner, J., Taha, H., Bornstein, R., Gillies, R. and Gallo, K., 1998. Project Atlanta (Atlanta Land use Analysis: Temperature and Air Quality): a study of how the urban landscape affects meteorology and air quality through time. *In: 2nd AMS Urban Environment Conference, 2–6 November 1998 Albuquerque, NM: American Meteorological Society*, 104–107.

Sharon, D., 1980. The distribution of hydrologically effective rainfall incident on sloping ground. *Journal of Hydrology*, 46 (1-2), 165–188.

Sharon, D., Adar, E. and Lieberman, G., 1983. Observations on the differential hydrological and/or erosional response of opposite-lying slopes, as related to incident rainfall. *Israel Journal of Earth Sciences*, 32, 71–74.

Shearman, R.J., 1977. The speed and direction of storm rainfall patterns with reference to urban storm sewer design. *Hydrological Sciences Bulletin*, 22 (3), 421–431.

Singh, V.P., 1998. Effect of the direction of storm movement on planar flow. *Hydrological Processes*, 12, 147–170.

Singh, V.P., 2002. Effect of the duration and direction of storm movement on infiltrating planar flow with full areal coverage. *Hydrological Processes*, 16, 1479–1511.

Tariku, F., Cornick, S., Lacasse, M., 2008. Simulation of Wind-Driven Rain Penetration Effects on the Performance of a Stucco-Clad Wall. In: *Thermal Performance of Exterior Envelopes of Whole Buildings X*, 2–7 December 2007, Clearwater Beach, FL. ASHRAE, 9pp.

United Nations, Department of Economic and Social Affairs, Population Division, 2005. *World Urbanization Prospects: The 2005 Revision*. New York: United Nations, ESA/P/WP/200.

Willems, P., 2001. A spatial rainfall generator for small spatial scales. *Journal of Hydrology*, 252 (1–4), 126–144.

Wilson, C.B., Valdes, J.B. and Rodrigues-Iturbe, I., 1979. On the influence of the spatial distribution of rainfall on storm runoff. *Water Resources Research*, 15 (2), 321–328.

Yen, B.C. and Chow, V.T., 1969. A laboratory study of surface runoff due to moving rainstorms. *Water Resources Research*, 5 (5), 989–1006.

CHAPTER 5

5. THE STUDY OF ROOFTOP CONNECTIVITY ON THE RAINFALL-RUNOFF PROCESS BY MEANS OF A RAINFALL SIMULATOR AND A PHYSICAL MODEL

Abstract: The influence of rooftop connectivity on the rainfall-runoff process associated to wind-driven rain and storm movement on highly urbanized areas is not yet well known. In order to study it, a rainfall simulator and a physical model of a hypothetical urban area were used to perform laboratory experiments. Thirty different scenarios were studied combining static and moving storms with/without wind-driven rainfall for five rooftops arrangements with different connectivity. These experiments show that rooftop connectivity, storm movement and wind-driven rain have an important effect on urban runoff, leading to changes in the overland flow hydrographs shapes. Increasing rooftop connectivity leads to a reduction in the peak discharge and an increase in the runoff base time. Regarding flood minimization, the lowest peak discharges and the longest runoff base times were obtained for the clustered rooftop arrangement. Wind-driven rain was shown to reduce peak discharges and rising limb's slopes, thus increasing runoff base times. Wind-driven rain effects are more evident in the static and downstream moving storms.

Keywords: Rainfall simulation; Moving storms; Experimental methods; Rooftop connectivity; Urban hydrology

5.1 INTRODUCTION

The world demographic growth in cities led to an increase in the urban population from 10% in 1900 to more than 50% nowadays, with rising trend (*e.g.*, Grimm *et al.*, 2008). This social, economical and demographical phenomenon, usually referred as “urbanization” and the consequent coverage of the natural soil by impervious areas (*e.g.*, roads, driveways, rooftops) is considered one of the most important causes for the increase of storm water runoff in urban areas (*e.g.*, Arnold Jr. and Gibbons, 1996; O’Driscoll *et al.*, 2007), with urban flooding and infrastructural damages as potential consequences (*e.g.*, McCluskey, 2001; Isidoro *et al.*, 2010).

The morphology of urban areas, which is mainly defined by the construction land plots, the street network and the buildings geometry, is a very important factor for

the rainfall-runoff process in those areas (Rodriguez *et al.*, 2008). Rooftop connectivity, a characteristic associated with buildings geometry and thus related to the morphology of urban areas, is very likely to have a strong impact on that process, affecting flow depths and velocities. The influence of rooftop connectivity on urban runoff has not yet been studied despite its importance stated by some authors (*e.g.*, Roy and Shuster, 2009).

When compared to stationary storms, moving storms modify the hydrologic behaviour of a drainage basin from the headwater scale to the drainage basin scale (*e.g.*, Nunes *et al.*, 2006; de Lima *et al.*, 2011). If the storm movement is not taken into account, over- or under-estimation of runoff peaks may occur (*e.g.*, Maksimov, 1964; Ngirane-Katashaya and Wheeler, 1985; Singh, 1998; de Lima and Singh, 2002; Vischel and Lebel, 2007). Wind also affects the spatial and temporal distribution of rainfall (*e.g.*, Disrud, 1970; de Lima, 1990; Pedersen and Hasholt, 1995; Erpul *et al.*, 2002; Blocken *et al.*, 2006) leading to considerable changes in overland flow and runoff processes (*e.g.*, de Lima 1989a; de Lima 1989b; de Lima 1989c).

Advantages on the use of rainfall simulators for hydrological studies (as opposed to numerical simulators (*e.g.*, Leandro *et al.*, 2009; Cea *et al.*, 2010)) have been referred by several authors, both in-situ (*e.g.*, Navas *et al.*, 1990; Cerdà *et al.*, 1997; Humphry *et al.*, 2002; Fernández-Gálvez *et al.*, 2008; Sheridan *et al.*, 2008; Yu *et al.*, 2009) and in the laboratory (*e.g.*, Chow and Harbaugh, 1965; Bryan and Posen, 1989; Andersen *et al.*, 1999; de Lima and Singh, 2003; Pappas *et al.*, 2008; Isidoro *et al.*, 2012). Rainfall simulators have been used with success in other fields of knowledge such as pollution control (*e.g.*, Baker *et al.*, 1978) and education (*e.g.*, Dillaha *et al.*, 1988). Wind-driven rain simulation, both numerical (*e.g.*, Blocken *et al.*, 2005) and experimental (*e.g.*, Fister *et al.*, 2011), has also been used in the fields of hydrology and soil conservation. Wind-driven raindrops fall through a wind field and thus have horizontal velocity, which does not happen in windless conditions where raindrops only suffer from the effects of gravitational and (vertical) drag forces. By modifying the raindrop impact frequency and angle on superficial flow and the spatial distribution of the rainfall intensity at ground level, wind-driven rain changes the flow roughness (Erpul *et al.*, 2004), thus having an important effect on the surface runoff. Moreover, on a built environment, the wind flow patterns around the buildings have a marked influence on the rainfall reaching the building facades. These patterns depend, among other factors, on the building volumes upwind and downwind, the building geometry and orientation regarding the wind direction and the neighbourhood building density (Hens, 2011).

This paper aims to study the influence of rooftop connectivity on the rainfall-runoff process in impervious urban areas. Particular attention is given to the hydrograph shapes and related characteristics (*e.g.*, peak discharge, runoff base time, rising limb slope) which are influenced by the rooftop connectivity. A rainfall simulator and a physical model were used for this study. The rainfall simulator had the capacity to simulate both static and moving storms, with or without wind, while the physical model allowed the representation of different rooftop connectivities.

5.2 METHODOLOGY

5.2.1 RAINFALL SIMULATOR

The rainfall simulator used in this work has been developed and constructed at the Laboratory of Hydraulics, Water Resources and Environment of the Civil Engineering Department of the Faculty of Sciences and Technology – University of Coimbra (Figure 5.1 left). This equipment was, for this paper, upgraded from previous studies which focused on the hydrologic response for windless conditions (*e.g.*, de Lima and Singh, 2003), namely by the installation of: (i) a set of fans to simulate the effect of wind on rainfall, (ii) an automatic panel to operate and control the rainfall simulator structure movement, (iii) an hydraulic system to assure constant pressure on the nozzle and (iv) a continuous discharge recording system.

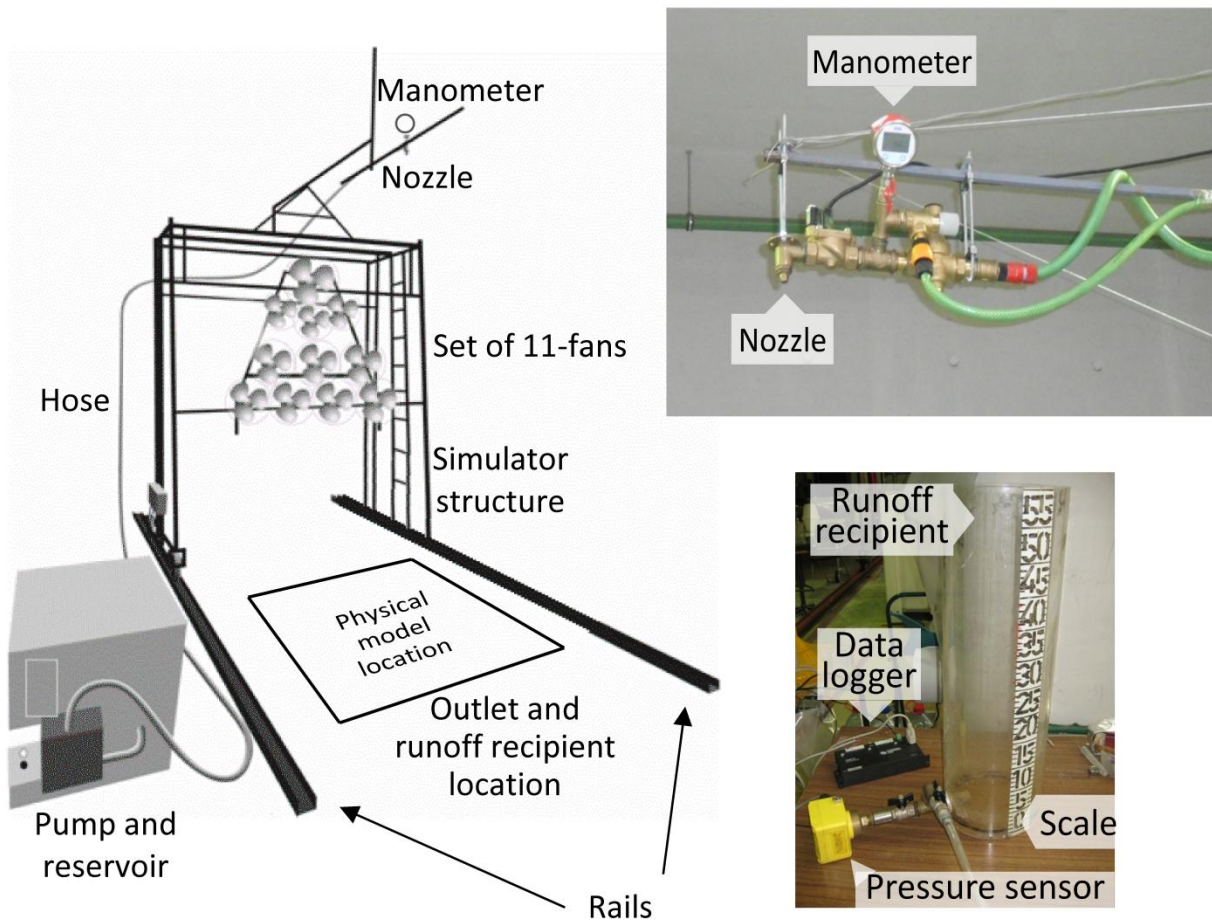


Figure 5.1 Left: Sketch of rainfall simulator comprising the pressurized system, moving structure and set of fans. Top right: Detail of constant pressure system and nozzle. Bottom right: Discharge measuring system consisting of a recipient equipped with a pressure sensor and data logger.

The rainfall simulator is comprised of three distinct elements: (i) a pressurized hydraulic system, (ii) a moving structure and (iii) a continuous discharge recording system. The pressurized system consists of a constant level water reservoir (intake from the public supply system), a pump, a set of hoses and a constant pressure sprinkling system (Figure 5.1 top right) with one downward-oriented nozzle (3/4 HH - 4 FullJet Nozzle Brass-Spraying Systems Co.) operated by an electric retention valve. The moving structure consists of a light steel frame to which the pressurized hydraulic system, the 11-fans set and the control panel are fixed, and two pairs of wheels which, power-driven by an electric engine, permit a uniform movement of the structure along the rails. The continuous discharge recording system (Figure 5.1 bottom right) comprises a reservoir (to collect the runoff) with a pressure transducer, a data logger and a computer (to operate the data logger and monitor the pressure transducer measurements).

5.2.2 PHYSICAL MODEL

The physical model (Figure 5.2) is comprised of: (i) a 4.00 m^2 square surface fixed to a stand, representing an impervious drainage basin and (ii) a set of parallelepiped elements, representing identical high-rise buildings. Each building represents 1% of the total drainage surface. Although the building elements are not scaled to the simulated raindrops (which are natural-sized), they allow the study of the effects of different rooftop connectivities, in impervious areas, on the rainfall-runoff process.

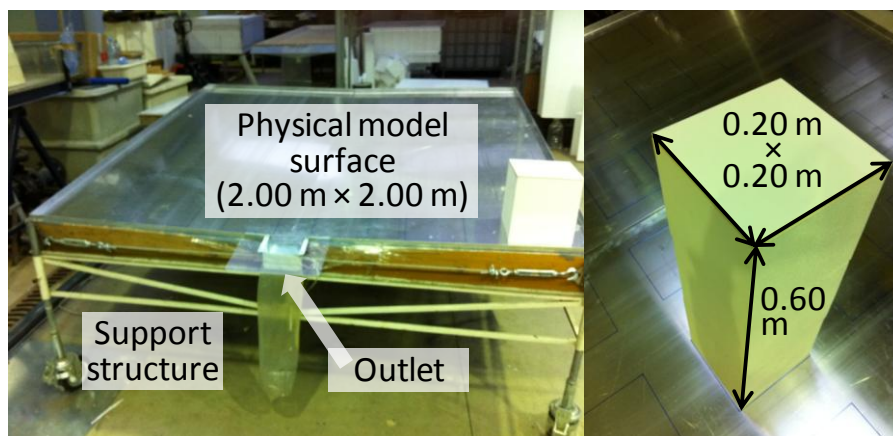


Figure 5.2 Physical model. Left: Stand with steel sheet surface. Right: Building element made of expanded polystyrene.

The square surface is attached to a rigid steel structure with four wheels. The square surface is composed of a solid wooden base over which lays a 2.0 mm thick steel sheet of $2.00 \times 2.00 \text{ m}^2$. The expanded polystyrene elements¹ with $0.60 \times 0.20 \times 0.20 \text{ m}^3$ painted with a solvent-free paint, were light and easy to dispose over the steel sheet. A $0.20 \times 0.20 \text{ m}^2$ ceramic tile was put on top of each element to keep them steady during the simulations. To obtain the desired arrangements (see Table 5.3) and assuring the rooftop connectivities, the polystyrene elements were manually placed in predefined positions amidst simulations, guarantying that all the element fronts were orthogonally displaced regarding the wind direction.

¹ These elements, representing high-rise buildings, were cut from a single polystyrene block with a hot wire. The sides were cut to different heights, so that the elements would stand vertically when placed in the square surface, which had transversal (2.5%) and longitudinal (10.0%) slopes. The 0.60 m height of each block is thus measured at its geometric centre.

5.2.3 RAINFALL AND WIND DISTRIBUTION

Static and moving storms were simulated, respectively, by immobilization or continuously moving the nozzle during each rainfall event. Finite duration rainfalls over the drainage basin (see table 1) were obtained by: (i) opening and closing the electrical valve for the static storms and (ii) adjusting the velocity of the rainfall simulator structure for the moving storms. Wind-driven rainfall scenarios were accomplished by running the 11-fan set (see Figure 1). The electrical valve, structure movement and fans were operated via control panel.

The spatial distributions of the simulated rainfall intensity and wind speed were measured on spatially fixed grids using gauges and anemometers. All experiments were carried out indoors, thus the obtained wind and wind-driven rain fields were noise-free. Rainfall intensity was obtained for both the no-wind and the wind-driven rainfall scenarios. Figure 5.3 shows the distribution of the rainfall intensity (mm/h) used in all simulations without wind (top) and with wind (bottom); in the latter, the wind speed field is also added. More details on the laboratory wind field measurements using anemometers (for wind-driven rain simulation) can be found in Isidoro *et al.* (2012).

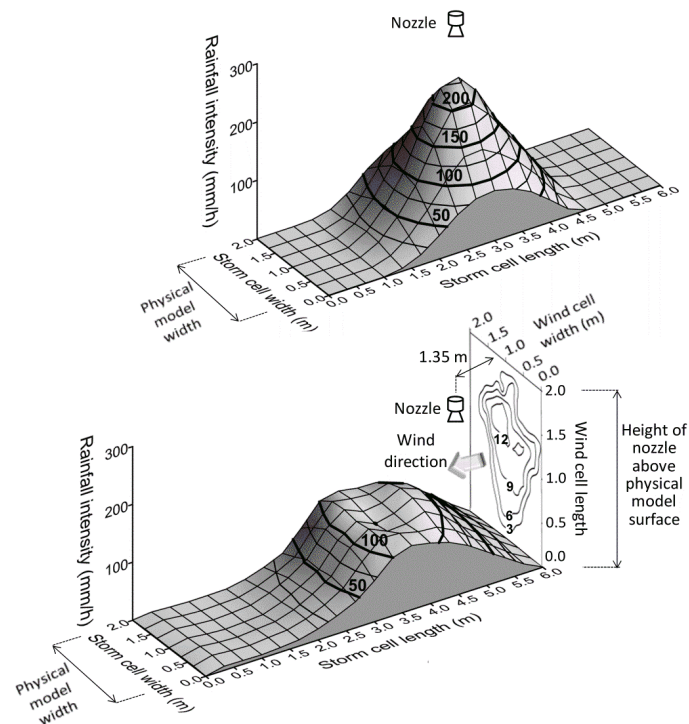


Figure 5.3 Spatial distributions of the storm cell rainfall intensity. Top: without wind. Bottom: with wind (and wind-speed spatial distribution at 1.35 m from the nozzle). Wind speed measured above physical model with no buildings.

The wind speed and rainfall intensity measurement procedures were both repeated 3 times to attain statistical representativeness. Average values were used to represent the respective fields. The wind speed field presents a range of 0–14 m/s and the rainfall intensity spatial distribution ranges 0–230 mm/h (no-wind rainfall – Figure 5.3 up) and 0–123 mm (wind-driven rainfall – Figure 5.3 bottom). These values are within the range of wind speeds and rainfall intensities found in natural systems (e.g., Shearman, 1977; Coutinho and Tomás, 1995).

The rainfall vector for the no-wind rainfall (Figure 5.3 top) had an average raindrop fall velocity of 3.4 m/s (approximately vertical rainfall), while for wind-driven rain (Figure 5.3 bottom) that velocity is 3.8 m/s with a raindrop fall angle of 27°. The diameter and fall velocity ranges of raindrops, measured at the scale model level, with no buildings, using a laser precipitation monitor (Thies LPM) were, respectively, 0.125–3.000 mm and 0.2–6.6 m/s.

5.2.3 LABORATORY EXPERIMENTS PROCEDURE

The steel structure in which the physical model stands was adjusted such that the longitudinal and transversal slopes of the steel sheet were, respectively, 10.0% and 2.5% (Figure 5.4).

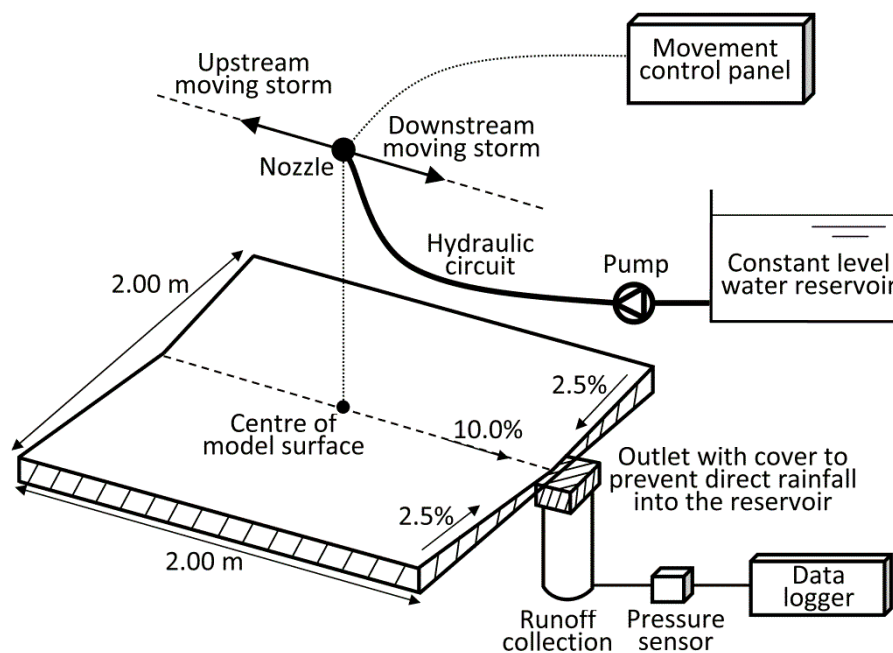


Figure 5.4 Sketch of the drainage basin geometry, storm movement directions, hydraulic circuit of the rainfall simulator, outlet and data collection.

Before each simulation the level of water in the recipient was reset to a predefined level (0.15 m). This procedure minimized the eventual turbulence caused by water falling from the physical model outlet, thus helping to obtain hydrographs with less wiggling.

All simulations were repeated twice, to assure their reliability. After completing the experimental runs, the runoff hydrographs were obtained using the data acquired by the pressure transducer and registered in the data-logger. Since both hydrographs obtained for each simulated scenario had a very good match, only one of these was chosen and used for posterior analysis.

Several preliminary simulations were carried out to establish, by mathematical regression, the duration of rainfall and simulator structure velocity used in the experiments (see Table 5.1). The established values allowed producing, for all the simulations, comparable overland flow hydrographs with a similar total runoff volume.

Before each simulation round, the physical model was wetted for 5 minutes and then let to rest for 10 minutes. An interval of 10 minutes was made between each simulation and so, at the beginning of each rainfall event, the water content accumulated on the steel sheet and elements surfaces was always the same. Because the steel sheet and the painted polystyrene elements are impervious and have a high water-repellence, this water content was negligible.

5.3 SIMULATION RUNS

In order to focus this study in the influence of rooftop connectivity on the discharge hydrographs, the following assumptions were set: a full impermeable surface, a single rainfall pattern with a constant moving velocity, all building elements and pavements with the same surface roughness. This study was thus confined to the influence of wind-driven rain and rooftop connectivity, while other factors such as roof shapes, house structures, ground surface characteristics and surface moisture were kept constant.

The 30 simulated storm scenarios presented in this paper include (i) static and dynamic (upstream and downstream moving) storms, (ii) no-wind and wind-driven

rainfall, and (iii) six groups of distinctive rooftop connectivities. In the static simulations the duration of rainfall is equal to the period when the nozzle valve is kept open whilst, in the dynamic simulations, is equal to the period that a storm cell takes to completely cross over the scale model (time interval from the instant the storm-cell enters until it leaves the scale model). This information is summarized in Table 5.1. In the case of moving storms (only uniform motion was used), the duration of rainfall (R_d) was calculated with Eq. (5.1).

$$R_d = \frac{L_f + L_s}{V_s} \tag{5.1}$$

where: L_f is the impervious drainage basin length (m); L_s is the storm length (m); and V_s is the storm speed (m/s)

Table 5.1 Storm types used in the laboratory simulations.

Simulated group index	Type of storm	Duration of precipitation (s)	Simulator speed ($\times 10^{-2}$ m/s)
①	Static / no-wind	49	---
②	Static / wind-driven	69	---
③	Upstream / no-wind	126	4.6
④	Upstream / wind-driven	170	4.1
⑤	Downstream / no-wind	126	4.6
⑥	Downstream / wind-driven	170	4.1

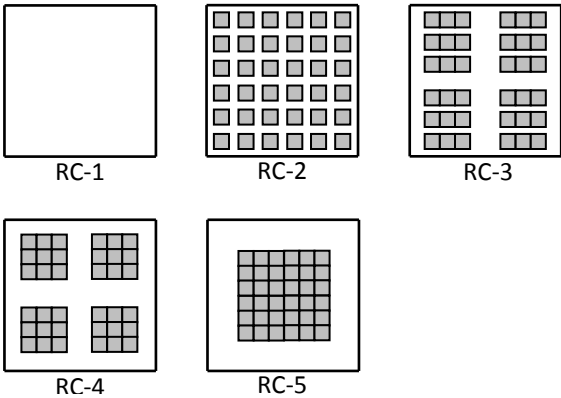


Figure 5.5 Rooftop connectivities used in the simulations.

Each simulation group corresponds to a distinct arrangement of the polystyrene elements over the impervious drainage basin: all arrangements have the same occupied area, except for the scenario without buildings (Figure 5.5). A rooftop is considered connected when water can flow freely from one of its ends to the other.

RC-1 represents inexistence of buildings, *i.e.*, no rooftops; each of the groups covers 36% of the drainage basin area (36 building elements). RC-2 simulates a uniform distribution over the drainage basin; RC-3 represents 12 groups of 3-buildings with connected rooftops; RC-4, 4 groups of 9-buildings; and RC-5 all the rooftops connected in a single large building group. Table 5.2 shows the clustering indexes (RC_i), representing the relation between clustered and total number of building rooftops Eq. (5.2), for each one of the rooftop connectivities (RC):

$$RC_i = \frac{N_{CR}}{N_R} \times 100 \quad (5.2)$$

where: N_{CR} is the number of buildings in clustered rooftops; and N_R is the maximum possible number of rooftops.

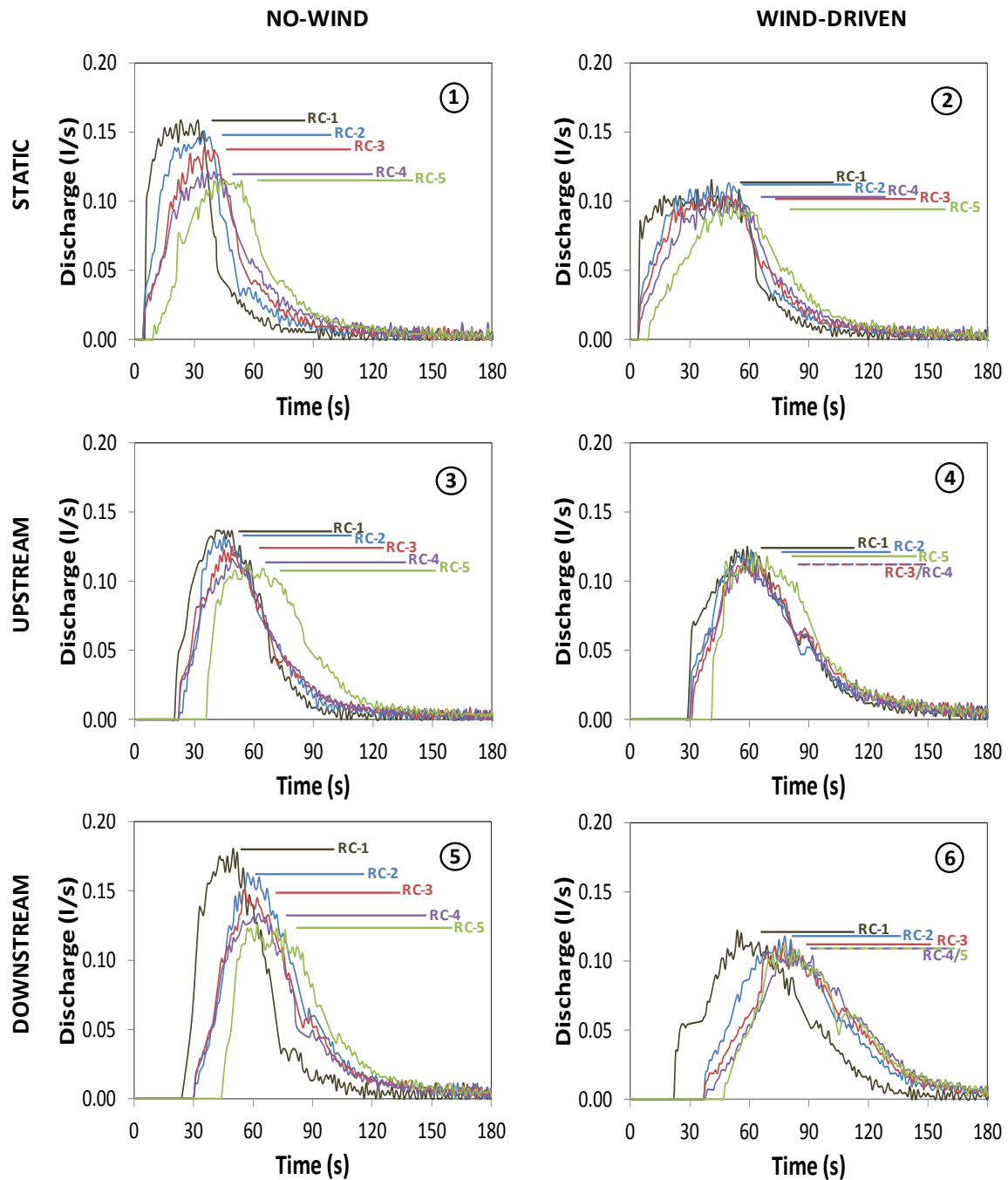
Table 5.2 Rooftop connectivities used in the laboratory simulations (see Figure 5.5).

Rooftop connectivity	N_{CR} (-)	RC_i (%)
RC-1*	0	0.0
RC-2	1	2.8
RC-3	3	8.3
RC-4	9	25.0
RC-5	36	100.0

* No buildings, assumes $RC_i=0$.

5.4 RESULTS

Runoff hydrographs obtained for all simulations referred in Table 5.1 are shown in Figure 5.6.



① - Group index i

RC-j - Rooftop connectivity j

Figure 5.6 Discharge hydrographs. Top: Static storms; Centre: Downstream storms; Bottom: Upstream storms. Left: No-wind; Right: Wind-driven. The obtained peak flows are shown in the hydrographs.

The following data was retrieved from the discharge hydrographs (see Figure 5.7): Q_p – Peak discharge (l/s), T_b – Base time of discharge (s), T_i – Time of runoff initiation at the physical model outlet (s), T_p – Time to peak discharge and α – Slope of the rising limb (l/s^2). This information is summarized in Table 5.3.

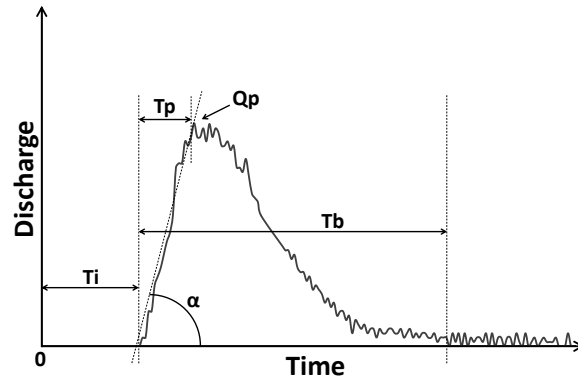


Figure 5.7 Notation used for the variables retrieved from the hydrographs. Discharge obtained from the output of the pressure sensor.

Table 5.3 Parameters obtained directly from the discharge hydrographs (see Figure 5.6).

Simulated group index	Type of storm	Rooftop connectivity	Qp (l/s)	Tb (s)	Ti (s)	Tp (s)	α ($\times 10^{-3}$ l/s ²)
①	Static no-wind	RC-1	0.158	87	6	15	17.00
		RC-2	0.151	117	5	19	9.36
		RC-3	0.139	131	5	28	5.83
		RC-4	0.121	137	5	33	3.93
		RC-5	0.117	136	10	42	3.31
②	Static wind-driven	RC-1	0.115	115	5	15	10.10
		RC-2	0.113	132	5	23	5.78
		RC-3	0.104	137	5	26	4.62
		RC-4	0.106	166	5	33	2.86
		RC-5	0.101	144	10	49	2.49
③	Upstream no-wind	RC-1	0.136	83	21	37	8.13
		RC-2	0.132	101	23	40	7.59
		RC-3	0.125	119	23	44	5.86
		RC-4	0.116	136	23	48	4.40
		RC-5	0.111	122	37	49	8.50
④	Upstream wind-driven	RC-1	0.125	130	31	52	5.38
		RC-2	0.122	133	31	55	5.00
		RC-3	0.115	140	31	57	4.35
		RC-4	0.115	153	31	50	4.84
		RC-5	0.120	166	42	48	2.17
⑤	Downstream no-wind	RC-1	0.181	87	29	37	12.50
		RC-2	0.162	131	31	40	6.23
		RC-3	0.150	138	31	44	5.87
		RC-4	0.133	148	31	48	4.57
		RC-5	0.125	136	45	49	10.18
⑥	Downstream wind-driven	RC-1	0.122	120	22	52	3.59
		RC-2	0.118	143	38	55	3.11
		RC-3	0.113	155	38	57	3.12
		RC-4	0.111	163	38	50	2.24
		RC-5	0.111	164	48	48	4.30

5.5 DISCUSSION

The laboratory experiments show that under different storm conditions, *i.e.*, moving or static storms, with or without wind, the rooftop connectivity influences the hydrologic response of the physical model. The observed overland flow hydrographs (see Figure 5.6 and Table 5.3) show clear variations in the maximum peak discharge, base time of runoff, runoff starting time and slope of the rising limb of the hydrograph. For benefit of the discussion, the information in Table 5.3 and Figure 5.6 has been compiled into Figure 5.8; the variations were quantified in terms of relative differences in static storms and visually cross-compared between group indexes for different storm conditions.

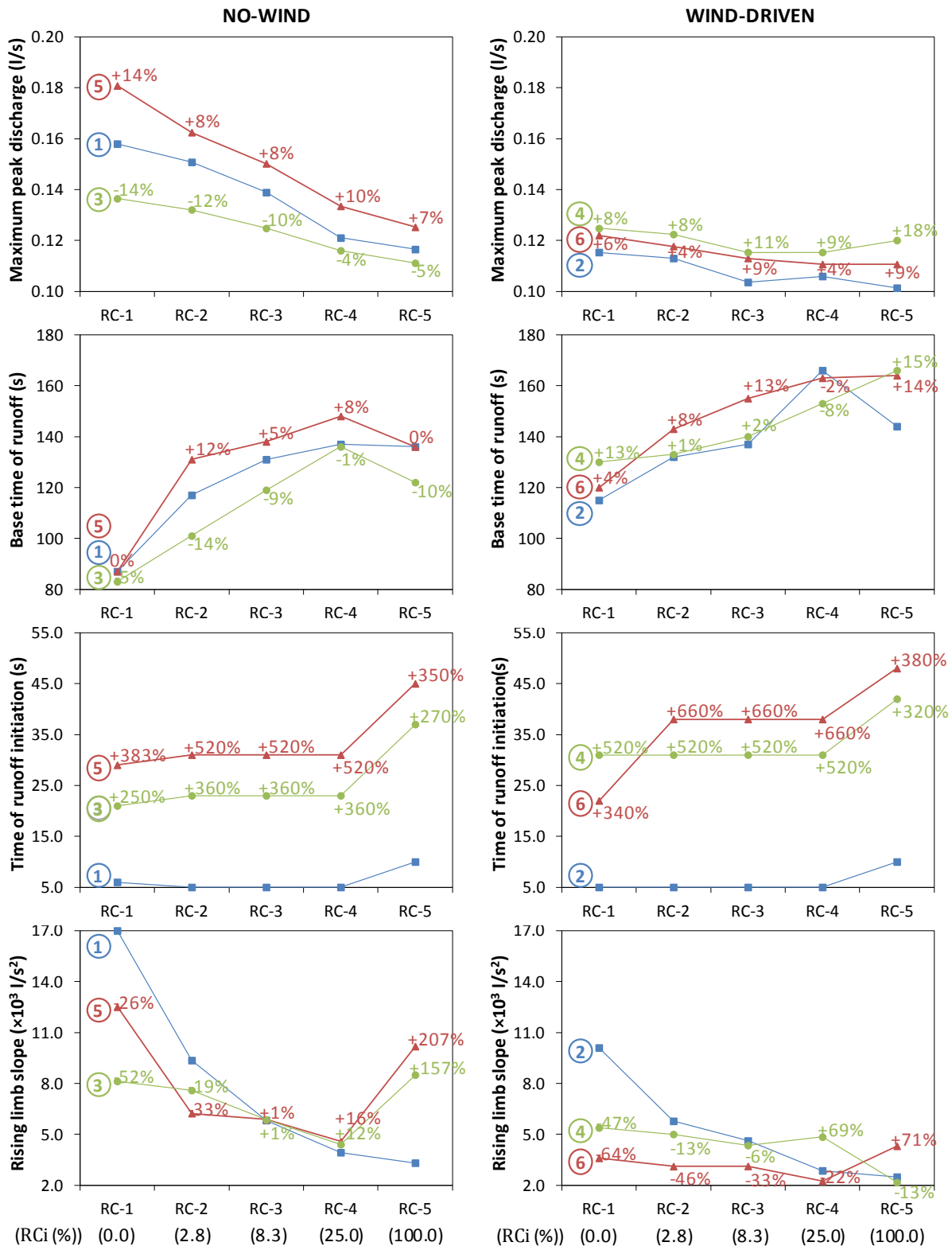


Figure 5.8 Variables retrieved from the hydrographs as a function of rooftop connectivity. Top: Maximum peak discharges; Centre top: Base time of runoff; Centre bottom: Time of runoff initiation; Bottom: Slope of the rising limb of the hydrograph, for all rooftop connectivities and storm types; Left: no-wind rainfall; and Right: wind-driven rainfall.

Rooftop connectivity reduces the maximum peak discharge (Figure 5.8 top) because the travel time that raindrops take to reach the outlet is increased by the collision with the building facades. This explains why the RC-1 (inexistence of buildings) configuration leads to the highest peak flows for all storm types, denoting a smaller time of concentration. The clustering of buildings therefore affects raindrops trajectories due to collision, as well as runoff streamlines due to path obstruction. This effect, which is more noticeable in the static and downstream moving storms, is strongly reduced by the effect of wind-driven rainfall (Figure 5.8 top right); the latter promotes a more homogenous spatial distribution of the rainfall intensity (see Figure 5.3) and an important horizontal component in the rainfall velocity, thus reducing the rooftop connectivity effect which is more susceptible to vertical rainfall interception. Highest maximum peak discharges in no-wind scenarios were attained with downstream moving storms (*e.g.*, for RC-1 and RC-4 peak discharges are respectively 14% and 10% higher than for static storms), followed by static and upstream moving storms. In wind-driven scenarios, upstream storms produce the highest maximum peak discharges (for RC-3 and RC-5 peak discharges are respectively 11% and 18% higher than for static storms), followed by downstream moving storms and static storms. These differences between storm types are consistent for all rooftop connectivities. Similar conclusions were found by Isidoro *et al.* (2012) when studying the influence of building density in overland flow under moving storms and wind-driven rainfall.

In an upstream storm, maximum peak discharge is not significantly affected by the buildings as much as the other storm types because rainfall starts near the outlet. On the other hand, downstream moving storms are seriously affected because all rainfall water has to travel through the building arrangements.

In downhill moving storms, the horizontal components of the raindrop vector are aligned with the main surface flow direction, while the opposite occurs in uphill moving storms. The momentum transferred by raindrop impact on the surface runoff is thus responsible for the higher peak discharges observed in downhill moving storms. Moreover, in an uphill moving storm raindrops will first start to fall near the outlet section which leads to a sooner rise of the discharge when compared to downhill moving storms. Figure 5.8 (centre top) shows that, in general, the increasing of rooftop connectivity leads to an increasing of runoff base time, with the highest values obtained in the RC-4 pattern, for both no-wind (downstream moving) and wind-driven (static) rainfall. Generally, if rooftops are clustered, the distance which the runoff must travel to reach the outlet is increased (runoff must go around the

cluster perimeter). However the RC-5 pattern, where the roof connectivity stretches across all the ground routes that were cut-off by the clustering effect, the rooftop runoff contribution (which now occupies a large area) is able to reduce the effect of the increase of base time runoff acted by the clustering (Figure 5.8 centre top).

The movement of rain cell causes, for all the simulated scenarios, a much later initiation of runoff (Figure 5.8 centre bottom) at the outlet (*e.g.*, regarding static storms, RC-2, RC-3 and RC-4 time of runoff initiation is, for downstream moving storms 5.2× higher, and for upstream moving storms 3.6× higher; in wind-driven scenarios and for the same rooftop connectivities, T_i for downstream moving storms is 6.6× higher, and for upstream moving storms is 5.2× higher than the T_i of static storms). This happens because the rain cell distribution in static storms (Figure 5.3 up) covers instantly the full physical model's surface. In moving storms the rain cell progressively moves over the physical model, initially covering only a small part of the drainage area, causing very low rainfall intensity at the beginning. In moving storm scenarios, runoff initiation takes place earlier in upstream than in downstream storms because it is less dependent on the overland flow, *i.e.*, the proximity of the physical model outlet with the area where rainfall starts to occur promotes the earlier rise of the hydrograph. Wind-driven rain is responsible for promoting increase of the time of runoff initiation for moving storms. These findings about the influence of storm movement on runoff are in accordance with de Lima and Singh (2003).

Wind-driven rainfall reduces, in all rooftop connectivity and storm types, the slope of the raising limb of the overland flow hydrographs when compared with no-wind rainfall (Figure 5.8 bottom). Rooftop connectivity has an important influence on the raising limb of hydrographs, mainly in no-wind rainfall situations, (*e.g.*, in the no-wind static storm scenario, α for RC-2 is much higher than for RC-5), however a clear trend is not visible, except for the static storm scenario where the increasing of rooftop connectivity is clearly responsible for lowering the slope of the rising limb of the hydrograph.

5.6 CONCLUSIONS

A rainfall simulator was used in order to study the influence of rooftop connectivity on the overland flow of a physical model, under the Influence of storm movement and wind-driven rain. Rooftop connectivity was shown to strongly influence the

rainfall-runoff process in impervious areas, particularly the flood hydrographs shapes. The main following conclusions could be reached:

1. Increasing the rooftop connectivity leads to a reduction in the peak discharge; this effect is attenuated by the effect of wind-driven rainfall because of raindrop collisions with the building facades;
2. Wind-driven rainfall effects are more evident in peak discharge and rising limb slope for the static and downstream moving storms, namely because upstream moving storms have later rise, lower peak discharge and longer base time;
3. Clustering of rooftops leads to an increase in the runoff base time;
4. Wind-driven rainfall reduces, in all rooftop connectivities and storm types, the peak discharges and slope of the rising limb of the overland flow hydrographs when compared with no-wind rainfall because of the raindrops trajectories against the buildings; in static storms, the increasing of rooftop connectivity is responsible for lowering the slope of the rising limb of the hydrographs.

Although the conclusions cannot be directly extended beyond the physical model studied (*e.g.*, urban drainage systems were not considered), this work shows evidence that rooftop connectivity has an important effect on the rainfall-runoff process in impervious urban areas which are influenced by the storm movement and direction, and by the combined effect of wind and rainfall which affects the rainfall vector. For example, the scenario with the rooftops connected into a single group was the most favourable rooftop connectivity in terms of reduced flood peak and rising limb's slopes, suggesting its possible use as a flood mitigation strategy.

5.7 ACKNOWLEDGMENTS

This research was supported by projects PTDC/ECM/105446/2008 and PTDC/AAC-AMB/101197/2008, funded by the Portuguese Foundation for Science and Technology (FCT) and by the Operational Programme "Thematic Factors of Competitiveness" (COMPETE) through the European Regional Development Fund (ERDF). The first author wishes to acknowledge FCT for PhD grant SFRH/PROTEC/49736/2009. The authors also wish to express their gratitude to Diana Coimbra for helping during the laboratory simulations.

5.8 NOTATION

The following symbols are used in this chapter:

i	group index;
j	rooftop connectivity index;
L_f	impervious drainage basin length;
L_s	storm length;
N_{CR}	buildings in clustered rooftops;
N_R	maximum possible number of rooftops;
Q_p	peak discharge;
RC	rooftop cluster;
R_d	duration of rainfall;
T_b	base time of discharge;
T_i	time of runoff initiation at the physical model outlet;
T_p	time to peak discharge;
V_s	storm speed;
α	slope of the rising limb.

5.9 REFERENCES

- Andersen, C.T., Foster, I.D.L. and Pratt, C.J., 1999. The role of urban surfaces (permeable pavements) in regulating drainage and evaporation: development of a laboratory simulation experiment. *Hydrological Processes*, 13 (4), 597–609.
- Arnold Jr., C.L. and Gibbons, C.J., 1996. Impervious Surface Coverage: The Emergence of a Key Environmental Indicator. *Journal of the American Planning Association*, 62 (2), 243–258.
- Baker, J.L., Laflen, J.M. & Johnson, H.P., 1978. Effect of Tillage Systems on Runoff Losses of Pesticides, A Rainfall Simulation Study. *Transactions of the American Society of Agricultural & Biological Engineers*, 21 (5), 886–892.
- Blocken, B., Carmeliet, J. and Poesen, J., 2005. Numerical simulation of the wind-driven rainfall distribution over small-scale topography in space and time. *Journal of Hydrology*, 315 (1–4), 252–273.
- Blocken, B., Poesen, J. and Carmeliet, J., 2006. Impact of wind on the spatial distribution of rain over micro-scale topography – numerical modelling and experimental verification. *Hydrological Processes* 20 (2), 345–368.
- Bryan, R.B. and Poesen, J., 1989. Laboratory experiments on the influence of slope length on runoff, percolation and rill development. *Earth Surface Processes and Landforms*, 14 (3), 211–231.

- Cea, L., Garrido, M. and Puertas, J., 2010. Experimental validation of two-dimensional depth-averaged models for forecasting rainfall-runoff from precipitation data in urban areas. *Journal of Hydrology*, 382 (1–4), 88–102.
- Cerdà, A., Ibáñez, S. and Calvo, A., 1997. Design and operation of a small and portable rainfall simulator for rugged terrain. *Soil Technology*, 11 (2), 163–170.
- Chow, V.T. and Harbaugh, T.E., 1965. Raindrop Production for Laboratory Watershed Experimentation. *Journal of Geophysical Research*, 70 (24), 6111–6119.
- Coutinho, M.A. and Tomás, P.P., 1995. Characterization of raindrop size distributions at the Vale Formoso Experimental Erosion Center. *Catena*, 25 (1–4), 187–197.
- de Lima, J.L.M.P. and Singh, V.P., 2002. The influence of the pattern of moving rainstorms on overland flow. *Advances in Water Resources*, 25 (7), 817–828.
- de Lima, J.L.M.P. and Singh, V.P., 2003. Laboratory experiments on the influence of storm movement on overland flow. *Physics and Chemistry of the Earth*, 28 (6–7), 277–282.
- de Lima, J.L.M.P., 1989a. Raindrop splash anisotropy: slope, wind and overland flow velocity effects. *Journal of Soil Technology*, 2 (1), 71–78.
- de Lima, J.L.M.P., 1989b. The influence of the angle of incidence of the rainfall on the overland flow process. In: M.L. KAVVAS, ed. *New Directions for Surface Water Modeling*. Wallingford: IAHS Publications, 73–82.
- de Lima, J.L.M.P., 1989c. Overland flow under simulated wind-driven rain. – In: V.A. DODD AND P.M. GRACE, eds. *Proceedings of the 11th International Congress on Agricultural Engineering*: 493–500; A.A. Balkema, The Netherlands.
- de Lima, J.L.M.P., 1990. The effect of oblique rain on inclined surfaces: A nomograph for the rain-gauge correction factor. *Journal of Hydrology*, 115 (1–4), 407–412.
- de Lima, J.L.M.P., Singh, V.P., Isidoro, J.M.G.P. and de Lima, M.I.P., 2011. Incorporating the effect of moving storms into hillslope hydrology: Results from a multiple-slope soil flume. In: R.E. Beighley II and M.W. Killgore, eds. *Proceedings of the 2011 World Environmental and Water Resources Congress: Bearing Knowledge for Sustainability*, 22–26 May 2011 Palm Springs, CA. Reston, VA: ASCE Publications, 1398–1407.
- Dillaha, T.A., Ross, B.B., Mostaghimi, S., Heatwole, C.D. and Shanholtz, V.O., 1988. Rainfall simulation: A tool for best management practice education. *Journal of Soil and Water Conservation*, 43 (4), 288–290.
- Disrud, L.A., 1970. Magnitude, probability and effect of kinetic energy of winds associated with rains in Kansas. *Transactions of Kansas Academy of Science*, 73, 237–246.
- Erpul, G., Gabriels, D. and Norton, L.D., 2004. Effect of wind on runoff. In: S. Visser and W. Cornelis, eds. *Wind and Rain Interaction in Erosion*. Tropical Resource Management Papers, No. 50. Wageningen: Wageningen University and Research Centre, 81–95.

- Erpul, G., Norton, L.D. and Gabriels, D., 2002. Raindrop-induced and wind-driven soil particle transport. *Catena*, 47 (3), 227–243.
- Fernández-Gálvez, J., Barahona, E. and Mingorance, M., 2008. Measurement of Infiltration in Small Field Plots by a Portable Rainfall Simulator: Application to Trace-Element Mobility. *Water, Air, & Soil Pollution*, 191 (1), 257–264.
- Fister, W., Iserloh, T., Ries, J.B. and Schmidt, R.G., 2011. Comparison of rainfall characteristics of a small portable rainfall simulator and a portable wind and rainfall simulator. *Zeitschrift für Geomorphologie*, 55 (3), 109–126.
- Grimm, N.B., Faeth, S.H., Golubiewski, N.E., Redman, C.L., Wu, J., Bai, X. and Briggs, J.M., 2008. Global Change and the Ecology of Cities. *Science*, 319, 756–760.
- Hens, H.S.L.C., 2011. *Applied Building Physics: Boundary Conditions, Building Performance and Material Properties*. Berlin: Wilhelm Ernst & Sohn.
- Humphry, J.B., Daniel, T.C., Edwards, D.R. and Sharpley, A.N., 2002. A portable rainfall simulator for plot-scale runoff studies. *Applied Engineering in Agriculture*, 18 (2), 199–204.
- Isidoro, J.M.G.P., de Lima, J.L.M.P. and Leandro, J.E.T. (2012). Influence of wind-driven rain on the rainfall-runoff process for urban areas: Scale model of high-rise buildings. *Urban Water Journal* (in press).
- Isidoro, J.M.G.P., Rodrigues, J.I.J., Martins, J.M.R. and de Lima, J.L.M.P., 2009. Evolution of urbanization in a small urban basin: DTM construction for hydrologic computation. In: A. Herrmann & S. Schumann, ed. *Status and Perspectives of Hydrology in Small Basins*, 30 March – 2 April 2009 Goslar-Hahnenklee, Germany: IAHS, 336, 109–114.
- Leandro, J., Chen, A.S., Djordjevic, S. and Dragan, S., 2009. A comparison of 1D/1D and 1D/2D coupled hydraulic models for urban flood simulation. *Journal of Hydraulic Engineering*, 6 (1), 495–504.
- Maksimov, V.A., 1964. Computing runoff produced by a heavy rainstorm with a moving center. *Soviet Hydrology*, 5, 510–513.
- McCluskey, J., 2001. Water supply, health and vulnerability in floods. *Waterlines*, 19 (3), 14–17.
- Navas, A., Alberto, F., Machin, J. and Galan, A., 1990. Design and operation of a rainfall simulator for field studies of runoff and soil erosion. *Soil Technology*, 3 (4), 385–397.
- Ngirane-Katashaya, G.G. and Wheeler, H.S., 1985. Hydrograph sensitivity to storm kinematics. *Water Resources Research*, 21 (3), 337–345.
- Nunes, J.P., de Lima, J.L.M.P., Singh, V.P., de Lima, M.I.P. and Vieira, G.N., 2006. Numerical modeling of surface runoff and erosion due to moving rainstorms at the drainage basin scale. *Journal of Hydrology*, 330 (3–4), 709–720.
- O’Driscoll, M., Clinton, S., Jefferson, A., Manda, A. and McMillan, S., 2010. Urbanization Effects on Watershed Hydrology and In-Stream Processes in the Southern United States. *Water*, 2, 605–648.

- Pappas, E.A., Smith, D.R., Huang, C., Shuster, W.D. and Bonta, J.V., 2008. Impervious surface impacts to runoff and sediment discharge under laboratory rainfall simulation. *Catena*, 72 (1), 146–152.
- Pedersen, H.S. and Hasholt, B., 1995. Influence of wind speed on rainsplash erosion. *Catena*, 24 (1), 39–54.
- Rodriguez, F., Andrieu, H. and Morena, F., 2008. A distributed hydrological model for urbanized areas – Model development and application to case studies. *Journal of Hydrology*, 351 (3–4), 268–287.
- Roy, A. and Shuster, D., 2009. Assessing Impervious Surface Connectivity and Applications for Watershed Management. *Journal of the American Water Resources Association*, 45 (1), 198–209.
- Shearman, R.J., 1977. The speed and direction of storm rainfall patterns with reference to characteristics on stream flow hydrograph. *Hydrological Processes*, 11 (12), 1649–1669.
- Sheridan, G.J., Noske, P.J., Lane, P.N.J. and Sherwin, C.B., 2008. Using rainfall simulation and site measurements to predict annual interrill erodibility and phosphorus generation rates from unsealed forest roads: Validation against in-situ erosion measurements. *Catena*, 73 (1), 49–62.
- Singh, V.P., 1998. Effect of the direction of storm movement on planar flow. *Hydrological Processes*, 12 (1), 147–170.
- Vischel, T. and Lebel, T., 2007. Assessing the water balance in the Sahel: Impact of small scale rainfall variability on runoff. Part 2: Idealized modeling of runoff sensitivity. *Journal of Hydrology*, 333 (2–4), 340–355.
- Yu, J., Yang, C., Liu, C., Song, X., Hu, S., Li, F. and Tang, C., 2009. Slope runoff study in situ using rainfall simulator in mountainous area of North China. *Journal of Geographical Sciences*, 19 (4), 461–470.

CHAPTER 6

6. LABORATORY SIMULATION OF THE INFLUENCE OF BUILDING HEIGHT AND STORM MOVEMENT ON THE RAINFALL-RUNOFF PROCESS IN IMPERVIOUS AREAS

Abstract: Conversion of land into impervious urban areas leads to more frequent and intense flash floods. Moving storms over impervious areas have a considerably influence in the rainfall-runoff process. A physical model of an urban catchment, with the ability to simulate different building heights, is used to study the changes in runoff caused by wind-driven moving storms. The laboratory experiments show that, for all the studied building heights, both wind and storm movement significantly influence the characteristics of the resulting hydrographs. These showed significantly dependence of the storm movement and the existence of wind, but less of the height of buildings. Downstream moving storms, compared with static or upstream moving storms, have higher discharge peaks thus being more prompt to cause flash flood events. For the simulated storm scenarios, wind-driven rainfall leads to lower peak discharges when compared to no-wind scenarios, for all storm types.

Keywords: Simulation modelling; Urban; Storm; Hydrology

6.1 INTRODUCTION

The expansion of urban area leads to increased impervious areas (*e.g.*, Yaun and Bauer, 2007; Grimm *et al.*, 2008), enhancing the magnitude and recurrence of floods, because urban drainage systems were not conceived for such soil occupation (*e.g.*, Isidoro *et al.*, 2010) or due to extreme storm conditions (*e.g.*, Schmitt *et al.*, 2004). Climate change places an additional motivation to anticipate extreme events and trends and to plan accordingly (Zevenbergen *et al.*, 2008). A better understanding of the rainfall-runoff process in urban areas is therefore a valuable tool for flood management. For a more in-depth review urban hydrologic models see, *e.g.*, Zoppou (2001).

Storm characteristics such as the spatial and temporal distribution of rainfall, highly dependent on the movement of storm cells, and the combined action of wind and rainfall govern, among other processes, overland flow. However, in hydrological models storm characteristics are usually simplified (*e.g.*, de Lima *et al.*, 2003).

Assuming that a storm after arriving instantaneously over a catchment remains stationary during the rainfall event and then disappears also instantaneously is a common simplification in hydrological models that can result in erroneous estimations of runoff (*e.g.*, de Lima *et al.*, 2009). Storm movement has long been recognized as an important factor in the rainfall-runoff process (*e.g.*, Maksimov, 1964; de Lima *et al.*, 2003). Wind-driven rain is also an important issue for runoff studies (*e.g.*, Blocken *et al.*, 2005).

The importance of building height in urban hydrology has been pointed out by some authors. Matheussen (2004) found that, among other factors, building height influence the melting of snow on rooftops, thus forcing the increase of runoff from these surfaces. Yudelson (2010) referred the possibility of combining rainwater and greywater harvesting systems, which depends on the buildings height. Isidoro *et al.* (2012a; 2012b) found that, in impervious areas, disregarding of the density of high-rise buildings can lead to under- or over-estimation of important hydrologic parameters (*e.g.*, peak discharge) and that rooftop connectivity strongly influences the rainfall-runoff process, particularly the flood hydrographs shapes. However, the influence of building height in the rainfall-runoff process has not been fully addressed.

This paper deals with the importance of storm movement and wind-driven rain on runoff, for different building heights, which has not been dealt with before using laboratory experiments. Focus is given on the analysis of the simulated hydrographs characteristics.

6.2 LABORATORY SET-UP AND PROCEDURE

The experimental set-up (Figure 6.1) consisted on an electrically-driven rainfall simulator with the ability to simulate moving storms and wind-driven rainfall, an impervious flume and polystyrene elements to simulate buildings with different heights.

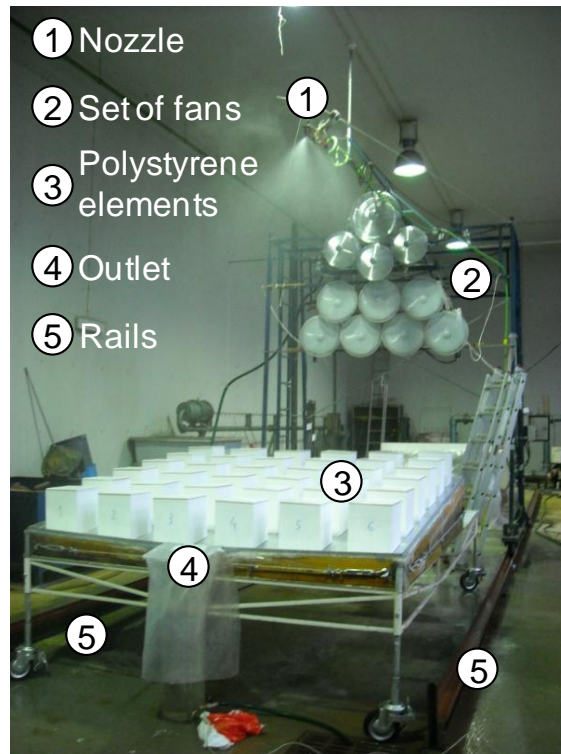


Figure 6.1 Experimental set-up comprising a wind-driven rainfall simulator (1, 2 and 5), an impervious flume (4) and polystyrene elements representing buildings (3) (elements with 0.20 m height, in the photograph).

6.2.1 RAINFALL SIMULATOR

The rainfall simulator comprises a constant water level reservoir, a pump, hoses, a light-framed-steel support structure driven over rails by two electric engines, a control switch panel, a single downward-oriented full-cone nozzle (3/8 HH – 22 FullJet – Spraying Systems Co.) and a set of eleven fans. Moving storms are restricted to forward and backward movements over the rails and are automatically controlled. The nozzle is fixed to the moving structure by a steel rod which maintains its relative position during the simulations. The vertical distance from the nozzle to the flume surface is 2.0 m. For a more detailed description of this simulator see Isidoro *et al.* (2012a).

6.2.2 IMPERVIOUS FLUME AND BUILDING ELEMENTS

The flume used for laboratory simulations, which was placed above a non-deformable steel support structure, has a 2.00 m side square shape and is coated with a steel sheet. The flume surface has a longitudinal slope of 10% and a transversal slope of 2.5% converging at the flume's middle axis. Overland flow was collected at

the centre of the flume’s downstream end (outlet; see Figure 6.1). For a more detailed description of this flume see Isidoro *et al.* (2012b).

6.2.3 RAINFALL AND WIND DISTRIBUTIONS

In this work rainfall cells were generated by a constant discharge and pressure at the nozzle. However, due to the wind effect, the rainfall cells have distinctive characteristics at the flume surface. No-wind and wind-driven storm cells were represented, respectively, by an approximately symmetrical spatial distribution (Figure 6.2; top) and a distorted (Figure 6.2; bottom) distribution of the rainfall intensity due to the added horizontal wind component. As in nature, this spatial distribution is not uniform, but with higher rainfall intensity areas encircled by lower intensity ones (*e.g.*, Willems, 2001). Rainfall water temperature was 14 ± 1 °C. The wind field used for wind-driven rainfall scenarios is presented in Figure 6.3.

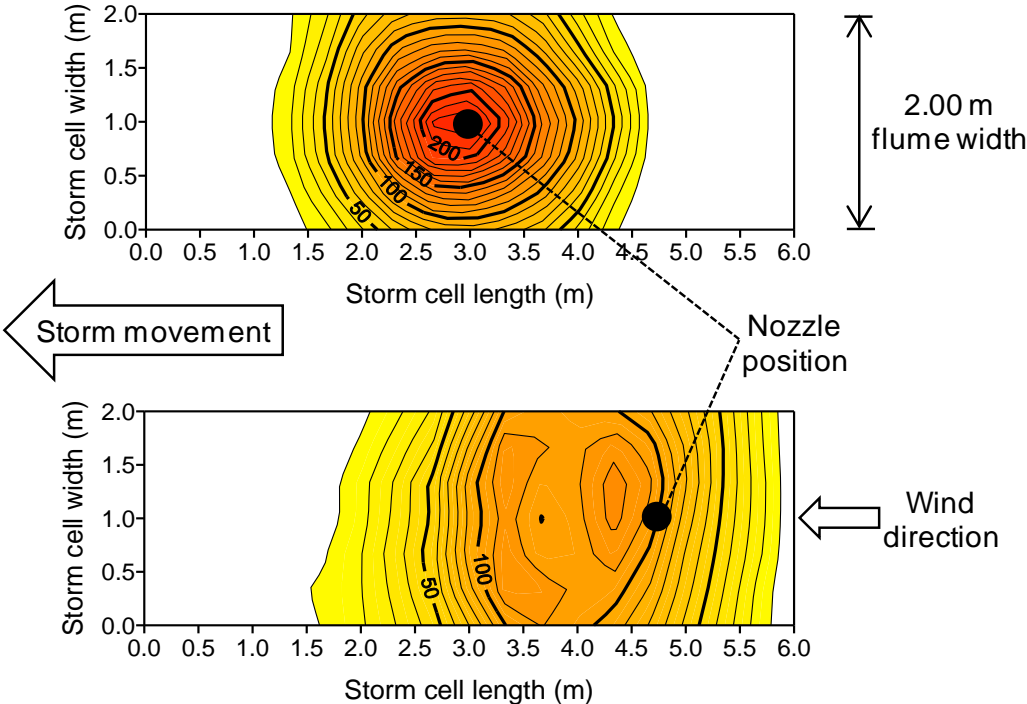


Figure 6.2 Spatial distribution of simulated rain cells rainfall intensities (mm/h) at the flume surface: Top: no-wind scenario; Bottom: wind-driven scenario.

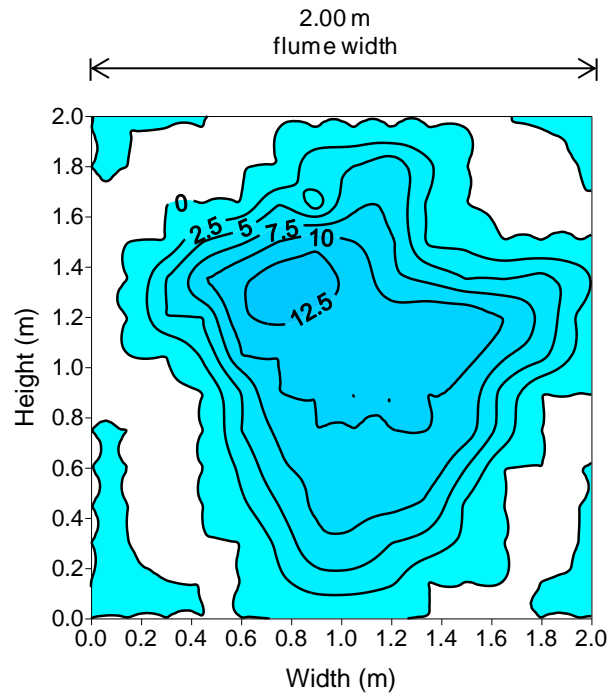


Figure 6.3 Wind speed field (m/s) at vertical plane 1.00 m away from of the set of fans. Height is measured upwards from the flume geometrical centre.

The rainfall cells (Figure 6.2) were displaced over the flume, with constant speed, simulating six different rainfall types: static, upstream and downstream moving storms; without wind and wind-driven rainfall. In the static storms scenarios (Figure 6.4a) the nozzle was placed in a fixed position for 49 s or 69 s, regarding if it was a no-wind or a wind-driven rainfall. In the no-wind rainfall the nozzle was over the geometric centre of the flume, while for the wind-driven rainfall it was at a distance of 1.00 m of the geometric centre of the flume to compensate the rainfall distribution offset caused by wind. In the moving storm scenarios (Figures 6.4b and 6.4c), the nozzle moved in both directions over the flume, respectively with a speed of 0.041 m/s or 0.046 m/s, regarding if it was a no-wind or a wind-driven rainfall scenario. The referred values of the duration of precipitation, for static storms, and of the rainfall simulator speed, for dynamic storms, were established, both for no-wind and wind-driven rainfall, in order to achieve comparable hydrographs with the same total discharged volume.

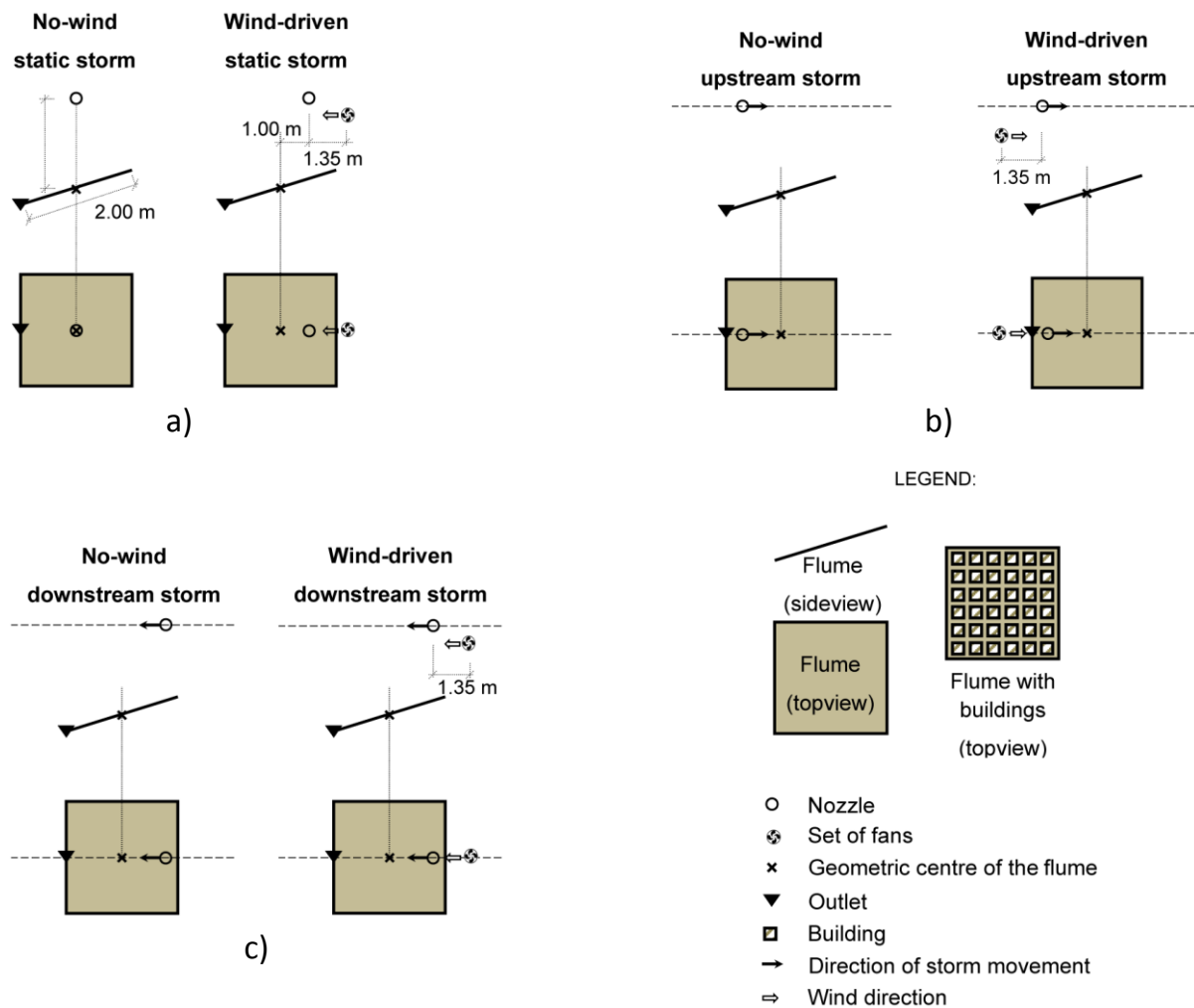


Figure 6.4 Sketch of different scenarios used in the laboratory experiments: a) static storm; b) upstream moving storm; and c) downstream moving storm. No-wind (left) and wind-driven (right) rainfalls are presented for each storm scenario.

6.3 RESULTS AND DISCUSSION

The hydrographs obtained from the laboratory experiments have common characteristics for each storm type scenario, despite the buildings height (Figure 6.5). Downstream moving storms produced the highest peak discharges. Wind-driven rainfall reduced the peak discharges and increase the runoff base times. Upstream storm movement promoted the lowest peak discharges and the highest base times. These findings are in accordance with the work of other authors (*e.g.*, de Lima *et al.*, 2003).

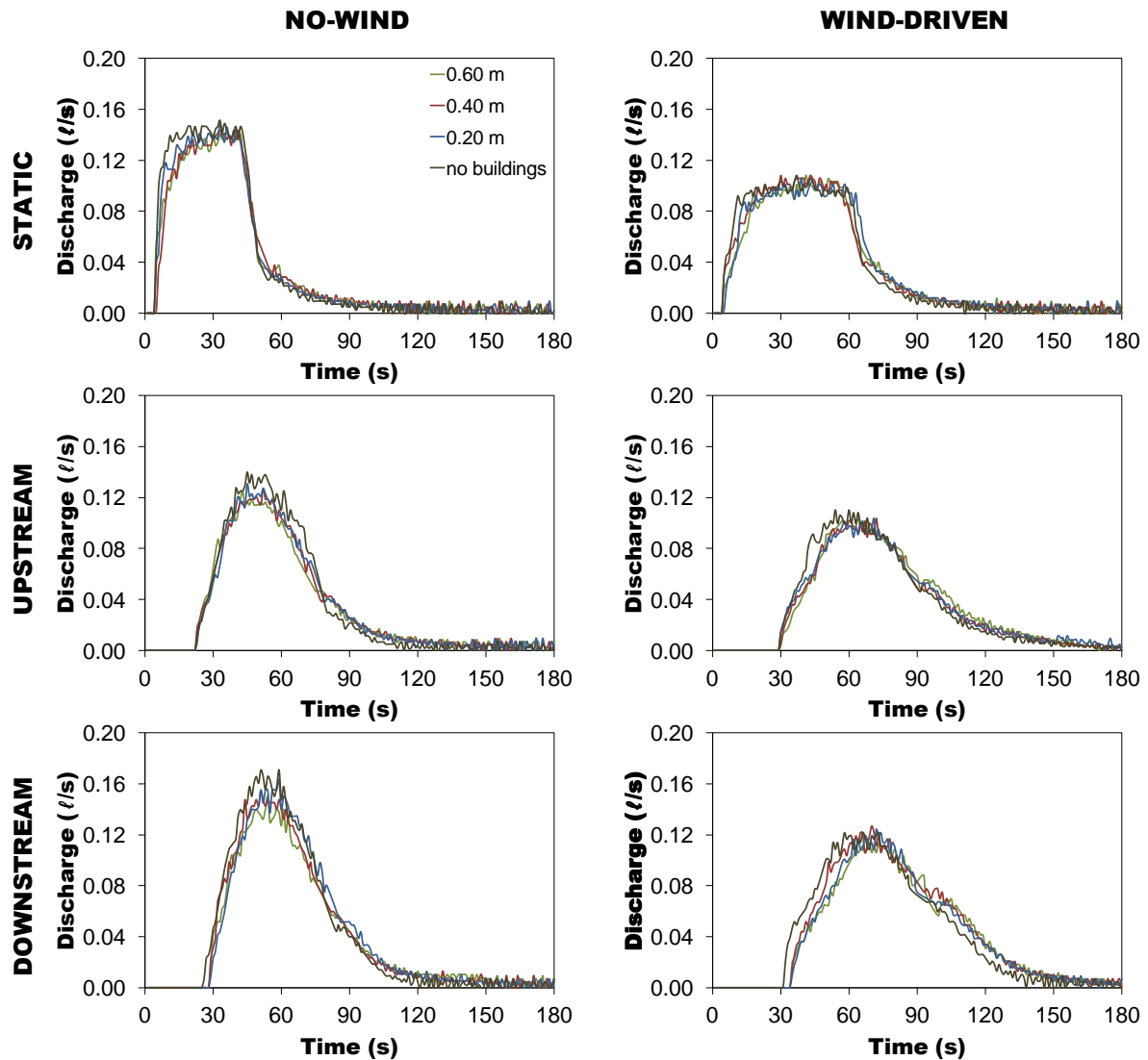


Figure 6.5 Experimental hydrographs. Left: no-wind rainfall; Right: wind-driven rainfall. Up: static storms; Centre: upstream moving storms; Bottom: downstream moving storms. Different building heights are represented by different colours.

Figure 6.6 (left) shows that peak discharges were significantly affected by the storm movement and by the occurrence of wind but not so much by the distinct building heights; for the same storm conditions, peak discharge is approximately the same independently of the building height. Figure 6.6 (right) shows that storm movement, occurrence of wind and building height have a marked influence on the overland flow base time. By promoting the collision of raindrops into the building facades, wind-driven rainfall leads to an increase in the runoff base time because raindrops have to travel a longer distance to reach the outlet.

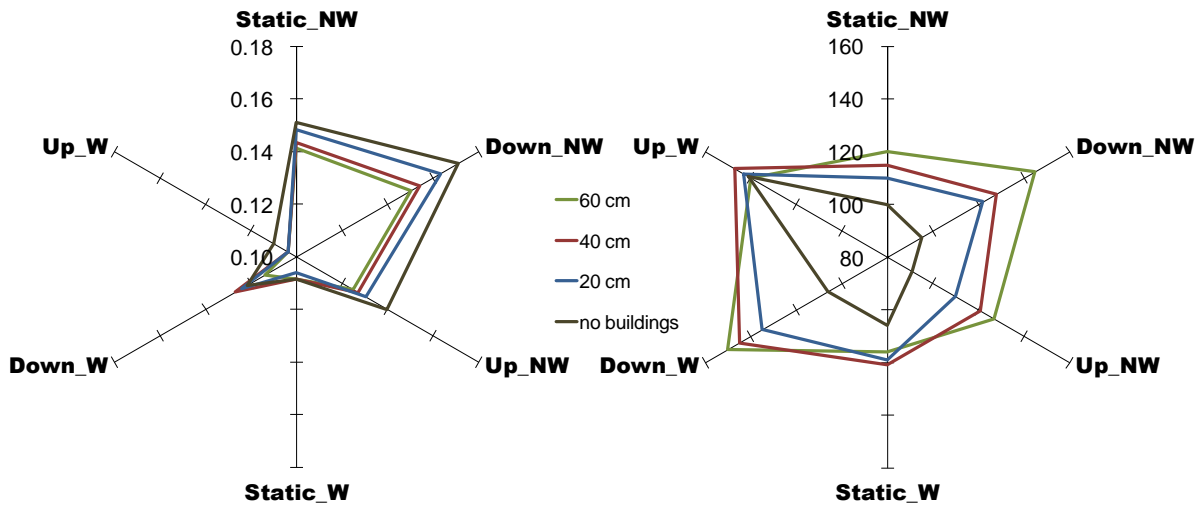


Figure 6.6 Runoff peak discharges (left, in l/s) and base times (right, in s) obtained for all the storm types and building heights. Different building heights are represented by different colours). In the figure NW stands for No-Wind rainfall and W for Wind-driven rainfall.

When compared to wind-driven rainfall events, no-wind rainfall consistently leads to higher peak discharges (Figures 6.5, 6.6 and 6.7) because of the less peaked rainfall input.

Figure 6.7 shows a comparison of the obtained peak discharges for all the scenarios. It is visible that the occurrence of wind and the storm movement have both a marked influence in the peak discharge, which is only slightly diminished by the increase in the height of buildings (the majority of points are under the 1:1 line).

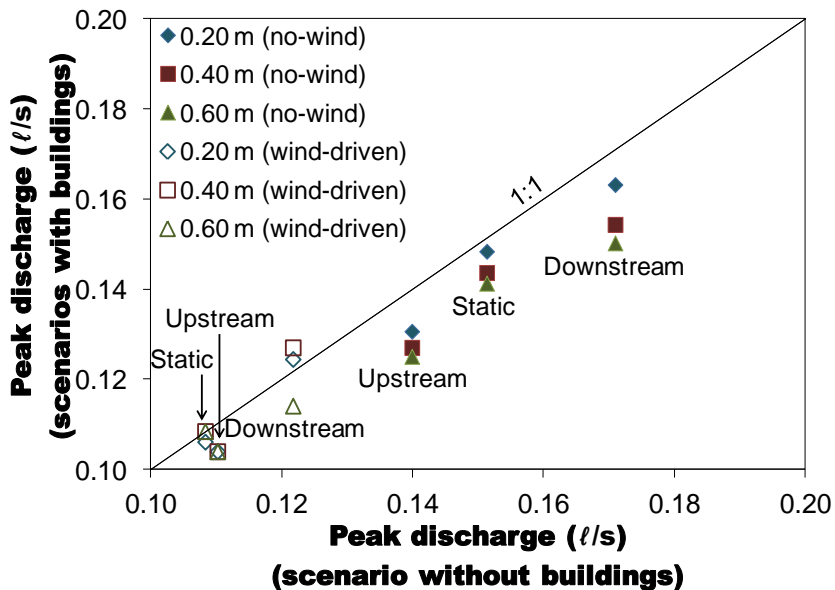


Figure 6.7 Comparison of runoff peak discharges for the scenarios with and without buildings, no-wind and wind-driven rainfall. Different building heights are represented by different colours. Storm types (static, upstream and downstream) are specified.

6.4 CONCLUSIONS

The laboratory experiments described in this work show that: (i) the highest peak discharges were generated by downstream moving storms; (ii) wind-driven rain reduced the peak discharges and increased runoff base times; (iii) upstream moving storms promoted the lowest peak discharges and the highest base times; (iv) increase in buildings height lead to higher runoff base times, but only slight decrease of the peak discharges. Thus, it is likely that ignoring the buildings height in real systems, as shown in the physical model, can derive in under- or over-estimation of important hydrologic parameters, such as peak discharge, which are indispensable to the design of urban drainage systems. Extrapolation of results to urban basins is not simple... but physical experimentation gives insight into the processes involved.

6.5 ACKNOWLEDGMENTS

This research was supported by projects PTDC/ECM/105446/2008 and PTDC/AAC-AMB/101197/2008, funded by the Portuguese Foundation for Science and Technology (FCT) and by the Operational Programme “Thematic Factors of Competitiveness” (COMPETE), shared by the European Regional Development Fund (ERDF). The first author wishes to acknowledge FCT for PhD grant SFRH/PROTEC/49736/2009. The authors also wish to express their gratitude to Diana Coimbra for helping during the laboratory simulations.

6.6 REFERENCES

- Blocken, B., Carmeliet, J. and Poesen, J., 2005. Numerical simulation of the wind-driven rainfall distribution over small-scale topography in space and time. *Journal of Hydrology*, 315 (1–4), 252–273.
- de Lima, J.L.M.P., Singh, V.P. and de Lima, M.I.P., 2003. The influence of storm movement on water erosion: Storm direction and velocity effects. *Catena*, 52, 39–56.
- de Lima, J.L.M.P., Tavares, P., Singh, V.P. and de Lima, M.I.P., 2009. Investigating the nonlinear response of soil loss to storm direction using a circular soil flume. *Geoderma*, 159 (1–2), 9–15.
- Grimm, N.B., Faeth, S.H., Golubiewski, N.W., Redman, C.L., Wu, J., Bai, X. and Briggs, J.M., 2008. Global Change and the Ecology of Cities. *Science*, 319, 756–760.

Isidoro, J.M.G.P., de Lima, J.L.M.P. and Leandro, J.E.T., 2012a. Influence of wind-driven rain on the rainfall-runoff process for urban areas: Scale model of high-rise buildings. *Urban Water Journal* (in press).

Isidoro, J.M.G.P., de Lima, J.L.M.P. and Leandro, J.E.T., 2012b. The study of rooftop connectivity on the rainfall-runoff process by means of a rainfall simulator and a physical model. *Zeitschrift für Geomorphologie* (in press).

Isidoro, J.M.G.P., Rodrigues, J.I.J., Martins, J.M.R. and de Lima, J.L.M.P., 2010. Evolution of urbanization in a small urban basin: DTM construction for hydrologic computation. In: A. Hermann, S.A. Schumann, L. Holko, I. Littlewood, L. Pfister, P. Warmerdam and U. Schroder, eds. *Proceedings of the International Workshop on Status and Perspectives of Hydrology in Small Basins*, IAHS Red Book Series No. 336, 30 March 2 April 2009 Goslar-Hahnenklee. Wallingford: IAHS, 109–114.

Maksimov, V.A., 1964. Computing runoff produced by a heavy rainstorm with a moving center. *Soviet Hydrology*, 5, 510–513.

Matheussen, B., 2004. Effects of anthropogenic activities on snow distribution, and melt in an urban environment. Thesis (PhD). Norway University of Science and Technology.

Schmitt, T.G., Thomas, M. and Ettrich, N., 2004. Analysis and modeling of flooding in urban drainage systems. *Journal of Hydrology*, 299 (3–4), 300–311.

Willems, P., 2001. A spatial rainfall generator for small spatial scales. *Journal of Hydrology*, 252 (1–4), 126–144.

Yuan, F. and Bauer, M.E., 2007. Comparison of impervious surface area and normalized difference vegetation index as indicators of surface urban heat island effects in Landsat imagery. *Remote Sensing of Environment*, 106 (3), 375–386.

Yudelson, J., 2010. *Dry Run: Preventing the Next Urban Water Crisis*. Gabriola Island, BC: New Society Publishers.

Zevenbergen, C., Veerbeek, W., Gersonius, B. and van Herk, S., 2008. Challenges in urban flood management: travelling across spatial and temporal scales. *Journal of Flood Risk Management*, 1 (2), 81–88.

Zoppou, C., 2001. Review of urban storm water models. *Environmental Modelling & Software*, 16 (3), 195–231.

CHAPTER 7

7. AN ANALYTICAL CLOSED FORM SOLUTION FOR 1D LINEAR KINEMATIC OVERLAND FLOW UNDER MOVING RAINSTORMS

Abstract: An analytical solution for overland flow under (upstream and downstream) moving storms that uses Laplace transformation to solve the 1D linear kinematic wave equation (Zarmi's hypothesis) is presented. This solution, which corresponds to a single continuous function for the total space-time domain of the overland hydrograph, enables evaluation of the discharge over time for the total drainage plane surface. The result was compared with another analytical solution, a numerical simulation and experimental runs using a laboratory flume. The comparison showed very good fit and the proposed analytical solution was thus regarded as validated. By applying the model to hypothetical catchments and storm patterns, distinct hydrologic responses for upstream and downstream moving storms were identified.

Keywords: Overland flow; Moving storms; Analytical solution; Kinematic wave

7.1 INTRODUCTION

Overland flow plays a major role in the water cycle in natural and urbanized environments. It is of vital importance in the study of catchment and hillslope hydrology, and its storm-response character gives it particular relevance in some engineering studies (*e.g.*, urban flooding; soil erosion). Since rainfall is a highly nonlinear natural phenomenon which exhibits spatial and temporal variability (*e.g.*, de Lima *et al.*, 2002; Meselhe *et al.*, 2009), modelling of the rainfall-runoff process involves several difficulties, particularly in obtaining reliable design hydrographs.

The influence of moving storms on overland flow (shape of the hydrographs and peak discharges) has been studied by a number of authors in the last 50 years (*e.g.*, Maksimov, 1964; Jensen, 1984; Singh, 1998; de Lima and Singh, 2002; Lee and Huang, 2007). Overlooking the storm movement may result in erroneous estimation of runoff volumes and peaks (*e.g.*, Yen and Chow, 1969; Wilson *et al.*, 1979). The movement of storm cells should therefore be considered for a more accurate simulation of overland flow, since the spatial distribution of rainfall is a dominant factor in the magnitude of runoff response (Villarini *et al.*, 2011). Previous studies on the influence of moving storms on overland flow have been based on: (i) empirical

analysis of available hydrological data (*e.g.*, Hindi and Kelway, 1977; Niemczynowicz, 1988); (ii) physical modelling using laboratory watersheds (*e.g.*, Black, 1972; de Lima *et al.*, 2003); (iii) numerical simulation of rainfall-runoff processes (*e.g.*, Stephenson, 1984; Ogden *et al.*, 1995) and, (iv) analytical solutions of the governing flow equations for specific scenarios (*e.g.*, de Lima and van der Molen, 1988; Singh, 1998; Mizumura, 2006; Mizumura and Ito, 2011).

The use of kinematic wave models in surface runoff analysis began with the work of (Lighthill and Whitham, 1955) for channel flow routing and became today's standard theory for modelling overland flow and other hydrological processes (Singh and Woolhiser, 2002). Kinematic wave models were used by Henderson and Wooding (1964) for watershed modelling and Eagleson (1970) for overland flow routing and hydrograph prediction. Several authors have continued researching the use of kinematic waves in hydrology (*e.g.*, Li *et al.*, 1975; Borah *et al.*, 1980; Govindaraju *et al.*, 1992; Smith *et al.*, 1995; Tayfur and Kavvas, 1998; de Lima and Singh, 2002; Xiong and Melching, 2005). The accuracy and applicability of kinematic wave models in hydrology have also been investigated (*e.g.*, Singh, 1994; Singh, 2002; Moramarco *et al.*, 2008a; Moramarco *et al.*, 2008b). For a review on the use of kinematic wave models in water resources see (*e.g.*, Singh, 1996; Singh, 2001).

Zarmi's hypothesis (Zarmi *et al.*, 1983) has been used in several hydrological studies to derive analytical solutions. Based on this hypothesis Franchini (1994) obtained an exact solution of the rising limb of the hydrograph and sediment discharge on an infiltrating surface and de Lima and van der Molen (1988) found an exact solution of the rising limb of the hydrograph on a parabolic infiltrating surface. Zarmi's hypothesis has also been used to derive analytical solutions for validating laboratory and field experimental work, *e.g.*, to assess runoff in water harvesting micro-catchments (Giakoumakis and Tsakiris, 2001) and to estimate the effects of weirs and weir boxes on flow rate measurements (Boers *et al.*, 1991).

The main objectives of this study were: (i) to present a single-equation closed form analytical solution for the entire space-time domain of the overland flow hydrograph; to verify this solution by comparing it with other solutions provided by (ii) numerical (de Lima and Singh, 2002) and (iii) analytical (Singh, 1998) simulations; and (iv) to compare the results with laboratory experiments making use of a flume to represent a hillslope and a rainfall simulator.

The analytical solution proposed in this study, valid for small impervious catchment areas, is a contribution to the study of the rainfall-runoff processes under moving storms. This solution has several uses in fundamental and applied hydrology (*e.g.*, sensitivity tests of the rainfall-runoff process underlying factors, calibration of numerical methods and estimation of hydrological parameters). In addition, the closed form analytical solution can also be used in real-world engineering applications, such as micro-catchments, water-harvesting systems, road drainage systems and rooftop downspouts. This solution, which is straightforward to apply, takes into account the spatial and temporal variability of rainfall at the plane surface, which is not possible with other methods often used by engineers (*e.g.*, Unit Hydrograph Method). The closed form analytical solution can thus be a useful tool in hydrologic engineering practice.

7.2 THEORY

This section describes the governing equations and assumed simplifications used for simulating the 1D shallow water kinematic wave flow, the mathematical description of the rainfall cell movement and the method used to solve the aforementioned equations.

The governing equations for 1D planar flow (unit width) are:

- The mass conservation (continuity) equation:

$$\frac{\partial h}{\partial t} + \frac{\partial q}{\partial x} = p(x, t) \quad (7.1)$$

where: h (m) is the flow depth at time t (s) and position x (m); q ($\text{m}^2 \cdot \text{s}^{-1}$) is the volumetric water flux per unit width; and p ($\text{m} \cdot \text{s}^{-1}$) is the rainfall intensity at time t and position x .

- The kinematic wave assumption equation:

$$q = Vh = \alpha h^n \quad (7.2)$$

where: V ($\text{m}\cdot\text{s}^{-1}$) is the flow velocity; α is an empirical hydraulic coefficient (related to the catchment's slope and surface roughness); and n is an empirical exponent (Bakhmeteff exponent). Units of α and n depend on the formulae used to estimate the flow resistance (de Lima and van der Molen, 1988).

According to Zarmi *et al.* (1983), the volumetric water flux can be represented by a linear kinematic approximation of Eq. (7.2), and so, this equations stands as:

$$q = \alpha h \quad (7.3)$$

This simplified linear approximation is valid for the steady flow of a thin layer of water over small impervious catchments (*e.g.*, urban impermeable areas). During a rainfall event, the thin layer of water is systematically struck by falling raindrops whose impacts cause a localized interruption of the flow at the point of collision, thus disturbing the flow lines. After the impact, runoff particles will accelerate until they are stopped by another raindrop. Because the flow is governed by the friction forces generated between the catchment surface and the thin runoff sheet, acceleration is low, and so it is reasonable to consider a steady flow (for a detailed description of this process see (Boers, 1994)). If there is uncertainty about the input data and/or the α and n parameters Zarmi's hypothesis can also lead to better results than the nonlinear approximation (Eq. (7.2)) due to the amplification of errors produced by the latter (Singh and Woolhiser, 1976). Using the linear kinematic approximation (Eq. (7.3)) and assuming the conditions expressed by Eqs. (7.5–7.6), we can rewrite Eq. (7.1) to obtain the following boundary value problem:

$$\frac{\partial h}{\partial t} + \alpha \frac{\partial h}{\partial x} = p(x, t) \quad (7.4)$$

$$h(0, t) = 0 \text{ (Boundary condition)} \quad (7.5)$$

$$h(x, 0) = 0 \text{ (Initial condition)} \quad (7.6)$$

The Laplace transform of Eq. (7.4) with respect to t yields:

$$s\mathcal{L}(h) - h(x, 0) + \alpha \frac{d}{dx} \mathcal{L}(h) = \psi(x, s) \quad (7.7)$$

where: s is an independent variable (Laplace transform s -domain); $\mathcal{L}(h)$ is the Laplace transform of $h(x,t)$; and $\psi(x,s)$ is the Laplace transform of $p(x,t)$.

Substituting Eq. (7.6) in Eq. (7.7), and dividing all terms of the resulting equation by α :

$$\frac{d}{dx} \mathcal{L}(h) + \frac{s}{\alpha} \mathcal{L}(h) = \frac{1}{\alpha} \psi(x,s) \quad (7.8)$$

Eq. (7.8) is a nonhomogeneous first-order linear differential equation in x .

The next two subsections will give solutions of Eq. (7.8) for the downstream and upstream movements of a storm cell moving with constant velocity.

7.2.1 SOLUTION OF THE 1D LINEAR KINEMATIC WAVE EQUATION FOR DOWNSTREAM (UNIFORM) MOVEMENT OF A STORM CELL

For the uniform movement of a single rainfall block (storm cell) in the same direction of flow (downstream), with velocity V_S , and assuming that the rainfall rate (p) is constant under the rainfall block, the rainfall rate at time t and position x , over a surface of length L and slope S (Figure 7.1), is given by:

$$p(x,t) = \begin{cases} p & \text{if } \frac{x}{V_S} \leq t \leq \frac{x+L_S}{V_S} \\ 0 & \text{if } t < \frac{x}{V_S} \vee t > \frac{x+L_S}{V_S} \end{cases} \quad (7.9)$$

where: V_S ($\text{m}\cdot\text{s}^{-1}$) and L_S (m) are, respectively, the rainfall block velocity and length.

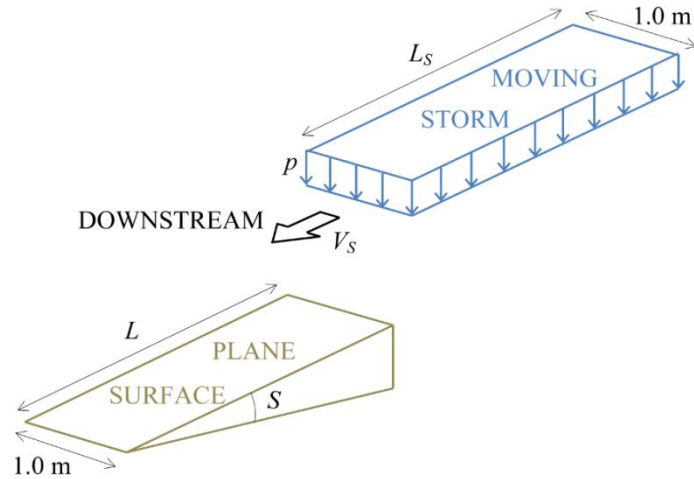


Figure 7.1 Sketch of a storm cell moving over a plane surface with unit width. “Downstream” refers to the storm cell’s movement in the flow direction.

The Laplace transform of the rainfall intensity $p(x,t)$ with respect to t yields:

$$\mathcal{L}[p(x,t)] = \psi(x,s) = \int_0^{\infty} e^{-st} p(x,t) dt = \frac{p}{s} \left(e^{-\frac{x}{V_s}s} - e^{-\frac{L_s+x}{V_s}s} \right) \quad (7.10)$$

The general solution of Eq. (7.8), for $V_s \neq \alpha$ is of the form (e.g., Piskounov, 1992):

$$\mathcal{L}(h) = e^{-\frac{x}{\alpha}s} \left(\frac{e^{\frac{V_s x - \alpha(L_s+x)}{\alpha V_s}s} \left(-1 + e^{\frac{L_s}{V_s}s} \right) p V_s}{s^2 (V_s - \alpha)} + C \right) \quad (7.11)$$

The constant of integration C follows from the boundary condition (Eq. (7.5)):

$$h(0,t) \Rightarrow \mathcal{L}(h) = 0 \Leftrightarrow C = \frac{\left(1 - e^{-\frac{L_s}{V_s}s} \right) p V_s}{s^2 (\alpha - V_s)} \quad (7.12)$$

The solution for the boundary value problem (Eqs. (7.4–7.6)) is consequently given by:

$$h(x,t) = \mathcal{L}^{-1} \left(\frac{e^{-\frac{2L_s+x}{V_s}s} \left(e^{\frac{L_s}{V_s}s} - 1 \right) \left(e^{\frac{L_s}{V_s}s} - e^{-\frac{\alpha(L_s+x)-V_s x}{\alpha V_s}s} \right) p V_s}{s^2 (V_s - \alpha)} \right) \quad (7.13)$$

Finally, the inverse Laplace transform of Eq. (7.13) is of the form:

$$\begin{aligned} h(x,t) = & \frac{P}{\alpha(\alpha - V_s)} \left(\alpha(tV_s - L_s - x) \mu \left(\frac{tV_s - L_s - x}{V_s} \right) + V_s(\alpha t - x) \mu \left(t - \frac{x}{\alpha} \right) \right. \\ & + \alpha L_s \mu \left(t - \frac{L_s}{V_s} - \frac{x}{\alpha} \right) - \alpha t V_s \mu \left(t - \frac{L_s}{V_s} - \frac{x}{\alpha} \right) + V_s x \mu \left(t - \frac{L_s}{V_s} - \frac{x}{\alpha} \right) \\ & \left. - \alpha t V_s \mu \left(t - \frac{x}{V_s} \right) + \alpha x \mu \left(t - \frac{x}{V_s} \right) \right) \end{aligned} \quad (7.14)$$

where: $0 \leq x \leq L$, $V_s \neq \alpha$ and μ is the Heaviside step function (with $\mu(0)=1$).

7.2.2 SOLUTION OF THE 1D LINEAR KINEMATIC WAVE EQUATION FOR UPSTREAM (UNIFORM) MOVEMENT OF A STORM CELL

For the uniform movement of a single rainfall block (storm cell) against the direction of flow (upstream), with velocity V_s , and assuming that the rainfall rate (p) is constant under the rainfall block, the rainfall rate at time t and position x , over a surface with length L and slope S (Figure 7.2), is given by:

$$p(x,t) = \begin{cases} p & \text{if } \frac{L-x}{V_s} \leq t \leq \frac{L-x+L_s}{V_s} \\ 0 & \text{if } t < \frac{L-x}{V_s} \vee t > \frac{L-x+L_s}{V_s} \end{cases} \quad (7.15)$$

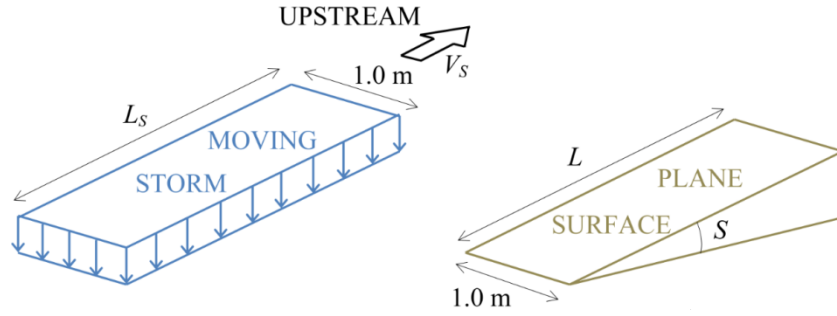


Figure 7.2 Sketch of a storm cell moving over a plane surface with unit width. “Upstream” refers to the storm cell’s movement opposite to the flow direction.

The Laplace transform of $p(x,t)$ with respect to t , yields:

$$\mathcal{L}[p(x,t)] = \psi(x,s) = \int_0^{\infty} e^{-st} p(x,t) dt = \frac{p}{s} \left(e^{\frac{L_s}{V_s} s} - 1 \right) e^{\frac{x-L-L_s}{V_s} s} \quad (7.16)$$

The general solution of Eq. (7.8) is of the form (e.g., Piskounov, 1992):

$$\mathcal{L}(h) = e^{-\frac{x}{\alpha} s} \left(\frac{e^{\frac{V_s x - \alpha(L+L_s-x)}{\alpha V_s} s} \left(e^{\frac{L_s}{V_s} s} - 1 \right) p V_s}{s^2 (V_s + \alpha)} + C \right) \quad (7.17)$$

The constant of integration C follows from the boundary condition (Eq. (7.5)):

$$h(0,t) \Rightarrow \mathcal{L}(h) = 0 \Leftrightarrow C = \frac{e^{-\frac{L+L_s}{V_s} s} \left(1 - e^{\frac{L_s}{V_s} s} \right) p V_s}{s^2 (V_s + \alpha)} \quad (7.18)$$

The solution for the boundary value problem (Eqs. (7.4–7.6)) is consequently given by:

$$h(x,t) = \mathcal{L}^{-1} \left(\frac{e^{-\left(\frac{L+L_s+x}{V_s} + \frac{x}{\alpha} \right) s} \left(e^{\frac{L_s}{V_s} s} - 1 \right) \left(e^{\frac{(V_s+\alpha)x}{\alpha V_s} s} - 1 \right) p V_s}{s^2 (V_s + \alpha)} \right) \quad (7.19)$$

Finally, the inverse Laplace transform of Eq. (7.19) is of the form:

$$\begin{aligned}
h(x,t) = & \frac{P}{\alpha(\alpha+V_s)} \left(\alpha(tV_s+x-L) \mu \left(\frac{tV_s+x-L}{V_s} \right) \right. \\
& + \alpha(L+L_s-tV_s-x) \mu \left(\frac{tV_s+x-L-L_s}{V_s} \right) + \alpha L \mu \left(t - \frac{L}{V_s} - \frac{x}{\alpha} \right) \\
& - \alpha t V_s \mu \left(t - \frac{L}{V_s} - \frac{x}{\alpha} \right) + V_s x \mu \left(t - \frac{L}{V_s} - \frac{x}{\alpha} \right) - \alpha L \mu \left(t - \frac{L+L_s}{V_s} - \frac{x}{\alpha} \right) \\
& \left. - \alpha L_s \mu \left(t - \frac{L+L_s}{V_s} - \frac{x}{\alpha} \right) + \alpha t V_s \mu \left(t - \frac{L+L_s}{V_s} - \frac{x}{\alpha} \right) - V_s x \mu \left(t - \frac{L+L_s}{V_s} - \frac{x}{\alpha} \right) \right)
\end{aligned} \tag{7.20}$$

where: $0 \leq x \leq L$ and μ is the Heaviside step function (with $\mu(0)=1$).

7.3 VERIFICATION OF THE ANALYTICAL SOLUTION

The developed 1D analytical solution for the kinematic wave equation under moving storms was verified using another analytical solution (Singh, 1998), a numerical approximation (de Lima and Singh, 2002), and laboratory simulations using a rainfall simulator able to simulate downstream and upstream moving storms.

7.3.1 COMPARISON WITH ANOTHER ANALYTICAL SOLUTION

Using the method of characteristics, Singh (1998) presented an analytical solution of the nonlinear kinematic wave equation for overland flow caused by storms moving up and down an impervious plane. The solution was used to study the influence of the storm movement on the flow hydrograph by comparing the flow resulting from moving and equivalent stationary storms. Dimensionless solutions were obtained to study how the duration of rain and the velocity of moving storm cells influenced the hydrograph shape (*e.g.*, discharge, peak discharge, time to peak discharge, steepness of the hydrograph).

For both the equilibrium and partial equilibrium hydrographs the solution is divided into 3 temporal domains, D_1 , D_2 and D_3 , respectively representing the hydrograph rising limb, crest (peak segment) and recession limb. For the equilibrium hydrograph the proposed solution is as follows:

– Downstream storm movement:

Domain D₁:

$$h(x,t) = \frac{p(tV_s - x)}{V_s - \alpha h^{(n-1)}} \quad (7.21)$$

Domain D₂:

$$h(x,t) = \left(\frac{px}{\alpha} \right)^{1/n} \quad (7.22)$$

Domain D₃:

$$h(x,t) = (T-t)np + \frac{n\alpha h^n}{V_s} + \frac{xp}{\alpha h^{(n-1)}} \quad (7.23)$$

– Upstream storm movement:

Domain D₁:

$$h(x,t) = \frac{ptV_s - (L - px)}{V_s - \alpha h^{(n-1)}} \quad (7.24)$$

Domain D₂:

$$h(x,t) = \left(\frac{px}{\alpha} \right)^{1/n} \quad (7.25)$$

Domain D₃:

$$h(x,t) = \left(T - t + \frac{nL + x}{nV_s} \right) + \frac{pnV_s}{nV_s + \alpha h^{(n-1)}} \quad (7.26)$$

where: T (s) is the storm duration.

Solutions for the rising and recession limbs are implicit for both the downstream and upstream storms (domains D_1 and D_3 ; Eqs. (7.21, 7.23, 7.24, 7.26)). Discharge $q(x,t)$ is obtained through Eq. (7.2).

This solution presented by Singh (1998) was compared, for a unit Bakhmeteff exponent ($n=1.0$; linear kinematic wave equation), with the one proposed in this study by evaluating the flood hydrograph caused by a $2.78 \cdot 10^{-5} \text{ m}\cdot\text{s}^{-1}$ ($100 \text{ mm}\cdot\text{h}^{-1}$) rainfall intensity and a 500 m long rainfall cell, which was moving over a 100 m plane at a velocity of $5.0 \text{ m}\cdot\text{s}^{-1}$. The plane's slope was 1.0% with a surface roughness Strickler coefficient (K) of $30 \text{ m}^{1/3}\cdot\text{s}^{-1}$, resulting in a hydraulic coefficient of 3.0.

The storm hydrographs obtained by the analytical solutions presented in this study (solid lines) and obtained by Singh (1998) (markers), show a perfect match for both the downstream and upstream storm movements (Fig. 3).

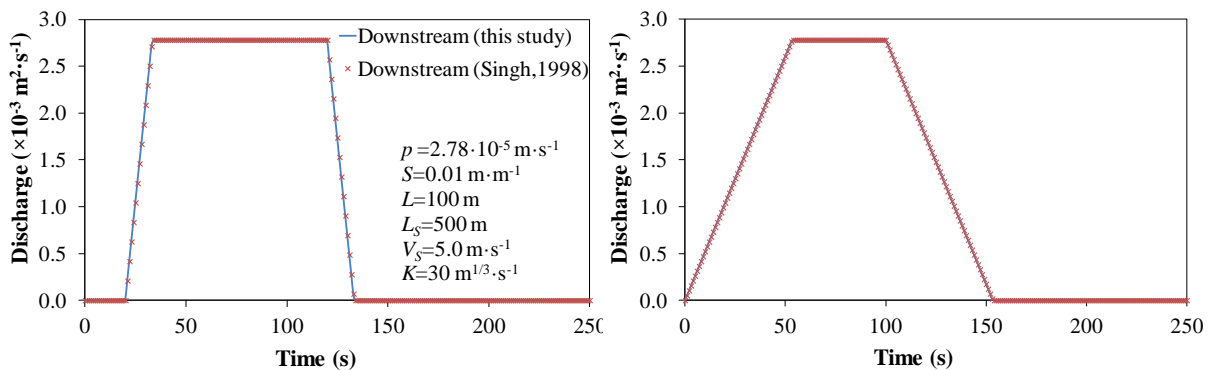


Figure 7.3 Flood hydrographs obtained with the analytical solutions presented in this study and in Singh (1998) for (left) downstream and (right) upstream storm movements.

7.3.2 COMPARISON WITH A NUMERICAL APPROXIMATION

A numerical approximation to the nonlinear kinematic wave equation for moving storms, solved with the second-order single step Lax-Wendroff scheme, was proposed by de Lima and Singh (2002). This approximation was used to compare the runoff hydrographs of hypothetical storms with different storm patterns, lengths, speeds and directions. Hypothetical storm patterns were determined by the arrangement of the rainfall intensity histogram. These storms moved up and down over an impervious plane surface to simulate one dry-wet-dry cycle.

To guarantee the stability of the discretised equation, the time-step/space-step ratio verified the Courant condition for linear numerical stability (e.g., Constantinides,

1981; Stephenson and Meadows, 1986). In this approximation the finite-difference form of the continuity equation (Eq. (7.1)) under the kinematic wave assumption (Eq. (7.2)) is expressed as:

$$\begin{aligned}
h_j^{i+1} = h_j^i + \Delta t & \left(p_j^i - n\alpha \frac{h_{j+1}^{i^{n-1}} + h_{j-1}^{i^{n-1}}}{2} \frac{h_{j+1}^i - h_{j-1}^i}{2\Delta x} \right) + \frac{(\Delta t)^2}{2} \frac{p_j^{i+1} - p_j^i}{\Delta t} \\
& - \frac{(\Delta t)^2}{2} n\alpha \left[\frac{h_{j+1}^{i^{n-1}} + h_j^{i^{n-1}}}{2} \left(\frac{p_{j+1}^i + p_j^i}{2} - n\alpha \frac{h_{j+1}^{i^{n-1}} + h_j^{i^{n-1}}}{2} \frac{h_{j+1}^i - h_j^i}{\Delta x} \right) \right. \\
& \left. - \frac{h_j^{i^{n-1}} + h_{j-1}^{i^{n-1}}}{2} \left(\frac{p_j^i + p_{j-1}^i}{2} - n\alpha \frac{h_j^{i^{n-1}} + h_{j-1}^{i^{n-1}}}{2} \frac{h_j^i - h_{j-1}^i}{\Delta x} \right) \right] / \Delta x
\end{aligned} \tag{7.27}$$

where: j denotes position and i denotes time, Δx is the space-step and Δt the time-step. For the downstream boundary, de Lima and Singh (2002) propose the following first-order scheme:

$$h_j^{i+1} = h_j^i + \Delta t \left(p_j^i - n\alpha \frac{h_j^{i^{n-1}} + h_{j-1}^{i^{n-1}}}{2} \frac{h_j^i - h_{j-1}^i}{\Delta x} \right) \tag{7.28}$$

This numerical approximation was used to evaluate for a unit Bakhmeteff exponent ($n=1.0$; linear kinematic wave equation), the flood hydrograph caused by a $2.78 \cdot 10^{-5} \text{ m}\cdot\text{s}^{-1}$ ($100 \text{ mm}\cdot\text{h}^{-1}$) rainfall intensity and 200 m long rainfall cell, which was moving over a 100 m plane at a velocity of $5.0 \text{ m}\cdot\text{s}^{-1}$. The plane's slope was 1.0% with a surface roughness Strickler coefficient of $30 \text{ m}^{1/3}\cdot\text{s}^{-1}$, resulting in a hydraulic coefficient of 3.0.

Storm hydrographs for a downstream and an upstream storm movement (Figure 7.4), were obtained by the analytical solution presented in this study (solid lines) and by the above-mentioned numerical approximation (markers). Very good consistency was found for both movements ($R^2=1.00$ for the downstream and the upstream storm movement).

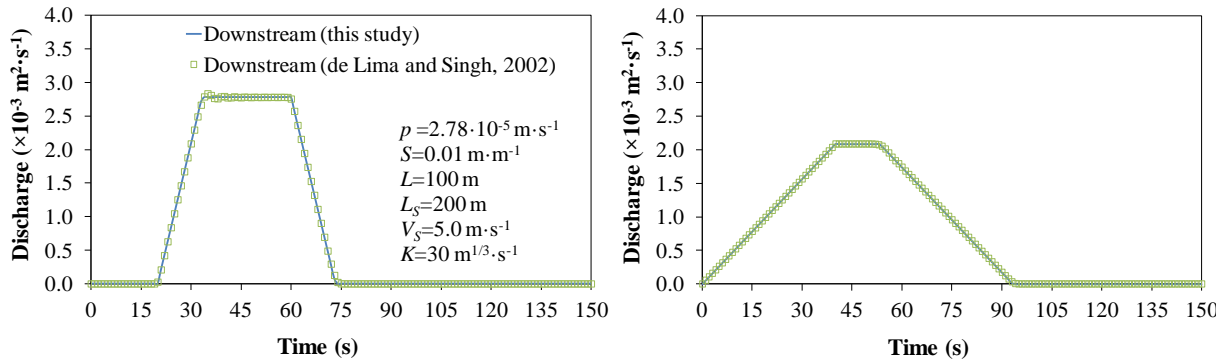


Figure 7.4 Analytical solution and numerical approximation (presented in de Lima and Singh (2002)) of flood hydrographs for (left) downstream and (right) upstream storm movements.

7.3.3 COMPARISON WITH LABORATORY SIMULATIONS

Laboratory runs were conducted on a flume as shown in Figure 7.5, to compare the analytical solution with experimental data. The laboratory apparatus consisted of a rainfall simulator fixed to an electrically-driven moving structure, a $2.00 \times 2.00 \text{ m}^2$ impermeable flume and a discharge measuring system.

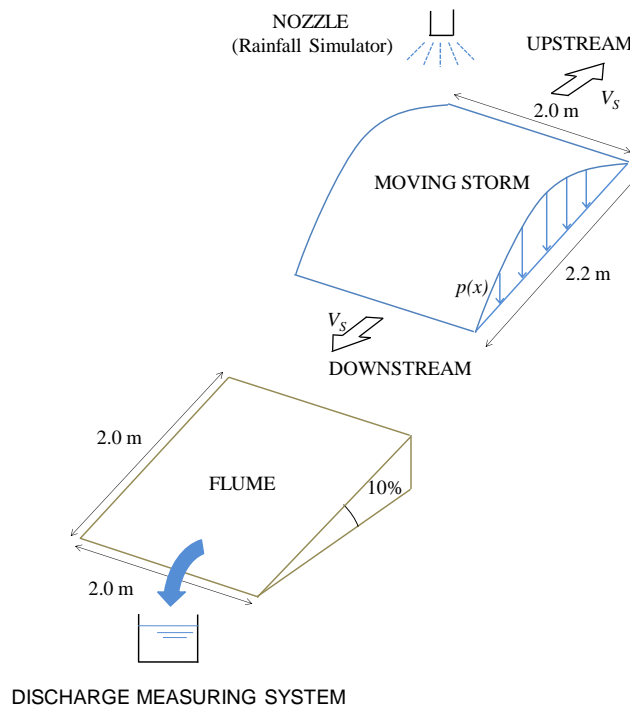


Figure 7.5 Sketch of the laboratory experiments. The simulated storm cell, generated by a moving sprinkler, moves over the laboratory flume.

The rainfall simulator comprised a constant level reservoir, a pump, a system of hoses, a stand, two electric engines, an automatic control panel to control the speed

at which the assembly moved (it was driven along a rail to simulate the rain cell movements), a sprinkler with flow control and a (constant) pressure gauge fixed to a connecting rod on the stand, 2.0 m above the flume. The nozzle's relative position did not change when the assembly moved. For a detailed description on the rainfall simulator see de Lima *et al.* (2003).

The 2.00×2.00 m² impermeable flume's surface is made of a single 2 mm steel sheet, in which the longitudinal slope is 10.0%. The rainfall simulator structure's downstream and upstream movements followed the flume's longitudinal slope. Rainfall water drained to an outlet located in the middle of the flume's downstream side.

The discharge measuring system comprised a cylindrical reservoir 0.14 m in diameter and 0.60 m deep which was positioned at the flume's outlet. The reservoir had a high-sensitivity pressure transducer (VEGA Bar 20) connected to a data logger (Campbell Scientific Ltd. CR510) and linked via an RS232 interface (Campbell Scientific Ltd. SC32A) to a computer (Intel Pentium III processor, 640 MB RAM), allowing the continuous monitoring of the pressure measurements and data logging (1.0 s intervals).

Experimental runs were performed to obtain flood hydrographs at the flume's outlet. Rainfall intensity and spatial distribution were determined by the sprinkler size and type (one downward-oriented full-cone nozzle – Spraying Systems Co.), the water operating pressure (145 kPa registered by the pressure gauge) and the nozzle height above the flume's surface (2.0 m). Rainfall water for a 240 s rainfall event was captured and weighed in a grid of plastic containers spaced 0.30 m apart, enabling the rainfall spatial distribution to be obtained. The measurements were taken 3 times. Average rainfall intensity was $3.33 \cdot 10^{-5} \text{ m} \cdot \text{s}^{-1}$ ($120 \text{ mm} \cdot \text{h}^{-1}$) and storm length was 2.2 m. Figure 7.6 shows the measured rainfall spatial distribution under the nozzle (static) which is different from the uniform rainfall distribution used as an input for the derivation of the analytical solution presented in this paper. The laboratory set-up used is not able to produce uniform rainfall.

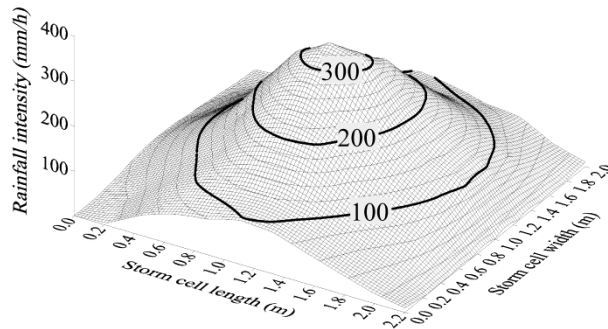


Figure 7.6 3D representation of the rainfall spatial distribution under the nozzle.

The roughness coefficient of the steel sheet defined by the Strickler coefficient was $100 \text{ m}^{1/3} \cdot \text{s}^{-1}$, which gives a hydraulic coefficient of 31.62 for a 10% slope. Fig. 7 shows the storm hydrographs provided by the analytical solution presented in this study (solid lines) and by the experimental runs (dashed lines), for a downstream and an upstream storm movement. Although the spatial distribution of rainfall over the flume is non-uniform, the analytical solution was able to reasonably describe the behaviour of the runoff hydrographs. Computed and experimental hydrograph shapes are similar, but the first shows a slight delay on the time to peak and a higher peak value, respectively for the downstream and the upstream storm movements. These slight differences are due to (i) the fact the experimental and simulated rainfall intensity histograms were respectively for non-uniform and uniform moving storms; (ii) the kinematic wave approach that assumes a constant empirical hydraulic coefficient (α), and (iii) adhesion and surface tension, which are not expressed in the kinematic wave model, but may be responsible for delaying the discharge of the last amount of water from the flume (as can be seen in Fig. 7.7 where, for both storm directions, the end of the recession limb of the experimental hydrographs decreases much more slowly than the simulated hydrograph).

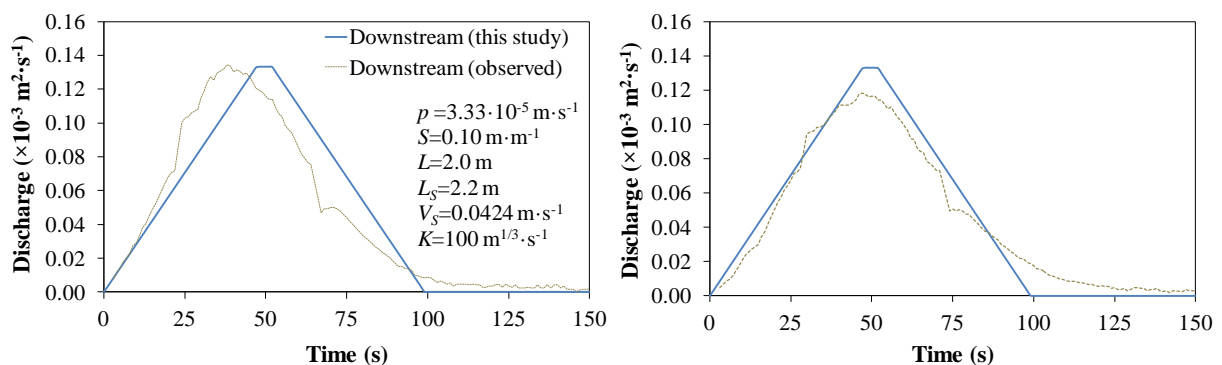


Figure 7.7 Analytical solution and experimental simulation of flood hydrographs for (left) downstream and (right) upstream storm movement.

The Nash-Sutcliffe coefficient of efficiency (*NSE*) was used to support the validity of the comparison of the results obtained from the laboratory simulations and the analytical solution (Eq. (7.29)). *NSE* coefficients of 0.95 and 0.84 were found, respectively for the upstream and the downstream storm movement, thus showing a very good correlation (Moriassi *et al.*, 2007) between the results obtained from the laboratory simulations and the analytical solution. This shows that, despite the simplification in the rainfall input, the analytical solution was able to simulate the behaviour of the experimental hydrographs.

$$NSE = 1 - \frac{\sum_k^m (Y_k^{obs} - Y_k^{sim})^2}{\sum_k^m (Y_k^{obs} - \bar{Y}_k^{obs})^2} \quad (7.29)$$

where: Y_k^{obs} is the k^{th} observed discharge, Y_k^{sim} is the k^{th} simulated discharge, \bar{Y}_k^{obs} is the mean of observed discharges, and m is the total number of observations.

7.4 APPLICATIONS

To evaluate the hydrologic response (flood hydrographs) to moving storms using the analytical solution, several hypothetical scenarios (catchment lengths (L) and surface roughnesses (K)) and storm patterns (lengths (L_s), velocities (V_s) and rainfall intensities (p)) were used. These hypothetical scenarios could represent examples of engineering applications since the input data (catchment and storm data) is within the range of real-world situations. The runoff hydrographs for the entire time-space domains were obtained so that the specified variables influence on the behaviour of the resulting hydrographs could be assessed.

An example is given of a catchment 100 m long and with a hydraulic coefficient (α ; see Eqs. (7.2–7.3)) of 2.0. Figure 7.8 shows the overland flow hydrograph for the entire space-time domain. The overland flow was caused by the movement of a storm cell with velocity of $0.5 \text{ m}\cdot\text{s}^{-1}$, rainfall intensity of $2.78 \cdot 10^{-5} \text{ m}\cdot\text{s}^{-1}$ ($100 \text{ mm}\cdot\text{h}^{-1}$) and length of 250 m. The discharge was calculated for a period of 1000 s. The discharge was evaluated over time (the hydrograph) for the total drainage surface, which may be important in urban flood risk assessment (*e.g.*, knowing *when* and *where* flow peaks occur). It can be seen that the downstream storm cell movement

leads to steeper rising and recession limbs of the hydrograph, for the entire drainage surface. Over the drainage surface there is an increase in the difference of the hydrographs (downstream and upstream) base time, and the maximum difference (100 s) occurs at the outlet.

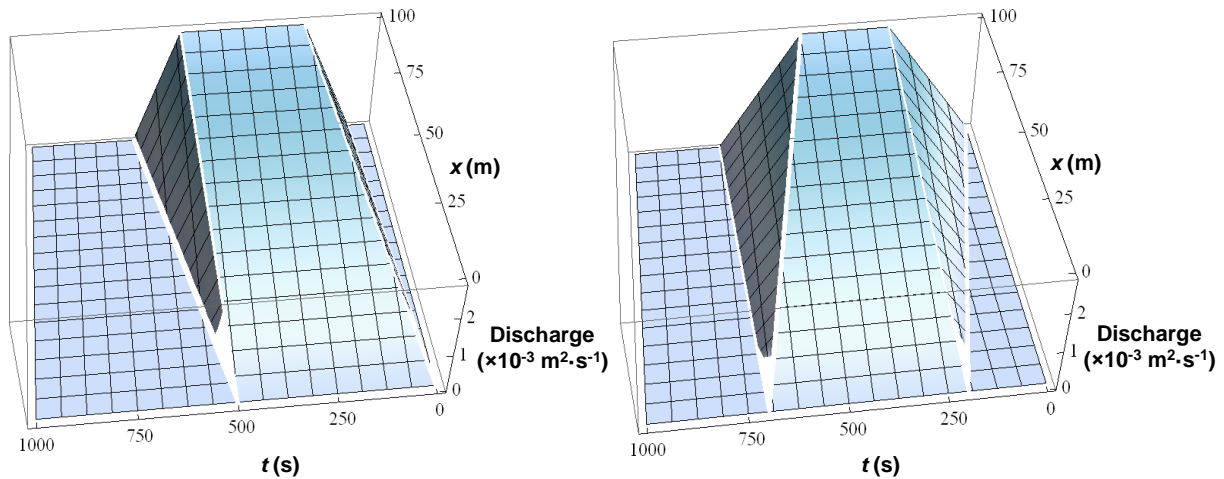


Figure 7.8 Entire time-space domain hydrographs provided by the analytical solution for a catchment 100 m long and with a hydraulic coefficient (α) of 2.0, caused by a storm cell moving with a velocity of $0.5 \text{ m} \cdot \text{s}^{-1}$ and having $2.78 \cdot 10^{-5} \text{ m} \cdot \text{s}^{-1}$ ($100 \text{ mm} \cdot \text{h}^{-1}$) rainfall intensity and a length of 250 m, for (left) downstream and (right) upstream storm movements.

The influence of storm cell velocity on hydrographs was analyzed by simulating an overland flow on an imaginary catchment with a length of 500 m, slope of 1.0% and Strickler roughness coefficient of $100 \text{ m}^{1/3} \cdot \text{s}^{-1}$ ($\alpha=10$), above which a storm cell with a rainfall intensity of $2.78 \cdot 10^{-5} \text{ m} \cdot \text{s}^{-1}$ ($100 \text{ mm} \cdot \text{h}^{-1}$) and a length of 1000 m moves with a velocity of 0.5, 1.0 and $5.0 \text{ m} \cdot \text{s}^{-1}$. Figure 7.9 shows that storm cell moving downstream (mainly at faster velocities) tend to promote higher runoff peaks than upstream-moving storm cells. Storm cells moving at faster velocities also lead to steeper hydrographs (both the rising and the recession limbs) and therefore shorter base times, which is physically explained by the shorter time over which rainfall take place in those instances.

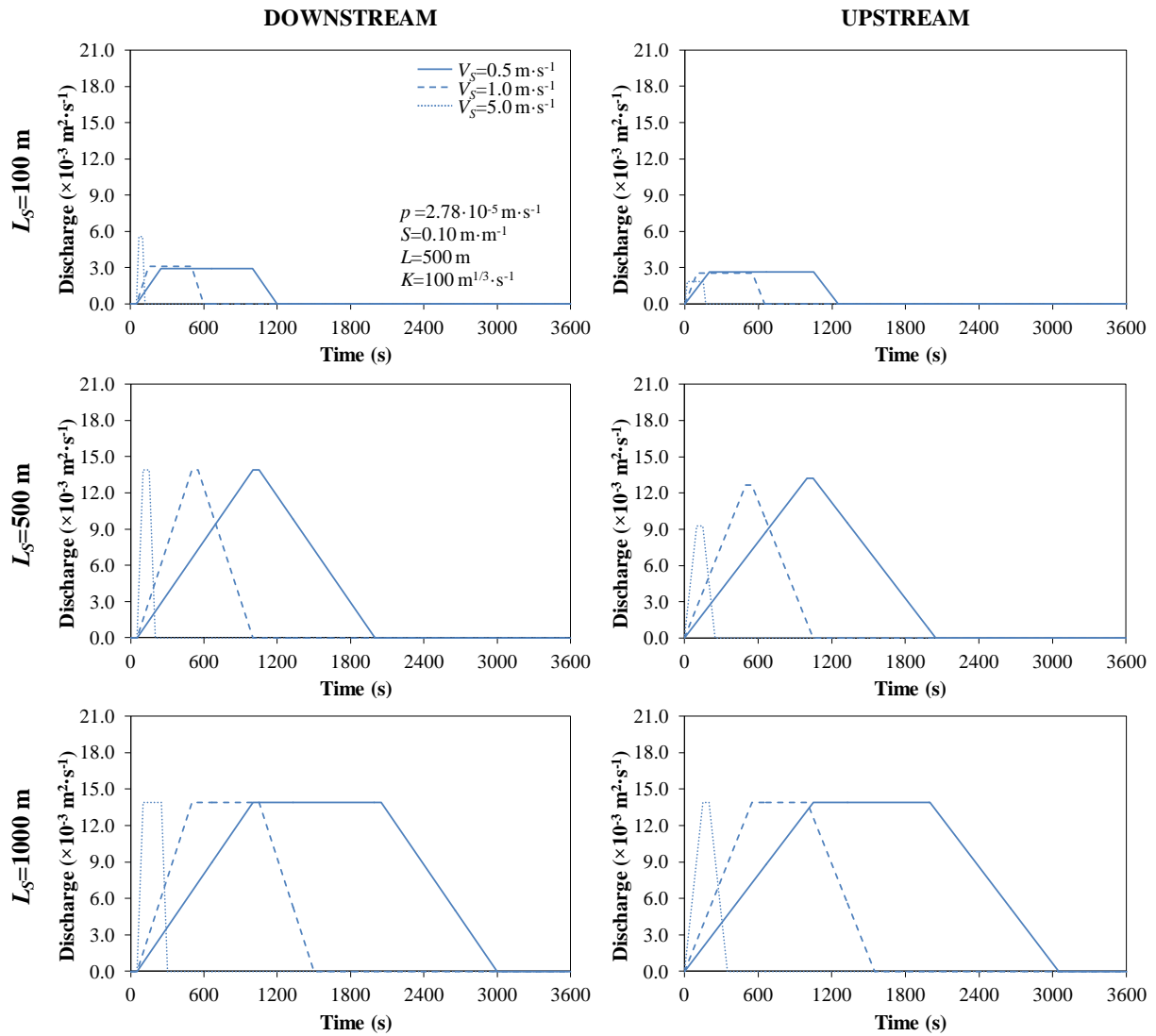


Figure 7.9 Hydrographs for a catchment with a length of 500 m, a slope of 1.0% and Strickler roughness coefficient of $100 \text{ m}^{1/3} \cdot \text{s}^{-1}$ ($\alpha=10$), caused by storm cells of (top) 100 m, (middle) 500 m and (bottom) 1000 m length and with a rainfall intensity of $2.78 \cdot 10^{-5} \text{ m} \cdot \text{s}^{-1}$ ($100 \text{ mm} \cdot \text{h}^{-1}$) moving (left) downstream and (right) upstream, at a velocity of 0.5, 1.0 and $5.0 \text{ m} \cdot \text{s}^{-1}$.

To understand the discharge evolution over the drainage surface for an imaginary catchment 100 m long and with a slope of 1.0% and Strickler roughness coefficient of $100 \text{ m}^{1/3} \cdot \text{s}^{-1}$ ($\alpha=10$), caused by the movement of a storm cell with rainfall intensity of $2.78 \cdot 10^{-5} \text{ m} \cdot \text{s}^{-1}$ ($100 \text{ mm} \cdot \text{h}^{-1}$) and 50 m long, moving at $2.0 \text{ m} \cdot \text{s}^{-1}$, the linear kinematic wave equation was solved for $t=20, 40$ and 60 s (Figure 7.10).

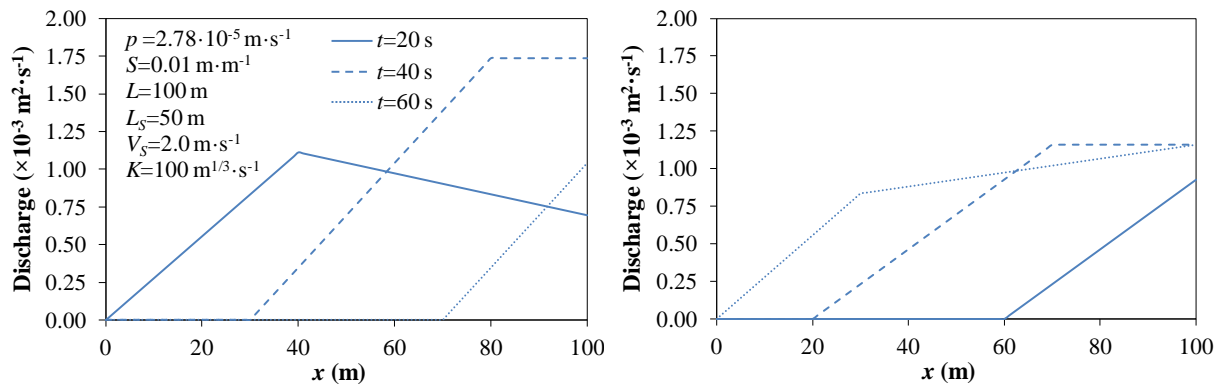


Figure 7.10 Discharge vs. drainage surface length in $t=20, 40$ and 60 s for (left) downstream and (right) upstream storm movements.

The following can be said of the above scenarios: (i) distinct hydrologic responses for storms moving upstream and downstream were identified; (ii) higher V_s lead to steeper rising limbs of the hydrograph, both for downstream and upstream storm movement; (iii) downhill storms lead to steeper rising limb of the hydrographs and higher peak flows than uphill storms. All of which are in accordance with the conclusions reported by other authors (*e.g.*, Yen and Chow, 1969; Singh, 1998; de Lima and Singh, 2002; de Lima *et al.*, 2003).

7.4 CONCLUSIONS

This study has presented and discussed an analytical solution of the 1D kinematic wave equation combined with Zarmi's hypothesis for overland flow under upstream and downstream moving storms. Moving storms are of particular importance when modelling urban environments because of their responsiveness to spatial and temporal variations of rainfall and fast hydrologic response. The analytical solution is easy to use and gives the solution for the overland flow in the full space-time domain in just one single explicit closed form equation which has never been presented before. For the assumed presumption of linearity, this is a clear advantage over other solutions.

The analytical solution was verified by comparing the computed hydrographs with the results attained by using another analytical solution and, a numerical approximation, both for the linearized kinematic wave equation, and laboratory observations using three different sets of parameters. The Results showed a perfect match with the other analytical solution and a very good fit with the numerical approximation, thereby validating the proposed solution. The analytical solution was

also able to capture the shape of hydrographs obtained in the laboratory, exhibiting high Nash-Sutcliffe coefficients of efficiency.

The particular simplicity of the analytical solution presented in this work contributes to a more straightforward and less time-consuming study of the rainfall-runoff processes under moving rainstorms. In addition to being a useful tool in fundamental hydrological studies, the proposed formulae may be used to calibrate more complex models, estimate hydrological parameters (*e.g.*, surface roughnesses) and quantify overland flow for design purposes (*e.g.*, micro-catchments, water harvesting systems and road drainage systems).

7.5 ACKNOWLEDGMENTS

The authors wish to acknowledge José Pereira, BSc and Dr. José Rodrigues for their valuable suggestions on the mathematical issues and to Mr. Joaquim Cordeiro for his help with the laboratory work. The authors also wish to acknowledge the comments and suggestions of the three anonymous Reviewers, the Associated Editor and the Editor-in-Chief of the Journal of Hydrologic Engineering. The availability of the Laboratory of Hydraulics, Water Resources and Environment of the Department of Civil Engineering of the Faculty of Science and Technology, University of Coimbra (Portugal), in which the laboratory experiments took place, is also acknowledged.

7.6 NOTATION

The following symbols are used in this chapter:

C	constant;
K	Strickler coefficient;
L	length of catchment;
L_S	length of storm block;
NSE	Nash-Sutcliffe coefficient of efficiency;
S	slope;
T	storm duration;
V	flow velocity;
V_S	storm block velocity;

Y_k^{obs}	k^{th} observed discharge;
\bar{Y}_k^{obs}	k^{th} observed mean discharge;
\bar{Y}_k^{sim}	k^{th} simulated discharge;
h	flow depth;
i	discretised time;
j	discretised position;
m	total number of observations;
n	empirical exponent;
p	rainfall intensity;
q	volumetric water flux per unit width;
s	independent variable (Laplace transform s -domain);
t	time;
x	position;
Δt	time-step;
Δx	space-step;
α	hydraulic coefficient;
μ	Heaviside step function;
ψ	Laplace transform of function p .

7.7 REFERENCES

- Black, P.E., 1972. Hydrograph responses to geomorphic model watershed characteristics and precipitation variables. *Journal of Hydrology*, 17 (4), 309–329.
- Boers, Th.M., 1994. Rainwater harvesting in arid and semi-arid zones. Thesis (PhD). The International Institute for Land Reclamation, Wageningen University.
- Boers, Th.M., van der Molen, W.H., Eppink, L.A.A.J. and Ben-Asher, J., 1991. Effect of the Thomson weir and weirbox on the measurement of flow rates from micro-catchments and runoff plots. *Journal of Hydrology*, 128 (1–4), 29–39.
- Borah, D.K., Prasad, S.N. and Alonso, C.V., 1980. Kinematic wave routing incorporating shock fitting. *Water Resources Research*, 16 (3), 529–541.
- Constantinides, C.A., 1981. Numerical techniques for a two-dimensional kinematic overland flow model. *Water SA*, 7 (4), 234–248.

- de Lima, J.L.M.P. and Singh, V.P., 2002. The influence of the pattern of moving rainstorms on overland flow. *Advances in Water Resources*, 25 (7), 817–828.
- de Lima, J.L.M.P. and van der Molen, W.H., 1988. An analytical kinematic model for the rising limb of overland flow on infiltrating parabolic shaped surfaces. *Journal of Hydrology*, 104 (1–4), 363–370.
- de Lima, J.L.M.P., Singh, V.P. and de Lima, M.I.P., 2003. The influence of storm movement on water erosion: Storm direction and velocity effects. *Catena*, 52 (1), 39–56.
- de Lima, M.I.P., Schertzer, D., Lovejoy, S. and de Lima, J.L.M.P., 2002. Multifractals and the study of extreme precipitation events: a case study from semi-arid and humid regions in Portugal. In: V.P. Singh, M. Al-Rashid and M.M. Sherif, eds. *Surface Water Hydrology*. Lisse: AA Balkema Publishers, 195–211.
- Eagleson, P.S., 1970. *Dynamic Hydrology*. New York, NY: McGraw-Hill Book Co.
- Franchini, M., 1994. Combined analytical solution of overland flow and sediment transport. *Water Resources Management*, 8 (3), 225–238.
- Giakoumakis, S. and Tsakiris, G., 2001. Experimental Validation of a Linearized Kinematic Wave Equation for Micro-Catchment Water Harvesting Design. *Water Resources Management*, 15 (4), 235–246.
- Govindaraju, R.S., Kavvas, M.L. and Tayfur, G., 1992. A simplified model for 2-Dimensional overland flows. *Advances in Water Resources*, 15 (2), 133–141.
- Henderson, F.M. and Wooding, R.A., 1964. Overland flow and groundwater flow from a steady rainfall of finite duration. *Journal of Geophysical Research*, 69 (8), 1531–1540.
- Hindi, W.N.A. and Kelway, P.S., 1977. Determination of storm velocities as an aid to the quality control of recording raingauge data. *Journal of Hydrology*, 32 (1–2), 115–137.
- Jensen, M., 1984. Runoff pattern and peak flows from moving block rains based on linear time-area curve. *Nordic Hydrology*, 15 (3), 155–168.
- Lee, K.T. and Huang, J.K., 2007. Effect of moving storms on attainment of equilibrium discharge. *Hydrological Processes*, 21 (24), 3357–3366.
- Li, R.M., Simons, D.B. and Stevens, M.A., 1975. Nonlinear kinematic wave approximation for water routing. *Water Resources Research*, 11 (2), 245–252.
- Lighthill, M.J. and Whitham, G.B., 1955. On kinematic waves I. Flood movement in long rivers. *Proceedings of the Royal Society of London*, 229 (1178), 281–316.
- Maksimov, V.A., 1964. Computing runoff produced by a heavy rainstorm with a moving center. *Soviet Hydrology*, 5, 510–513.
- Meselhe, E.A., Habib, E.H., Oche, O.C. and Gautam, S., 2009. Sensitivity of conceptual and physically based hydrologic models to temporal and spatial rainfall sampling. *Journal of Hydrologic Engineering*, 14 (7), 711–720.

- Mizumura, K., 2006. Analytical solutions of nonlinear kinematic wave model. *Journal of Hydrologic Engineering*, 11 (6), 539–546.
- Mizumura, K. and Ito, Y., 2011. Influence of moving rainstorms on overland flow of an open book type using kinematic wave. *Journal of Hydrologic Engineering*, 16 (9), 736–745.
- Moramarco, T., Pandolfo, C. and Singh, V.P., 2008a. Accuracy of kinematic wave and diffusion wave approximations for flood routing. I: Steady analysis. *Journal of Hydrologic Engineering*, 13 (11), 1078–1088.
- Moramarco, T., Pandolfo, C. and Singh, V.P., 2008b. Accuracy of kinematic wave approximation for flood routing. II: Unsteady analysis. *Journal of Hydrologic Engineering*, 13 (11), 1089–1096.
- Moriasi, D.N., Arnold, J.G., van Liew, M.W., Bingner, R.L., Harmel, R.D. and Veith, T.L., 2007. Model evaluation guidelines for systematic quantification of accuracy in watershed simulation. *Transactions of the American Society of Agricultural and Biological Engineers*, 50 (3), 885–900.
- Niemczynowicz, J., 1988. The rainfall movement - A valuable complement to short-term rainfall data. *Journal of Hydrology*, 104 (1–4), 311–326.
- Ogden, F.L., Richardson, J.R. and Julien, P.Y., 1995. Similarity in Catchment Response: 2. Moving Rainstorms. *Water Resources Research*, 31 (6), 1543–1547.
- Piskounov, N., 1992. *Cálculo Diferencial e Integral*, Vol. 2. Porto: Lopes da Silva edições (in Portuguese).
- Singh, V.P., 1994. Accuracy of Kinematic-Wave and Diffusion-Wave Approximations for Space-Independent Flows. *Hydrological Processes*, 8 (1), 45–62.
- Singh, V.P., 1996. *Kinematic Wave Modelling in Water Resources: Surface-Water Hydrology*. New York, NY: Wiley-Interscience.
- Singh, V.P., 1998. Effect of the direction of storm movement on planar flow. *Hydrological Processes*, 12 (1), 147–170.
- Singh, V.P., 2001. Kinematic Wave Modeling in Water Resources: a Historical Perspective. *Hydrological Processes*, 15 (4), 671–706.
- Singh, V.P., 2002. Is Hydrology Kinematic? *Hydrological Processes*, 16 (3), 667–716.
- Singh, V.P. and Woolhiser, D.A., 1976. Sensitivity of linear and nonlinear surface runoff models to input errors. *Journal of Hydrology*, 29 (3–4), 243–249.
- Singh, V.P. and Woolhiser, D.A., 2002. Mathematical Modeling of Watershed Hydrology. *Journal of Hydrological Engineering*, 7 (4), 270–292.
- Smith, R.E., Goodrich, D.C., Woolhiser, D.A. and Unkrich, C.L., 1995. KINEROS: A kinematic runoff and erosion model. In: V.P. Singh, ed. *Computer Models of Watershed Hydrology*. Littleton, CO: Water Resources Publications, 697–732.
- Stephenson, D., 1984. Kinematic study of effects of storm dynamics on runoff hydrographs. *Water SA*, 10 (4), 189–196.

Stephenson, D. and Meadows, M.E., 1986. *Kinematic hydrology and modeling*. Amsterdam: Elsevier Science Publications Co.

Tayfur, G. and Kavvas, M.L., 1998. Areal-averaged overland flow equations at hillslope scale. *Hydrological Sciences Journal*, 43 (4), 361–378.

Villarini, G., Smith, J.A., Baeck, M.L., Smith, B.K. and Stedevant-Rees, P., 2012. Hydrologic analyses of the 17–18 July 1996 flood in Chicago and the role of urbanization. *Journal of Hydrologic Engineering*, doi:10.1061/(ASCE)HE.1943-5584.0000462, (in press).

Wilson, C.B., Valdes, J.B. and Rodrigues-Iturbe, I., 1979. On the influence of the spatial distribution of rainfall on storm runoff. *Water Resources Research*, 15 (2), 321–328.

Xiong, Y. and Melching, C.S., 2005. Comparison of kinematic-wave and nonlinear reservoir routing of urban watershed runoff. *Journal of Hydrologic Engineering*, 10 (1), 39–49.

Yen, B.C. and Chow, V.T., 1969. A laboratory study of surface runoff due to moving rainstorms. *Water Resources Research*, 5 (5), 989–1006.

Zarmi, Y., Asher, J.B. and Greengard, T., 1983. Constant velocity kinematic analysis of an infiltrating microcatchment hydrograph. *Water Resources Research*, 19 (1), 277–283.

CHAPTER 8

We know more about the movement of celestial bodies than about the soil underfoot.

Leonardo da Vinci

8. INCORPORATING MOVING STORM EFFECTS INTO HILLSLOPE HYDROLOGY: RESULTS FROM MULTIPLE-SLOPE SOIL FLUME

Abstract: The spatial and temporal characteristics of rainfall are altered by wind. Nevertheless, for simplicity, rainfall is typically assumed spatially uniform in conventional hydrological modelling of rainfall–runoff processes. The implications of this simplification for rainfall-runoff and soil loss estimation are sometimes not adequately evaluated. However, the importance of storm movement on surface flows has long been acknowledged, at scales ranging from headwater scales to drainage basins: different studies have shown that moving rainstorms substantially affect surface flow hydrographs although some of the results reported are in need of further insight. Difficulties in assessing the effect of storm movement in hydrological systems come from the extreme variability typically exhibited by all the relevant processes involved: *e.g.*, rainfall, wind, runoff, soil erosion. The combined effect of wind and rain assume an increasing importance in geographical areas where intense rainfall events are common, particularly in the context of climate change scenario projections pointing out to an increase in rainfall variability. This subject is particularly important for agriculture, soil and water conservation, urban hydrology and water resources management.

The main objective of this study is to quantify, at the hillslope scale, the hydrologic response to both non-moving and moving rainstorms, in terms of discharge and soil loss. Controlled laboratory experiments were carried out using a 6 m long multiple-slope soil flume and a movable sprinkling-type rainfall simulator. To simulate moving rainstorms, the rainfall simulator was moved upstream and downstream over the soil surface at different speeds. During runoff events overland flow and sediment transport were measured over time.

Results for different hillslope shapes are reported, taking advantage of the multiple-slope feature of the soil flume used in the experiments. In general, results show that the direction of storm movement, especially for very high intensity rainfall events, significantly affected runoff and water erosion processes. Downstream-moving storms caused significantly higher peak runoff and erosion than did upstream-moving storms. The hydrograph shapes were also different: for downstream-moving storms, runoff started later and the rising limb was steeper, whereas for upstream moving storms, runoff started earlier and the rising limb was less steep. The effect of the

direction of moving storms on the sediment loss quantity and quality was also studied, with downslope moving storms being potentially more erosive than their upstream counterparts.

Keywords: Hillslope hydrology; Moving storms; Overland flow; Soil loss

8.1 INTRODUCTION

Natural rainfall of low and high intensities is highly variable in both time and space (*e.g.*, Eagleson, 1978; Fofoula-Georgiou and Georgakakos, 1991; Ladoy *et al.*, 1993). The spatial and temporal characteristics of rainfall are affected by wind, and the importance of storm movement due to the combined effect of wind and rain on superficial flows, has long been recognised from the headwater to the larger catchment basins scales. Maksimov (1964) was probably the first to investigate the influence of rain storms movement on surface runoff and demonstrated that it modifies peak discharge. Nevertheless, for simplicity, rainfall is assumed spatially uniform in conventional hydrological modelling of the rainfall–runoff process. Moving rainstorms affects substantially surface flow hydrographs (*e.g.*, Yen and Chow, 1968; Jensen, 1984; Singh, 1998; de Lima and Singh, 2002 and 2003; Nunes *et al.*, 2006; and de Lima *et al.*, 2009) and in geographical areas where intense rainfall events are common, the combined effect of wind and rain assume an increasing importance in a context of a possible climate change scenario, pointing out to an increase in rainfall variability, thus, of extreme hydrological events. Regarding that soil loss from rainstorms moving in different directions across drainage areas are clearly the result of the corresponding overland flow dynamics, this subject gains particular importance for agriculture, soil and water conservation, urban hydrology, water resources management, environmental decision making and ecosystems sustainability, among other study areas.

All the referred involved processes (rainfall, wind, runoff, soil erosion) were investigated in this study in a laboratory equipped with a storm simulator, as this kind of equipment allow for a better control of parameters and thus to obtain improved results, benefits which have been discussed by Meyer (1965), Bryan and Poesen (1989), Cerdà *et al.* (1997). However, most of these studies did not take into account the combined effect of rainfall and wind and its effect on runoff. Failure to consider the movement of rainfall (*i.e.*, the combined action of wind and rainfall) can result in

under- or over-estimation of peak discharge (*e.g.*, Jensen, 1984; Singh, 1998; de Lima and Singh, 2002). The importance of this combined action, especially the changes in rainfall characteristics (*e.g.*, spatial and temporal distribution, trajectory of drops) and runoff (*e.g.*, height of runoff and velocity), has been recognized by a number of investigators (*e.g.*, Maksimov, 1964; Yen and Chow, 1968; Wilson *et al.*, 1979; Singh, 1998; Lima and Singh, 2000), and some authors (*e.g.*, de Lima and Singh, 2002) have considered the movement of rainfall over basins, particularly upstream or downstream.

The main objective of this study is to evaluate the hydrologic response of drainage systems (in terms of discharge and soil loss caused by both non-moving and moving rainstorms) and the influence of rainfall storm movement, through a characterization of the runoff hydrographs and sediment flux (by quantifying sediments transported on runoff and identifying their granulometry), and thus to contribute to increase understanding of water erosion factors and processes at a hillslope scale.

8.2 METHODS AND MATERIALS

Laboratory experiments were carried out using an articulated soil flume and a movable sprinkling-type rainfall simulator. To simulate moving rainstorms, the rainfall simulator was moved upstream and downstream over the soil flume surface at different velocities. The simulator could also produce non-moving precipitation at any part of the flume.

The methodology used to conduct the experiments was divided into two phases: (i) Simulation of rainfall events and obtaining the hydrographs of direct runoff; and (ii) characterization of the transported solid (granulometry analysis).

8.2.1 RAINFALL SIMULATOR

The rainfall simulator system (Figure 8.1) comprises a constant level reservoir, a pump, a system of hoses, a stand, 2 electric engines, 1 switch panel to control the apparatus velocity, and sprinklers (3/8 HH – 22 FullJet nozzles – Spraying Systems Co.) attached to a connecting rod and standing 2.20m above the soil flume surface. Position of nozzles, rainfall simulator movement and discharge point regarding the soil flume can be seen on Figure 8.2.

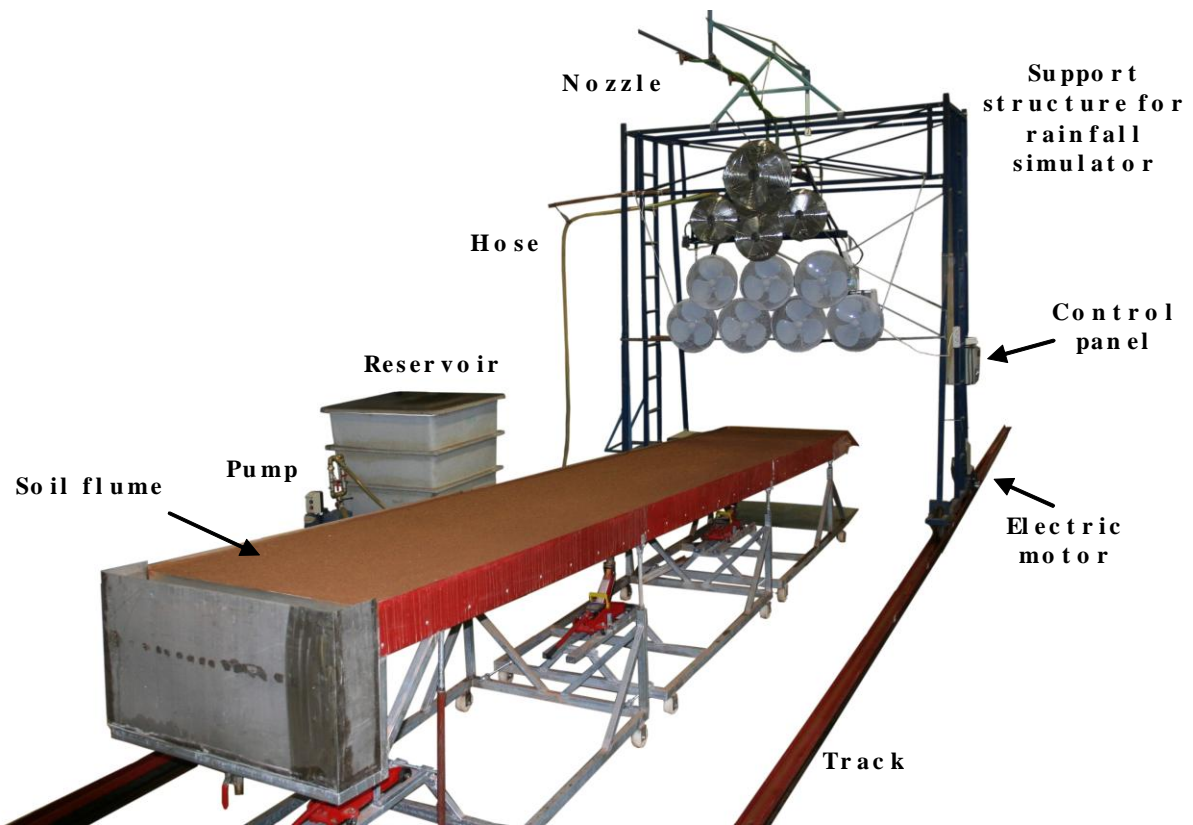


Figure 8.1 Rainfall simulator system and soil flume.

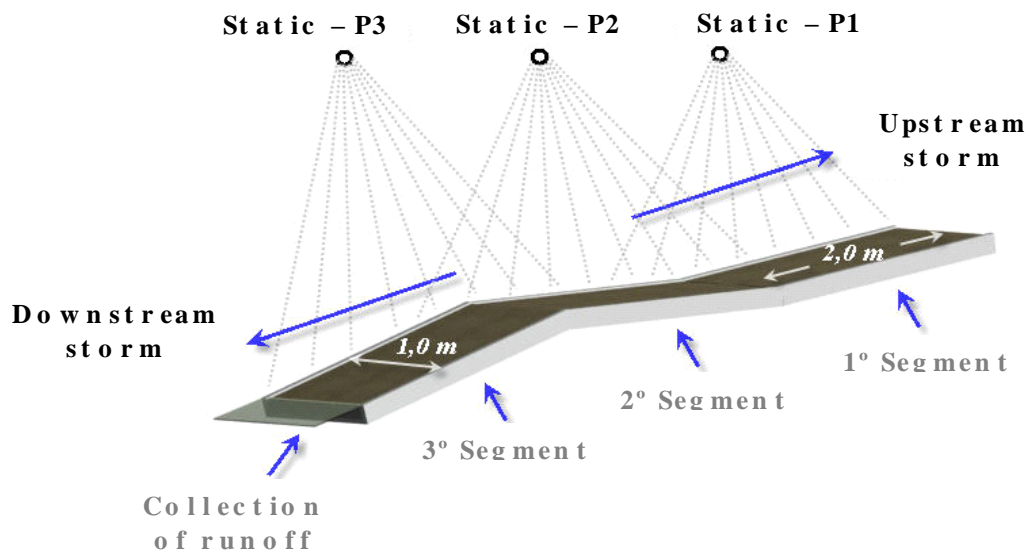


Figure 8.2 Position of nozzles, rainfall simulator movement and discharge point regarding the soil flume.

8.2.2 SOIL FLUME

The soil flume, made of zinc-coated iron was 6.00 m long (2.00 m each segment), 1.00 m wide and 0.10 m deep. Hillslope types varied by using the following segment slopes: 6 – 2 – 13%; 6 – 13 – 2%; 7 – 7 – 7%; 2 – 6 – 13% and 13 – 6 – 2% (Figure 8.3). The original soil consisted of 6.64% clay, 9.53% silt and 83.83% sand and gravel.






HILLSLOPE TYPES	NOMENCLATURES
	6 - 2 - 13%
	6 - 13 - 2%
	7 - 7 - 7%
	2 - 6 - 13%
	13 - 6 - 2%

Figure 8.3 Hillslope types used in the laboratory experiences.

8.2.3 STORM CHARACTERIZATION

The soil surface water content was controlled by imposing a 30 minutes interval between each simulated rainstorm event. The volumetric soil water content was of approximately 20% (determined by Time-Domain-Reflectometer measurements) just before the start all storm events. During experimentation, it was observed that there was always a higher quantity of fine particles transported in the first simulated rains; so each rainfall type of simulation was repeated for 4 times to observe differences in granulometric characteristics.

Rainfall used in the laboratory experiments had a constant pressure of 2 bar, corresponding to a discharge of 2.07 l/min (Figure 8.2). The velocity of the rainfall simulator was kept at a constant velocity of 4.00 m/min, which corresponds to a total of 9.70 litres of water falling on the flume surface. Storm proprieties, namely rainfall

intensity, sizes and velocities of rain drops were characterized by several equipments (Laser Precipitation Monitor – Thies, classic udometer and Weather Transmitter – Vaisala).

8.2.4 GRANULOMETRIC CHARACTERIZATION

Overland flow and sediment loss caused by each rainfall event were measured by collecting samples every 15 s in metal containers placed at the downstream end of the soil flume (discharge point). Time measurement for each storm event started at the initiation of overland flow at the flume outlet. The amount of sediment transported by overland flow was estimated by weighting after a low temperature oven drying of runoff samples.

The granulometric characterization of transported sediments consisted in two distinct methods: by use of optical spectrophotometry, and by conventional sieving. A laser diffraction particle size analyzer – LS 230 (Beckman Coulter, Inc.) was used. A sieving “cut” was applied in accordance with the moisture of the material in the 0.250 mm mesh sieve. The material whose particle size was smaller than the sieve mesh size was suspended in liquid and analyzed with the spectrophotometer, and the other fraction was dried and sieved in a conventional way.

8.3 RESULTS AND DISCUSSION

During runoff events, overland flow and sediment transport were measured in order to obtain hydrographs and evaluate sediment production over time.

8.3.1 HYDROGRAPHS AND SEDIMENT FLUX

Figures 8.4 and 8.5 presents runoff hydrographs and their respective sediment fluxes (4 rainfall events) for different storms as a function of hillslope types. It is observed that the distribution of both discharge and transported sediments by runoff depend on the storm and hillslope types.

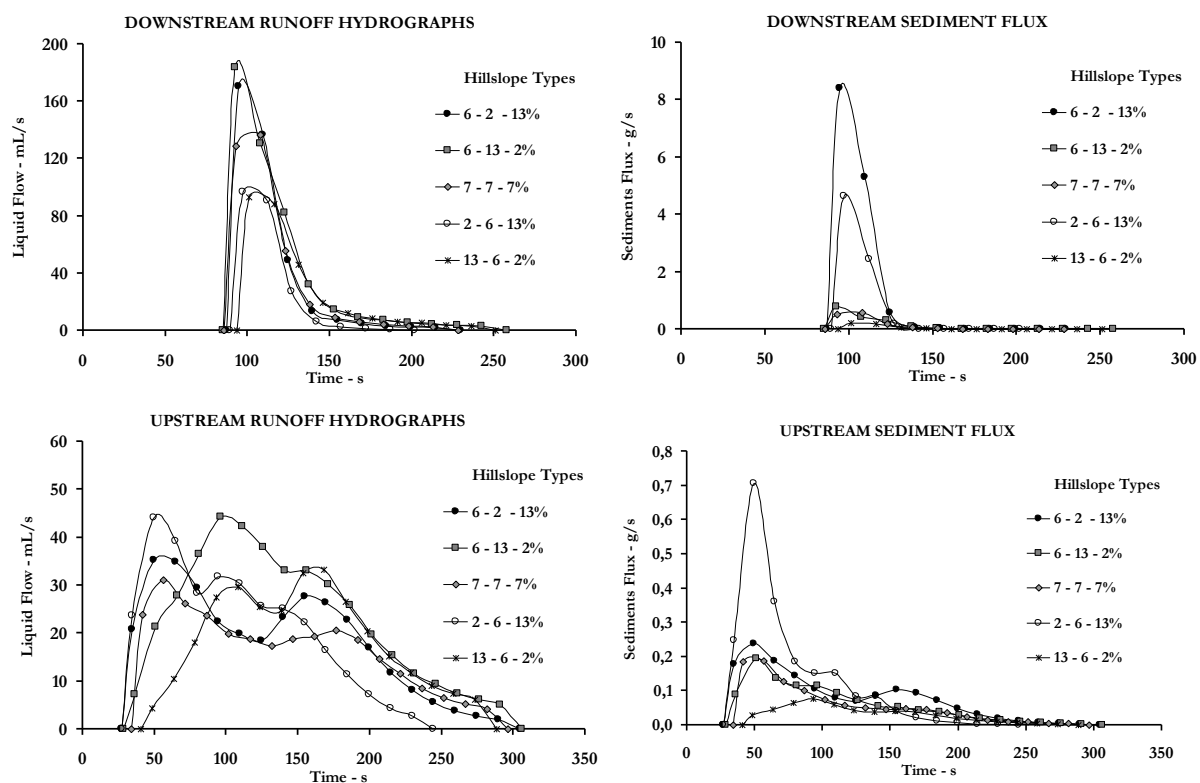


Figure 8.4 Runoff hydrographs and respective sediments fluxes for different storms and hillslopes types, for moving rains.

It can be observed that the hillslope types had a smaller effect on the hydrograph shape (and particularly on the peak discharge), but it a strong influence on the transport of sediments. This is because a steeper gradient increases the transport capacity of runoff, regardless of the storm type. Types of hillside that provide a bigger loss of sediments, and consequently, greater superficial erosion is the ones that possess the inclination of 13% next to the collection point of runoff. Amongst these, the hillside with a convex geometry (2-6-13%) is the one that presents the configuration most favourable to the transport of sediments. Table 8.1 summarizes the main characteristics of the runoff hydrographs and sediment flux.

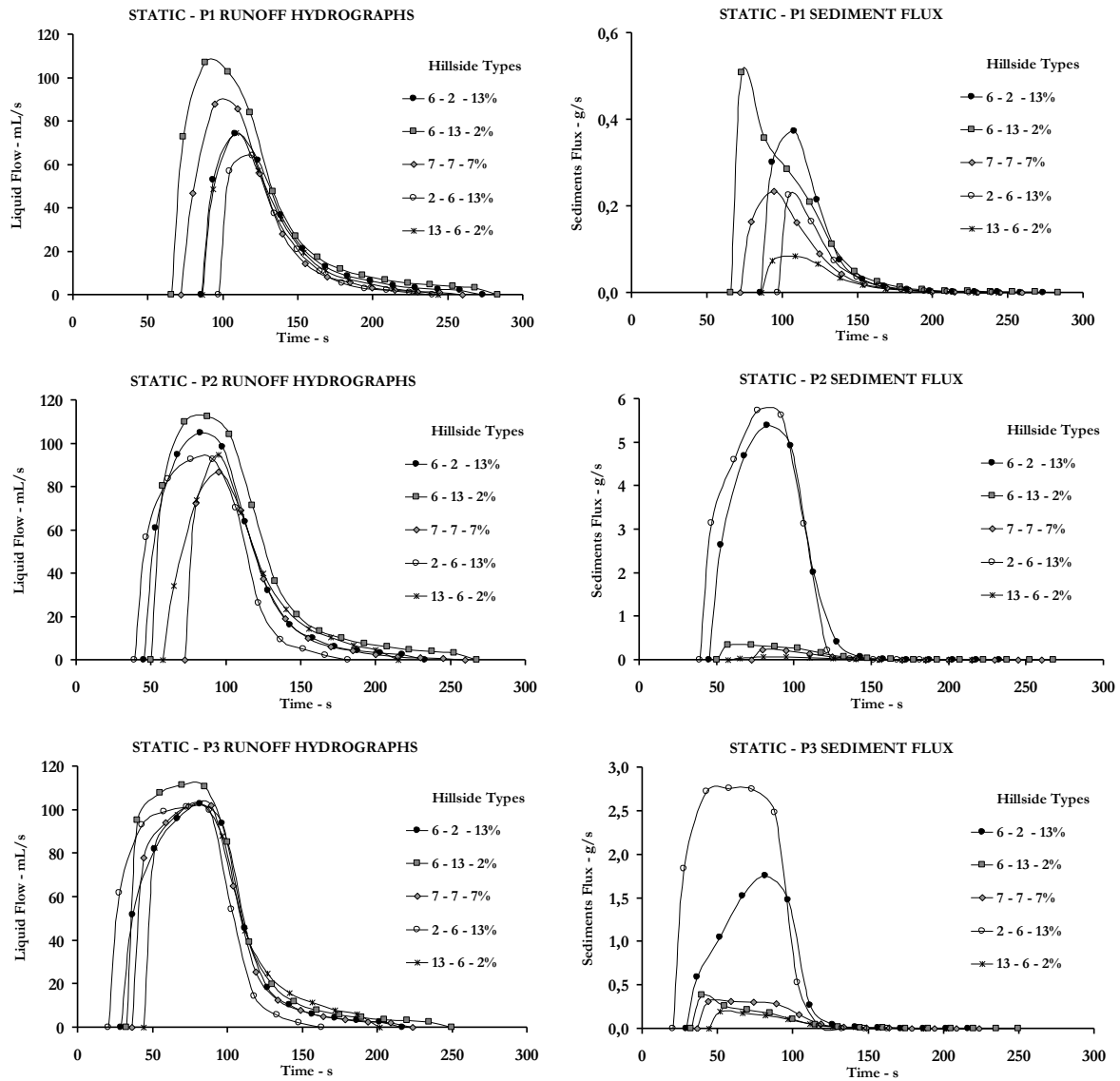


Figure 8.5 Runoff hydrographs and respective sediments fluxes for different storms and hillslopes types, for static rains.

Table 8.1 Runoff hydrographs and respective sediments fluxes for different storms and hillslopes types, for moving rains.

Hillslope types	Storm types	Total runoff flow (mL)	Peak runoff (mL/s)	Total sediments transported (g)	Sediments flow in the peak (g/s)	Time to peak (s)	Time of runoff initiation (s)
6-2-13%	Downstream	5817.22	170.14	215.53	8.40	94.50	87,00
	Upstream	4985.40	35.23	22.30	0.24	49.50	27,00
	Static P1	4314.60	74.33	15.35	0.37	108.25	85,75
	Static P2	7469.82	104.78	302.31	5.38	82.75	45,25
	Static P3	7759.45	102.84	101.13	1.75	81.50	29,00
6-13-2%	Downstream	7126.88	183.57	25.14	0.79	92.50	85,00
	Upstream	6210.05	44.19	16.43	0.12	96.00	28,50
	Static P1	7545.72	107.15	23.65	0.36	88.25	65,75
	Static P2	8764.85	112.47	23.08	0.30	87.50	50,00
	Static P3	9123.59	111.25	18.56	0.21	69.75	32,25
7-7-7%	Downstream	5458.96	136.46	20.51	0.57	93.00	85,50
	Upstream	4330.11	31.16	15.24	0.19	56.50	34,00
	Static P1	5111.95	87.87	11.00	0.23	94.50	72,00
	Static P2	4659.96	86.75	10.94	0.23	94.75	72,25
	Static P3	7496.28	101.89	22.34	0.32	88.75	36,25
2-6-13%	Downstream	3361.85	96.49	108.62	4.63	97.00	89,50
	Upstream	4691.59	44.17	30.88	0.71	49.50	27,00
	Static P1	3020.83	64.04	7.94	0.23	119.50	97,00
	Static P2	6584.48	92.63	336.87	5.73	91.50	39,00
	Static P3	7982.22	101.31	196.48	2.75	72.75	20,25
13-6-2%	Downstream	4279.19	93.00	7.96	0.22	101.00	93,50
	Upstream	4541.32	33.28	7.81	0.08	168.25	40,75
	Static P1	3944.03	74.54	4.43	0.09	108.50	86,00
	Static P2	5565.54	94.65	4.46	0.08	95.00	57,50
	Static P3	7236.58	102.98	11.12	0.20	81.50	44,00

8.3.2 SOIL GRANULOMETRIC EVOLUTION

Granulometric curves for each simulation as function of the storm and hillslope types were drawn. From those it was obtained the soil components (sand, silt and clay) percentages for the diverse combinations between storms and hillslopes, which is presented in Figure 8.6.

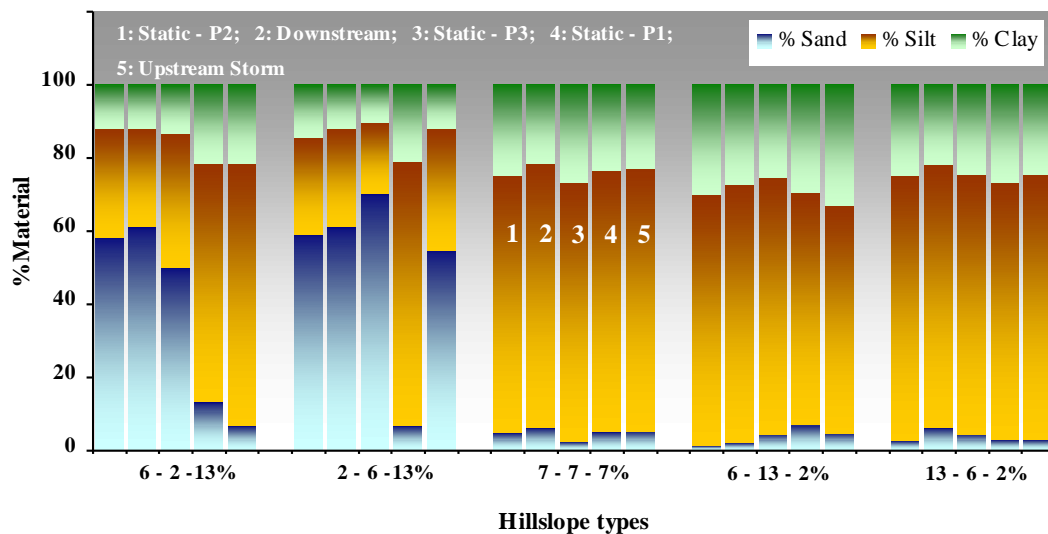
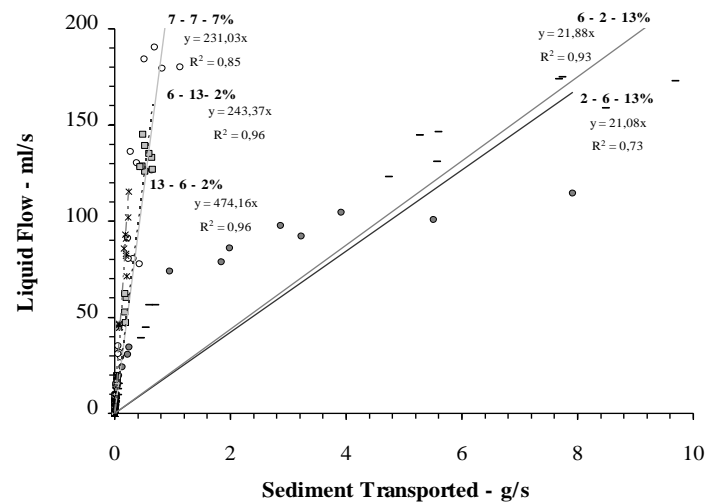


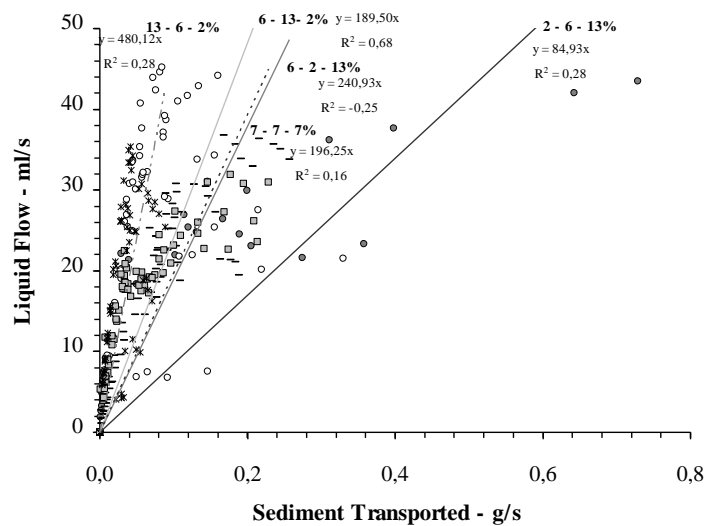
Figure 8.6 Percentages of the sand, silt and clay by the different storm types and hillslope.

8.3.3 RELATION BETWEEN THE SEDIMENT TRANSPORTED AND DISCHARGE

Figure 8.7 presents the obtained relations between discharge and sediment flux. Trend lines were drawn and regression equations obtained. It is visible that the static – P2 and downstream storms are the ones that presents higher transport capacity despite hillslope geometry, and that hillslope type with the segment more inclined near the discharge point (3^o segment, in this in case, 13%), cause higher superficial erosion and sediment flux.

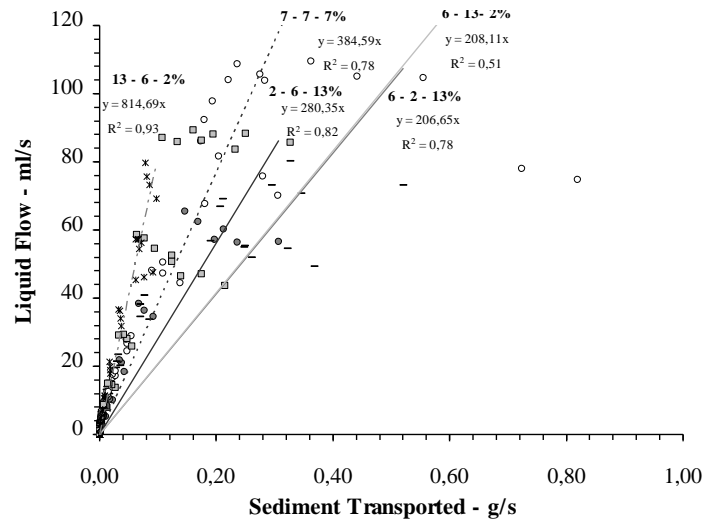


(a)

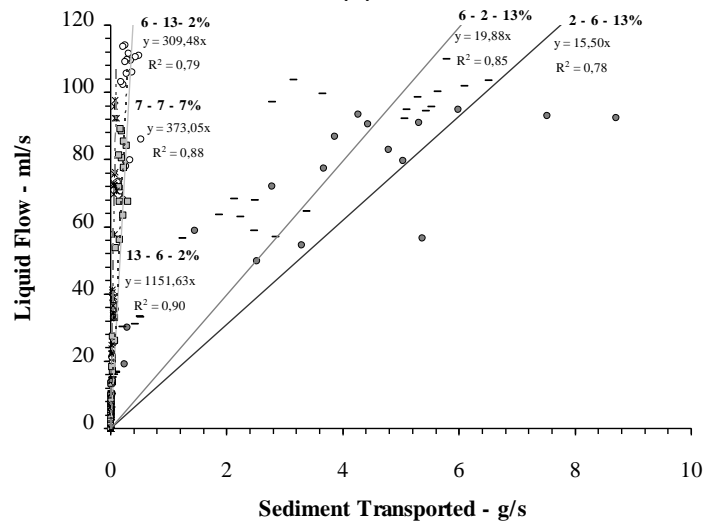


b)

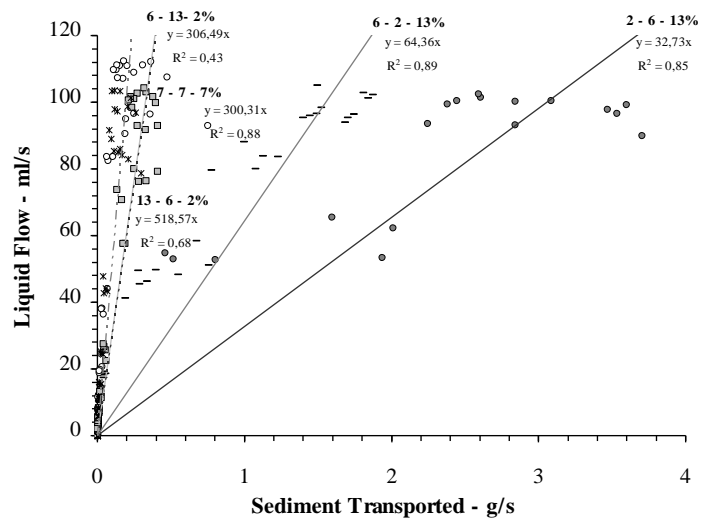
Figure 8.7 Relation between the sediment flux and discharge by the different combinations of the storm and hillslope types: Downhill moving storm (a); Uphill moving storm (b); Static – P1 (c); Static – P2 (d) and Static – P3 (e).



(c)



(d)



(e)

Figure 8.7 (cont.) Relation between the sediment flux and discharge by the different combinations of the storm and hillslope types: Downhill moving storm (a); Uphill moving storm (b); Static – P1 (c); Static – P2 (d) and Static – P3 (e).

8.4 CONCLUSIONS

The following conclusions can be drawn from this study: (1) hillslope shape affects the water erosion process for both non-moving and moving rainstorms; (2) upstream and downstream moving storms cause different hydrologic responses; (3) soil loss by sheet erosion caused by the downstream moving rainstorm and the static P2 was higher than the caused by identical upstream moving rainfall storms or non-moving storms P1 and P3; (4) hillslope with lower slope near discharge section will erode less, while sediment deposits in that area; (5) when the hillslope possess higher slope near discharge section, the superficial erosion strong is evidenced, forming deeper superficial ridges, and (6) granulometric curves similar to the original soil promotes a larger percentage of coarse material, and consequently, higher superficial erosion.

8.5 ACKNOWLEDGEMENTS

The authors wish to acknowledge the Portuguese Foundation for Science and Technology (FCT) for support of project PTDC/ECM/105446/2008. The authors wish to express their gratitude to Célio Duarte, MSc and Cristiano Souza, BSc for conducting the preliminary simulations and the laboratory runs.

8.6 REFERENCES

- Bryan, R.B. and Poesen, J., 1989. Laboratory experiments on the influence of slope length on runoff, percolation and rill development. *Earth Surface Processes and Landforms*, 14 (3), 211–231.
- Cerdà, A., Ibáñez, S. and Calvo, A., 1997. Design and operation of a small and portable rainfall simulator for rugged terrain. *Soil Technology*, 11 (2), 163–170.
- de Lima, J.L.M.P., and Singh V.P., 2000. The influence of storm movement on overland flow – Laboratory experiments under simulated rainfall *In*: V.P. Singh, I.W., Seo, J.H. Sonu, ed. *Hydrologic Modeling – Proceedings of the International Conference on Water, Environmental, Ecology, Socio-economics and Health Engineering*, 18–21 1999 October, Seoul. Fort Collins, CO: Water Resources, 101–11.
- de Lima, J.L.M.P. and Singh V.P., 2002. The influence of the pattern of moving rainstorms on overland flow. *Advances on Water Resources*, 25 (7), 817–828.
- de Lima, J.L.M.P. and Singh, V.P., 2003. Laboratory experiments on the influence of storm movement on overland flow. *Journal Physics and Chemistry of the Earth*, 28 (6–7), 277–282.

de Lima, J.L.M.P., Tavares, P., Singh, V.P. and de Lima, M.I.P., 2009. Investigating the nonlinear response of soil loss to storm direction using a circular soil flume. *Geoderma*, 152 (1–2), 9–15.

Eagleson, P.S., 1978. Climate, soil and vegetation: the distribution of annual precipitation derived from observed storm sequences. *Water Resources Research*, 14 (5), 713–721.

Foufoula-Georgiou, E. and Georgakakos, K.P., 1991. Hydrologic advances in space time precipitation modelling and forecasting. In: D.S. Bowles and P.E. O’Connell, eds. *Recent Advances in the Modelling of Hydrologic Systems*, NATO ASI Series, Serie C: Mathematical and Physical Sciences, vol. 345. Dordrecht: Kluwer Academic Publishers, 47–65.

Jensen, M., 1984. Runoff pattern and peak flows from moving block rains based on linear time-area curve. *Nordic Hydrology*, 15, 155–168.

Ladoy, P., Schmitt, F., Schertzer, D. and Lovejoy, S., 1993. Variabilité temporelle multifractale des observations pluviométriques à Nîmes. *Comptes Rendus de l’Académie des Sciences Serie II*, 317, 775–782.

Maksimov, V.A., 1964. Computing runoff produced by a heavy rainstorm with a moving center. *Soviet Hydrology*, 5, 510–513.

Mayer, L.D., 1965. Simulation of rainfall for soil erosion research. *Transactions of the ASAE*, 8, 63–64.

Nunes, J.P., de Lima, J.L.M.P., Singh, V.P., de Lima, M.I.P. and Vieira, G.N., 2006. Numerical modelling of surface runoff and erosion due to moving rainstorms at the drainage basin scale. *Journal of Hydrology*, 330, (3–4), 709–720.

Singh, V.P., 1998. Effect of the direction of storm movement on planar flow. *Hydrological Processes*, 12, 147–170.

Wilson, C.B., Valdes, J.B. and Rodrigues-Iturbe, I., 1979. On the influence of the spatial distribution of rainfall on storm runoff. *Water Resources Research*, 15 (2), 321–328.

Yen, B.C. and Chow, V.T., 1968. *A Study of Surface Runoff Due to Moving Rain Storms*. Civil Engineering Studies, Hydraulic Engineering Series No. 17. Champaign, IL: University of Illinois at Urbana-Champaign.

CHAPTER 9

There are in fact two things, science and opinion; the former begets knowledge, the latter ignorance.

Hippocrates

Science is organized knowledge. Wisdom is organized life.

Immanuel Kant

There are no such things as applied sciences, only applications of science.

Louis Pasteur

9. CONCLUSIONS AND FUTURE RESEARCH

This chapter summarizes the main conclusions reached during the course of this thesis. They are presented in a complete form in the previous chapters. Short answers to the open-questions defined in Chapter 1 are offered here to show that the proposed objectives for this work were accomplished. These short answers should be regarded as contributions to the clarification of the issues raised in this thesis; they are limited by the constraints and assumptions associated to the particular cases studied in each of the chapters (*e.g.*, laboratory facilities, model simplification). Finally, some potential research lines in this field are outlined.

9.1 CONCLUSIONS

The overall scope of this thesis was to assess the influence of storm movement and wind-driven rain on the rainfall-runoff process in urban areas under intense rainfall events. Since urban areas are characterized by having large impervious coverings, such as roads, paths and buildings this research focused especially on impermeable areas. Special attention was given to the relations between storm movement, wind-driven rainfall, some specific characteristics of urban areas (*e.g.*, building height) and the resulting overland flow hydrographs. Other issues were also discussed and presented (*e.g.*, the influence of hillslope configuration on overland flow and sediment loss).

This research shows that storm movement and wind-driven rain have a marked influence on the rainfall-runoff process and that their interactions strongly affect the resulting overland flood hydrographs. Urban features such as building density and the connectivity of rooftops were found to play a major role in the rainfall-runoff process.

The following statements summarize the main conclusions of this thesis by answering to the open-questions listed in Chapter 1. As referred before, these answers are partial and limited to the scope and assumptions of this thesis.

For urban (impervious) areas:

- How does storm movement affect overland flow?

During the physical rainfall-runoff experiments (Chapters 4, 5 and 6) and when applying the analytical solution to the linear kinematic wave equation (Chapter 7), consistent differences were found in the flood hydrographs. These were caused by static and moving storms (downstream and upstream). Simulated storm cell movement affected the peak discharge, base time and steepness of the hydrograph's limbs. When compared with storms moving upstream, downstream moving storms produced higher peak discharges, steeper limbs of the hydrographs, lower base times and earlier start of runoff (*e.g.*, Figure 4.8).

- How does wind-driven rainfall affect overland flow?

Wind-driven rainfall reduces the differences in the overland flow hydrographs mentioned above. This is mainly because the raindrops are spread over a larger area than in a windless situation. Wind-driven rainfall thus leads to less-peaked spatial patterns of rainfall intensity (*e.g.*, Figure 5.3) which causes smaller peak discharges, less steep limbs of the hydrographs and longer base times (*e.g.*, Figure 5.6) than windless rainfall conditions. Wind-driven rainfall effects are more evident for static and downstream moving storms, where the hydrographs show significant changes in comparison with hydrographs of upstream moving storms (*e.g.*, Figure 6.5). The existence of high-rise buildings also plays a major role in wind-driven rainfall conditions. The higher lateral interception by the buildings was found to delay raindrops from falling onto the basin surface, thus leading to a higher concentration time and a more uniform discharge over time (*e.g.*, Figures 4.8a and 4.8b).

- Which effects does building density have on overland flow? How are these effects altered by the occurrence of wind-driven moving rainstorms?

In the laboratory simulations of overland flow using models of high-rise buildings, it was seen that increasing building density lowers the discharge peak, reduces the steepness of the hydrograph's limbs and increases the base time. Reduction of differences between peak discharges for different building densities is particularly noticeable for static rainfall (*e.g.*, Figure 4.8a). Wind-driven rainstorms considerably attenuate these differences (*e.g.*, Figure 4.8b). The steepness of rising limbs of hydrographs was found to be linearly reduced by the increasing building density, regardless of the type of storm movement (static, upstream or downstream) and of the presence or absence of wind (*e.g.*, Figure 4.10).

- What effects do rooftop connectivities have on overland flow? How are these effects altered by the occurrence of wind-driven moving rainstorms?

In the laboratory simulations of overland flow using models of connected rooftops, it was seen that, for static storms, increasing rooftop connectivity is responsible for lowering the slope of the rising limb of the hydrographs and the peak discharge, although the latter is mostly noticeable in windless conditions (*e.g.*, Figure 5.6 top left). Clustering of rooftops leads to an increase in the runoff base time, for both moving and static storms, with or without wind (*e.g.*, Figure 5.8; centre top). Regardless of the rooftop connectivity and storm type, wind-driven rainfall reduces the peak discharge and slope of the rising limb of the overland flow hydrographs compared with windless rainfall (*e.g.*, Figures 5.8 top and 5.8 bottom).

- What effects do building heights have on overland flow? How are these effects altered by the occurrence of wind-driven moving rainstorms?

In the laboratory simulations of overland flow using models of buildings of different heights, it was seen that when buildings were taller runoff base times were longer, but there was only a slight decrease in the peak discharges (*e.g.*, Figure 6.6). Storm movement proved to be more important than building height to the hydrograph's shape. The highest peak discharges were generated by downstream moving storms, while upstream moving storms promoted the lowest peak discharges and the largest base times (*e.g.*, Figure 6.5). Wind-driven rainfall significantly reduced the peak discharge, in particular for static storms, and increased runoff base times (*e.g.*, Figure 6.5 top).

- Based on the linear kinematic wave theory is it possible to establish an exact solution of 1D overland flow under moving rainstorms? If so, what are the constraints, advantages and possible applications of that solution?

Yes. An exact solution of 1D overland flow under (downstream and upstream) moving rainstorms was derived from the linear kinematic wave equation. The solution is valid according to the suppositions of the kinematic wave theory (*e.g.*, valid for small impervious drainage basins). The main advantages of the analytical solution are that it is easy to use and gives, in a single closed form equation that is more straightforward and less time-consuming to compute, the overland flow discharge and depth for the full space-time domain (*e.g.*, Figure 7.8). This exact solution can be used as a tool in fundamental

hydrological studies to calibrate more complex models, estimate hydrological parameters (*e.g.*, surface roughness) and quantify overland flow for design purposes (*e.g.*, micro drainage basins).

- Can building density, rooftop connectivity and building height contribute to flood prevention or mitigation?

According to the experiments carried out in the laboratory, the results achieved, as set out in Chapters 4, 5 and 6, show that building density, rooftop connectivity and building height do have an influence on the overland flow hydrographs. Some of these results, such as lower peak discharges and increased base times associated with higher building densities, suggest that some urban characteristics can contribute to the prevention of flooding events caused by high-intensity rainstorms and to mitigating the effects of flooding.

For natural (pervious) surfaces:

- How does hillslope configuration affect overland flow and erosion? How are these effects altered by storm movement?

In the laboratory simulations of overland flow and erosion using an articulated soil flume, it was observed that hillslope shape affects overland flow and the water erosion process for both static and moving rainstorms. The hillslope shapes have more influence on the transport of sediments than on runoff (and especially on the peak discharge), regardless of the storm type. Hillslopes with a lower slope near the discharge section suffer less sediment yield, while sediment is deposited in that area. Static and downhill moving storms promote higher peak flows and sediment transport than uphill storms.

- What are the most hazardous hillslope configurations for soil loss?

In the laboratory simulations it was observed that convex-shaped hillslopes, characterized by higher slopes near the discharge (lower) sections, promote stronger surface erosion and the development of surface ridges, and is the most hazardous in terms of soil loss.

9.2 FUTURE RESEARCH

The process by which rainfall becomes runoff is complex in natural and urban areas alike. Storm movement and the simultaneous action of wind and rainfall give it extra complexity. In urban areas, large impervious surfaces and typical urban features such as buildings complicate matters even further. Some aspects related to the rainfall-runoff process have been studied in this thesis. But many other issues can be raised in this context. Further research may include:

- Monitoring a real-scale experimental basin by using a synchronized network of meteorological sensors and flow/level gauges to obtain field data on the influence of storm movement on runoff;
- Implementing physically-based numerical models to simulate the influence of storm movement on hydrological connectivity, at different drainage basin scales;
- Evaluating the influence of impervious areas connectivity on overland flow and erosion by using scale models with distinct patterns of pervious and impervious surfaces;
- Quantifying the increase of the magnitude and recurrence of floods associated with urban expansion by means of implementing a dynamic (temporal) GIS-based hydrological model;
- Studying the influence of storm acceleration in overland flow and erosion by means of numerical and/or analytical simulation of the rainfall-runoff process under accelerated or decelerated storm movement;
- Performing laboratory simulations to evaluate the effectiveness of soil conservation measures, like furrows or terraces on hillslopes under wind-driven rainfall.